Mathematical Problems in Engineering

Discrete Fractional-Order Systems with Applications in Engineering and Natural Sciences

Lead Guest Editor: Abdelalim Elsadany
Guest Editors: Abdulrahman Al-khedhairi, Hamdy Nabih Agiza, Baogui Xin, and Amr Elsonbaty

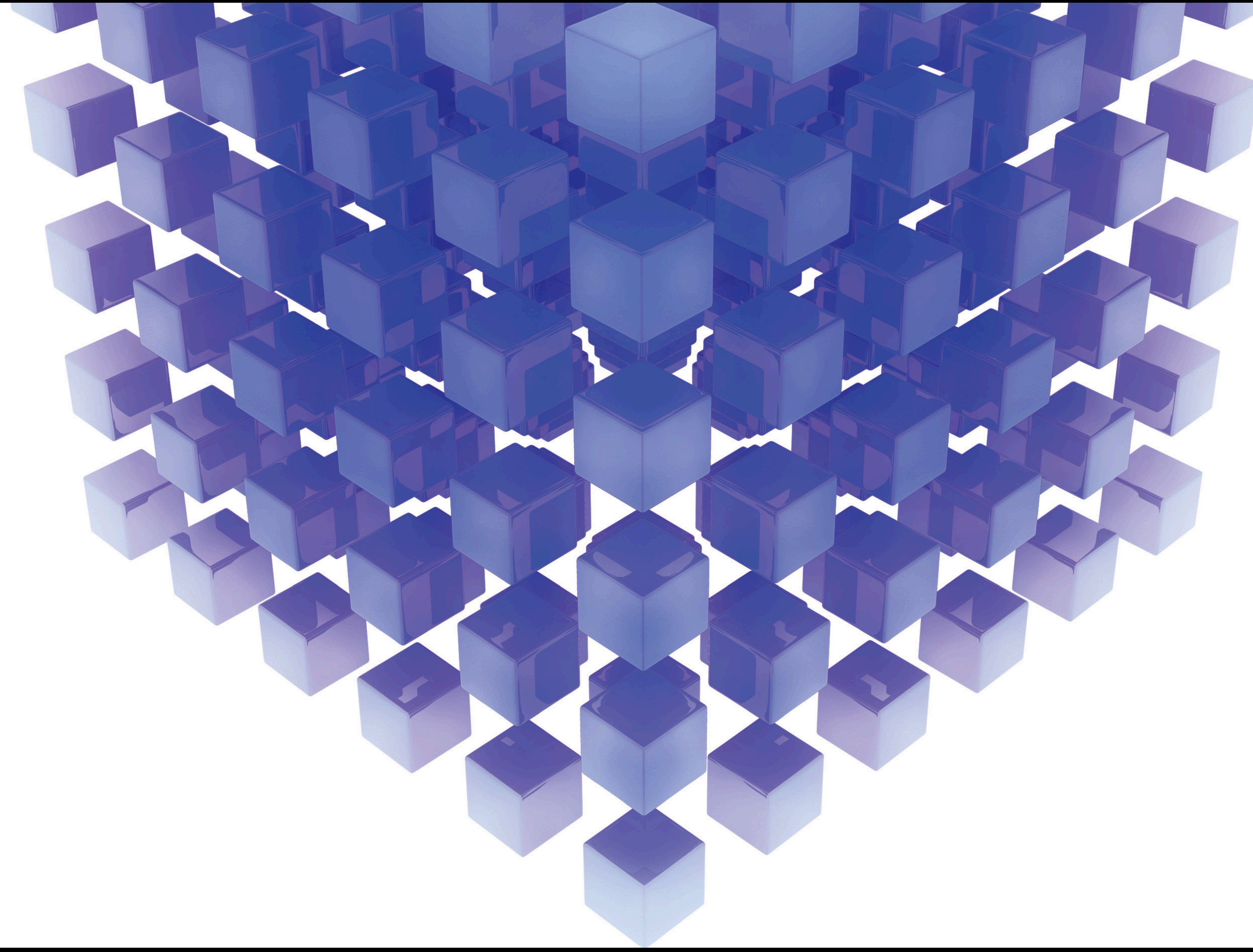

Discrete Fractional-Order Systems with Applications in Engineering and Natural Sciences

Mathematical Problems in Engineering

Discrete Fractional-Order Systems with Applications in Engineering and Natural Sciences

Lead Guest Editor: Abdelalim Elsadany
Guest Editors: Abdulrahman Al-khedhairi, Hamdy Nabih Agiza, Baogui Xin, and Amr Elsonbaty

Guido Bolognesi, United Kingdom
Rodolfo Bontempo, Italy
Alberto Borboni, Italy
Marco Bortolini, Italy
Paolo Boscariol, Italy
Daniela Boso, Italy
Guillermo Botella-Juan, Spain
Boulaïd Boulkroune, Belgium
Abdesselem Boulkroune, Algeria
Fabio Bovenga, Italy
Francesco Braghin, Italy
Ricardo Branco, Portugal
Maurizio Brocchini, Italy
Julien Bruchon, France
Matteo Bruggi, Italy
Michele Brun, Italy
Maria Elena Bruni, Italy
Vasilis Burganos, Greece
Maria Angela Butturi, Italy
Raquel Caballero-Águila, Spain
Guillermo Cabrera-Guerrero, Chile
Filippo Cacace, Italy
Pierfrancesco Cacciola, United Kingdom
Salvatore Caddemi, Italy
zuowei cai, China
Roberto Caldelli, Italy
Alberto Campagnolo, Italy
Eric Campos, Mexico
Salvatore Cannella, Italy
Francesco Cannizzaro, Italy
Maosen Cao, China
Javier Cara, Spain
Raffaele Carli, Italy
Ana Carpio, Spain
Rodrigo Carvajal, Chile
Caterina Casavola, Italy
Sara Casciati, Italy
Federica Caselli, Italy
Carmen Castillo, Spain
Inmaculada T. Castro, Spain
Miguel Castro, Portugal
Giuseppe Catalanotti, United Kingdom
Nicola Caterino, Italy
Alberto Cavallo, Italy
Gabriele Cazzulani, Italy
Luis Cea, Spain
Fatih Vehbi Celebi, Turkey
Song Cen, China
Miguel Cerrolaza, Venezuela
M. Chadli, France
Gregory Chagnon, France
Ludovic Chamoin, France
Qing Chang, USA
Ching-Ter Chang, Taiwan
Xiaoheng Chang, China
Kuei-Lun Chang, Taiwan
Dr. Prasenjit Chatterjee, India
Kacem Chehdi, France
Peter N. Cheimets, USA
Xinkai Chen, Japan
Xizhong Chen, Ireland
Xue-Bo Chen, China
Chih-Chiang Chen, Taiwan
Shyi-Ming Chen, Taiwan
Zhiwen Chen, China
He Chen, China
Xiao Chen, China
Kebing Chen, China
Chien-Ming Chen, China
Qiang Cheng, USA
Zeyang Cheng, China
Luca Chiapponi, Italy
Ryoichi Chiba, Japan
Francisco Chicano, Spain
Nicholas Chileshe, Australia
Tirivanhu Chinyoka, South Africa
Adrian Chmielewski, Poland
Seongim Choi, USA
Ioannis T. Christou, Greece
Hung-Yuan Chung, Taiwan
Simone Cinquemani, Italy
Roberto G. Citarella, Italy
Joaquim Ciurana, Spain
John D. Clayton, USA
Francesco Clementi, Italy
Piero Colajanni, Italy
Giuseppina Colicchio, Italy
Vassilios Constantoudis, Greece
Francesco Conte, Italy
Enrico Conte, Italy
Alessandro Contento, USA
Mario Cools, Belgium
Gino Cortellessa, Italy
Juan Carlos Cortés, Spain

Shangce Gao, Japan
Xingbao Gao, China
Giovanni Garcea, Italy
José García, Chile
Luis Rodolfo Garcia Carrillo, USA
Jose M. Garcia-Aznar, Spain
Akhil Garg, China
Harish Garg, India
Alessandro Gasparetto, Italy
Gianluca Gatti, Italy
Oleg V. Gendelman, Israel
Stylianos Georgantzinos, Greece
Fotios Georgiades, India
Parviz Ghadimi, Iran
Georgios I. Giannopoulos, Greece
Agathoklis Giaralis, United Kingdom
Pablo Gil, Spain
Anna M. Gil-Lafuente, Spain
Ivan Giorgio, Italy
Gaetano Giunta, Luxembourg
Alessio Gizzi, Italy
Jefferson L.M.A. Gomes, United Kingdom
HECTOR GOMEZ, Chile
José Francisco Gómez Aguilar, Mexico
Emilio Gómez-Déniz, Spain
Antonio M. Gonçalves de Lima, Brazil
Chris Goodrich, USA
Rama S. R. Gorla, USA
Veena Goswami, India
Xunjie Gou, Spain
Jakub Grabski, Poland
Antoine Grall, France
George A. Gravvanis, Greece
Fabrizio Greco, Italy
David Greiner, Spain
Jason Gu, Canada
Federico Guarracino, Italy
Michele Guida, Italy
Muhammet Gul, Turkey
Dong-Sheng Guo, China
Zhaoxia Guo, China
Hu Guo, China
Jian-Ping Guo, China
Quang Phuc Ha, Australia
Li Haitao, China
Petr Hájek, Czech Republic
Muhammad Hamid, United Kingdom
Shigeyuki Hamori, Japan
Weimin Han, USA
Renke Han, United Kingdom
Xingsi Han, China
Zhen-Lai Han, China
Thomas Hanne, Switzerland
Xinan Hao, China
Mohammad A. Hariri-Ardebili, USA
Khalid Hattaf, Morocco
Yu-Ling He, China
Defeng He, China
Fu-Qiang He, China
Xiao-Qiao He, China
salim HEDDAM, Algeria
Ramdane Hedjar, Saudi Arabia
Jude Hemanth, India
Reza Hemmati, Iran
Nicolae Herisanu, Romania
Alfredo G. Hernández-Diaz, Spain
M.I. Herreros, Spain
Eckhard Hitzer, Japan
Paul Honeine, France
Jaromir Horacek, Czech Republic
S. Hassan Hosseinnia, The Netherlands
Xiaorong Hou, China
Yingkun Hou, China
Lei Hou, China
Yunfeng Hu, China
Can Huang, China
Gordon Huang, Canada
Sajid Hussain, Canada
Asier Ibeas, Spain
Wubshet Ibrahim, Ethiopia
Orest V. Iftime, The Netherlands
Przemyslaw Ignaciuk, Poland
Muhammad Imran, Pakistan
Giacomo Innocenti, Italy
Emilio Insfran Pelozo, Spain
Alessio Ishizaka, France
Nazrul Islam, USA
Benoit Iung, France
Benjamin Ivorra, Spain
Breno Jacob, Brazil
Tushar Jain, India
Amin Jajarmi, Iran
Payman Jalali, Finland
Mahdi Jalili, Australia

Prashant Kumar Jamwal, Kazakhstan
Łukasz Jankowski, Poland
Fahd Jarad, Turkey
Samuel N. Jator, USA
Juan C. Jauregui-Correa, Mexico
Kandasamy Jayakrishna, India
Reza Jazar, Australia
Khalide Jbilou, France
Isabel S. Jesus, Portugal
Chao Ji, China
Linni Jian, China
Bin Jiang, China
Qing-Chao Jiang, China., China
Peng-fei Jiao, China
Ricardo Fabricio Escobar Jiménez, Mexico
Emilio Jiménez Macías, Spain
Xiaoliang Jin, Canada
Maolin Jin, Republic of Korea
Zhuo Jin, Australia
Dylan F. Jones, United Kingdom
Viacheslav Kalashnikov, Mexico
Mathiyalagan Kalidass, India
Tamas Kalmar-Nagy, Hungary
Zhao Kang, China
Tomasz Kapitaniak, Poland
Julius Kaplunov, United Kingdom
Konstantinos Karamanos, Belgium
Michal Kawulok, Poland
Irfan Kaymaz, Turkey
Vahid Kayvanfar, Iran
Krzysztof Kecik, Poland
Chaudry M. Khalique, South Africa
Abdul Qadeer Khan, Pakistan
Mukhtaj Khan, Pakistan
Mostafa M. A. Khater, Egypt
MOHAMMAD REZA KHEDMATI, Iran
Kwangki Kim, Republic of Korea
Nam-Il Kim, Republic of Korea
Philipp V. Kiryukhantsev-Korneev, Russia
P.V.V Kishore, India
Jan Koci, Czech Republic
Ioannis Kostavelis, Greece
Sotiris B. Kotsiantis, Greece
Frederic Kratz, France
Vamsi Krishna, India
Kamalanand Krishnamurthy, India
Petr Krysl, USA
Edyta Kucharska, Poland
Krzysztof S. Kulpa, Poland
Kamal Kumar, India
Michal Kunicki, Poland
Cedrick A. K. Kwuimy, USA
Kyandoghere Kyamakya, Austria
Ivan Kyrchei, Ukraine
Davide La Torre, Italy
Márcio J. Lacerda, Brazil
Risto Lahdelma, Finland
Giovanni Lancioni, Italy
Jaroslaw Latalski, Poland
Antonino Laudani, Italy
Hervé Laurent, France
Agostino Lauria, Italy
Aimé Lay-Ekuakille, Italy
Nicolas J. Leconte, France
Kun-Chou Lee, Taiwan
Dimitri Lefebvre, France
Eric Lefevre, France
Marek Lefik, Poland
Yaguo Lei, China
Gang Lei, Saudi Arabia
Kauko Leiviskä, Finland
Thibault Lemaire, France
Ervin Lenzi, Brazil
Roman Lewandowski, Poland
ChenFeng Li, China
Jian Li, USA
Jun Li, China
Yueyang Li, China
Yang Li, China
Zhen Li, China
Yao-Jin Lin, China
Jian Lin, China
Mingwei Lin, China
En-Qiang Lin, USA
Zhiyun Lin, China
Wanquan Liu, China
Sixin Liu, China
Lei Liu, China
Jianxu Liu, Thailand
Bin Liu, China
Heng Liu, China
Yuanchang Liu, United Kingdom
Yu Liu, China
Bo Liu, China

Bonifacio Llamazares, Spain
Alessandro Lo Schiavo, Italy
Jean Jacques Loiseau, France
Francesco Lolli, Italy
Paolo Lonetti, Italy
Sandro Longo, Italy
António M. Lopes, Portugal
Sebastian López, Spain
Pablo Lopez-Crespo, Spain
Cesar S. Lopez-Monsalvo, Mexico
Luis M. López-Ochoa, Spain
Ezequiel López-Rubio, Spain
Vassilios C. Loukopoulos, Greece
Jose A. Lozano-Galant, Spain
Gabriele Maria Lozito, Italy
Rongxing Lu, Canada
Songtao Lu, USA
Zhiguo Luo, China
Gabriel Luque, Spain
Valentin Lychagin, Norway
Dazhong Ma, China
Junhai Ma, China
Antonio Madeo, Italy
Alessandro Magnani, Belgium
Toqeer Mahmood, Pakistan
Fazal M. Mahomed, South Africa
Arunava Majumder, India
Paolo Manfredi, Italy
Adnan Maqsood, Pakistan
Giuseppe Carlo Marano, Italy
Damijan Markovic, France
Filipe J. Marques, Portugal
Luca Martinelli, Italy
Rodrigo Martinez-Bejar, Spain
Guiomar Martín-Herrán, Spain
Denizar Cruz Martins, Brazil
Francisco J. Martos, Spain
Elio Masciari, Italy
Franck Massa, France
Paolo Massioni, France
Alessandro Mauro, Italy
Jonathan Mayo-Maldonado, Mexico
Fabio Mazza, Italy
Pier Luigi Mazzeo, Italy
Laura Mazzola, Italy
Driss Mehdi, France
Dr. Zahid Mehmood, Pakistan
YUE MEI, China
Roderick Melnik, Canada
Xiangyu Meng, USA
Debiao Meng, China
Jose Merodio, Spain
Alessio Merola, Italy
Mahmoud Mesbah, Iran
Luciano Mescia, Italy
Laurent Mevel, France
Constantine Michailides, Cyprus
Mariusz Michta, Poland
Prankul Middha, Norway
Aki Mikkola, Finland
Giovanni Minafò, Italy
Hiroyuki Mino, Japan
Dimitrios Mitsotakis, New Zealand
saleh mobayen, Taiwan, R.O.C., Iran
Nikunja Mohan Modak, India
Sara Montagna, Italy
Roberto Montanini, Italy
Francisco J. Montáns, Spain
Gisele Mophou, France
Rafael Morales, Spain
Marco Morandini, Italy
Javier Moreno-Valenzuela, Mexico
Simone Morganti, Italy
Caroline Mota, Brazil
Aziz Moukrim, France
Shen Mouquan, China
Dimitris Mourtzis, Greece
Emiliano Mucchi, Italy
Taseer Muhammad, Saudi Arabia
Josefa Mula, Spain
Jose J. Muñoz, Spain
Giuseppe Muscolino, Italy
Dino Musmarra, Italy
Marco Mussetta, Italy
Ghulam Mustafa, Pakistan
Hariharan Muthusamy, India
Hakim Naceur, France
Alessandro Naddeo, Italy
Benedek Nagy, Turkey
Omar Naifar, Tunisia
Mariko Nakano-Miyatake, Mexico
Keivan Navaie, United Kingdom
Adrian Neagu, USA
Erivelton Geraldo Nepomuceno, Brazil

AMA Neves, Portugal
Luís C. Neves, United Kingdom
Dong Ngoduy, New Zealand
Nhon Nguyen-Thanh, Singapore
Papakostas Nikolaos, Ireland
Jelena Nikolic, Serbia
Tatsushi Nishi, Japan
Shanzhou Niu, China
Xesús Nogueira, Spain
Ben T. Nohara, Japan
Mohammed Nouari, France
Mustapha Nourelfath, Canada
Kazem Nouri, Iran
Ciro Núñez-Gutiérrez, Mexico
Wlodzimierz Ogryczak, Poland
Roger Ohayon, France
Krzysztof Okarma, Poland
Mitsuhiro Okayasu, Japan
Diego Oliva, Mexico
Alberto Olivares, Spain
Enrique Onieva, Spain
Calogero Orlando, Italy
Sergio Ortobelli, Italy
Naohisa Otsuka, Japan
Taoreed Owolabi, Nigeria
Cenap Özel, Turkey
Pawel Packo, Poland
Arturo Pagano, Italy
Roberto Palma, Spain
Alessandro Palmeri, United Kingdom
Pasquale Palumbo, Italy
Li Pan, China
Weifeng Pan, China
Chandan Pandey, India
K. M. Pandey, India
Jürgen Pannek, Germany
Elena Panteley, France
Achille Paolone, Italy
George A. Papakostas, Greece
Xosé M. Pardo, Spain
You-Jin Park, Taiwan
Manuel Pastor, Spain
Petr Páta, Czech Republic
Pubudu N. Pathirana, Australia
Surajit Kumar Paul, India
Sitek Paweł, Poland
Luis Payá, Spain
Alexander Paz, Australia
Igor Pažanin, Croatia
Libor Pekař, Czech Republic
Francesco Pellicano, Italy
Marcello Pellicciari, Italy
Zhi-ke Peng, China
Mingshu Peng, China
Haipeng Peng, China
Zhengbiao Peng, Australia
Jian Peng, China
Xindong Peng, China
Yuexing Peng, China
Bo Peng, China
Marzio Pennisi, Italy
Maria Patrizia Pera, Italy
Matjaz Perc, Slovenia
A. M. Bastos Pereira, Portugal
Ricardo Perera, Spain
F. Javier Pérez-Pinal, Mexico
Michele Perrella, Italy
Francesco Pesavento, Italy
Ivo Petras, Slovakia
Francesco Petrini, Italy
Hoang Vu Phan, Republic of Korea
Lukasz Pieczonka, Poland
Dario Piga, Switzerland
Antonina Pirrotta, Italy
Marco Pizzarelli, Italy
Javier Plaza, Spain
Goutam Pohit, India
Kemal Polat, Turkey
Dragan Poljak, Croatia
Jorge Pomares, Spain
Hiram Ponce, Mexico
Sébastien Poncet, Canada
Volodymyr Ponomaryov, Mexico
Jean-Christophe Ponsart, France
Mauro Pontani, Italy
Cornelio Posadas-Castillo, Mexico
Francesc Pozo, Spain
Aditya Rio Prabowo, Indonesia
Anchasa Pramuanjaroenkij, Thailand
Christopher Pretty, New Zealand
Leonardo Primavera, Italy
Luca Pugi, Italy
Krzysztof Puszynski, Poland
Goran D. Putnik, Portugal

Xiaofei Zhang, China
Xuping Zhang, Denmark
Kai Zhang, China
Xianming Zhang, Australia
Yifan Zhao, United Kingdom
Yongmin Zhong, Australia
Zebo Zhou, China
Debao Zhou, USA
Zhe Zhou, China
Jian G. Zhou, United Kingdom
Quanxin Zhu, China
Wu-Le Zhu, China
Gaetano Zizzo, Italy
Zhixiang Zou, China

Contents

Design of Static Output Feedback Controller for Fractional-Order T-S Fuzzy System
Zhile Xia
Research Article (9 pages), Article ID 7898109, Volume 2020 (2020)

Hindawi
Mathematical Problems in Engineering
Volume 2022, Article ID 9767920, 2 pages
https://doi.org/10.1155/2022/9767920

Editorial

Discrete Fractional-Order Systems with Applications in Engineering and Natural Sciences

Abdelalim Elsadany,[1] **Abdulrahman Al-khedhairi**,[2] **Hamdy Nabih Agiza**,[3] **Baogui Xin**,[4] **and Amr Elsonbaty**[5]

[1]*Suez Canal University, Ismailia, Egypt*
[2]*King Saud University, Riyadh, Saudi Arabia*
[3]*Mansoura University, Mansoura, Egypt*
[4]*Shandong University of Science and Technology, Qingdao, China*
[5]*Prince Sattam Bin Abdulaziz University, Al-Kharj, Saudi Arabia*

Correspondence should be addressed to Abdelalim Elsadany; aelsadany1@yahoo.com

Received 5 January 2022; Accepted 5 January 2022; Published 27 January 2022

Discrete fractional calculus (DFC) research is gaining a lot of attention, both theoretically and practically. Some DFC systems such as the discrete fractional-order logistic, the fractional-order Henon maps, and their applications in image encryption have been studied. Recent publications in this field include the novel discrete fractional order in engineering, physical, biological, and economical models, analytical insights into such models, stability analysis, bifurcation analysis, determination of chaotic behaviour, and implementation of chaos control methods and synchronization applications in many applied models.

We are delighted to announce the publication of this Special Issue devoted to fresh problems in discrete fractional calculus (DFC) and its applications in engineering and natural sciences. The main goal of this Special Issue is to provide an opportunity to study new developments in the discrete fractional-order models in relevant areas of engineering and natural sciences, as well as bifurcation and chaos analysis of discrete fractional-order models and their applications. Our editorial team chose ten pieces for publishing from among those submitted for consideration. These articles cover the topics of feedback controller for fractional-order T-S fuzzy system, delta partial difference equations, forecasting confirmed cases, deaths, and recoveries from COVID-19 in China, discrete fractional-order Prion model, n-dimensional fractional frequency Laplace transform, fractional Black–Scholes model, impulsive problem under Caputo fractional boundary conditions, discrete-time fractional-order system and its hidden chaotic attractors, algorithm for R-L fractional nonlinear control systems, and social welfare of a two-stage game under R&D spillovers. We are hopeful that this Special Issue will contribute to a better understanding and research of discrete fractional calculus and its applications.

Conflicts of Interest

The Guest Editors declare that they have no conflicts of interest regarding the publication of this Special Issue.

Abdelalim Elsadany
Abdulrahman Al-khedhairi
Hamdy Nabih Agiza
Baogui Xin
Amr Elsonbaty

Hindawi
Mathematical Problems in Engineering
Volume 2021, Article ID 2096868, 19 pages
https://doi.org/10.1155/2021/2096868

Research Article

Stability, Global Dynamics, and Social Welfare of a Two-Stage Game under R&D Spillovers

Wei Zhou, [1,2] **Tong Chu**, [3] **and Xiao-Xue Wang** [2]

[1] *School of Mathematics and Physics, Lanzhou Jiaotong University, Lanzhou, Gansu 730070, China*
[2] *Research Centre of Game Theory and Economics Mathematics, Lanzhou Jiaotong University, Lanzhou, Gansu 730070, China*
[3] *School of Law, Zhejiang University of Finance and Economics, Hangzhou, Zhejiang 310018, China*

Correspondence should be addressed to Wei Zhou; wei_zhou@vip.126.com

Received 24 June 2020; Revised 22 December 2020; Accepted 4 January 2021; Published 18 January 2021

Academic Editor: Abdelalim Elsadany

In this paper, a repeated two-stage oligopoly game where two boundedly rational firms produce homogeneous product and apply gradient adjustment mechanism to decide their individual R&D investment is considered. Results concerning the equilibrium in the built model and the stability are discussed. The effects of system parameters on the complex dynamical behaviors of the built game are analyzed. We find that the system can lose stability through a flip bifurcation or a Neimark–Sacker bifurcation. In addition, the coexistence of multiattractors is also discussed using the so-called basin of attraction. At the end of this research, the social welfare of the given duopoly game is also studied.

1. Introduction

Technological innovation is the first driving force for the development of social progress and economy. Research and development (denoted as R&D for short) activities are the main driving force for enterprises, which are the microeconomic foundation to carry out technological innovation and have become an important way for enterprises to gain greater competitive advantage. Therefore, the research about R&D has attracted more and more attention of both theoretical and applied researchers.

There are many tools to analyze the R&D behavior of enterprises, among which the industrial organization theory mainly uses two or three stages of noncooperative game model to investigate R&D competition. The problems studied by industrial organization theory are more in line with the actual situation of enterprises, and the results obtained from the research of industrial organization theory also have stronger explanatory power for R&D problems.

Along this line, D'Aspremont and Jacquemin [1] first put forward a famous AJ model of two-stage duopoly game, which laid a foundation for later scholars to study R&D problems by using game theory. Since then, Kamien et al. [2] have extended the AJ model to many enterprises and analyzed four different R&D forms, which are R&D competition, R&D cartel, RJV competition, and RJV cartel. Amir et al. [3] analyzed the impact of endogenous spillovers on cooperative and noncooperative game and compared them. On the research of R&D competition among enterprises, using multistage game theory can be further referenced by Qiu [4]; Brod et al. [5]; Matsumura [6]; and so on.

However, the above literature usually assumes that every enterprise has complete information of profit function and complete rationality, so the established models are often static game models. However, in the real market economy, enterprises cannot grasp enough complete decision-making information. Considering that the decision-makers of enterprises are limited by objective conditions such as perception ability, the decision-making of enterprises cannot be completely rational, but they can be only boundedly rational. They often adopt a simpler dynamic adjustment process in the decision-making process. In the process of dynamic adjustment, the competition among enterprises will converge to Nash equilibrium or never converge to Nash equilibrium through repeated games, and even chaos will occur.

As one of the three main research topics of nonlinear science, chaos has become an important research object of the economic system since its inception. In recent years, more and more scholars began to apply chaos theory to the economic system so as to explore the law of development in economy and reveal the complex economic phenomena [7–9]. Oligopoly game, as a very important economic model, has also become a hot issue for scholars. Firstly, some scholars prove the existence of chaos in the oligopoly game model by mathematical methods. Li et al. [10] proved the Kato chaos in the duopoly game model. Pireddu [11] assumed that the three oligarchs in the same market are heterogeneous and the existence of chaos in the built game is proved by using a topological approach. In addition, some scholars have studied the stability of equilibrium in the competitions of multi-oligarchs. For example, Elsadany [12] considered the Nash equilibrium stability of the duopoly Cournot model with relative profit maximization, where he supposed the cost function has external effects. Tramontana et al. [13] discussed the effect of increasing numbers of competitors on the stability of Cournot–Nash equilibrium and found that the Nash equilibrium would become unstable when the number of competitors increased. Matsumoto et al. [14] constructed an oligopoly model with bounded rationality and discussed the existence of the unique equilibrium state of the model with simple price and cost functions. Based on isoelastic demand function, Snyder et al. [15] established a continuous Cournot model of oligopoly competition and discussed the stability of the given model. Askar [16] established a duopoly Cournot model and analyzed the stability of duopoly competition in the case of concave demand function and uncertain cost function. In addition, more scholars have focused on the complex dynamic behavior of multi-oligarch game according to the degree of product differentiation (see [17, 18]), the difference of dynamic adjustment strategy (see [19–21]), the existence of delayed decision-making (see [22, 23]), and so on. Finally, a model with time varying delays and a multiscale time approach is proposed by Cavalli and Naimzada [24] for a monopoly and then generalized to a Cournotian competition in Cavalli et al. [25].

In recent years, more and more scholars began to use the multistage dynamic game model to analyze the complexity and formation mechanism of R&D competition among enterprises in order to reveal the decision-making rules of R&D competition. Bischi and Lamantia [26] used a two-stage game model to simulate the complexity of the R&D network. Matsumura et al. [6] established a two-stage model and discussed the impact of cooperation degree between enterprises on rival profits. Shibata [27] extended Matsumura's model and analyzed the impact of R&D spillovers on the profits of enterprises. By assuming that firms cooperate in the production stage and compete in the R&D stage, Zhang et al. [28] built a duopoly game model with semi-collusion and discussed the complex dynamical behaviors in the built model. Zhou et al. [29] first established a two-stage R&D game model based on product differentiation. And then they discussed the intermittent chaos, bifurcation, and coexisting attractors using basin of attraction.

However, the complex dynamical behavior of the two-stage duopoly game considering R&D spillover, where the duopoly firms produce homogeneous products and compete in both stages, has not been studied yet. The main purpose of this research is to establish a two-stage duopoly Cournot model and investigate the effects of parameters on the dynamical behaviors of the built game. In this paper, we suppose that the boundedly rational duopoly firms produce homogeneous products in a market and conduct R&D activities to reduce the production cost. Therefore, the model we built here would be a two-stage game. At the first stage, the duopoly firms compete with R&D investments, and we also allow the existence of R&D spillovers in order to better simulate the real situation. While at the second stage, we presume that the firms choose the outputs as their decision variables.

The rest of this research is organized as follows: the two-stage duopoly model will be built in Section 2. In Section 3, the local stability of the equilibrium points and the stability region of Nash equilibrium will be discussed. While in Section 4, a series of numerical simulations will be conducted in order to disclose the complex dynamical behaviors of the built model. The effects of parameters on the social welfare will be analyzed in Section 5. At last, this research is summarized in the final section.

2. The Duopoly Model

In this section, we first introduce a Cournot duopoly model. We assume that there are two firms producing homogeneous products in an oligopolistic industry, and the firms are labeled by i, $(i = 1, 2)$ for convenience. Both firms conduct R&D to reduce their respective product costs and improve the quality of their products. Furthermore, the competition between these two firms can be simulated by a two-stage duopoly game. At the first stage, these two firms compete in R&D level in order to reduce the product cost and further maximize their respective profits. Since the limited access to market information, these two firms are considered as boundedly rational. While at the second stage, the two firms conduct quantity competition and will share their information so as to maximize their own profits after the selection of R&D investment in the first stage. Following D'Aspremont and Jacquemin [1], the market, in which the quantity-setting firms operate, can be characterized by a linear inverse demand function (the inverse demand function is the inverse function of the demand function), which can be given as

$$p(q_i, q_j) = a - b(q_i + q_j), \quad i = 1, 2,\ i \neq j, \tag{1}$$

where $q_i \geq 0$ is the production output of firm i $(i = 1, 2)$ and $a, b > 0$ are positive constants. Parameter a represents the reservation price of produced goods, i.e., the maximum possible price that consumers are willing to pay. The production cost of firm i can be given by

$$c_i(x_i, x_j)q_i = (c - x_i - \beta x_j)q_i, \quad i = 1, 2, i \neq j, \tag{2}$$

where $c \in (0, a)$ is some constant, which means the marginal costs of these two firms (it is supposed that firm 1 and firm 2 have the same marginal costs in this research). $x_i \geq 0$ is the R&D investment of firm i, and $\beta \in [0,1]$ measures the R&D spillovers between firm i and its rival. Here, $\beta = 0$ means that the protection of intellectual rights is perfect. That is, firm i's knowledge acquired through R&D can only affect its own product cost, whereas $\beta = 1$ means that the two firms share their R&D achievements completely. Or it can be understood as the R&D spillover is perfect. According to D'Aspremont and Jacquemin [1], the R&D cost of firm i can be represented as

$$g(x_i) = \frac{1}{2}\gamma {x_i}^2, \quad i = 1, 2, \tag{3}$$

where $\gamma > 0$ is a positive parameter, which can be used to measure the R&D efficiency of these two firms. In view of the built game is two-stage game, we know that the competitive strategies of these two firms should be composed of a level of R&D investment and a subsequent quantity competition strategies based on the R&D choice. We shall now analyze the duopoly game in which both firms do not cooperate in R&D level and output level. It is obvious that the firm i's profit can be given as

$$\pi_i = \left[a - b\left(q_i + q_j\right)\right]q_i - \left(c - x_i - \beta x_j\right)q_i - \frac{1}{2}\gamma x_i^2, \quad i = 1, 2, i \neq j. \tag{4}$$

It is clear that equation (4) can be regarded as the residue that subtracts the production cost and the R&D cost from sales volume. The marginal profit for firm i at any given point can be given by

$$\frac{\partial \pi_i}{\partial q_i} = a - 2bq_i - bq_j - c + x_i + \beta x_j, \quad i = 1, 2, i \neq j. \tag{5}$$

It is obvious that the maximum profit of firm i can be solved by setting the derivative of π_i with respected to q_i to zero. That is,

$$\begin{cases} \dfrac{\partial \pi_1}{\partial q_1} = a - 2bq_1 - bq_2 - c + x_1 + \beta x_2 = 0, \\ \\ \dfrac{\partial \pi_2}{\partial q_2} = a - 2bq_2 - bq_1 - c + x_2 + \beta x_1 = 0. \end{cases} \tag{6}$$

Equation (6) can be regarded as a linear system of equations about unknowns q_1 and q_2. Through solving the above two equations simultaneously, we can obtain the optimal output of firm i, which is given by

$$q_i = \frac{a - c + (2-\beta)x_i + (2\beta - 1)x_j}{3b}, \quad i = 1, 2, i \neq j. \tag{7}$$

Substituting equation (7) into equation (4), then the expected profit of firm i can be written as

$$\pi_i^{(ex)} = \frac{1}{9b}\left[(a-c) + (2-\beta)x_i + (2\beta - 1)x_j\right]^2 - \frac{1}{2}\gamma {x_i}^2, \quad i = 1, 2, i \neq j. \tag{8}$$

It is worth noting that equation (8) can be regarded as a function with variables x_i and x_j. All the firms will maximize their own profits by choosing the proper R&D investment x_i. Then, an optimization problem can be obtained. Differentiating the function $\pi_i^{(ex)}$ with respect to the variable x_i, then we can get

$$\frac{\partial \pi_i^{(ex)}}{\partial x_i} = \frac{2}{9b}(2-\beta)\left[(a-c) + (2-\beta)x_i + (2\beta - 1)x_j\right] - \gamma x_i, \quad i = 1, 2, i \neq j. \tag{9}$$

It is necessary to presume that the firms are boundedly rational owing to the limited market information. That is to say, all the firms can only make decisions on the basis of the market information they have. Furthermore, the process of decision-making is also dynamic for the boundedly rational firms. Namely, if $x_i(t)$ is used to represent the R&D investment decision of firm i at the period t, then the R&D investment of firm i at the period $t+1$ (i.e., $x_i(t+1)$) will depend on the marginal profit of firm i at period t. According to Bischi and Naimzada [30], the dynamical adjustment mechanism employed here is $x_i(t+1) = x_i(t) + \alpha_i x_i \Phi_i(x_i)$, $i = 1, 2$.

Where $\Phi_i(x_i) = (\partial \pi_i^{(ex)}/\partial x_i)$ is marginal relative profit of firm i, the specific form of it has been given in equation (9). And $\alpha_i (i = 1, 2)$ are the adjustment speeds (or speeds of adjustment by some researchers) of firm i's investment in R&D. This parameter reflects the response speed of firm i to its marginal profit signal. In period t, if the estimated marginal profit firm i $\Phi_i(x_i)$ is positive/negative, then firm i will increase/decrease its respective R&D investment at period $t+1$ with a rate of α_i. According the above analysis, the final dynamic game can be expressed as

$$\begin{cases} x_1(t+1) = x_1(t) + \alpha_1 x_1(t)\left\{\frac{2}{9b}(2-\beta)\left[(a-c)+(2-\beta)x_1+(2\beta-1)x_2\right]-\gamma x_1\right\}, \\ x_2(t+1) = x_2(t) + \alpha_2 x_2(t)\left\{\frac{2}{9b}(2-\beta)\left[(a-c)+(2-\beta)x_2+(2\beta-1)x_1\right]-\gamma x_2\right\}. \end{cases} \tag{10}$$

3. Stability Analysis for the Duopoly Model

Obviously, previous duopoly model (10) consists of two nonlinear difference equations. The dynamical behaviors of it can be very complex. If we want to study the complex dynamical behaviors of system (10), the equilibrium points (also called fixed points) should be solved in the first place. Therefore, if we set $x_i(t+1) = x_i(t)$ in equation (10), then a set of nonlinear algebraic equations can be obtained. Through solving the nonlinear algebraic equations, four equilibrium points can be found, which are $E_0 = (0,0)$, $E_1 = (((2(a-c)(2-\beta))/(9b\gamma - 2(2-\beta)^2)), 0)$, $E_2 = (0, ((2(a-c)(2-\beta))/(9b\gamma - 2(2-\beta)^2)))$, and $E^* = (x_1^*, x_2^*)$, where $x_1^* = x_2^* = x^* = ((2(a-c)(2-\beta))/(9b\gamma - 2(2-\beta)(1+\beta)))$.

It is clear that the equilibrium points E_0, E_1, and E_2 are on the coordinate axes of phase plane (x_1, x_2), so they are often called boundary equilibrium points. In addition, E^* is usually called internal equilibrium point as it is located in the interior of phase plane (x_1, x_2). We stress that it could be shown that E^* corresponds to the Nash equilibrium of the two-stage static game. The stability of all these equilibrium points and the complex dynamical behaviors of model (10) after these equilibrium points lose their stability are our major concern in the future discussion. Both the analytical method and numerical method would be employed in order to analyze the stability of all these equilibrium points and the complex dynamical behavior of system (10). However, the nonnegativity of all these equilibrium points should be ensured before the discussion of these issues, as negative equilibrium has no economic significance. According to economic meaning of the parameters, we know that a, b, c, γ, and β are all positive, so it can be inferred that the boundary equilibrium points E_1, E_2 and the unique Nash equilibrium point E^* are positive if and only if the inequalities given below hold:

$$\begin{cases} a > c, \\ 2 > \beta, \\ 9b\gamma > 2(2-\beta)^2, \\ 9b\gamma > 2(2-\beta)(1+\beta). \end{cases} \tag{11}$$

Otherwise, there will be at least one firm out of the game. In this case, the duopoly market will become a monopoly market. The following discussion will mainly focus on the local stability analysis of all the boundary equilibrium points. It is generally known that the Jacobian matrix is a primary tool to analyze the local stability of these boundary equilibrium points. For simplicity purposes, we use the symbol $J(x_1, x_2)$ to represent the Jacobian matrix of game (10) at any given point (x_1, x_2), which has a specific form as

$$J(x_1,x_2) = \begin{bmatrix} 1+\alpha_1\left\{\frac{2}{9b}(2-\beta)\left[a-c+2(2-\beta)x_1+(2\beta-1)x_2\right]-2\gamma x_1\right\}, & \frac{2}{9b}\alpha_1 x_1(2-\beta)(2\beta-1), \\ \frac{2}{9b}\alpha_2 x_2(2-\beta)(2\beta-1), & 1+\alpha_2\left\{\frac{2}{9b}(2-\beta)\left[a-c+2(2-\beta)x_2+(2\beta-1)x_1\right]-2\gamma x_2\right\}. \end{bmatrix} \tag{12}$$

The characteristic equation of $J(x_1, x_2)$ can be given as

$$P(\lambda) = \lambda^2 - \mathrm{Tr}\lambda + \mathrm{Det} = 0, \tag{13}$$

where Tr and Det are the trace and the determinant of $J(x_1, x_2)$, respectively.

According to the theory of nonlinear dynamics, we know that any fixed point $E(\overline{x}_1, \overline{x}_2)$ will be locally asymptotically stable if all the eigenvalues $\lambda_i (i = 1, 2, \ldots)$ of the Jacobian matrix evaluated at $E(\overline{x}_1, \overline{x}_2)$ are located inside the unit circle of the complex plane. That is, all the eigenvalues need to satisfy $|\lambda_i| < 1$ $(i = 1, 2, \ldots)$.

Proposition 1. *The trivial equilibrium point E_0 is a repelling node.*

Proof. Obviously, the Jacobian matrix evaluated at the trivial equilibrium point E_0 can be rewritten as

$$J(E_0) = \begin{bmatrix} 1+\alpha_1\frac{2}{9b}(2-\beta)(a-c), & 0, \\ 0, & 1+\alpha_2\frac{2}{9b}(2-\beta)(a-c). \end{bmatrix} \tag{14}$$

Quite evidently, the eigenvalues of $J(E_0)$ are $\lambda_1 = 1 + \alpha_1(2/9b)(2-\beta)(a-c)$ and $\lambda_2 = 1 + \alpha_2(2/9b)(2-\beta)(a-c)$. Since all the parameters are positive constants and the conditions $a > c$, $b > 0$, $\alpha_i > 0$ $(i = 1, 2)$, and $0 < \beta < 1$ always meet according to the economic meaning, then we have

$\lambda_1 > 1$ and $\lambda_2 > 1$. Therefore, we can easily draw a conclusion that E_0 is a repelling node. □

In the same way, the similar results about the boundary equilibrium points E_1 and E_2 can be obtained as follows.

Proposition 2. *The boundary equilibrium points E_1 and E_2 are saddle points or attracting nodes.*

Proof. The Jacobian matrix evaluated at the equilibrium point E_1 is

$$J(E_1) = \begin{bmatrix} 1 - \alpha_1 \frac{2}{9b}(2-\beta)(a-c), & \frac{4}{9b}\alpha_1 (a-c)(2-\beta)^2(2\beta-1), \\ 0, & 1 + \alpha_2 \frac{2}{9b}(2-\beta)(a-c)\frac{9b\gamma - 6(2-\beta)(1-\beta)}{9b\gamma - 2(2-\beta)^2}. \end{bmatrix} \tag{15}$$

It is clear that the Jacobian matrix $J(E_1)$ given above is an upper triangular matrix. The eigenvalues of this matrix can be easily gained, which are $\lambda_1 = 1 - \alpha_1 (2/9b)(2-\beta)(a-c)$ and $\lambda_2 = 1 + \alpha_2\ (2/9b)(2-\beta)(a-c)((9b\gamma - 6(2-\beta)(1-\beta))/\ (9b\gamma - 2(2-\beta)^2))$. According to inequalities (11) and the nonnegative conditions $\alpha_1 > 0$, $\alpha_2 > 0$, we know that $|\lambda_1| < 1$ and $|\lambda_2| > 1$ if and only if the inequalities $(1/2) \le \beta \le 1$ and $9b\gamma > 6(2-\beta)(1-\beta)$ meet. While if the condition $0 < \beta < (1/2)$ and $2(2-\beta)^2 < 9b\gamma < 6\ (2-\beta)(1-\beta)$ meet, then the modules of the eigenvalues will be less than one, i.e., $|\lambda_1| < 1$ and $|\lambda_2| < 1$. Therefore, the fixed point E_1 would be an attracting node in such a situation.

Similarly, we can also prove that the boundary equilibrium point E_2 is a saddle point or an attracting node. □

3.1. Local Stability Analysis of the Internal Equilibrium Point.

Another topic of this research is the local stability of the internal equilibrium point $E^* = (x_1^*, x_2^*)$, $(x_1^* = x_2^* = x^*)$. Actually, the local stability analysis of the internal equilibrium point is more complicated than that of the boundary equilibrium points. The Jacobian matrix at E^* is

$$J(E^*) = \begin{bmatrix} 1 + \alpha_1 \left\{ \frac{2}{9b}(2-\beta)\left[(a-c) + 3x^*\right] - 2\gamma x^* \right\}, & \frac{2}{9b}\alpha_1 x^*(2-\beta)(2\beta-1), \\ \frac{2}{9b}\alpha_2 x^*(2-\beta)(2\beta-1), & 1 + \alpha_2 \left\{ \frac{2}{9b}(2-\beta)\left[(a-c) + 3x^*\right] - 2\gamma x^* \right\}. \end{bmatrix} \tag{16}$$

The specific forms of trace and determinant of $J(E^*)$ are given as

$$\begin{aligned} \operatorname{Tr} J(E^*) &= 2 + (\alpha_1 + \alpha_2)\Delta_1, \\ \operatorname{Det} J(E^*) &= 1 + (\alpha_1 + \alpha_2)\Delta_1 + \alpha_1\alpha_2\left(\Delta_1^2 - \Delta_2^2\right), \end{aligned} \tag{17}$$

where $\Delta_1 = (2/9b)(2-\beta)[(a-c) + 3x^*] - 2\gamma x^*$ and $\Delta_2 = (2/9b)x^*(2-\beta)(2\beta-1)$.

According to the expression of Jury discriminant in stability analysis [31], we know that the internal equilibrium point is asymptotically stable if the following nonlinear inequalities hold. That is,

$$\begin{cases} P(1) = 1 - \operatorname{Tr} J(E^*) + \operatorname{Det} J(E^*) > 0, \\ P(-1) = 1 + \operatorname{Tr} J(E^*) + \operatorname{Det} J(E^*) > 0, \\ \left|\operatorname{Det} J(E^*)\right| < 1. \end{cases} \tag{18}$$

The dual inequalities of these three conditions (18) correspond to three different ways that one of the eigenvalues may cross the unit circle. If $P(1) < 0$, then one of the real eigenvalues of $J(E^*)$ is larger than 1. While if $P(-1) < 0$, then one of the real eigenvalues of$J(E^*)$ will cross the unit circle of complex plane from $(-1, 0)$. Finally, if $|\mathrm{Det}| > 1$, then $J(E^*)$ has a complex conjugate pair of eigenvalues lying outside the unit circle of complex plane. It can be obtained by calculation that the first condition of (18) is

$$1 - \operatorname{Tr} J(E^*) + \operatorname{Det} J(E^*) = \alpha_1 \alpha_2 \left[\frac{2(2-\beta)(a-c)}{9b} \right]^2 \left(\frac{9b\gamma - 6(2-\beta)(1-\beta)}{9b\gamma - 2(2-\beta)(1+\beta)} \right) > 0. \tag{19}$$

The equation (19) can be expressed equivalently as $b\gamma > (2/3)(2-\beta)(1-\beta)$. In addition, condition (19) would be always fulfilled according to the nonnegative conditions. It means that all the eigenvalues cannot cross the unit circle in the complex plane through the point $(1, 0)$. In other words, the pitchfork bifurcation will never happen. Nevertheless, the other two conditions of (18) are equivalent to

$$54b^2 + x^* \alpha_1 \alpha_2 (2-\beta)(a-c)[3b\gamma - 2(2-\beta)(1-\beta)] - 3bx^* (\alpha_1 + \alpha_2)\left[9br - 2(2-\beta)^2\right] > 0, \tag{20}$$

$$\frac{x^*}{27b^2} \left\{ 2\alpha_1 \alpha_2 (2-\beta)(a-c)[3b\gamma - 2(2-\beta)(1-\beta)] - 3b(\alpha_1 + \alpha_2)\left[9br - 2(2-\beta)^2\right] \right\} < 0. \tag{21}$$

The above two inequalities together constitute the stability region of system (10) in the parameter space. That is, the internal equilibrium point would be stable if the parameters meet these two conditions. However, we can draw a conclusion that the internal equilibrium point will lose its stability, when one (or both) of conditions (20) and (21) is violated. When one of the system parameters crosses this stability region, the system will undergo a flip bifurcation or a Neimark–Sacker bifurcation. As we will mainly discuss the influence of speed of adjustment α_i on the system's dynamical behavior in this research, the bifurcation curve of flip bifurcation is defined by

$$\alpha_1^f = \frac{3b\alpha_2\left[9br - 2(2-\beta)^2\right] - 27b^2[9b\gamma - 2(2-\beta)(1+\beta)]}{(2-\beta)(a-c)\left\{\alpha_2(2-\beta)(a-c)[3b\gamma - 2(2-\beta)(1-\beta)] - 3b\left[9br - 2(2-\beta)^2\right]\right\}}, \tag{22}$$

and the Neimark–Sacker bifurcation curve is defined by $\alpha_1 = \alpha_1^{ns}$, where α_1^{ns} is shown as

$$\alpha_1^{ns} = \frac{3b\alpha_2\left[9br - 2(2-\beta)^2\right]}{2\alpha_2(2-\beta)(a-c)[3b\gamma - 2(2-\beta)(1-\beta)] - 3b\left[9br - 2(2-\beta)^2\right]}, \tag{23}$$

where α_1^f and α_1^{ns} are defined by the system parameters except for α_1. They give the flip bifurcation curve and the Neimark–Sacker bifurcation curve, respectively. If the values of parameters cross the bifurcation curves, then a bifurcation will arise and the stable/unstable internal equilibrium point will become unstable/stable. Based on the above discussions, we can get the following proposition.

Proposition 3. *The internal equilibrium point E^* is a*

(i) sink if $\alpha_1^f < \alpha_1 < \alpha_1^{ns}$

(ii) source if $\alpha_1 > \alpha_1^f$ and $\alpha_1 > \alpha_1^{ns}$

(iii) saddle if $\alpha_1 > \alpha_1^f$ and $\alpha_1 > \alpha_1^{ns}$ or $\alpha_1 < \alpha_1^f$ and $\alpha_1 > \alpha_1^{ns}$

(iv) nonhyperbolic point if either $\alpha_1 = \alpha_1^f$ or $\alpha_1 = \alpha_1^{ns}$

The specific mathematical expressions of the stability region in the parameter space have been studied analytically in the above discussion. However, the stability region of the internal equilibrium point can also be analyzed numerically.

In the following discussion, we will analyze the influence of each parameter on the stability region of system (10). As an example, the numerical stability region of adjustment speeds (α_1, α_2) for the internal equilibrium point is shown in Figure 1(a), where the parameters are fixed as $a = 50$, $c = 42$, $r = 0.8$, $b = 1$, and $\beta = 0.7$, which are also the reference parameters set of Figure 1. From Figure 1(a), we can see that the stability region is formed by coordinate axes and a curve, and the stability region is symmetric about the diagonal of plane (α_1, α_2). It means that the position of parameters α_1 and α_2 is equivalent, which can also be discovered from system (10). Furthermore, we can also find that an increasing of α_1 and/or α_2 can bring the internal equilibrium point out of the stability region, and then a flip (or Neimark–Sacker) bifurcation may occur.

Moreover, the influence of other parameters on the stability region is also worth studying. For example, the value of the parameter b is positively related to the size of the stability region. If we choose the values of the parameters as

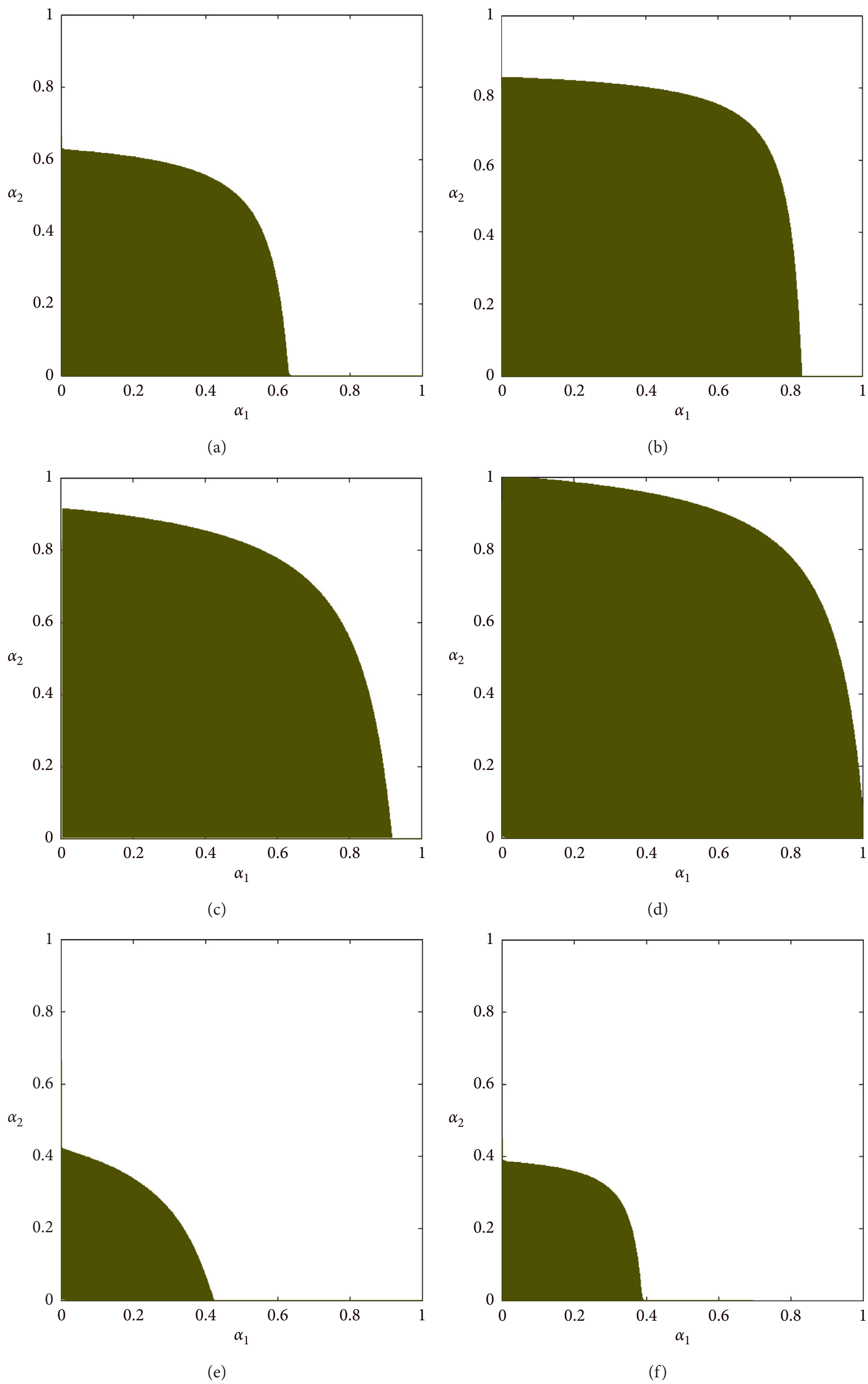

Figure 1: The stability region of system (10) in the (α_1, α_2) parameter space with different sets of parameters. (a) The parameter set is chosen as $a = 50$, $c = 42$, $r = 0.8$, $b = 1$, and $\beta = 0.7$. (b) The parameter set is chosen as $b = 1.2$, $a = 50$, $c = 42$, $\gamma = 0.8$, and $\beta = 0.7$. (c) The parameter set is chosen as $\beta = 0.4$, $a = 50$, $c = 42$, $b = 1$, and $\gamma = 0.8$. (d) The parameter set is chosen as $c = 45$, $a = 50$, $\gamma = 0.8$, $b = 1$, and $\beta = 0.7$. (e) The parameter set is chosen as $\gamma = 0.6$, $a = 50$, $c = 42$, $b = 1$, and $\beta = 0.7$. (f) The parameter set is chosen as $a = 55$, $c = 42$, $b = 1$, $\beta = 0.7$, and $\gamma = 0.8$.

$b = 1.2$, $a = 50$, $c = 42$, $\gamma = 0.8$, and $\beta = 0.7$, where only the parameter b is different compared with the reference parameters set, the stability region can be seen from Figure 1(b). Comparing with Figure 1(a), we can find that the size of stability region in Figure 1(b) has increased. Similar argument holds true if the value of the parameter c increases; when all the other parameters are fixed, the region of stability will become larger (see Figure 1(d)). In Figure 1(d), the parameters values are chosen as $c = 45$, $a = 50$, $\gamma = 0.8$, $b = 1$, and $\beta = 0.7$. However, the value of the parameter β is negatively correlated with the stability region. If the parameters set are taken as $\beta = 0.4$, $a = 50$, $c = 42$, $b = 1$, and $\gamma = 0.8$, we will find that the stability region will be become larger as the value of β decreases (see Figure 1(c)). While when the parameter γ decreases, the region of stability will become smaller than Figure 1(a), as shown in Figure 1(e), where the parameters set are fixed as $\gamma = 0.6$, $a = 50$, $c = 42$, $b = 1$, and $\beta = 0.7$. If we fix the values of α_1, α_2, b, c, γ, and β and increase the value of parameter a, we will find that the region of stability will become smaller than Figure 1(a) (see Figure 1(f)). The values of the parameters in Figure 1(f) are given as $a = 55$, $c = 42$, $b = 1$, $\beta = 0.7$, and $\gamma = 0.8$.

4. Numerical Illustrations of Dynamical Economy Model

It is well known that many complex dynamical behaviors in nonlinear dynamical systems can only be studied by numerical methods. Therefore, a numerical analysis is employed in this section to analyze the effects of varying parameters on the stability of the Nash equilibrium point of nonlinear system (10), as well as the irregular dynamical behaviors after the Nash equilibrium point loses its stability.

In the following discussion, a lot of numerical tools, such as 1-D bifurcation diagram, 2-D bifurcation diagram, phase portrait, and the largest Lyapunov exponent plot, are employed to reveal the complex dynamical behaviors of system (10). It is worth emphasizing that the 2-D bifurcation diagram is a more effective tool [32] (see Figure 2) in the numerical analysis of nonlinear dynamics. Hence, the 2-D bifurcation diagram is chosen as the principal tool in our analysis. In the next discussion, let us start with a set of parameters, which are chosen as $a = 50$, $c = 42$, $r = 0.8$, $b = 1$, and $\beta = 0.7$. In fact, this set of parameters is the same with that of Figure 1(a). Based on this set of parameters, the unique Nash equilibrium point is reached after some iterations, if the values of α_1 and α_2 are chosen in the green area of Figure 2(a). However, an increasement of α_1 and/or α_2 will bring the point (α_1, α_2) out the stability region and result in the instability of the Nash equilibrium point. As a consequence, a stable period-2 cycle arises. This phenomenon is mainly caused by the so-called flip bifurcation (see the boundary between the green area and the light blue area in Figure 2(a)). From Figure 2(a), we can also obtain the direct effect of parameter α_1 and $\alpha_2$on the local stability of the Nash equilibrium point. In particular, a further increasement of parameter $\alpha_i (i = 1, 2)$, with the other parameters are held fixed, may turn the period-2 points unstable through a flip bifurcation or a Neimark–Sacker bifurcation. This research result has very important economic significance and wide applications. This destabilizing effect owing to larger adjustment speed has attracted a lot of attention and has already been proved by Flam [33]. Figure 2(b) presents the 2-D bifurcation diagram in the parameter plane of (α_1, α_2), in which different colors represent different periods. The dark green indicates stable period-1 state, green for stable period-2 cycles, yellow for period-4, little green for period-8, and so on. However, the states of quasiperiodic, chaos, and divergent trajectories are all expressed in dark black, as the restriction of color numbers we can used here.

4.1. Global Dynamical Behavior Analysis. The local stability analysis given above mainly focuses on the dynamical behavior of system (10) near the equilibrium point. It means that the initial conditions should be chosen in the neighborhood of equilibrium point, if we want to analyze the local stability of an equilibrium point. However, the initial state of a real economic system often does not belong to the neighborhood of an equilibrium point, so the necessity of a global dynamical behavior analysis is highlighted. Moreover, the global dynamical analysis of a nonlinear system can also help us to know well the long run behavior of the system [18].

For the sake of better understanding of some global dynamic characteristics that may arise in the preset quantity-setting game, the 2-D bifurcation diagram is mainly employed. To clarify the problem more clearly, the parameters in Figure 3(a) are chosen as the same with that of in Figure 2(a). Firstly, we analyze the dynamical behavior around the line I_3, which is shown in Figure 2(a). In this region, the period-2 cycle will lose stability through a Neimark–Sacker bifurcation and the system will enter quasiperiodic state after this kind of bifurcation. However, if the parameter combination (α_1, α_2) passes through the line I_1 or I_2, the period-2 cycle will develop into a state of period-4 cycle, and the system will ultimately enter into chaotic state through a flip bifurcation. In Figure 3(a), we can find that different colors are associated to different periodic cycles and the detailed corresponding relationship between colors and period number can be found from the colorbar, which is given in the rightmost of Figure 3(a). Furthermore, we can also find a lot of areas of different color overlap; that is, some parts of light green area are overlapped by the pink area. This phenomenon is due to the coexistence of several attractors, which will be studied in the next section. It should be pointed out that the color of dark black may correspond to four different states, which may be chaotic state, quasiperiodic state, large periodic state, and unfeasible trajectories (or divergent trajectories by some researchers). To distinguish the states in dark black area of Figure 3(a), the 2-D largest Lyapunov exponent diagram is employed (see Figure 3(b)). The gradient colors are shown in Figure 3(b). We can obtain from Figure 3(b) that different colors represent different values of the largest Lyapunov exponent. The dark gray, which represents the relatively small values (negative), is for the stable state. As the color gradually fades, the value of the largest Lyapunov exponent also increases

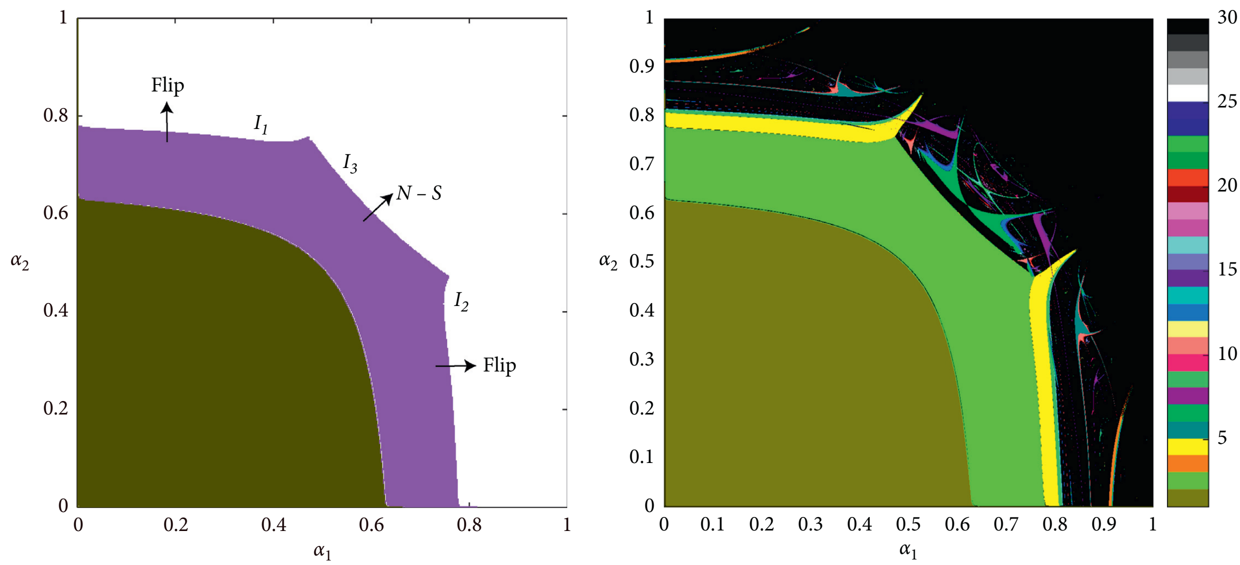

(a) (b)

Figure 2: (a) The stability region of the internal equilibrium point and the period-2 cycle with the parameters $a = 50, c = 42, r = 0.8, b = 1$, and $\beta = 0.7$. (b) The 2-D bifurcation diagram in the (α_1, α_2) plane with the same parameter selection in Figure 2(a).

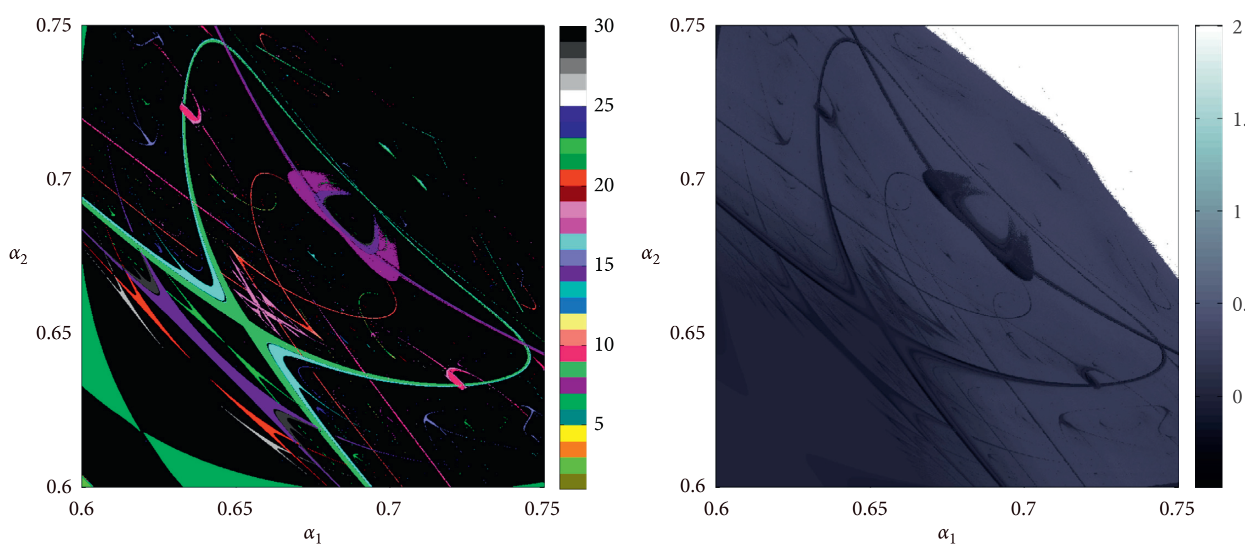

(a) (b)

Figure 3: (a) The 2-D bifurcation diagram in the (α_1, α_2) parameter space with parameters $a = 50, c = 42, r = 0.8, b = 1$, and $\beta = 0.7$. (b) The 2-D largest Lyapunov exponent diagram corresponding to Figure 3(a).

little by little. However, the maximum is set to 2 because of the limitation of the algorithm, and it corresponds to the white area in Figure 3(a). In addition, it is worth pointing out that the largest Lyapunov exponent is zero at the bifurcation point. By comparing the differences between these two figures, we can find the divergent trajectories very clearly, which is shown in the white region of Figure 3(b). Furthermore, we can find that Figures 3(a) and 3(b) have similar fractal structures.

Similarly, there is also a symmetric fractal structure in Figure 4(a). All the parameters of Figure 4(a) are the same with the parameters in Figure 3(a) except for β. In Figure 4(a), the value of β is set as 0.75, and it is little bigger than that of in Figure 3(a). Figure 4(b) gives the largest Lyapunov exponent diagram against the parameter (α_1, α_2), which corresponds to the 2-D bifurcation diagram of Figure 4(a). Comparing with Figure 3(b), we can find that in addition to the reduction of the stability region of E^*, the divergent area has also increased.

Through the above discussion, we can see that when other parameters are fixed, an increase of parameters $\alpha_i (i = 1, 2)$ will lead to the instability of Nash equilibrium

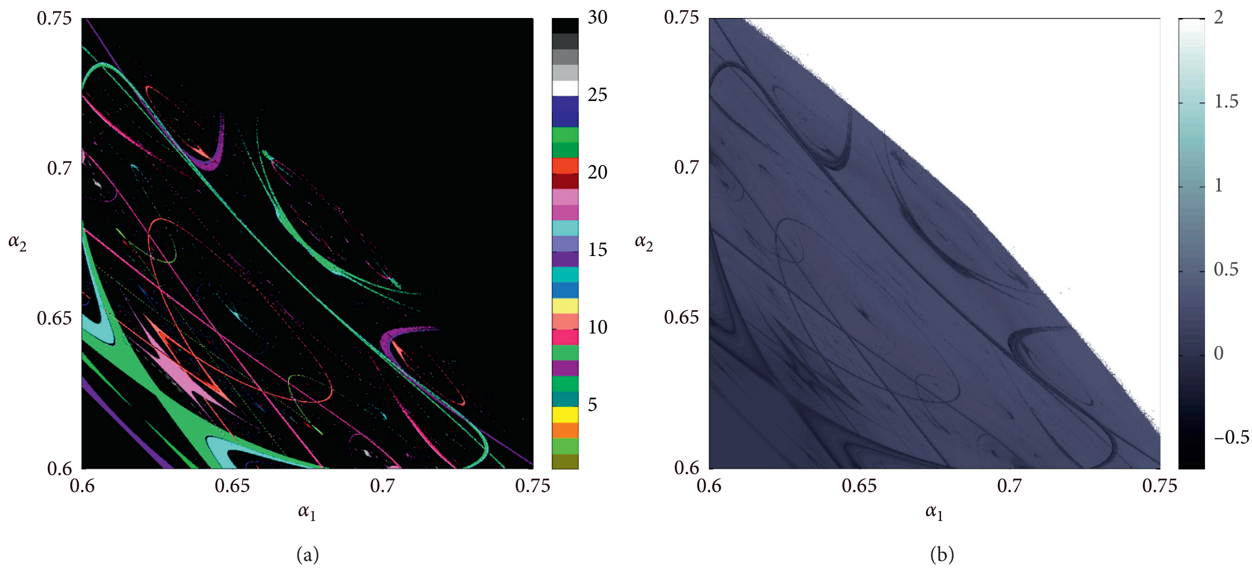

FIGURE 4: (a) The 2-D bifurcation diagram against parameters α_1 and α_2 with $a = 50$, $c = 42$, $r = 0.8$, $b = 1$, and $\beta = 0.75$. (b) The corresponding 2-D largest Lyapunov exponent diagram.

through a flip bifurcation or a Neimark–Sacker bifurcation (see Figure 2(b)). For example, if the parameter set is chosen as $a = 50$, $c = 42$, $r = 0.8$, $b = 1$, and $\beta = 0.75$ and the parameters α_1 and α_2 are chosen as the bifurcation parameter, we can find that the Nash equilibrium point is stable until a flip bifurcation occurs at which a set of stable period-2 points arise as the parameter α_1 grows. Then, with the speed of adjustment α_1 further increases, a series of period-doubling bifurcations occurs, and the cycles with higher periods and chaotic state will arise eventually. However, if the value of α_2 meets $0.476 < \alpha_2 < 0.800$, the period-2 cycle can also lose its stability through a Neimark–Sacker bifurcation as the value of α_1 increases.

Figure 5(a) gives a series of period-doubling bifurcations that cause instability, where the set of parameters are chosen as $\alpha_2 = 0.15$, $a = 50$, $c = 42$, $r = 0.8$, $b = 1$, and $\beta = 0.7$. We can notice that the Nash equilibrium point is stable for $0 \le \alpha_1 \le 0.6105$, and the Nash equilibrium point will lose stability through a flip bifurcation at $\alpha_1 \approx 0.6105$. Successively, a series of different state of period-2, period-4, period-8, etc., will appear constantly. At last, the system will enter into chaotic state when $\alpha_1 > 0.8012$.

Another useful tool to study the complex dynamical behaviors of nonlinear systems is the so-called Lyapunov exponent. The Lyapunov exponent describes the convergence or divergence of adjacent orbits in nonlinear dynamical systems, which is suitable for distinguishing the regular attractors and the strange attractors. If there is no positive Lyapunov exponent, we can make sure that the attractor is a regular attractor. If there is at least one positive Lyapunov exponent, then we can induce that a strange attractor (or chaotic attractor) exists. Zero Lyapunov exponent corresponds to bifurcation point or quasiperiodic orbit, while the especially large Lyapunov exponent always implies that there is an unfeasible trajectory that would evolve to infinity. Therefore, the largest Lyapunov exponent will be employed to distinguish the regular orbits, the quasiperiodic orbits, the chaotic orbit, and the unfeasible orbits (or divergent trajectories). The largest Lyapunov exponent with parameter α_1 is calculated and plotted in Figure 5(b), which also corresponds to Figure 5(a). It can be seen from Figure 5(b) that the largest Lyapunov exponent is negative when the bifurcation parameter is chosen as $\alpha_1 < 0.6105$. When $\alpha_1 \approx 0.6105$, the first period-doubling bifurcation takes place. As the value of parameter α_1 further increases, the occurrence of period-doubling bifurcation leads to chaos, eventually.

Similarly, the bifurcation diagram of system (10) with α_1 under the parameter set $\alpha_2 = 0.35$, $a = 50$, $c = 42$, $r = 0.8$, $b = 1$, and $\beta = 0.7$ is shown in Figure 5(c). The largest Lyapunov exponent associated with Figure 5(c) is disposed in Figure 5(d). The bifurcation diagram and the corresponding largest Lyapunov exponents of system (10) with the parameters set $\alpha_2 = 0.5$, $a = 50$, $c = 42$, $r = 0.8$, $b = 1$, and $\beta = 0.7$ are shown in Figures 5(e) and 5(f), respectively. From these two figures, we can see that the Nash equilibrium is locally stable when $\alpha_1 < 0.4851$. While if $\alpha_1 \approx 0.4581$, a period-doubling bifurcation occurs. Then, the period-2 cycle loses stability through a Neimark–Sacker bifurcation at $\alpha_1 = 0.715$. Subsequently, an attracting invariant circle appears when the parameter α_1 exceeds 0.715 and finally the chaotic attractor arises. The Neimark–Sacker bifurcation occurs when the modulus of a pair of complex eigenvalues crosses the unit circle. When a Neimark–Sacker bifurcation appears, the dynamics of market suddenly becomes quasiperiodic, and this is more difficult to deal with for a boundedly rational firm. The time series plot of a quasiperiodic trajectory is sometimes hardly distinguishable from a chaotic state or even a random state.

According to the previous method, more complex phenomena can also be revealed. If we chose the parameters as $\alpha_2 = 0.76$, $a = 50$, $c = 42$, $r = 0.8$, $b = 1$, and $\beta = 0.7$, the

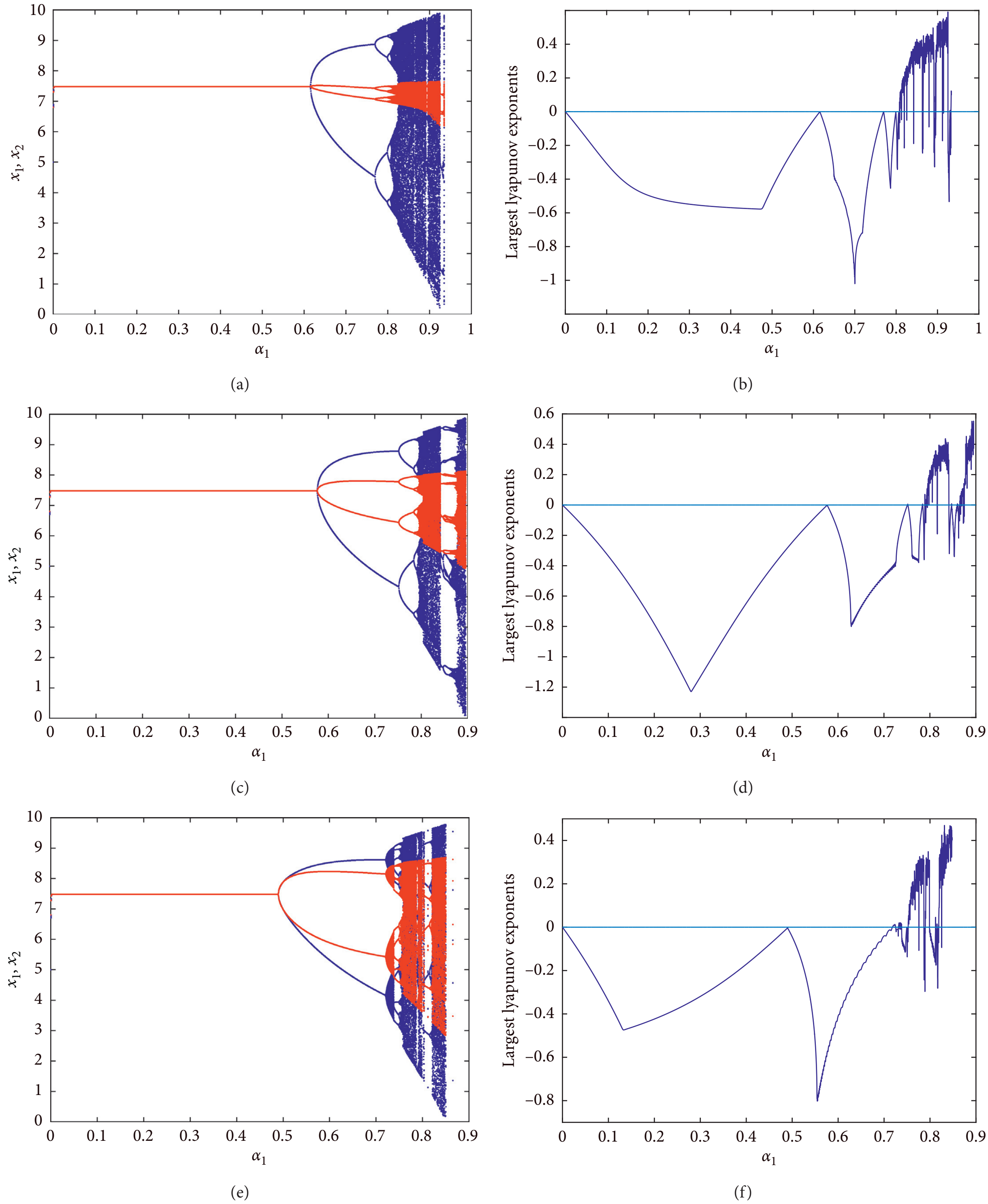

FIGURE 5: Continued.

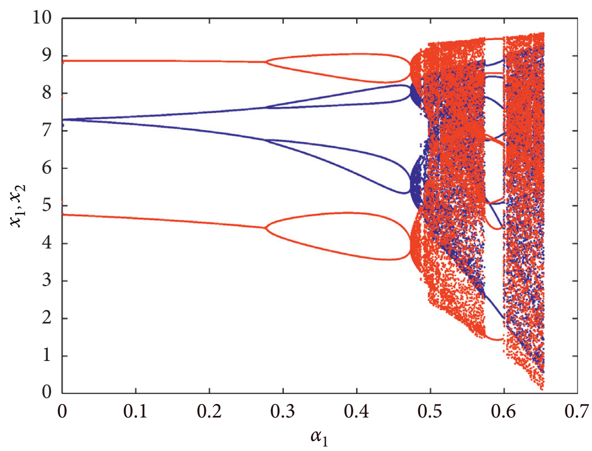

(g)

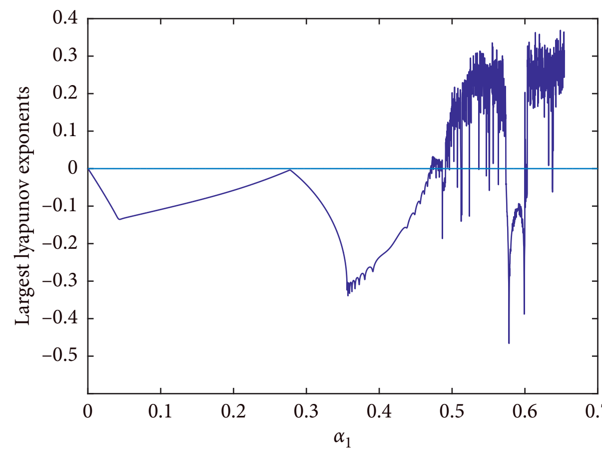

(h)

Figure 5: (a) The 1-D bifurcation diagram of α_1, where the reset of parameters is chosen as $\alpha_2 = 0.15$, $a = 50$, $c = 42$, $r = 0.8$, $b = 1$, and $\beta = 0.7$. (b) The largest Lyapunov exponent of $\alpha_1$corresponding to Figure 5(a). (c) The 1-D bifurcation diagram of α_1, where the reset of parameters is chosen as $\alpha_2 = 0.35$, $a = 50$, $c = 42$, $r = 0.8$, $b = 1$, and $\beta = 0.7$. (d) The largest Lyapunov exponent of $\alpha_1$corresponding to Figure 5(c). (e) The 1-D bifurcation diagram of α_1, where the reset of parameters is chosen as $\alpha_2 = 0.50$, $a = 50$, $c = 42$, $r = 0.8$, $b = 1$, and $\beta = 0.7$. (f) The largest Lyapunov exponent of α_1 corresponding to Figure 5(e). (g) The 1-D bifurcation diagram of α_1, where the reset of parameters is chosen as $\alpha_2 = 0.76$, $a = 50$, $c = 42$, $r = 0.8$, $b = 1$, and $\beta = 0.7$. (h) The largest Lyapunov exponent of α_1 corresponding to Figure 5(g).

bifurcation diagram of system (10) with respect to α_1 and the corresponding largest Lyapunov exponent can be plotted, which are shown in Figures 5(g) and 5(h), respectively. When $\alpha_1 = 0.2628$, a period-4 cycle appears and then it will lose stability through Neimark–Sacker bifurcation at $\alpha_1 = 0.4716$. In Figure 5(h), the positive largest Lyapunov exponent corresponds to chaotic state. This means that the dynamics of market becomes unstable and easily accesses to the chaotic state for large value of α_1.

In the following discussion, we will discuss the impact of other parameters on the complex dynamical behaviors of system (10). It can be seen from Figure 6(a) that the internal equilibrium point E^* is stable for small value of parameter a. However, as the value of parameter a increases, the internal equilibrium point becomes unstable, suddenly. Gradually, the irregular dynamical behaviors arise, including high-periodic cycles, chaotic states, and so on. In Figure 6(b), the bifurcation diagram about parameter b is plotted. We can see that there is a mixed bifurcation process with period-doubling bifurcation and inverse Neimark–Sacker bifurcation merged together. In this process of bifurcation, there is also a phenomenon called "chaotic bubbles." The "chaotic bubbles" begin in a multiperiodic state and end in a multiperiodic state, but there exists chaotic state between these two multiperiodic states. As the parameter value of b goes further, there exists a period-halving bifurcation. So, we can conclude that it is an effective way to make system (10) more stable by improving the product differentiation. Or we can say that the greater the degree of product differentiation, the more stable the market is.

Similarly, from Figures 6(c) and 6(d), we can see that the system is chaotic if the marginal cost c or the efficient measure of R&D investment cost γ is small enough. As c or γ increases, there exist mixed bifurcation processes, too. The bifurcation diagram of investment spillovers parameter β about the R&D investment is even more complicated (see Figure 6(e)). We can see from Figure 6(e) that the stable period-2 cycle loses its stability via a series of period-doubling bifurcations and Neimark–Sacker bifurcation, successively. Irregular states appear ultimately. Moreover, we can also observe "chaotic bubbles" in this bifurcation process. These numerical results fit very well with Proposition 3. The largest Lyapunov exponent plot corresponding to Figure 6(e) is displayed in Figure 6(f). In addition, a lot of irregular points can be found from Figure 6(e). These irregular points correspond to the coexistence of multiple attractors, which is the key issue of our research and will be discussed in the coming discussion.

4.2. Basins of Attraction and Multistability. A dramatic change in the long run dynamics occurs if we take different parameters and choose α_1 as the bifurcation parameter. By assuming $\alpha_2 = 0.76$, $a = 50$, $c = 42$, $r = 0.8$, $b = 1$, and $\beta = 0.7$, some interesting events take place when the bifurcation parameter α_1 belongs to the interval (0.2628, 0.6491) (see Figure 5(g)). We have shown in Figure 5(g) that a supercritical Neimark–Sacker bifurcation happens after the period-2 stable cycle loses its stability. Then, the annular attractor, which consists of two closed curves, arises in the phase space, as shown in Figure 7(a). If the parameter α_1 further increases, different phase-locking situations will take place and the periodic-7 cycle undergoes a period-doubling sequence that gives rise to a periodic-14 attractor as shown in Figure 7(b). Then, a homoclinic bifurcation of the two period-14 saddle cycle happens, and it leads to the

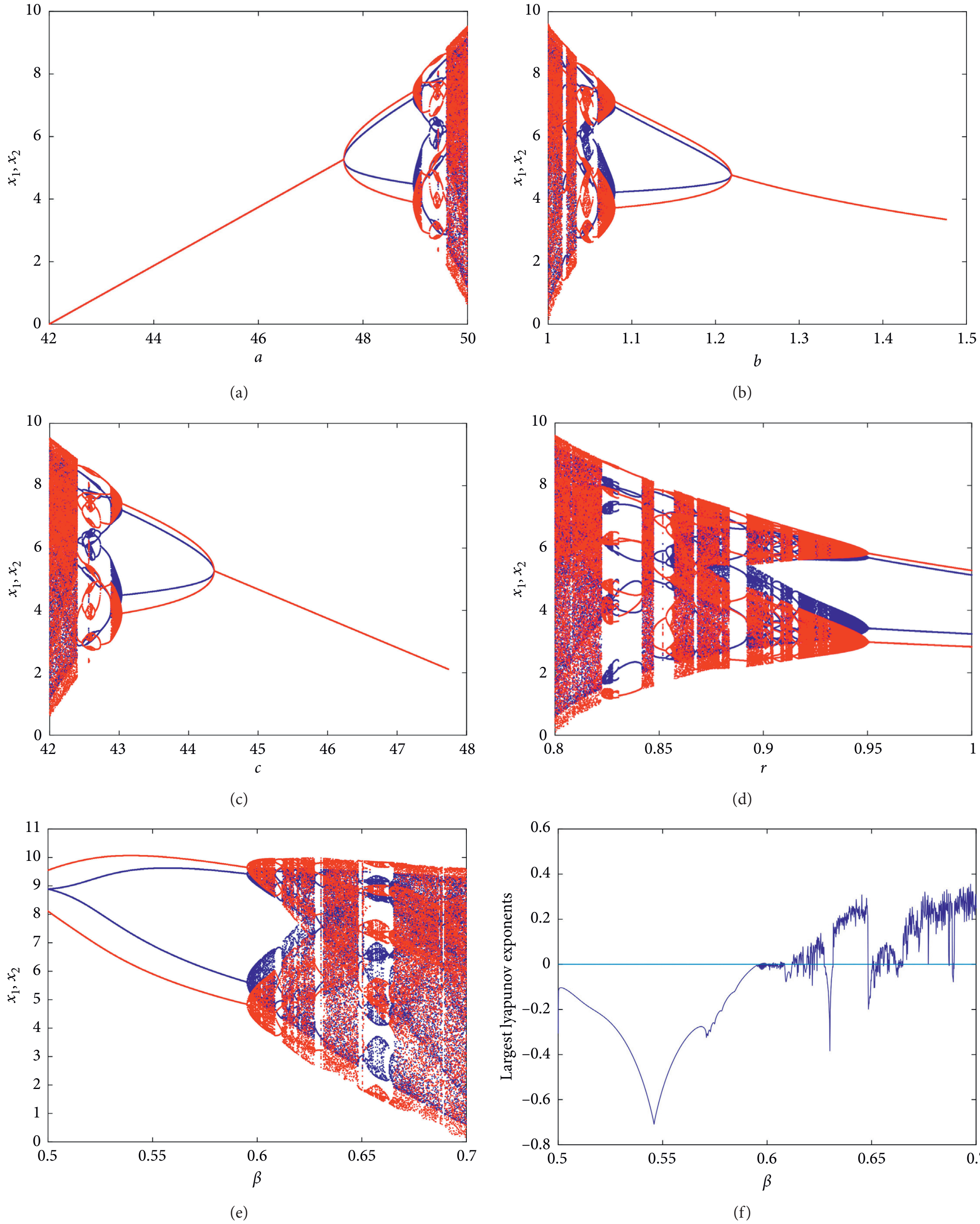

Figure 6: The bifurcation diagrams and the largest Lyapunov exponent diagram of system (10) with fixed values of α_1 and α_2, where $\alpha_1 = 0.63$ and $\alpha_2 = 0.76$. (a) The bifurcation diagram of parameter$a$, where the rest parameters are $b = 1$, $c = 42$, $\beta = 0.7$, and $\gamma = 0.8$. (b) The bifurcation diagram of parameter$b$, where the rest parameters are$a = 50$, $c = 42$, $\beta = 0.7$, and$\gamma = 0.8$. (c) The bifurcation diagram of parameter c, where the rest parameters are $a = 50$, $b = 1$, $\beta = 0.7$, and $\gamma = 0.8$. (d) The bifurcation diagram of parameter γ, and the rest parameters are$a = 50$, $b = 1$, $c = 42$, and $\beta = 0.7$. (e) The bifurcation diagram of parameter β, where the rest parameters are $a = 50$, $b = 1$, $c = 42$, and $\gamma = 0.8$. (f) The largest Lyapunov exponents of β corresponding to Figure 6(e).

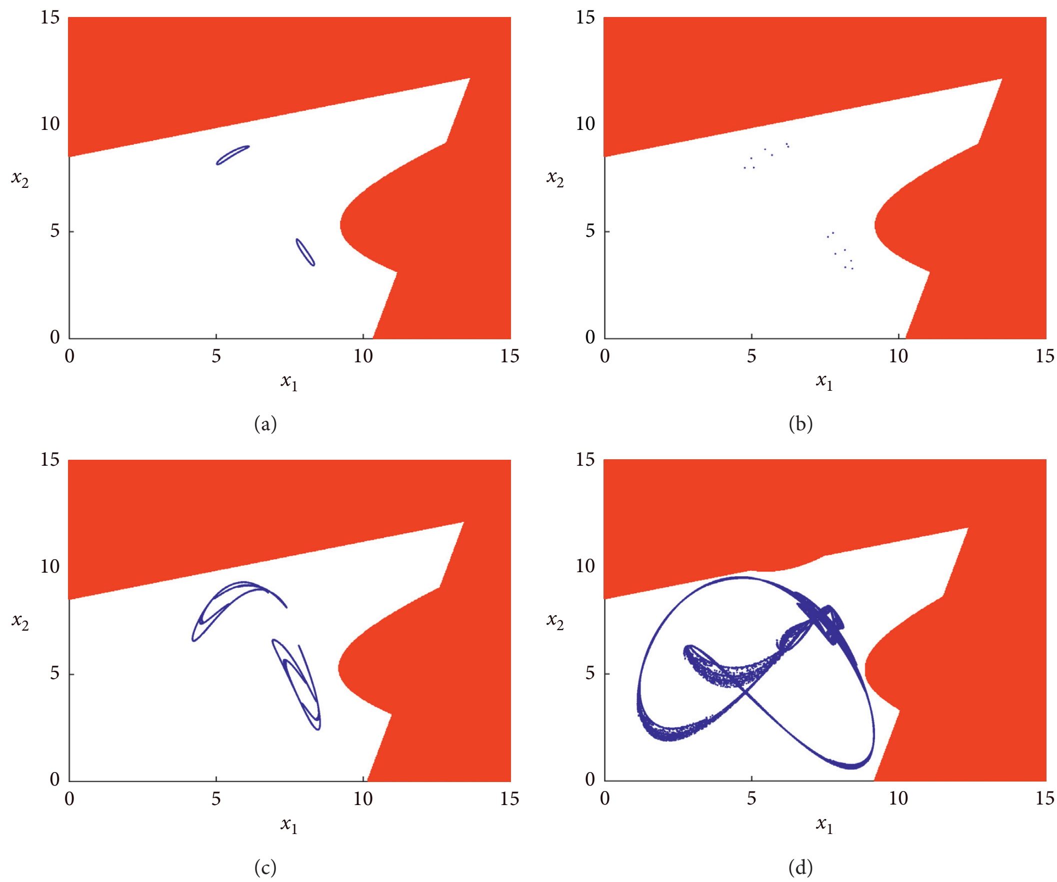

FIGURE 7: The basins of attraction and the attractors with varying α_1, where the rest parameters are chosen as $\alpha_2 = 0.76$, $a = 50$, $c = 42$, $r = 0.8$, $b = 1$, and $\beta = 0.7$. In these figures, the red region is the divergent area and the white region is the basin of attractors. (a) $\alpha_1 = 0.48$, the period-2 limit cycles (two attracting closed orbits) arise after the Neimark–Sacker bifurcation. (b) $\alpha_1 = 0.49$, the phenomenon of phase-locking appears, where we can find a period-14 cycle. (c) $\alpha_1 = 0.50$, an attractor made up by 2 weakly chaotic rings comes up. (d) A chaotic attractor and its basin of attraction when $\alpha_1 = 0.63$.

emergence of a "cyclical chaotic attractor," see Figure 7(c). The enlargement of one piece of the attractor allows us to appreciate that each of the closed curve exhibits loops and self-intersections. It means that the cyclical chaotic attractor is made up of two weakly chaotic rings, which merge into a unique annular chaotic attractor, when α_1 is further increased and the homoclinic bifurcation arises again, as shown in Figure 7(d). In addition, the basins of attraction of these attractors are also given in Figure 7. In Figure 7, the white region represents the attracting domain, while the red region indicates the divergent area. We can find that the shape of basin of attraction has scarcely changed in the process of variation of α_1. However, the attractors are getting bigger and bigger. In Figure 7(d), the attractor has almost connected with the boundary of the basin of attraction. Then, a global bifurcation called "contact bifurcation" will happen if the value of α_1 further increases. The chaotic attractor will be destroyed and the so-called "ghost" will occupy the entire basin of attraction after the "contact bifurcation" happens.

Another interesting phenomenon may arise in system (10) is the coexistence of multiple attractors. When the parameter α_1 is chosen as the bifurcation parameter, and the values of other parameters are fixed as $\alpha_2 = 0.8$, $a = 50$, $c = 42$, $r = 0.8$, $b = 1$, and $\beta = 0.7$, the basins of attraction at this circumstances can be plotted numerically, see Figure 8. In these two pictures, we can find the emergence of very complex basins of attraction with fractal boundaries. The value of parameter α_1 in Figure 8(a) is chosen as $\alpha_1 = 0.4952$. From Figure 8(a), we can see that there is a period-2 cycle coexisting with a chaotic attractor, where the purple region is the attracting area of the period-2, while the yellow region is the attracting area of the chaotic attractor, and the red region is the divergent area. However, the purple region and the yellow region are intertwined, and it is difficult to separate them. It means that the initial conditions have a great influence on the final state of system (10). This fact also tells us to be very cautious in choosing the initial state of the system. As the value of α_1 further increases to $\alpha_1 = 0.4996$, the yellow region is replaced by numerous yellow spots, and this is due to the contact between the chaotic attractor and the boundary of its basin of attraction. Hence, only the "ghost" of the chaotic attractor survives in the yellow region, see Figure 8(b). If the value of α_1 increases further, we will find that all the yellow spots will eventually

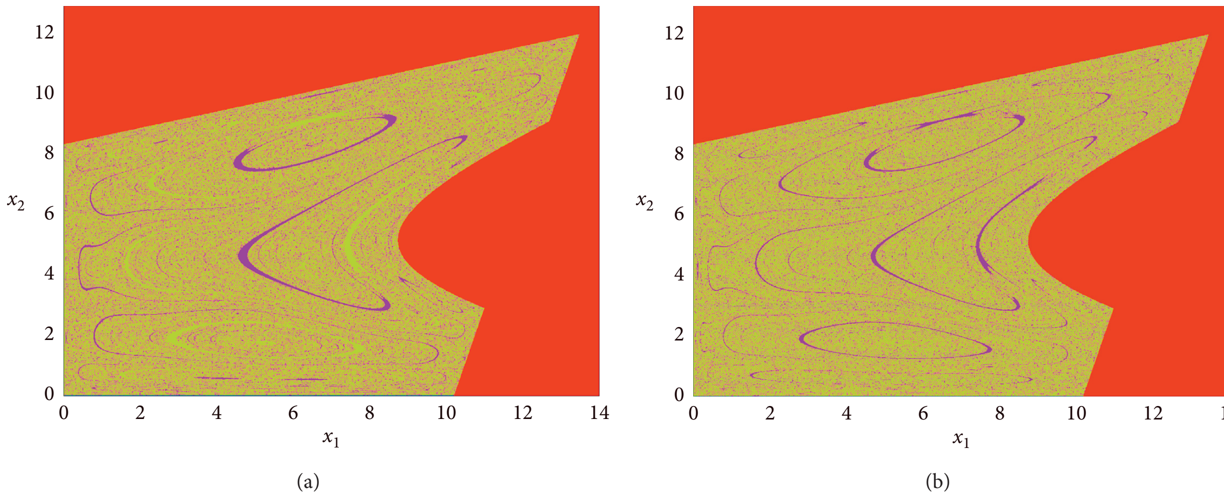

FIGURE 8: The basins of attraction with varying α_1 in the phase plane with the rest parameters are chosen as $\alpha_2 = 0.8$, $a = 50$, $c = 42$, $r = 0.8$, $b = 1$, and $\beta = 0.7$. (a) $\alpha_1 = 0.4952$, a period-2 cycles coexist with a chaotic attractors. (b)$\alpha_1 = 0.4996$, the basin becomes very complex after the disappearance of the chaotic attractor.

disappear, and these yellow spots will also be replaced by purple. This means that the coexistence of multiattractors has also disappeared.

5. Social Welfare

Based on the numerical simulations of R&D investment x_i given above, we can further analyze the dynamic evolution mechanism of the social welfare in built system (10). From equation (5), we can get that the maximum outputs of firm 1 and firm 2, which are given as

$$q_1 = \frac{a - c + (2-\beta)x_1 + (2\beta - 1)x_2}{3b},$$
$$q_2 = \frac{a - c + (2-\beta)x_2 + (2\beta - 1)x_1}{3b}. \tag{24}$$

From equation (6), we can get that the maximum profits of all the two firms, which are

$$\pi_1 = \frac{1}{9b}\left[(a-c) + (2-\beta)x_1 + (2\beta-1)x_2\right]^2 - \frac{1}{2}\gamma x_1^2,$$
$$\pi_2 = \frac{1}{9b}\left[(a-c) + (2-\beta)x_2 + (2\beta-1)x_1\right]^2 - \frac{1}{2}\gamma x_2^2. \tag{25}$$

The social welfare (denoted by SW) is the total surplus of the market, including the producer's surplus (for short PS) and the consumer's surplus (abbreviation: CS) [34]. That is,

$$\mathrm{SW} = \mathrm{PS} + \mathrm{CS}, \quad \text{with } \mathrm{PS} = \pi_1 + \pi_2, \mathrm{CS} = U(Q) - pQ. \tag{26}$$

According to Qiu [4], we know that the utility function of consumers can be represented as $U(Q) = aQ - (b/2)Q^2$, where $Q = q_1 + q_2$ is the total outputs of these two firms. By substituting this relation into (26), we can get the corresponding mathematic expression of the consumer's surplus, which is given as

$$CS = aQ - \frac{b}{2}Q^2 - (a - bQ)Q = \frac{b}{2}Q^2. \tag{27}$$

Correspondingly, the social welfare can be rewritten as

$$\mathrm{SW} = \pi_1 + \pi_2 + \frac{b}{2}Q^2, \tag{28}$$

where the forms of π_1 and π_2 can be founded in equation (8). On the basis of the above formulas, the final form of the social welfare can be represented as

$$\mathrm{SW} = \frac{1}{9b}\left[(a-c) + (2-\beta)x_1 + (2\beta-1)x_2\right]^2 + \frac{1}{9b}\left[(a-c) + (2-\beta)x_2 + (2\beta-1)x_1\right]^2 - \frac{1}{2}\gamma\left(x_1^2 + x_2^2\right) + \frac{\left[2(a-c) + (1+\beta)(x_1+x_2)\right]^2}{6b}. \tag{29}$$

According to system (10) and equation (29), we can obtain the bifurcation diagram of social welfare, numerically. In Figure 9, both the bifurcation diagram of social welfare and the bifurcation diagram of R&D investment are plotted under the parameter set $\alpha_2 = 0.35$, $a = 50$, $c = 42$, $r = 0.8$, $b = 1$, and $\beta = 0.7$, whereas the adjusting speed of firm 1 α_1 is chosen as the bifurcation parameter.

From Figure 9(a), we can see that the social welfare is stable when $0 \le \alpha_1 \le 0.5715$. And then the balanced social welfare loses its stability via a period-doubling bifurcation

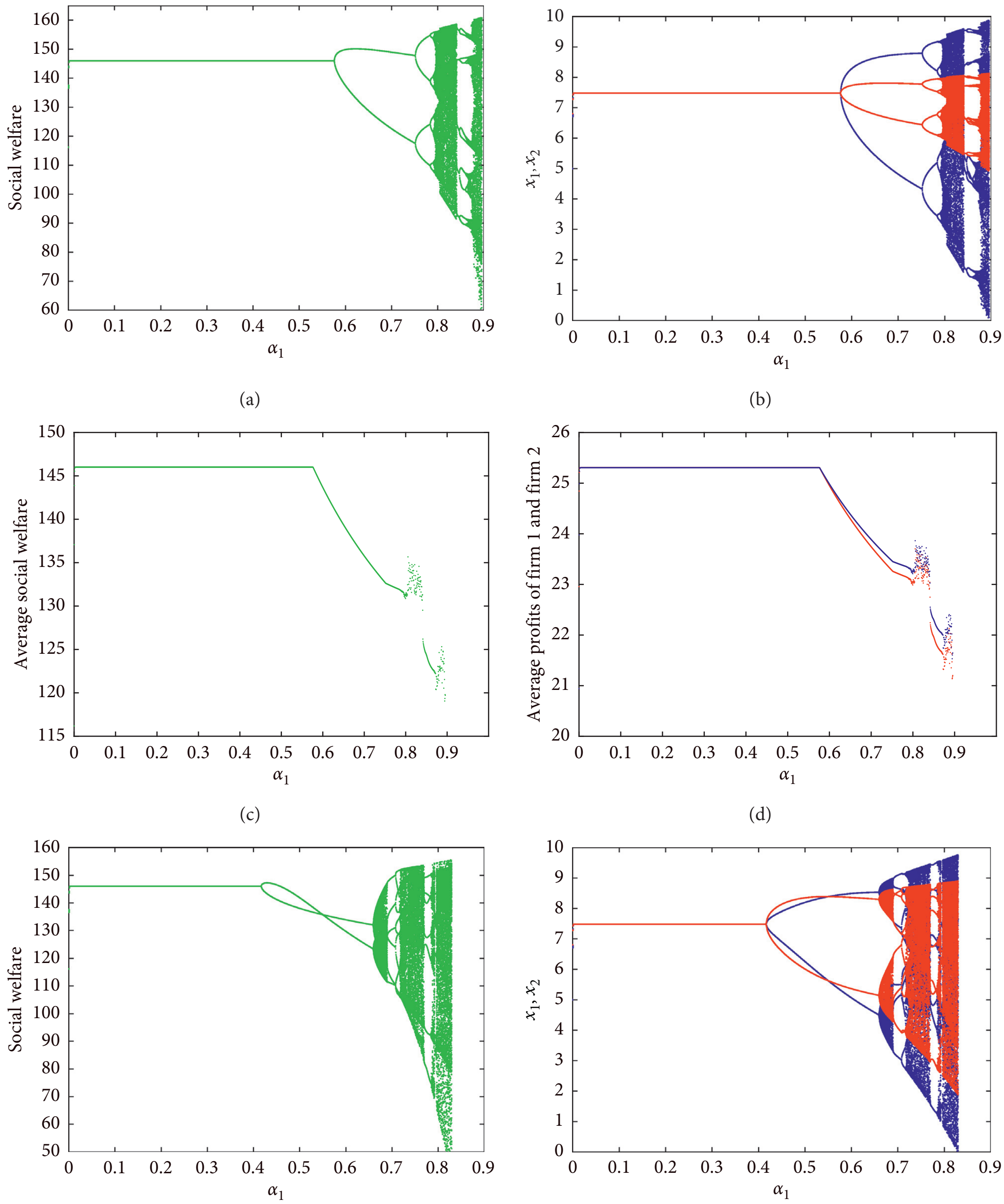

Figure 9: Continued.

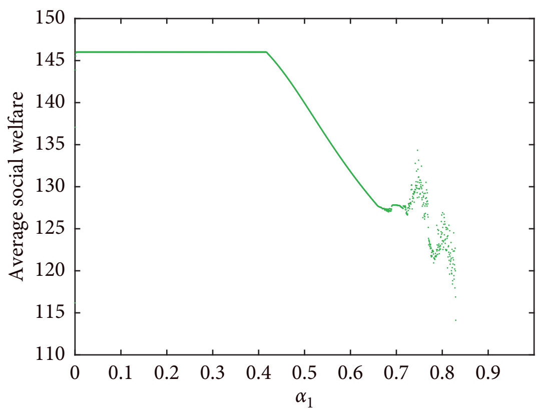

(g)

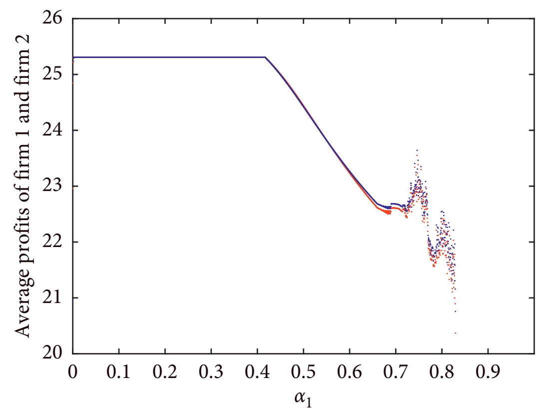

(h)

Figure 9: (a) The bifurcation diagrams of the social welfare with parameter α_1, where the parameters are chosen as $\alpha_2 = 0.35$, $a = 50$, $c = 42$, $r = 0.8$, $b = 1$, and $\beta = 0.7$. (b) The bifurcation diagram of R&D investments $x_i (i = 1, 2)$ corresponding to Figure 9(a). (c) The average social welfare with parameter α_1 and the rest parameters are the same with Figure 9(a). (d) The average profits of firm 1 and firm 2 with parameter α_1 and the rest parameters are the same with Figure 9(a). (e) The bifurcation diagrams of the social welfare with parameter α_1, where the parameters are chosen as $\alpha_2 = 0.55$, $a = 50$, $c = 42$, $r = 0.8$, $b = 1$, and $\beta = 0.7$. (f) The bifurcation diagram of R&D investments $x_i (i = 1, 2)$ corresponding to Figure 9(e). (g) The average social welfare with parameter α_1 and the rest parameters are the same with Figure 9(e). (h) The average profits of firm 1 and firm 2 with parameter α_1 and the rest parameters are the same with Figure 9(e).

when the parameter value meets $\alpha_1 \le 0.5715$. Then, a series of period-doubling bifurcations occur. The period-2 cycle, period-4 cycle, period-8 cycle, and the chaotic attractors appear successively. And then, another period-doubling bifurcation appears when $\alpha_1 > 0.8515$. As the value of α_1 increases further, the chaotic state occurs again. From the above analysis, we can see that both social welfare and R&D investment of these two firms will converge to an equilibrium, when the value of α_1 is small enough. By comparing Figures 9(a) and 9(b), we can find that these two figures have same bifurcation structure. Moreover, when the system is in chaotic state, the level of social welfare may be higher than that of periodic state in some certain time periods. However, it does not mean that chaos is conducive to improving the level of social welfare. If we calculate the average social welfare and the average profits (see Figures 9(c) and 9(d)), we will find that both the level of average social welfare and the level of average profit would be reduced, when the system is in a chaotic state.

Similarly, if we choose the parameter set $\alpha_2 = 0.55$, $a = 50$, $c = 42$, $r = 0.8$, $b = 1$, and $\beta = 0.7$, the bifurcation diagram of social welfare is shown in Figure 9(e). The corresponding bifurcation diagram of R&D investment is given in Figure 9(f). We can observe from these two figures that the equilibrium point will lose stability through flip bifurcation and Neimark–Sacker bifurcation successively, as the value of α_1 increases. The varying curves of average social welfare and average profit with parameter α_1 are also plotted in Figures 9(g) and 9(h), respectively. However, unlike Figures 9(c) and 9(d), the quasiperiodic state arises at this set of parameters. We can find both the average social welfare and the average profits have increased to a certain extent, when the system is in a quasiperiodic state.

6. Conclusion

In this research, a two-stage Cournot duopoly game, where the duopoly firms produce homogeneous goods and conduct R&D to reduce the production costs, is built. In the built model, we also allow the existence of R&D spillovers in order to better simulate the real situation. And then, the existence and the stability of the fixed points are discussed, and the effects of the system parameters on the size of stability region are discussed. We find that the adjusting speeds of the duopoly firms have a negative effect on the stability region. It means that the larger adjusting speed will lead the loss of stability of the Nash equilibrium point. We also find that the system will become more stable, if the R&D efficiency is improved. However, the higher degree of R&D spillover will make the system more unstable. It suggests that the firms should pay attention to the protection of intellectual property rights in the process of R&D.

In addition, the complex behaviors of the given model are also investigated numerically. The numerical tools, such as 2-D bifurcation diagram, 2-D largest Lyapunov exponent, and basins of attraction, are employed to study the complex dynamical behaviors. We find that the given system can present very complex dynamical behaviors. The equilibrium may lose stability through a Neimark–Sacker bifurcation or a flip bifurcation. Through analyzing the bifurcation diagram, the phenomenon of "chaotic bubble" is found in our research. The system will fall into a multiperiodic state, or a quasiperiodic state, or a chaotic state, or even divergent state eventually. The four different states can be distinguished using the 2-D bifurcation diagram combined with the 2-D largest Lyapunov exponent diagram. Moreover, the coexistence of multiattractors is also researched in this study using the so-called basin of attraction. We find the basins of the coexisting attractors can be very complex and present fractal structure. The effects of system parameters on the social welfare of the given system are discussed in the end of this paper. We find that chaos is harmful to the economic system, and it can lead to a decline in social welfare.

Data Availability

No data were used to support the study.

Conflicts of Interest

The authors declare that they have no conflicts of interest.

Acknowledgments

This research was supported by the National Natural Science Foundation of China (grant no. 61863022), the Young Scholars Science Foundation of Lanzhou Jiaotong University (grant no. 2015029), and the Foundation of Humanities and Social Sciences from the Ministry of Education of China (grant no. 15YJC820007).

References

[1] C. D'Aspremont and A. Jacquemin, "Cooperative and non-cooperative R&D in duopoly with spillovers," *American Economic Review*, vol. 78, no. 5, pp. 1133–1137, 1988.
[2] M. I. Kamien, E. Muller, and I. Zang, "Research joint ventures and R&D cartels," *American Economic Review*, vol. 82, no. 5, pp. 1293–1306, 1992.
[3] R. Amir, I. Evstigneev, and J. Wooders, "Noncooperative versus cooperative R&D with endogenous spillover rates," *Games and Economic Behavior*, vol. 42, no. 2, pp. 183–207, 2003.
[4] L. D. Qiu, "On the dynamic efficiency of bertrand and Cournot equilibria," *Journal of Economic Theory*, vol. 75, no. 1, pp. 213–229, 1997.
[5] A. Brod and R. Shivakumar, "Advantageous semi-collusion," *Journal of Industrial Economics*, vol. 47, no. 2, pp. 221–230, 1999.
[6] T. Matsumura, N. Matsushima, and S. Cato, "Competitiveness and R&D competition revisited," *Economic Modelling*, vol. 31, pp. 541–547, 2013.
[7] N. Schmitt, J. Tuinstra, and F. Westerhoff, "Side effects of nonlinear profit taxes in an evolutionary market entry model: abrupt changes, coexisting attractors and hysteresis problems," *Journal of Economic Behavior & Organization*, vol. 135, pp. 15–38, 2017.
[8] M. Akhmet, Z. Akhmetova, and M. O. Fen, "Chaos in economic models with exogenous shocks," *Journal of Economic Behavior & Organization*, vol. 106, pp. 95–108, 2014.
[9] L. Fanti, "The dynamics of a banking duopoly with capital regulations," *Economic Modelling*, vol. 37, pp. 340–349, 2014.
[10] R. Li, H. Wang, and Y. Zhao, "Kato's chaos in duopoly games," *Chaos, Solitons & Fractals*, vol. 84, pp. 69–72, 2016.
[11] M. Pireddu, "Chaotic dynamics in three dimensions: a topological proof for a triopoly game model," *Nonlinear Analysis: Real World Applications*, vol. 25, pp. 79–95, 2015.
[12] A. A. Elsadany, "Dynamics of a Cournot duopoly game with bounded rationality based on relative profit maximization," *Applied Mathematics and Computation*, vol. 294, pp. 253–263, 2017.
[13] F. Tramontana, A. A. Elsadany, B. Xin, and H. N. Agiza, "Local stability of the Cournot solution with increasing heterogeneous competitors," *Nonlinear Analysis: Real World Applications*, vol. 26, pp. 150–160, 2015.
[14] A. Matsumoto and F. Szidarovszky, "Complex dynamics of monopolies with gradient adjustment," *Economic Modelling*, vol. 42, pp. 220–229, 2014.
[15] B. C. Snyder, R. A. Van Gorder, and K. Vajravelu, "Continuous-time dynamic games for the Cournot adjustment process for competing oligopolists," *Applied Mathematics and Computation*, vol. 219, no. 12, pp. 6400–6409, 2013.
[16] S. S. Askar, "The impact of cost uncertainty on Cournot oligopoly game with concave demand function," *Applied Mathematics and Computation*, vol. 232, pp. 144–149, 2014.
[17] E. Ahmed, A. A. Elsadany, and T. Puu, "On Bertrand duopoly game with differentiated goods," *Applied Mathematics and Computation*, vol. 251, pp. 69–179, 2015.
[18] A. Agliari, A. K. Naimzada, and N. Pecora, "Nonlinear dynamics of a Cournot duopoly game with differentiated products," *Applied Mathematics and Computation*, vol. 281, pp. 1–15, 2016.
[19] F. Cavalli and A. Naimzada, "A multiscale time model with piecewise constant argument for a boundedly rational monopolist," *Journal of Difference Equations and Applications*, vol. 22, pp. 1–10, 2016.
[20] L. Baiardi, F. Lamantia, and D. Radi, "Evolutionary competition between boundedly rational behavioral rules in oligopoly games," *Chaos, Solitons & Fractals*, vol. 79, pp. 204–225, 2015.
[21] G. I. Bischi, F. Lamantia, and D. Radi, "An evolutionary Cournot model with limited market knowledge," *Journal of Economic Behavior & Organization*, vol. 116, pp. 219–238, 2015.
[22] A. A. Elsadany and A. M. Awad, "Dynamical analysis of a delayed monopoly game with a log-concave demand function," *Operations Research Letters*, vol. 44, no. 1, pp. 33–38, 2016.
[23] A. Matsumoto and F. Szidarovszky, "Nonlinear Cournot duopoly with implementation delays," *Chaos, Solitons & Fractals*, vol. 79, pp. 157–165, 2015.
[24] F. Cavalli and A. Naimzada, "Complex dynamics and multistability with increasing rationality in market games," *Chaos, Solitons & Fractals*, vol. 93, pp. 151–161, 2016.
[25] F. Cavalli, A. Naimzada, and M. Sodini, "Oligopoly models with different learning and production time scales," *Decisions in Economics and Finance*, vol. 41, no. 2, pp. 297–312, 2018.
[26] G. I. Bischi and F. Lamantia, "A dynamic model of oligopoly with R&D externalities along networks. Part II," *Mathematics and Computers in Simulation*, vol. 84, pp. 66–82, 2012.
[27] T. Shibata, "Market structure and R&D investment spillovers," *Economic Modelling*, vol. 43, pp. 321–329, 2014.
[28] Y.-h. Zhang, W. Zhou, T. Chu, Y.-d. Chu, and J.-n. Yu, "Complex dynamics analysis for a two-stage Cournot duopoly game of semi-collusion in production," *Nonlinear Dynamics*, vol. 91, no. 2, pp. 819–835, 2018.
[29] J. Zhou, W. Zhou, T. Chu, Y.-x. Chang, and M.-j. Huang, "Bifurcation, intermittent chaos and multi-stability in a two-stage Cournot game with R&D spillover and product differentiation," *Applied Mathematics and Computation*, vol. 341, pp. 358–378, 2019.
[30] G. I. Bischi and A. Naimzada, "Global analysis of a dynamic duopoly game with bounded rationality," *Advances in Dynamic Games and Applications*, vol. 5, pp. 361–385, 2000.
[31] H. N. Agiza and A. A. Elsadany, "Chaotic dynamics in nonlinear duopoly game with heterogeneous players," *Applied*

Mathematics and Computation, vol. 149, no. 3, pp. 843–860, 2004.

[32] C. Diks, C. Hommes, V. Panchenko, and W. R. van der, "E&F chaos: a user friendly software package for nonlinear economic dynamics," *Computational Economics*, vol. 32, no. 1-2, pp. 221–244, 2008.

[33] S. D. Flam, "Oligopolistic competition; from stability to chaos," *Lecture Notes in Economics and Mathematical Systems*, vol. 399, pp. 232–237, 1993.

[34] A. Agliari, P. Commendatore, I. Foroni, and I. Kubin, "Expectations and industry location: a discrete time dynamical analysis," *Decisions in Economics and Finance*, vol. 37, no. 1, pp. 3–26, 2014.

Hindawi
Mathematical Problems in Engineering
Volume 2021, Article ID 6661543, 9 pages
https://doi.org/10.1155/2021/6661543

Research Article

Robustness Analysis of a Type of Iterative Algorithm for R-L Fractional Nonlinear Control Systems in the Sense of L_p Norm

Yanfang Li, Xianghu Liu, and Guangjun Xu

Department of Mathematics, Zunyi Normal College, Zunyi 563006, Guizhou, China

Correspondence should be addressed to Xianghu Liu; liouxianghu04@126.com

Received 28 October 2020; Revised 4 December 2020; Accepted 31 December 2020; Published 16 January 2021

Academic Editor: Abdelalim Elsadany

The paper is concerned with the robustness analysis of a type of iterative algorithm for R-L fractional nonlinear control systems in the sense of L_p norm. Firstly, according to the Laplace transform and M-L function, the concept of mild solutions of the system is derived. Secondly, we give the sufficient conditions of robustness analysis of the PD^α-type ILC algorithm with uncertain disturbances and then study the robust analysis of the second-order PD^α-type ILC algorithm. At last, two fractional examples are given to demonstrate the results.

1. Introduction

The aim of the paper is to analyze the robustness of a type of iterative algorithm in the sense of L_p norm of the following R-L fractional system:

$$\left\{ {}^{\mathrm{RL}}D_t^\alpha z(t) = Az(t) + Bu(t), \quad t \in J = [0,b], \left(g_{1-\alpha} * z\right)(0) = z_0, y(t) = Cz(t) + Du(t), \right. \tag{1}$$

where ${}^{\mathrm{RL}}D_t^\alpha$ denotes the R-L derivative of order α, $0 < \alpha < 1$, $A,B,C \in R^{n\times n}$, $u(t)$ is a control vector, and $g_{1-\alpha} = (t^{1-\alpha}/\Gamma(1-\alpha))$.

Iterative learning control (ILC) was shown by Uchiyama in 1978 (in Japanese), and in recent years, more and more scholars have paid attention to the problems, among which are experts who study fractional calculus. The work of the fractional-order system in iterative learning control appeared in 2001. In the following decade, extensive attention has been paid to this field, great progress has been made [1–8], and many fractional nonlinear systems were investigated [9–17]. In recent years, the fractional ILC algorithm has played a great role in multiagent control information transmission, and for more information, one can see the references [13–16].

In Li et al.'s study [17], the authors discussed a P-type ILC scheme for a class of fractional-order nonlinear systems with delay by using the λ-norm and Gronwall inequality and obtained the sufficient condition for the robust convergence of the tracking errors.

In view of that the λ-norm often causes tracking errors that exceed the actual engineering range and cause inaccurate data, the authors Lan and Lin [18] used the L_p norm to discuss the convergence of iterative learning algorithms, and it objectively quantifies the essential characteristics of the tracking error and comprehensively reflects the behavior of the system. Zhang and Peng [19] used the generalized Young inequality of convolution and discussed the robustness of the PD-type fractional-order iteration and learning control algorithm in the sense of L_p norm, and the conditions of its robust convergence are obtained.

The above references have analyzed the robustness of the algorithm of the Caputo-type fractional system, and we find the Caputo fractional derivative is often used to solve general diffusion problems. The R-L type fractional derivative has a wider application in viscoelastic problems because it does not require the function to be differentiable at the origin. As far as we all know, analyzing robustness with interference of the R-L type fractional system is an extremely interesting and challenging work.

The rest of this paper is organized as follows. In Section 2, according to the Laplace transform and M-L function, the concept of mild solutions of the system is derived. In Section 3, we give the sufficient conditions of robustness analysis of the PD^{α}-type ILC algorithm with uncertain disturbances and then study the robust analysis of the second-order PD^{α}-type ILC algorithm. In Section 4, two fractional examples are given to demonstrate the results.

2. Some Preliminaries for Fractional Systems

In this section, we show some definitions and preliminaries of the L_p norm and Mittag–Leffler function. From [20–23], one can see the definitions of the R-L fractional integral and derivative.

Definition 1. The norm for the n-dimensional vector $Z = (z_1, z_2, \ldots, z_n)$ is defined as $\|Z\| = \max_{1\le i\le n}|z_i|$, and the L_p norm is defined as $|Z|_p = [\int_0^T (\max|z_i|)^p \mathrm{d}t]^{(1/p)}$, where $t \in [0, T]$.

Definition 2. The definition of the two-parameter function of the Mittag–Leffler type is described by

$$E_{\alpha,\beta}(z) = \sum_{k=0}^{\infty} \frac{z^k}{\Gamma(\alpha k + \beta)}, \quad \alpha > 0, \beta > 0, z \in C. \tag{2}$$

If $\beta = 1$, one has the Mittag–Leffler function of one parameter as follows:

$$E_{\alpha}(z) = \sum_{k=0}^{\infty} \frac{z^k}{\Gamma(\alpha k + 1)}. \tag{3}$$

Now, according to the results of the papers [17, 24–27], we will give the following lemma.

Lemma 1 (Lemma 3, see [25]). The general solution of equation (1) is given by

$$z(t) = t^{\alpha-1}E_{\alpha,\alpha}(A,t)z_0 + \int_0^t (t-s)^{\alpha-1}E\left(A(t-s)^{\alpha}\right)Bu(s)\mathrm{d}s, \tag{4}$$

where

$$E_{\alpha,\beta}(A,t) = \sum_{k=0}^{\infty} \frac{A^k t^{\alpha k+\beta-1}}{\Gamma(\alpha k + \beta)}. \tag{5}$$

Lemma 2 (Definition 2.4, see [27]). The operators $E_{\alpha,\alpha}(t)$ are exponentially bounded, and there is a constant $C_0 = (1/\alpha)\|A\|^{((1-\alpha)/\alpha)}$, $e_{\alpha}(t) = e^{\|A\|^{(1/\alpha)}t}$, $M = e_{\alpha}(b)$, and $\|E_{\alpha,\alpha}(A,t)\| \le C_0 e_{\alpha}(t) \le C_0 M$.

Lemma 3 (Hölder inequality). Set $p > 0, q > 0$, and $(1/p) + (1/q) = 1$; if $f \in L^p(\Omega)$, $g \in L^q(\Omega)$, and $f \cdot g \in L^1(\Omega)$, then $\|f\cdot g\|_{L^1} \le \|f\|_{L^p}\|g\|_{L^q}$.

3. Robustness Analysis of the PD^{α}-Type ILC Algorithm with Uncertain Disturbances

In this section, we consider the following fractional equation:

$$\left\{ {}^{\mathrm{RL}}D_t^{\alpha} z_k(t) = Az_k(t) + Bu_k(t) + \omega(t), \quad t \in J = [0,b], y_k(t) = Cz_k(t) + Du_k(t) + \nu(t), \right. \tag{6}$$

where $k = 0, 1, 2, 3, \ldots$, and $\omega(t)$ and $\nu(t)$ are uncertain disturbances.

For system (6), we apply the following open- and closed-loop PD^{α}-type ILC algorithm:

$$u_{k+1}(t) = u_k(t) + \gamma_1 e_k(t) + \gamma_2 e_{k+1}^{(\alpha)}(t), \tag{7}$$

where $t \in [0, b]$, γ_1 and γ_2 are the parameters which will be determined, $y_d(t)$ is the given function, $e_k = y_d(t) - y_k(t)$, and $e_k^{(\alpha)}(t) = {}^{\mathrm{RL}}D_t^{\alpha} e_k$. For convenience, one can see Figure 1. The initial state of each iterative learning is as follows:

$$z_{k+1}(0) = z_k(0) + B\gamma_1 e_k(t). \tag{8}$$

We denote that

$$\begin{aligned}
\kappa_1 &= \left\|I + \gamma_2 D\right\| - \frac{b^{\alpha-(1/p)}\left\|\gamma_2 C\right\| C_0 M\|B\|}{\sqrt[q]{q(\alpha-1)+1}}, \\
\kappa_2 &= \left\|I - \gamma_1 D\right\| - \frac{b^{\alpha-(1/p)}\left\|\gamma_1 C\right\| C_0 M\|B\|}{\sqrt[q]{q(\alpha-1)+1}}, \\
\kappa_3 &= \frac{b^{\alpha-(1/p)}\left(\left\|\gamma_1 C\right\| + \left\|\gamma_2 C\right\|\right)C_0 M\|B\|\|\omega\|_{L_p}}{\sqrt[q]{q(\alpha-1)+1}} \\
&\quad + \left(\left\|\gamma_1\right\| + \left\|\gamma_2\right\|\right)\|\nu\|_{L_p}.
\end{aligned} \tag{9}$$

Theorem 1. *Assume that each iteration state meets algorithm (7) and the initial state is $z_k(0) = z_d(0)$; then, there exists $m > 0$ such that $\kappa_1 > 0, \kappa_2 > 0, \kappa_3 < m$, and $\kappa_1 > \kappa_2$, and then, the sufficient condition for being uniformly bounded on J is $\lim_{k\longrightarrow\infty}\|u_k\|_{L_p} \le (\kappa_3/(\kappa_1 - \kappa_2))$.*

Proof. Define

$$\begin{cases} \Delta z_k(t) = z_d(t) - z_k(t), \\ \Delta u_k(t) = u_d(t) - u_k(t). \end{cases} \tag{10}$$

For $t \in J$, one has $\Delta z_k^{(\alpha)}(t) = {}^{\mathrm{RL}}D_t^{\alpha}\Delta z_k(t) = A\Delta z_k(t) + B\Delta u_k(t)$ and $e_{k+1}^{(\alpha)}(t) = C(A\Delta z_{k+1}(t) + B\Delta u_{k+1}(t))$.

According to system (6), we have

$$\begin{aligned} z_{k+1}(t) &= t^{\alpha-1}E_{\alpha,\alpha}(A,t)z_0 + \\ &\cdot \int_0^t (t-s)^{\alpha-1}E_{\alpha,\alpha}(A(t-s)^{\alpha})(Bu_{k+1}(s) + \omega(t))\mathrm{d}s, \\ z_d(t) &= t^{\alpha-1}E_{\alpha,\alpha}(A,t)z_0 + \\ &\cdot \int_0^t (t-s)^{\alpha-1}E_{\alpha,\alpha}(A(t-s)^{\alpha})Bu_d(s)\mathrm{d}s, \end{aligned} \tag{11}$$

and thus, using the ILC algorithms (7) and (8), we derive

$$\begin{aligned} \Delta z_{k+1}(t) &= \int_0^t (t-s)^{\alpha-1}E_{\alpha,\alpha}(A(t-s)^{\alpha})B \\ &\cdot (\Delta u_{k+1}(s) + \omega(t))\mathrm{d}s, \\ \Delta z_k(t) &= \int_0^t (t-s)^{\alpha-1}E_{\alpha,\alpha}(A(t-s)^{\alpha})B \\ &\cdot (\Delta u_k(s) + \omega(t))\mathrm{d}s, \end{aligned} \tag{12}$$

so

$$\begin{aligned} \Delta u_{k+1}(t) &= \Delta u_k(t) - \gamma_1(y_d(t) - y_k(t)) - \gamma_2(y_d(t) - y_{k+1}(t)), \\ &= \Delta u_k(t) - \gamma_1(C\Delta z_k(t) + D\Delta u_k(t) - \nu(t)) - \gamma_2(C\Delta z_{k+1}(t) + D\Delta u_{k+1}(t) - \nu(t)), \\ &= \Delta u_k(t) - \left(\gamma_1 C\int_0^t (t-s)^{\alpha-1}E_{\alpha,\alpha}(A(t-s)^{\alpha})B(\Delta u_k(s) + \omega(t))\mathrm{d}s + \gamma_1 D\Delta u_k(t) - \gamma_1\nu(t)\right), \\ &\quad -\left(\gamma_2 C\int_0^t (t-s)^{\alpha-1}E_{\alpha,\alpha}(A(t-s)^{\alpha})B(\Delta u_{k+1}(s) + \omega(t))\mathrm{d}s + \gamma_2 D\Delta u_{k+1}(t) - \gamma_2\nu(t)\right). \end{aligned} \tag{13}$$

Hence,

$$\begin{aligned} \Delta u_{k+1}(t)(I + \gamma_2 D) &= \Delta u_k(t)(I - \gamma_1 D) \\ &-\left(\gamma_1 C\int_0^t (t-s)^{\alpha-1}E_{\alpha,\alpha}(A(t-s)^{\alpha})B(\Delta u_k(s)\right. \\ &\left. + \omega(t))\mathrm{d}s - \gamma_1\nu(t)\right) \\ &-\left(\gamma_2 C\int_0^t (t-s)^{\alpha-1}E_{\alpha,\alpha}(A(t-s)^{\alpha})B(\Delta u_{k+1}(s)\right. \\ &\left. + \omega(t))\mathrm{d}s - \gamma_2\nu(t)\right). \end{aligned} \tag{14}$$

By taking the L_p norm, we obtain

$$\begin{aligned} \|\Delta u_{k+1}\|_{L^p}\|(I + \gamma_2 D)\| &\le \|\Delta u_k\|_{L^p}\|(I + \gamma_2 D)\| \\ &+ \frac{b^{\alpha-(1/p)}\|\gamma_1 C\|C_0 M\left(\|B\|\|\Delta u_k\|_{L^p} + \|\Delta\omega\|_{L^p}\right)}{\sqrt[q]{q(\alpha-1)+1}} + \|\gamma_1\|\|\nu\|_{L^p} \\ &+ \frac{b^{\alpha-(1/p)}\|\gamma_2 C\|C_0 M\left(\|B\|\|\Delta u_{k+1}\|_{L^p} + \|\Delta\omega\|_{L^p}\right)}{\sqrt[q]{q(\alpha-1)+1}} + \|\gamma_2\|\|\nu\|_{L^p}, \end{aligned} \tag{15}$$

denoting

$$\begin{aligned} \kappa_1 &= \|I + \gamma_2 D\| - \frac{b^{\alpha-(1/p)}\|\gamma_2 C\|C_0 M\|B\|}{\sqrt[q]{q(\alpha-1)+1}}, \\ \kappa_2 &= \|I - \gamma_1 D\| - \frac{b^{\alpha-(1/p)}\|\gamma_1 C\|C_0 M\|B\|}{\sqrt[q]{q(\alpha-1)+1}}, \\ \kappa_3 &= \frac{b^{\alpha-(1/p)}\left(\|\gamma_1 C\| + \|\gamma_2 C\|\right)C_0 M\|B\|\|\omega\|_{L_p}}{\sqrt[q]{q(\alpha-1)+1}} \\ &\quad + \left(\|\gamma_1\| + \|\gamma_2\|\right)\|\nu\|_{L_p}. \end{aligned} \tag{16}$$

Consequently, $\kappa_1\|\Delta u_{k+1}\|_{L^p} \le \kappa_2\|\Delta u_k\|_{L^p} + \kappa_3$. So, there exists a positive m, such that $\kappa_3 < m$ and $\kappa_1 > 0, \kappa_2 > 0$, and $\kappa_1 > \kappa_2$, and then $\lim_{k\longrightarrow\infty}\|u_k\|_{L_p} \le (\kappa_3/(\kappa_1 - \kappa_2))$, which implies $e_k(t)$ is uniformly bounded on J. □

4. Robust Analysis of the Second-Order PD^{α}-Type ILC Algorithm

In this section, we consider the following second-order PD^{α}-type ILC algorithm:

$$\begin{aligned} u_2(t) &= u_1(t) + \gamma_1 e_1(t) + \gamma_2 e_1^{(\alpha)}(t), \\ u_{k+1}(t) &= r_1\left[u_k(t) + \gamma_1 e_k(t) + \gamma_2 e_k^{(\alpha)}(t)\right] \\ &\quad + r_2\left[u_{k-1}(t) + \gamma_3 e_{k-1}(t) + \gamma_4 e_{k-1}^{(\alpha)}(t)\right], \quad k = 2, 3, \ldots, \end{aligned} \tag{17}$$

where $r_1 + r_2 = 1$.

The initial state of the system is as follows:

$$z_{k+1}(0) = z_k(0) + BL_1 e_k(t) + BL_2 e_k^{(\alpha)}(t). \tag{18}$$

For convenience, one can see Figure 2.

Assume that the initial state of each iterative learning meets (18), where L_1 and L_2 are the parameters which will be determined.

Note

$$\begin{aligned} K_1 &= \left\|r_1 + r_1\gamma_1 D + r_1\gamma_2 CB\right\| \\ &\quad + \left\|r_1\gamma_1 C + r_1\gamma_2 CA\right\| \frac{b^{\alpha-(1/p)} C_0 M \|B\|}{\sqrt[q]{q(\alpha-1)+1}}, \\ K_2 &= \left\|r_2 + r_2\gamma_3 D + r_2\gamma_4 CB\right\| \\ &\quad + \left\|r_2\gamma_3 C + r_2\gamma_4 CA\right\| \frac{b^{\alpha-(1/p)} C_0 M \|B\|}{\sqrt[q]{q(\alpha-1)+1}}, \\ K_3 &= \left(\left\|r_1\gamma_1 C + r_1\gamma_2 CA\right\| \right. \\ &\quad \left. + \left\|r_2\gamma_3 C + r_2\gamma_4 CA\right\|\right) \frac{b^{\alpha-(1/p)} C_0 M}{\sqrt[q]{q(\alpha-1)+1}} \|\omega\|_{L_p}. \end{aligned} \tag{19}$$

Theorem 2. *Suppose system (6) satisfies the second-order PD^{α}-type ILC algorithm and the initial state of each iteration satisfies (18), then there exists positive p such that $K_1 + K_2 < 1$, and $K_3 \longrightarrow 0$. Since $k \longrightarrow \infty$, $\|\Delta u_{k+1}\|_{L^p}$ is uniformly bounded, which guarantees that $\lim_{k\longrightarrow\infty}\|e_k\|_{\lambda} = 0$ and $t \in J$.*

Proof. According to Lemma 1, we yield

$$\begin{aligned} z_{k+1}(t) &= t^{\alpha-1}\mathscr{E}_{\alpha,\alpha}(A, t) z_0 + \int_0^t (t-s)^{\alpha-1} E_{\alpha,\alpha}\left(A(t-s)^{\alpha}\right) \\ &\quad \cdot \left(Bu_{k+1}(s) + \omega(t)\right) ds, \\ \Delta z_{k+1}(t) &= \int_0^t (t-s)^{\alpha-1} E_{\alpha,\alpha}\left(A(t-s)^{\alpha}\right) B\left(\Delta u_{k+1}(s) + \omega(t)\right) ds, \\ \Delta z_k(t) &= \int_0^t (t-s)^{\alpha-1} E_{\alpha,\alpha}\left(A(t-s)^{\alpha}\right) B\left(\Delta u_k(s) + \omega(t)\right) ds, \end{aligned} \tag{20}$$

and then,

$$\begin{aligned} \Delta u_{k+1}(t) &= r_1\left[\Delta u_k(t) + \gamma_1 C\Delta z_k(t) + \gamma_1 D\Delta u_k(t) \right. \\ &\quad \left. + \gamma_2 C\left(A\Delta z_k(t) + B\Delta u_k(t)\right)\right] \\ &\quad + r_2\left[\Delta u_{k-1}(t) + \gamma_3 C\Delta z_{k-1}(t) + \gamma_3 D\Delta u_{k-1}(t) \right. \\ &\quad \left. + \gamma_4 C\left(A\Delta z_{k-1}(t) + B\Delta u_{k-1}(t)\right)\right], \\ &= \left(r_1 + r_1\gamma_1 D + r_1\gamma_2 CB\right)\Delta u_k(t) \\ &\quad + \left(r_2 + r_2\gamma_3 D + r_2\gamma_4 CB\right)\Delta u_{k-1}(t) \\ &\quad + \left(r_1\gamma_1 C + r_1\gamma_2 CA\right)\int_0^t (t-s)^{\alpha-1} E_{\alpha,\alpha} \\ &\quad \cdot \left(A(t-s)^{\alpha}\right) B\left(\Delta u_k(s) + \omega(t)\right) ds \\ &\quad + \left(r_2\gamma_3 C + r_2\gamma_4 CA\right)\int_0^t (t-s)^{\alpha-1} E_{\alpha,\alpha} \\ &\quad \cdot \left(A(t-s)^{\alpha}\right) B\left(\Delta u_{k-1}(s) + \omega(t)\right) ds. \end{aligned} \tag{21}$$

By taking the L_p norm, it yields

$$\begin{aligned} \left\|\Delta u_{k+1}\right\|_{L^p} &\le \left\|r_1 + r_1\gamma_1 D + r_1\gamma_2 CB\right\| \left\|\Delta u_k(t)\right\|_{L^p} + \left\|r_1\gamma_1 C + r_1\gamma_2 CA\right\| \frac{b^{\alpha-(1/p)} C_0 M \|B\|}{\sqrt[q]{q(\alpha-1)+1}} \left\|\Delta u_k(t)\right\|_{L^p} \\ &\quad + \left\|r_2 + r_2\gamma_3 D + r_2\gamma_4 CB\right\| \left\|\Delta u_{k-1}(t)\right\|_{L^p} + \left\|r_2\gamma_3 C + r_2\gamma_4 CA\right\| \frac{b^{\alpha-(1/p)} C_0 M \|B\|}{\sqrt[q]{q(\alpha-1)+1}} \left\|\Delta u_{k-1}(t)\right\|_{L^p} \\ &\quad + \left\|r_1\gamma_1 C + r_1\gamma_2 CA\right\| \frac{b^{\alpha-(1/p)} C_0 M}{\sqrt[q]{q(\alpha-1)+1}} \|\omega\|_{L_p} + \left\|r_2\gamma_3 C + r_2\gamma_4 CA\right\| \frac{b^{\alpha-(1/p)} C_0 M}{\sqrt[q]{q(\alpha-1)+1}} \|\omega\|_{L_p}. \end{aligned} \tag{22}$$

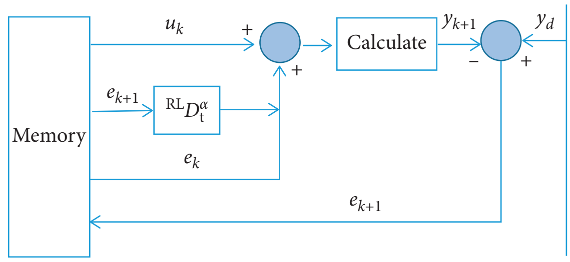

FIGURE 1: Block diagram of the open- and closed-loop PD^α-type ILC algorithm.

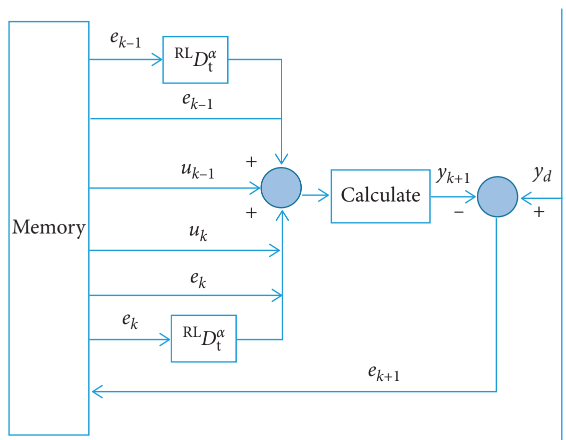

FIGURE 2: Block diagram of the second-order PD^α-type ILC algorithm.

For brevity, note that

$$\begin{aligned} K_1 &= \left\| r_1 + r_1\gamma_1 D + r_1\gamma_2 CB \right\| + \left\| r_1\gamma_1 C + r_1\gamma_2 CA \right\| \frac{b^{\alpha-(1/p)} C_0 M \|B\|}{\sqrt[q]{q(\alpha-1)+1}}, \\ K_2 &= \left\| r_2 + r_2\gamma_3 D + r_2\gamma_4 CB \right\| + \left\| r_2\gamma_3 C + r_2\gamma_4 CA \right\| \frac{b^{\alpha-(1/p)} C_0 M \|B\|}{\sqrt[q]{q(\alpha-1)+1}}, \\ K_3 &= \left(\left\| r_1\gamma_1 C + r_1\gamma_2 CA \right\| + \left\| r_2\gamma_3 C + r_2\gamma_4 CA \right\| \right) \frac{b^{\alpha-(1/p)} C_0 M}{\sqrt[q]{q(\alpha-1)+1}} \|\omega\|_{L_p}, \end{aligned} \tag{23}$$

and one can deduce $\|\Delta u_{k+1}\|_{L^p} \le K_1 \|\Delta u_k\|_{L^p} + K_2 \|\Delta u_{k-1}\|_{L^p} + K_3$.

There exists a constant $p > 0$, which satisfies $K_1 + K_2 < 1$ and $K_3 \longrightarrow 0$. Since $k \longrightarrow \infty$, $\|\Delta u_{k+1}\|_{L^p}$ is uniformly bounded. The proof is completed. □

5. Simulations

In this section, we will give two simulation examples to demonstrate the validity of the algorithms.

5.1. PD^α-Type ILC with Initial State Error. Consider the following one-dimensional systems as follows:

$$\left\{ {}^{\mathrm{RL}}D_t^{0.6} x(t) = x_k^2(t) + 0.1u(t) + \omega_k(t), \quad t \in J = [1,2], x(0) = 2, y(t) = x(t) + 0.3u_k(t) + \nu(t), \right. \tag{24}$$

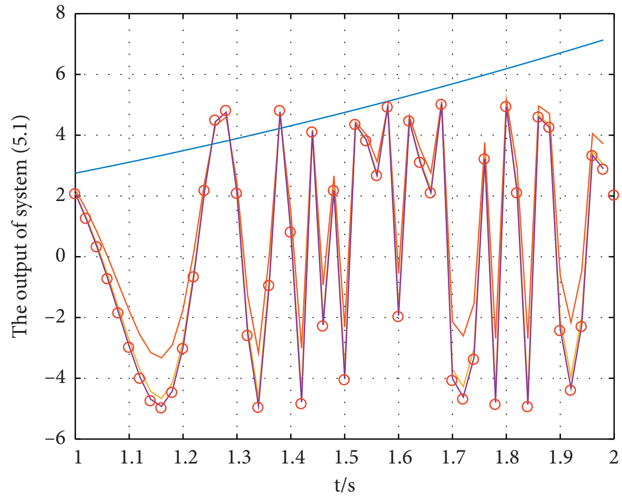

Figure 3: Simulation results of output y_k.

Table 1: Numerical simulation of the output of the system in Section 5.1 and the desired trajectory.

k	y_k	$y_d(t_k)$	k	y_k	$y_d(t_k)$	k	y_k	$y_d(t_k)$
1	2.0818	2.0539	18	−4.9051	−4.9774	35	5.0183	4.9945
2	1.2580	1.2454	19	−0.9237	−0.9645	36	−4.0133	−4.0915
3	0.3294	0.3088	20	4.7684	4.7910	37	−4.6198	−4.7037
4	−0.7118	−0.7414	21	0.8193	0.7912	38	−3.3214	−3.3956
5	−1.8284	−1.8677	22	−4.7823	−4.8564	39	3.2206	3.1983
6	−2.9501	−2.9989	23	4.1016	4.0857	40	−4.7914	−4.8791
7	−3.9613	−4.0190	24	−2.2443	−2.2993	41	4.9318	4.9216
8	−4.6935	−4.7576	25	2.1803	2.1603	42	2.1176	2.0840
9	−4.9269	−4.9936	26	−3.9964	−4.0669	43	−4.8627	−4.9535
10	−4.4206	−4.4837	27	4.3542	4.3339	44	4.5943	4.5790
11	−2.9888	−3.0410	28	3.8435	3.7982	45	4.2592	4.2403
12	−0.6484	−0.6824	29	2.6705	2.6515	46	−2.3747	−2.4479
13	2.1738	2.1620	30	4.9469	4.9048	47	−4.3241	−4.4139
14	4.4456	4.4755	31	−1.9316	−1.9891	48	−2.2423	−2.3162
15	4.7533	4.7927	32	4.4846	4.4505	49	3.3387	3.3090
16	2.0844	2.0698	33	3.1067	3.0883	50	2.8945	2.8603
17	−2.5569	−2.6095	34	2.1099	2.0826			

with the iterative learning control and initial state error

$$\begin{cases} u_{k+1}(t) = u_k(t) + 0.5e_k(t) + 0.5e_{k+1}^{(\alpha)}(t), \\ x_{k+1}(0) = x_k(0) + 0.1e_k(t), \end{cases} \tag{25}$$

where $Ax(\cdot) = x(\cdot)^2$. Now, we can choose $\alpha = 0.6$, $B = 0.1$, $C = 1$, $p = 2$, $\gamma_1 = \gamma_2 = 0.5$, $\omega(t) = 10^{-3}\sin(0.001t)$, and $\nu(t) = 10^{-5}(t)$. For the system, we use the PD^α-type ILC algorithm and set the initial control $u_0(\cdot) = 0$, $y_d(t) = 5\sin(e^{t^2})$, and $t \in (0, 2)$. One can calculate $M \approx 3 > 0$, $\kappa_1 = 0.47$, $\kappa_2 = 0.17$, and $\kappa_3 < 0.01 = m$, and then, all conditions of Theorem 1 are satisfied.

The state trajectories of system (24) with initial conditions are given in Figure 3 and Table 1, and with the increase of the number of iterations, it can track the desired trajectory gradually. Consistent with the theoretical analysis in the previous section, the algorithm has a faster convergence speed. At the end of the fourth iteration, the algorithm has converged. From Figures 3 and 4, the curve is basically completely fitted, showing that the system algorithm is well robust.

5.2. PD^α-Type ILC with Random Disturbance. Consider a two-dimensional ILC system; we set $\alpha = 0.7$, $\omega(t) = 10^{-10}\sin((\pi t)/1000)$, $\nu(t) = 10^{-3}$, $A\begin{pmatrix} x_1 \\ x_2 \end{pmatrix} = \begin{pmatrix} 2x_1^2 \\ x_2^2 \end{pmatrix}$, $B = \begin{pmatrix} 0 & 1 \\ 1 & 1 \end{pmatrix}$, $C = \begin{pmatrix} 1 & 1 \\ 0 & 1 \end{pmatrix}$, and $D = \begin{pmatrix} 0 & 1 \\ 1 & 1 \end{pmatrix}$ and construct the second-order PD^α-type ILC algorithm as follows:

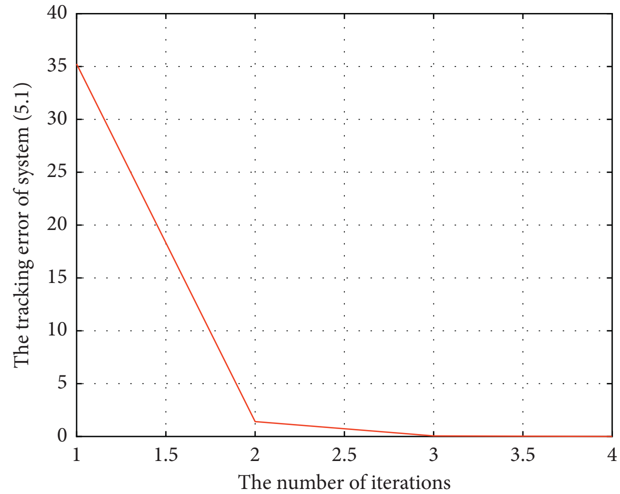

Figure 4: The tracking error of the systems.

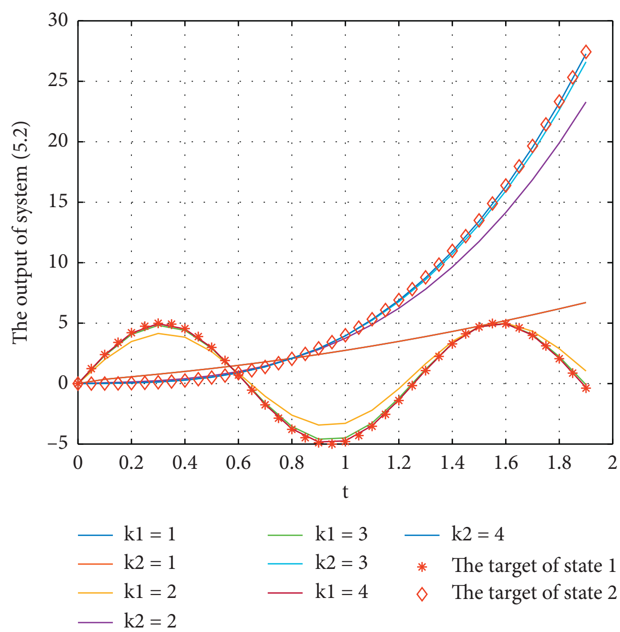

Figure 5: Simulation results of output y_k.

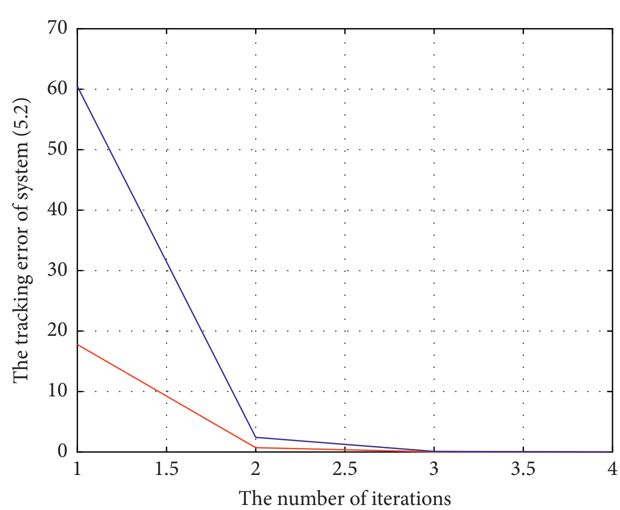

Figure 6: The tracking error of the system.

Table 2: Numerical simulation of the output of the system in Section 5.2 and the desired trajectory.

k	y_k	$y_d(t_k)$	k	y_k	$y_d(t_k)$
1	0	0	1	0	0
2	2.3808	2.3971	2	0.0181	0.0040
3	4.1782	4.2073	3	0.0534	0.0320
4	4.9538	4.9874	4	0.1349	0.1080
5	4.5182	4.5464	5	0.2860	0.2560
6	2.9784	2.9923	6	0.5299	0.5000
7	0.7378	0.7056	7	0.8898	0.8640
8	−1.7256	−1.7539	8	1.3887	1.3720
9	−3.7370	−3.7840	9	2.0900	2.0480
10	−4.8293	−4.8876	10	2.8958	2.9160
11	−4.7343	−4.7946	11	3.9500	4.0000
12	−3.4746	−3.5277	12	5.3063	5.3240
13	−1.3580	−1.3970	13	6.8846	6.9120
14	1.0981	1.0755	14	8.7488	8.7880
15	3.3259	3.2849	15	10.9227	10.9760
16	4.7019	4.6899	16	13.4300	13.5000
17	4.9573	4.9467	17	16.2946	16.3840
18	4.0060	3.9924	18	19.5403	19.6520
19	2.0936	2.0605	19	23.1909	23.3280
20	−0.3191	−0.3757	20	27.2702	27.4360

$$\begin{aligned} u_{k+1}(t) &= 0.1\left[u_k(t) + 0.1e_k(t) + 0.1e_k^{(\alpha)}(t)\right] \\ &\quad + 0.1\left[u_{k-1}(t) + 0.2e_{k-1}(t) + 0.2e_{k-1}^{(\alpha)}(t)\right], \\ k &= 2, 3, \ldots \end{aligned} \tag{26}$$

We also select other parameters and initial values of the algorithm as follows: $u_0(\cdot) = 0$, $y_d(t) = \begin{pmatrix} y_{1d}(t) \\ y_{2d}(t) \end{pmatrix} = \begin{pmatrix} 5\sin(t) \\ 4t^3 \end{pmatrix}$, $t \in (0, 1.9)$, $r_1 = 1$, $r_2 = 0.5$, $\gamma_1 = 1$, and $\gamma_2 = 0.5$. It is easy to show that $M \approx 3 > 0$, $K_1 = 0.264$, $K_2 = 0.428$, and $K_3 \longrightarrow 0$, and all conditions of Theorem 2 are satisfied. In the simulation, $\ast\ast\ast$ denotes the desired trajectory of state 1, ◇◇◇ denotes the desired trajectory of state 2, and solid lines (—–) in different colors denote the output of the system. In Figure 5, we use k1 to represent the iteration of state 1 and use k2 to represent the iteration of state 2, and the tracking error is shown in Figure 6, which implies the number of iterations and tracking error.

From Figure 6 and Table 2, one can find that the tracking error tends to zero quickly, so the output of the system can track the desired trajectory almost perfectly.

6. Conclusion

In this paper, we show the concept of mild solutions of the R-L fractional system and considered two cases of the PD^α-type ILC algorithm. The sufficient conditions of robustness analysis of the PD^α-type ILC algorithm with uncertain disturbances were given by the corresponding theorems and proved. At last, two R-L fractional examples are given to demonstrate the results.

Data Availability

The data used to support the findings of this study are included within the article.

Conflicts of Interest

The authors declare that they have no conflicts of interest regarding the publication of this paper.

Authors' Contributions

The authors contributed equally to this work, and all authors read and approved the final manuscript.

Acknowledgments

This work was supported by the NSF of China (no. 11661084) and Guizhou Province Department of Education Fund ([2016]046, Qian Jiao He KY[2020]093, and Qian Ke He Ping Tai Ren Cai [2018]5784-08).

References

[1] X. Liu, J. Wang, and D. O'Regan, "On the approximate controllability for fractional evolution inclusions of sobolev and clarke subdifferential type," *IMA Journal of Mathematical Control and Information*, vol. 36, no. 1, pp. 1–17, 2019.

[2] Z. Bien and J. X. Xu, *Iterative Learning Control Analysis: Design, Integration and Applications*, Springer, Berlin, Germany, 1998.

[3] Y. Q. Chen and C. Wen, *Iterative Learning Control: Convergence, Robustness and Applications*, Springer-Verlag, Berlin, Germany, 1999.

[4] M. Norrlof, "Iterative learning control: Analysis, Design, and Experiments, Linkoping Studies in Science and Technology," Dissertations, Linköping University, Linköping, Sweden, 2000.

[5] J. X. Xu and Y. Tan, *Linear and Nonlinear Iterative Learning Control*, Spring-Verlag, Berlin, Germany, 2003.

[6] Y. Wang, F. Gao, and F. J. Doyle III, "Survey on iterative learning control, repetitive control, and run-to-run control," *Journal of Process Control*, vol. 19, no. 10, pp. 1589–1600, 2009.

[7] J. V. Wijdeven, T. Donkers, and O. Bosgra, "Iterative Learning Control for uncertain systems: robust monotonic convergence analysis," *Automatica*, vol. 45, no. 10, pp. 2383–2391, 2009.

[8] J. X. Xu, "A survey on iterative learning control for nonlinear systems," *International Journal of Control*, vol. 84, no. 3, pp. 1275–1294, 2011.

[9] Y. Li, Y. Q. Chen, and H. S. Ahn, "Fractional-order iterative learning control for fractional-order systems," *Asian Journal of Control*, vol. 13, no. 1, pp. 1–10, 2011.

[10] Y.-H. Lan, "Iterative learning control with initial state learning for fractional order nonlinear systems," *Computers & Mathematics with Applications*, vol. 64, no. 10, pp. 3210–3216, 2012.

[11] X. Liu, Y. Li, and Y. Liu, "The convergence of iterative learning control for some fractional system," *Advances in Difference Equations*, vol. 132, pp. 1–12, 2017.

[12] M.-T. Lin, C.-L. Yen, M.-S. Tsai, and H.-T. Yau, "Application of robust iterative learning algorithm in motion control system," *Mechatronics*, vol. 23, no. 5, pp. 530–540, 2013.

[13] D. A. Haghighi and S. Mobayen, "Design of an adaptive super-twisting decoupled terminal sliding mode control scheme for a class of fourth-order systems," *ISA Transactions*, vol. 75, pp. 216–225, 2018.

[14] S. Mobayen, "Chaos synchronization of uncertain chaotic systems using composite nonlinear feedback based integral sliding mode control," *ISA Transactions*, vol. 77, pp. 100–111, 2018.

[15] S. Mobayen, "A novel global sliding mode control based on exponential reaching law for a class of underactuated systems with external disturbances," *Journal of Computational and Nonlinear Dynamics*, vol. 11, Article ID 021011, 9 pages, 2016.

[16] S. Mobayen, "Design of LMI-based sliding mode controller with an exponential policy for a class of underactuated systems," *Complexity*, vol. 21, no. 5, pp. 117–124, 2014.

[17] Y. Li and W. Jiang, "Fractional order nonlinear systems with delay in iterative learning control," *Applied Mathematics and Computation*, vol. 257, no. 15, pp. 546–552, 2015.

[18] T. Lan and H. Lin, "Accelerated modify approach for initial state error iterative learning control in sense of Lebesgue-p norm," *Control and Decision*, vol. 31, no. 3, pp. 429–434, 2016.

[19] K. Zhang and G. Peng, "Convergence analysis of PD^{03b1}-type fractional order iterative learning control in the sense of $L_p$norm," *Systems Engineering and Electronics*, vol. 39, no. 10, pp. 2285–2290, 2017.

[20] K. S. Miller and B. Ross, *An Introduction to the Fractional Calculus and Differential Equations*, John Wiley, Hoboken, NJ, USA, 1993.

[21] A. A. Kilbas, H. M. Srivastava, and J. J. Trujillo, "Theory and applications of fractional differential equations," in *North-Holland Mathematics Studies*Elsevier Science B.V., Amsterdam, The Netherlands, 2006.

[22] V. Lakshmikantham, S. Leela, and J. Vasundhara Devi, *Theory of Fractional Dynamic Systems*, Cambridge Academic Publishers, Cambridge, UK, 2009.

[23] K. Diethelm, *The Analysis of Fractional Differential Equations*, Springer-Verlag, Berlin, Germany, 2010.

[24] G. M. Mophou and G. M. N'Guérékata, "Existence of mild solutions of some semilinear neutral fractional functional evolution equations with infinite delay," *Applied Mathematics and Computation*, vol. 216, no. 1, pp. 61–69, 2010.

[25] X. Liu, Z. Liu, and M. Bin, "Approximate controllability of impulsive fractional neutral evolution equations with Riemann-Liouville fractional derivatives," *Journal of Computational Analysis and Applications*, vol. 17, no. 3, pp. 468–485, 2014.

[26] W. Jiang, "The controllability of fractional control systems with control delay," *Computers & Mathematics with Applications*, vol. 64, no. 10, pp. 3153–3159, 2012.

[27] E. Bazhlekova, *Fractional Evolution Equations in Banach Spaces*, Ph.D Thesis, Eindhoven University of Technology, Eindhoven, Netherlands, 2001.

Hindawi
Mathematical Problems in Engineering
Volume 2021, Article ID 6768215, 10 pages
https://doi.org/10.1155/2021/6768215

Research Article

An Unprecedented 2-Dimensional Discrete-Time Fractional-Order System and Its Hidden Chaotic Attractors

Amina Aicha Khennaoui[1], **A. Othman Almatroud**[2], **Adel Ouannas**[1], **M. Mossa Al-sawalha**[2], **Giuseppe Grassi**[3], **Viet-Thanh Pham**[4], and **Iqbal M. Batiha**[5]

[1]*Department of Mathematics and Computer Science, University of Larbi Ben M'hidi, Oum El Bouaghi, Algeria*
[2]*Department of Mathematics, Faculty of Science, University of Ha'il, Ha'il 81451, Saudi Arabia*
[3]*Universita Del Salento, Dipartimento Ingegneria Innovazione, Lecce 73100, Italy*
[4]*Nonlinear Systems and Applications, Faculty of Electrical and Electronics Engineering, Ton Duc Thang University, Ho Chi Minh City, Vietnam*
[5]*Department of Mathematics, University of Jordan, Amman, Jordan*

Correspondence should be addressed to Amina Aicha Khennaoui; kamina_aicha@yahoo.fr

Received 12 August 2020; Revised 30 October 2020; Accepted 22 December 2020; Published 6 January 2021

Academic Editor: Abdelalim Elsadany

Some endeavors have been recently dedicated to explore the dynamic properties of the fractional-order discrete-time chaotic systems. To date, attention has been mainly focused on fractional-order discrete-time systems with "self-excited attractors." This paper makes a contribution to the topic of fractional-order discrete-time systems with "hidden attractors" by presenting a new 2-dimensional discrete-time system without equilibrium points. The conceived system possesses an interesting property not explored in the literature so far, i.e., it is characterized, for various fractional-order values, by the coexistence of various kinds of chaotic attractors. Bifurcation diagrams, computation of the largest Lyapunov exponents, phase plots, and the 0-1 test method are reported, with the aim to analyze the dynamics of the system, as well as to highlight the coexistence of chaotic attractors. Finally, an entropy algorithm is used to measure the complexity of the proposed system.

1. Introduction

Exploring chaotic dynamics has received considerable attention during the past few years [1]. Numerous attempts have been dedicated to analyze the classical systems (outlined by differential or difference equations of integer order), as well as fractional-order systems (outlined by differential or difference equations of fractional order) [2]. Generally speaking, regardless of the type of system, chaos can appear in the form of "hidden attractors" or "self-excited attractors" [3–6]. On the first occasion, the initial conditions, for the purpose of getting chaos, are situated near the saddle points of the motion [3], whereas, on the last occasion, the initial conditions may only be set up via a wide range of computer-based search [4], given that the corresponding dynamic systems are distinguished by the presence of stable equilibrium points [5] or else by the absence of them at all [6].

Referring to fractional-order chaotic discrete-time systems (i.e., systems outlined by difference equations of fractional order), many scholars have mainly focused on the system's dynamics characterized by the presence of "self-excited attractors" [7, 8]. For example, the so-called generalized Hénon map of three dimensions has been studied in [9], while some dynamics of the fractionalized logistic map were examined in [10]. In [11], three different fractional-order discrete-time systems (FoDs) have been investigated, i.e., Wang's, Rossler's, and Stefanski's maps. In [12], the chaotic behaviors of the fractional-order sine and standard maps were analyzed, whereas in [13], the dynamic properties of the fractional-order Grassi–Miller map have been illustrated in detail. Additionally, the presence of chaos in the fractional-order discrete double scroll map has been investigated in [14], whereas in [12], the fractional-order delayed logistic map was analyzed regarding to its chaotic behavior. It is worthy to state that all these FoDs have shown "self-excited attractors." On the other hand, very few FoDs characterized by "hidden attractors" have been investigated in the previously published works up to this time [15–19]. For example, in [15], the dynamics of the fractional-order version of the standard iterated map have been investigated, whereas in [18], a 2-Dimensional FoDs (2D-FoDs) without discontinuity for all equations of the system has been presented. However, these FoMs with "hidden attractors" do not show any coexisting chaotic attractors. Based on these considerations, this paper aims to make a contribution to the topic of FoDs with "hidden attractors" by presenting a new 2D-FoD without equilibrium points. The conceived system possesses an interesting property, i.e., it is characterized by the coexistence of various kinds of chaotic attractors. Here is how this paper is arranged. Section 2 introduces a new 2D-FoD time system without equilibria, along with some primary preliminaries associated with discrete-time non-integer-order calculus. In Section 3, the dynamic properties of the conceived map are analyzed via bifurcation diagrams and computation of the Largest Lyapunov Exponents (LLEs). In Section 4, a 0-1 test is reported to highlight the existence of chaotic hidden attractors. Also, an entropy algorithm is used to measure the complexity of the proposed system. Finally, a number of phase plots are reported, which highlight the coexistence of several types of chaotic attractors for various fractional-order values of the conceived system.

2. A New 2D-FoDs

This paper considers the following 2D-difference system:

$$\left\{ {}^{c}\Delta_a^{\gamma} x(t) = y(t-1+\gamma) - x(t-1+\gamma), {}^{c}\Delta_a^{\gamma} = -\alpha y(t-1+\gamma) - 0.37y^2(t-1+\gamma) + 0.81x(t-1+\gamma)y(t-1+\gamma) + 1.79, \right. \tag{1}$$

where x and y stand for state variables of the FoDs, $\alpha$is the system's parameter, and ${}^{c}\Delta_a^{\gamma}$ is the Caputo-like difference operator of fractional-order γ, where $\gamma \in]0,1]$.

Next, two main definitions that will pave the way for obtaining novel results are given below for completeness. Such two definitions are stated for the ${}^{c}\Delta_a^{\gamma}$ in its γ^{th}- order version and also for the γ^{th}-fractional sum operator, $\Delta^{-\gamma}$, respectively.

Definition 1. Let $\gamma > 0$ and $\mathbf{y}(\mathbf{t}) \in \mathbb{N}_a$. We define the $\gamma^{\mathbf{th}}$-order Caputo-like operator as [20]

$${}^{c}\Delta_a^{\gamma} y(t) = \frac{1}{\Gamma(1-\gamma)} \sum_{\tau=a}^{t-(1-\gamma)} (t-\tau-1)^{-\gamma} \Delta_\tau y(\tau), \tag{2}$$

where $\Gamma(.)$ denotes the gamma function and $t \in \mathbb{N}_{a+1-\gamma}$.

Definition 2. Let $\gamma > 0$; we define the γ^{th}-fractional sum, $\Delta^{-\gamma}$ as

$$\Delta_a^{-\gamma} y(t) = \frac{1}{\Gamma(\gamma)} \sum_{\tau=a}^{t-\gamma} (t-\tau-1)^{(\gamma-1)} \Delta_\tau y(\tau). \tag{3}$$

Using $\Delta^{-\gamma}$ makes (1) to be also rewritten as an integral equation in the Volterra sense as follows:

$$\begin{cases} x(t) = x_0 + \dfrac{1}{\Gamma(\gamma)} \displaystyle\sum_{\tau=a+1-\gamma}^{t-\gamma} (t-\tau-1)^{(\gamma-1)} \left(y(\tau+\gamma-1) - x(\tau+\gamma-1) \right), \\ y(t) = y_0 + \dfrac{1}{\Gamma(\gamma)} \displaystyle\sum_{\tau=a+1-\gamma}^{t-\gamma} (t-\tau-1)^{(\gamma-1)} \begin{pmatrix} -\alpha y(\tau+\gamma-1) - 0.37y^2(\tau+\gamma-1) + \\ 0.81x(\tau+\gamma-1)y(\tau+\gamma-1) + 1.79 \end{pmatrix}. \end{cases} \tag{4}$$

In the present work, some numerical methods are adopted to examine the complex dynamics of the proposed FoDs. First of all, we discuss the equilibrium points of the model at hand. Actually, the equilibrium points can be determined by finding the solution of the following system:

$$\begin{cases} y - x = 0, \\ -\alpha y - 0.37y^2 + 0.81xy + 1.79 = 0. \end{cases} \tag{5}$$

From system (5), it follows that

$$-\alpha y - 1.18y^2 + 1.79 = 0. \tag{6}$$

Thus, FoDs (1) has no equilibrium point when $-2.9067 < \alpha < 2.9067$. This result shows that FoDs (1) is able to produce a chaotic hidden attractor for appropriate choice of initial conditions and fractional order as well.

Secondly, we present the numerical formulae corresponding to all equations given in FoDs (1). This is can be carried out by first setting the initial point a to be equal to 0, then assuming $\tau + \gamma = \kappa$, and finally, replacing $(t-\tau-1)^{(\gamma-1)}/\Gamma(\gamma)$ by $\Gamma(t-\tau)/(\Gamma(\gamma)\Gamma(t-\tau-\gamma+1))$. Thus, (4) becomes

$$\begin{cases} x(n) = x_0 + \dfrac{1}{\Gamma(\gamma)} \displaystyle\sum_{\kappa=1}^{n} \dfrac{\Gamma(n-\kappa+\gamma)}{\Gamma(n-\kappa+1)} (y(\kappa-1) - x(\kappa-1)), \\ y(n) = y_0 + \dfrac{1}{\Gamma(\gamma)} \displaystyle\sum_{\kappa=1}^{n} \dfrac{\Gamma(n-\kappa+\gamma)}{\Gamma(n-\kappa+1)} \left(-\alpha y(\kappa-1) - 0.37 y^2(\kappa-1) + 0.81 x(\kappa-1) y(\kappa-1) + 1.79\right), \end{cases} \tag{7}$$

where x_0 and y_0 are the initial states. According to the discrete equation (7), the proposed fractional system (1) has memory effects, which means that the iterated solutions x and y are determined by all the previous states. In the next section, some dynamic characteristics of the novel 2D-FoD system are analyzed numerically.

3. Bifurcations and LLEs

When plotting bifurcation diagrams, two sets of symmetrical initial states are considered. The bifurcation diagram is plotted in blue for the initial state $x_0 = 1.78$, $y_0 = -0.79$ and in red for the initial states $x_0 = -1.78$, $y_0 = 0.79$.

3.1. Bifurcation and LLEs versus the System's Parameter α. Firstly, the bifurcation diagram of FoDs (1) is studied as α varies from 1.35109 to 1.9199. Besides, the bifurcation diagrams and LLEs of the state variable $x(n)$ are also studied corresponding to two distinct fractional-order values of γ, as exhibited in Figures 1 and 2. It can be seen that the states of FoDs (1) change qualitatively with the variation of α and γ. In particular, the bifurcation diagram of FoDs (1) is illustrated in Figure 1(a), for $\gamma = 0.9362$. When α increases from 1.35109 to 1.9199, the states of the system go, via period-doubling bifurcation, to chaotic motion. It is noteworthy that FoDs (1) exhibits chaotic behavior in larger intervals for the initial condition $x_0 = 1.78$, $y_0 = -0.79$. As shown in Figure 2, when γ is increased starting from 0.9362 up to 0.992, FoDs (1) shows chaotic motion over most of the range $(1.7387, 1.9136)$.

3.2. Bifurcation versus Fractional-Order γ. In order to highlight the effect of γ on the dynamic behavior of FoDs (1), its bifurcation with respect to γtoo is considered. We fix the parameter α to be equal to 1.73 and change γ within $[0, 1]$. The bifurcation diagram and the LLE are illustrated in Figures 3(a) and 3(b), respectively. As one can see, the system has positive LE when γ takes the smallest values, indicating that FoDs (1) is chaotic. Besides, when $\gamma \in [0.9362, 0.9402] \bigcup]0.9816, 0.9834]$, FoDs (1) shows chaotic behavior. The phase diagrams are plotted in Figure 4 for different values of γ. From these diagrams, it is clear that as the value of γ increases, different chaotic attractors are observed. Moreover, these figures indicate that the fractional order γ is another bifurcation parameter.

3.3. Coexisting Chaotic Attractors. Herein, the dynamics of FoDs (1) are analyzed using the phase portraits, obtained by fixing the parameter α and by considering the two previous different sets of initial conditions. For $\gamma = 0.992$, as shown in Figure 5(a), FoDs (1) highlights the coexistence of a hidden chaotic attractor corresponding to the two initial conditions $(1.78, -0.79)$. Similarly, when the order γ is selected to be equal 0.9992 in FoDs (1), Figure 5(b) highlights the coexistence chaotic hidden attractors corresponding to the two initial conditions $(-1.78, 0.79)$ and $(1.78, -0.79)$, respectively. Finally, when γ is taken to be equal to 0.96, the coexisting chaotic hidden attractors are plotted as in Figure 5(c). One might deduce that the dynamic behavior of the new FoDs given in (1) is complex and interesting, by virtue of the presence of different types of coexisting hidden chaotic attractors.

4. Test for Chaos and Approximate Entropy

In the following section, we present the influence of both fractional-order and initial-conditions on the dynamical behavior of the suggested discrete-time system by considering the 0-1 test method. Then, we introduce the approximate entropy to further investigate the complexity of fractional-order discrete-time system (1).

4.1. Test for Chaos. To reflect the sensitivity of the FoDs, the 0-1 test is considered. This test was proposed in [21] for fractional-order systems to distinguish regular and chaotic dynamics. As opposed to the Lyapunov exponents method, the 0-1 test is applied to known or unknown systems regarding the phase plane. Thus, it is able to identify the chaos in a series of data where the phase space reconstruction is not necessary. For model (1), this method works for the finite points $(y_i)_{i=1,\ldots,N}$ and is a suitable choice of $c \in (0, 2\pi)$. Using the approach in [21], one can define the two terms for $m = \overline{1, N}$ as

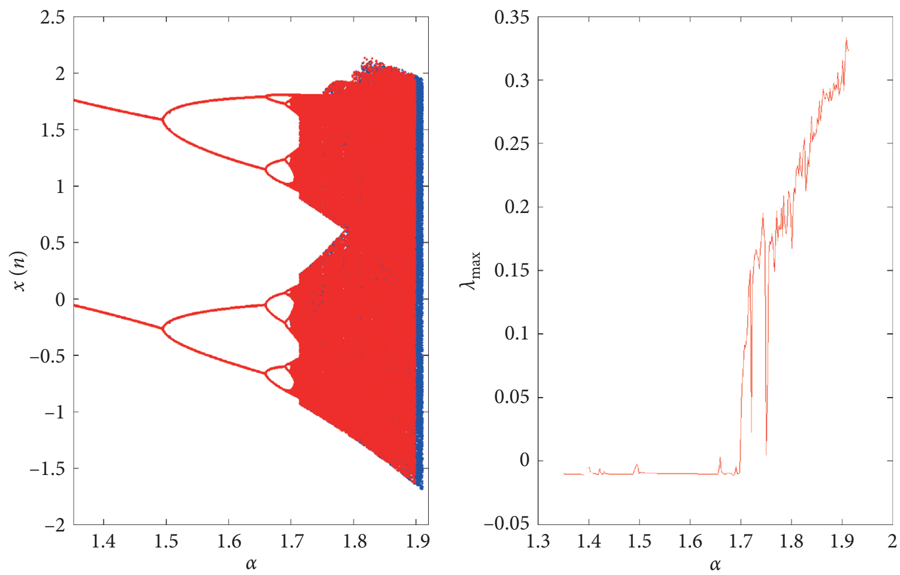

(a) (b)

Figure 1: (a) Bifurcation diagrams of FoDs (1) vs. α when $\gamma = 0.9362$; (b) LLE diagram according to (a).

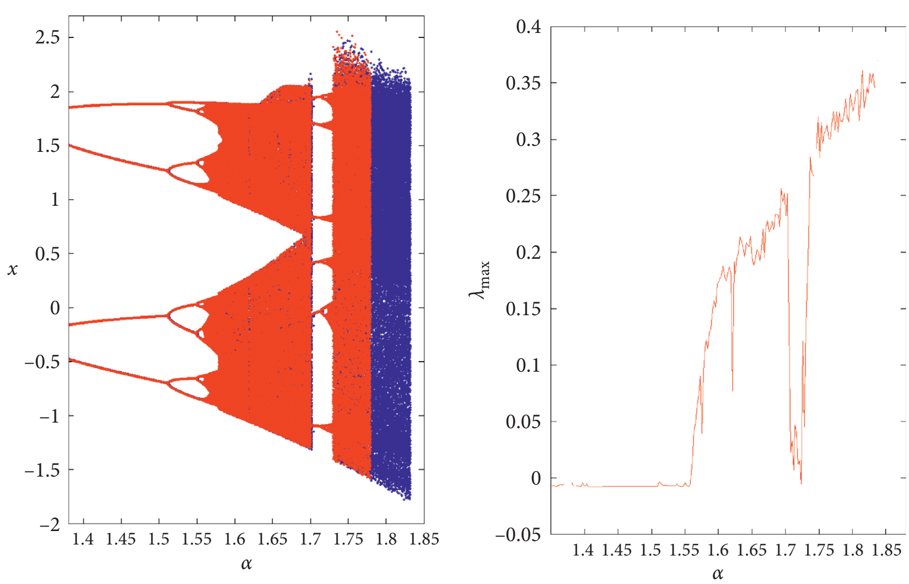

(a) (b)

Figure 2: (a) Bifurcation diagrams of FoDs (1) vs. α when $\gamma = 0.992$; (b) LLE diagram according to (a).

$$
\begin{aligned}
p_m &= \sum_{i=1}^{m} y_i \cos(ic), \\
s_m &= \sum_{i=1}^{m} y_i \sin(ic).
\end{aligned}
\tag{8}
$$

Such terms are called the translation components. In order to study the boundedness or unboundedness of the functions p_m and s_m, we calculate the time-averaged mean-square displacement, which can be defined as

$$M_m = \lim_{N\longrightarrow+\infty} \frac{1}{N} \sum_{j=1}^{N} \left(\left(p_{j+m} - p_j\right)^2 + \left(s_{j+m} - s_j\right)^2 \right). \tag{9}$$

In practice $n \ll N$. Finally, we obtain the asymptotic growth rate K via

$$K = \mathrm{median}\left(K_c\right), \tag{10}$$

where $K_c = \lim_{m\longrightarrow\infty} (\log M_m / \log m)$.

On the other hand, the "0-1 test" has been developed in [22], such that the output K of the test is obtained using

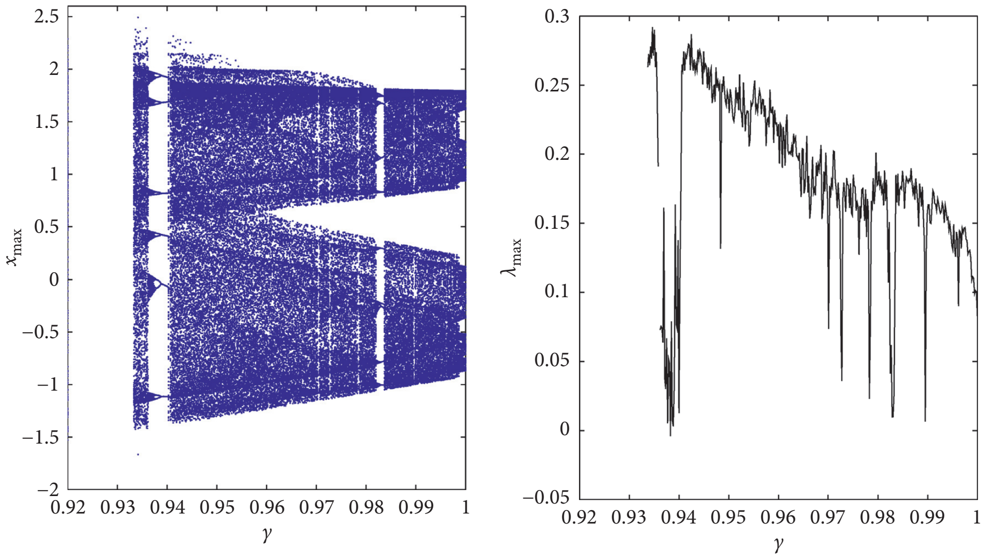

(a) (b)

Figure 3: (a) Bifurcation diagram vs. γ, when $\alpha = 1.73$; (b) LLE according to diagram (a).

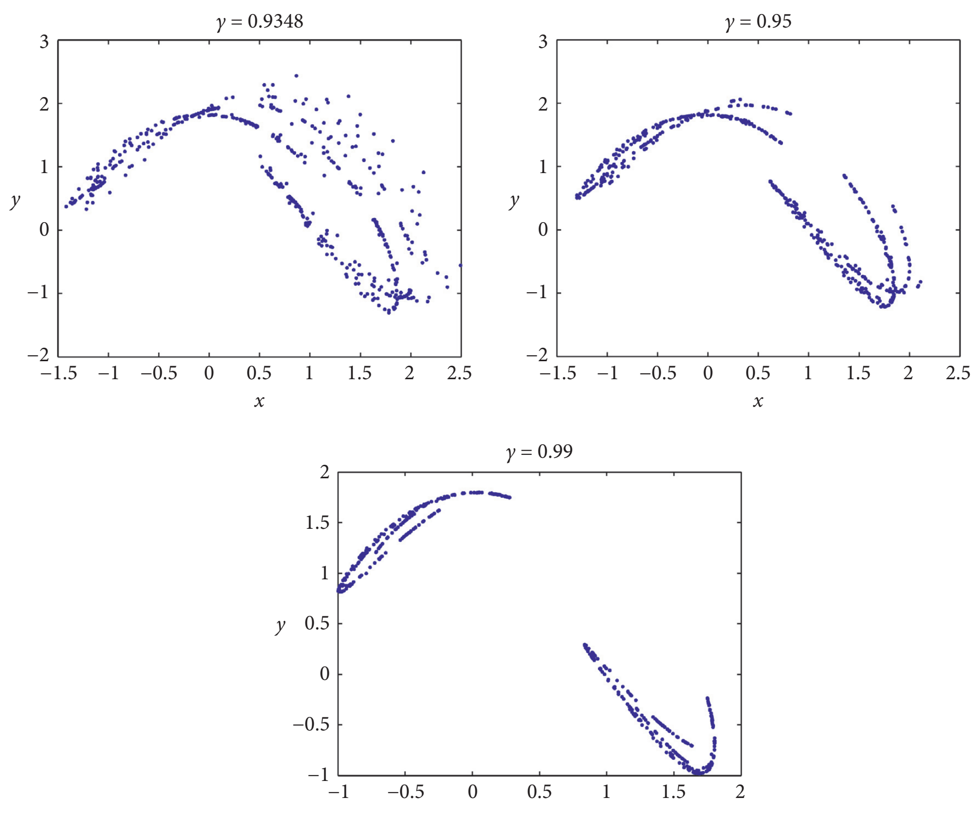

Figure 4: Phase diagrams of fractional-order map (1) for different values of fractional order.

correlation to measure the growth rate of the mean-square displacement D_m for better convergence property. Generally, D_m is calculated as

$$D_m = M_m - V_{osc}, \tag{11}$$

where V_{osc} is the oscillatory term:

$$V_{osc}(c, n) = \left(\lim_{N \longrightarrow \infty} \frac{1}{N} \sum_{j=1}^{N} x(j) \right)^2 \frac{1 - \cos(mc)}{1 - \cos(c)}. \tag{12}$$

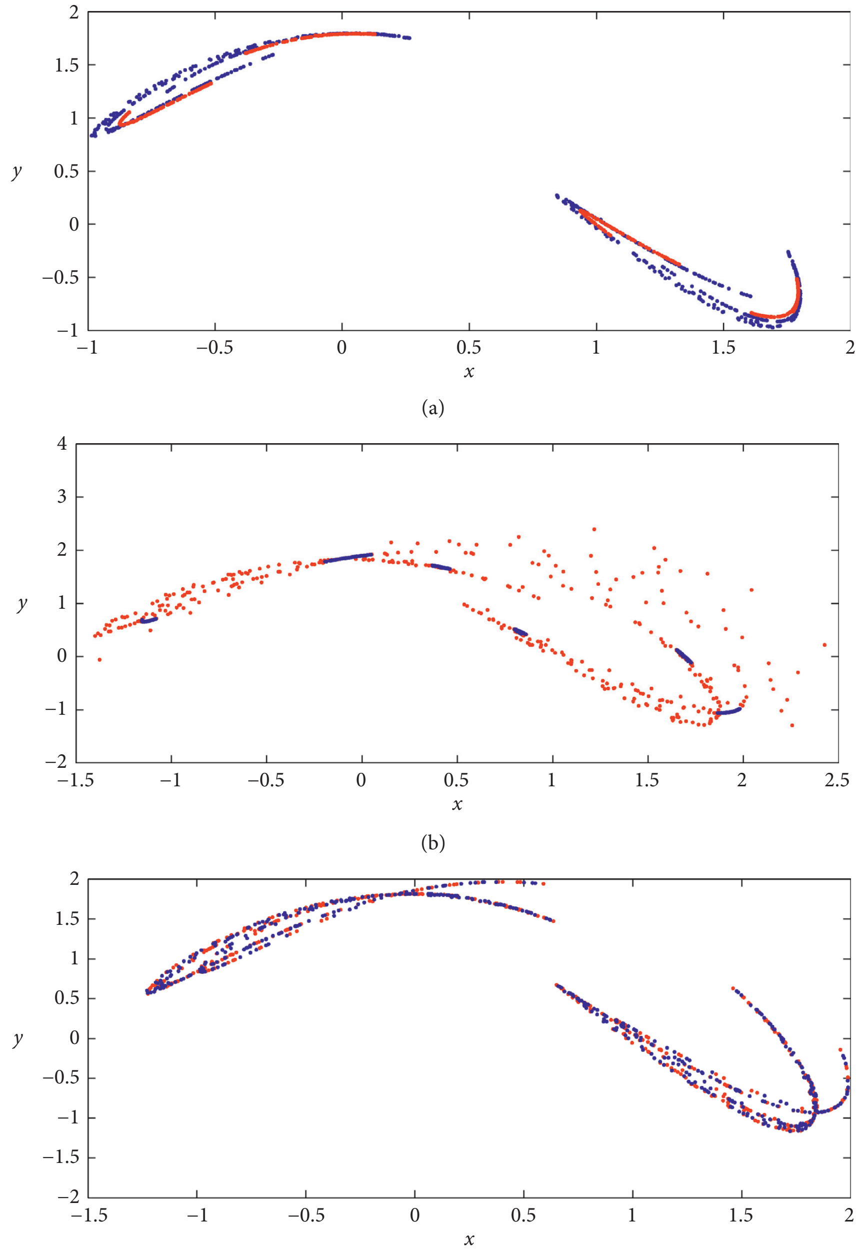

Figure 5: The coexisting attractors of FoDs (1) with $\alpha = 1.73$ and subject to the two initial conditions $(-1.78, 0.79)$ and $(1.78, -0.79)$ for the red and the blue attractors, respectively: (a) $\gamma = 0.9992$; (b) $\gamma = 0.9362$; and (c) $\gamma = 0.96$.

It is shown in [22] that the modified mean-square deplacement $D_c$processes better convergence than M_c. Therefore, the output K can now be performed as the co-variance $\mathrm{cov}(x, y) = (1/m)\sum_{i=1}^{m}(x(i)-\overline{x})(y(i)-\overline{y})$ and variation $\mathrm{var}(x) = \mathrm{cov}(x, x)$ of m element as follows:

$$K_c = \frac{\mathrm{cov}(r, s)}{\sqrt{\mathrm{var}(r)\mathrm{var}(s)}} \in [1, 1], \qquad (13)$$

where $r = \{1, 2, \ldots, m\}$ and s is the vector formed by the mean-square displacement D_m.

In both methods, fractional-order discrete-time system (1) is evaluated to be chaotic if the plot of p and s in the $p-s$ plane present Brownian-like trajectories and if K approaches 1, while it becomes regular as K approaches 0, and p and s display bounded-like trajectories. Figure 6, however, depicts the results of the test for different values of fractional order γ in which $(x_0, y_0) = (-1.78, 0.79)$. Based on this figure, one can observe that the output K has appeared in a similar manner to the results of the maximum LE and bifurcation diagram, shown in Figure 3, which clearly confirms the abovementioned results.

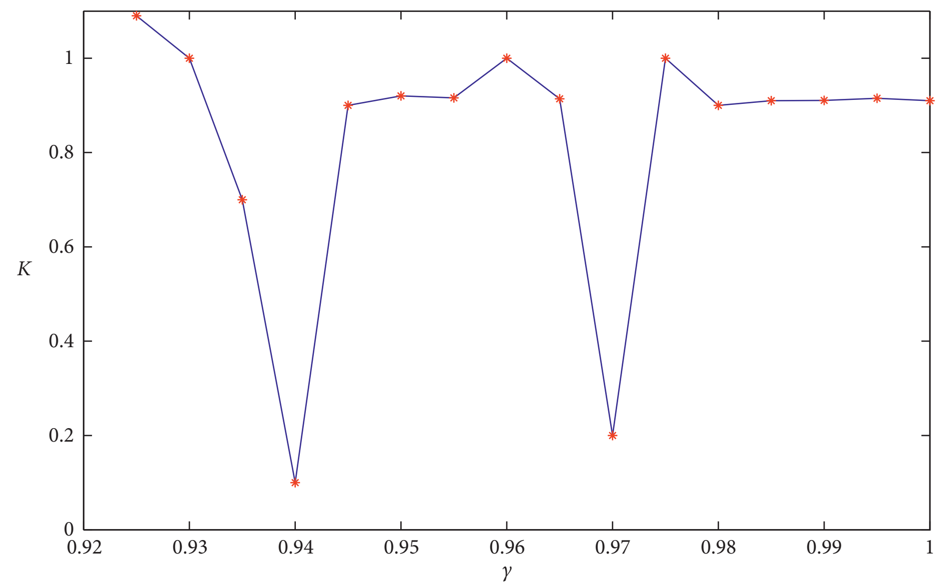

Figure 6: Asymptotic growth rate K vs. γ, when $\alpha = 1.73$.

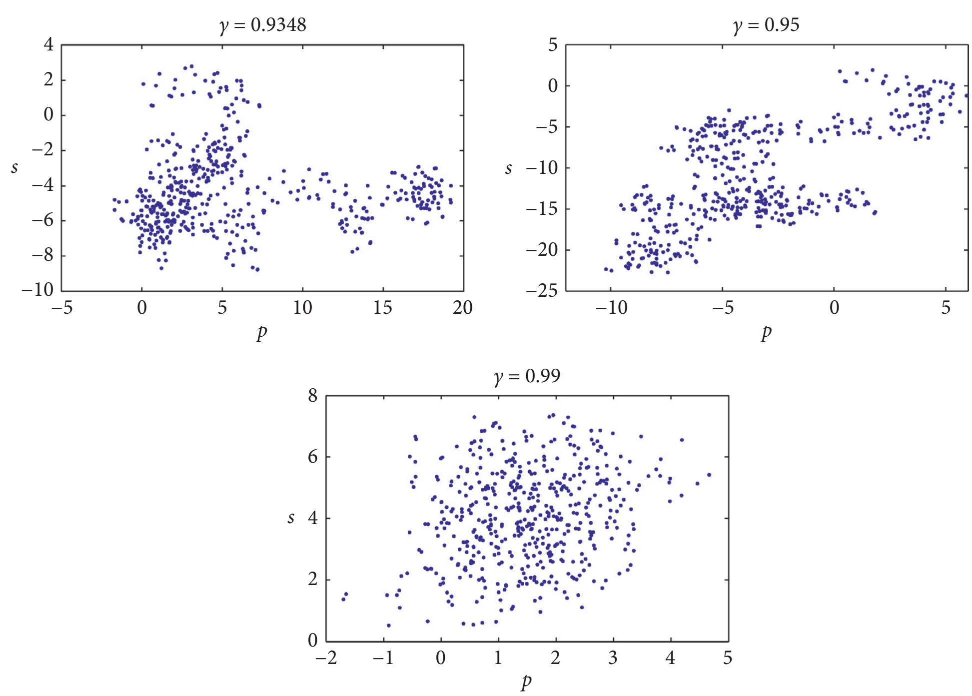

Figure 7: 0-1 test of the FoDs (1) for $\alpha = 1.73$ and subject to the initial conditions $(-1.78, 0.79)$ and for different values of γ.

Next, the translations functions p and s of the 0-1 test for different fractional-order values are plotted in Figure 7, and it fits well with the phase diagrams in Figure 4. In particular, Figure 7 depicts the Brownian-like trajectories for all the three fractional-order values indicating that the suggested map is chaotic in this case. To further confirm the results, we choose to plot a 3D view of the asymptotic growth rate K of the 0-1 test when $1.3 < \alpha \leq 1.9$ and by varying γ from 0.92 to 1 (see Figure 8). It is clear that the dynamics of system (1) shift to small intervals of α as the fractional order γ decreases and disappears as the fractional order and system parameter α values decrease.

4.2. Approximate Entropy. The approximate entropy (ApEn) [23] is the measurement of the degree of complexity of a series of data from a multidimensional perspective. This method estimates the regularity by assigning a nonnegative number, where higher values indicate higher complexity. By applying the technique in [23], we consider $(x_i)_{i=1,..,N}$ points that are obtained from discrete formula (4). The value of the approximate entropy depends on two important parameters, i.e., m and τ, where the input τ is the similar tolerance whereas m is the embedding dimension. We reconstruct a subsequence of x such that $\chi(i) = [x(i), \ldots, x(i+m-1)]$, where

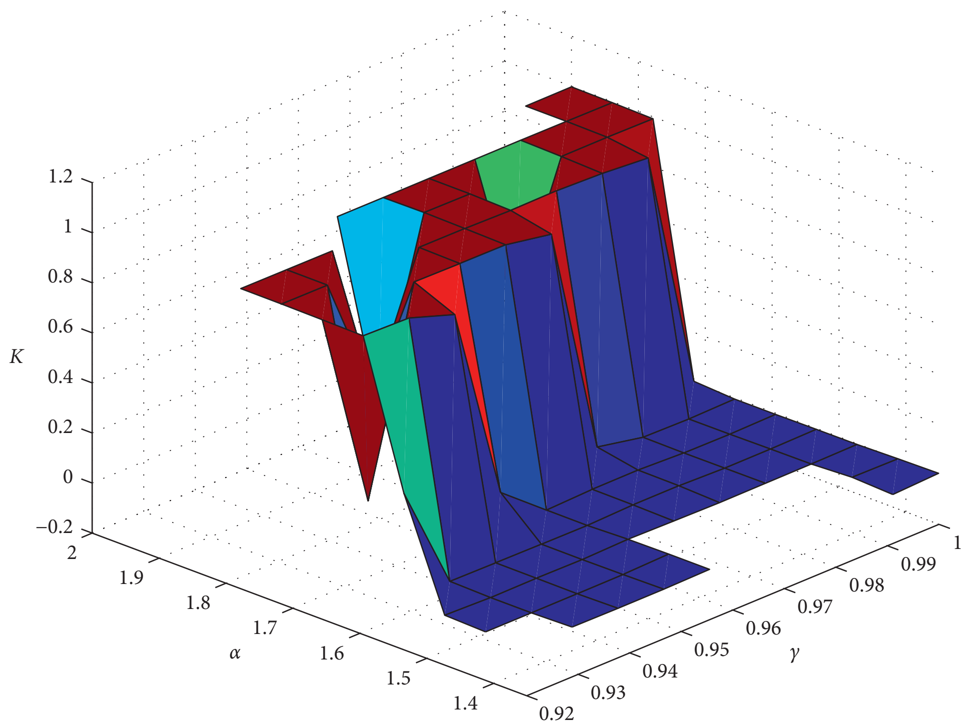

FIGURE 8: Asymptotic growth rate of the 0-1 test method of the fractional-order map (1) in three-dimensional space with the variation of system parameter α and fractional order γ.

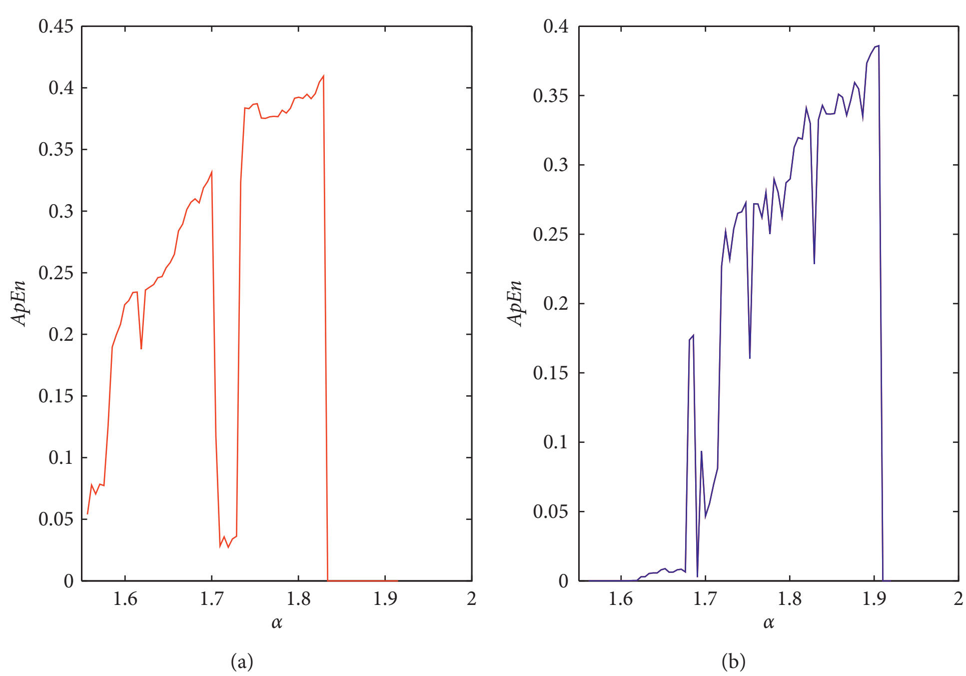

FIGURE 9: The approximate entropy (ApEn) of FoDs (1) versus α for (a) \$$\gamma = 0.9362$ and (b) $\gamma = 0.992$.

m presents the points from $x(i)$ to $x(i+m-1)$. Let K be the number of $\chi(i)$ such that the maximum absolute difference of two vectors $\chi(i)$ and $\chi(j)$ is lower or equal to the tolerance τ. The relative frequency of $\chi(i)$ is similar to $\chi(j)$, and it has the form $C_i^m(\tau) = K/(N-m+1)$. From C_i^m, we calculate the logarithm and then define the average for all i as follows:

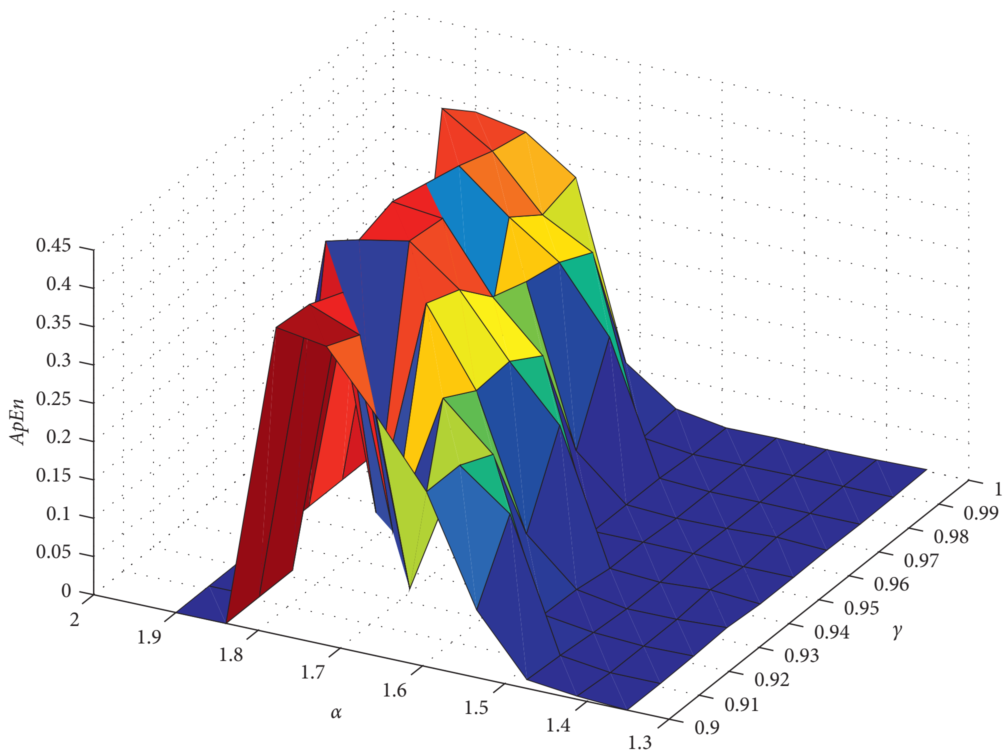

Figure 10: The approximate entropy (ApEn) of the fractional-order map (1) in three-dimensional space with the variation of system parameter α and fractional order γ.

$$\phi^m(r) = \frac{1}{N-m-1}\sum_{i=1}^{N-m+1}\log C_i^m(r). \tag{14}$$

Thus, the approximate entropy of order m is set as

$$\text{ApEn} = \phi^m(r) - \phi^{m+1}(r). \tag{15}$$

Herein, the structural complexity of FoDs (1) is analysed via equation (15) by varying the control parameter α and the fractional order γ as reported in Figures 9 and 10. In particular, the approximate entropy (ApEn) diagrams with two different initial conditions are plotted in Figure 9. It can be seen that the complexity of FoDs (1) strongly depends on the variations of γ and α. In particular, Figure 10 highlights that there are some combined values of α and γ for which the approximate entropy ApEn is high, indicating that FoDs (1) is characterized by complex dynamic behaviors for both initial conditions. The results agree will with the bifurcation diagrams in Figures 1 and 2.

5. Conclusions

Referring to a fractional-order discrete-time system (FoDs) with "hidden attractors," this paper has introduced a new 2D system without equilibrium points. The system possesses the interesting property of being characterized by the coexistence of various kinds of chaotic attractors, for various fractional-order values. Bifurcation diagrams, computation of the Largest Lyapunov Exponents (LLEs), and phase plots have been reported to investigate the dynamics of the map, indicating the effectiveness of the approach developed herein along with the 0-1 test. Finally, an entropy algorithm is used to measure the complexity of the proposed system.

Data Availability

The data that support the findings of this study are available within the article.

Conflicts of Interest

The authors declare no conflicts of interest.

Authors' Contributions

Adel Ouannas, Amina-Aicha Khennaoui, A. Othman Almatroud, and Iqbal M. Batiha conceptualized the study; data curation was performed by Amina-Aicha Khennaoui, M. Mossa Al-sawalha, Adel Ouannas, and Viet-Thanh Pham; Amina-Aicha Khennaoui, A. Othman Almatroud, Viet-Thanh Pham, and Iqbal M. Batiha conducted investigation; Adel Ouannas and Giuseppe Grassi formulated the methodology; Giuseppe Grassi supervised the work; and Adel Ouannas and Iqbal M. Batiha were involved in validation.

Acknowledgments

This work was supported by the Scientific Research Deanship at University of Ha'il- Saudi Arabia, though Project No. RG-191307.

References

[1] J. C. Sprott, *Elegant Chaos: Algebraically Simple Chaotic Flows*, World Scientific, Singapore, 2010.

[2] G. M. Zaslavsky and G. M. Zaslavskij, *Hamiltonian Chaos and Fractional Dynamics*, Oxford University Press on Demand, Oxford, England, 2005.

[3] G. A. Leonov, N. V. Kuznetsov, and V. I. Vagaitsev, "Hidden attractor in smooth Chua systems," *Physica D: Nonlinear Phenomena*, vol. 241, no. 18, pp. 1482–1486, 2012.

[4] G. A. Leonov and N. V. Kuznetsov, "Hidden attractors in dynamical systems. From hidden oscillations in hilbert-Kolmogorov, Aizerman, and Kalman problems to hidden chaotic attractor in chua circuits," *International Journal of Bifurcation and Chaos*, vol. 23, no. 01, p. 1330002, 2013.

[5] M. Molaie, S. Jafari, J. C. Sprott, and S. M. R. H. Golpayegani, "Simple chaotic flows with one stable equilibrium," *International Journal of Bifurcation and Chaos*, vol. 23, no. 11, p. 1350188, 2013.

[6] Z. Wei, "Dynamical behaviors of a chaotic system with no equilibria," *Physics Letters A*, vol. 376, no. 2, pp. 102–108, 2011.

[7] A. Ouannas, A.-A. Khennaoui, Z. Odibat, V.-T. Pham, and G. Grassi, "On the dynamics, control and synchronization of fractional-order Ikeda map," *Chaos, Solitons & Fractals*, vol. 123, pp. 108–115, 2019.

[8] A.-A. Khennaoui, A. Ouannas, S. Bendoukha, G. Grassi, R. P. Lozi, and V.-T. Pham, "On fractional-order discrete-time systems: chaos, stabilization and synchronization," *Chaos, Solitons & Fractals*, vol. 119, pp. 150–162, 2019.

[9] L. Jouini, A. Ouannas, A. A. Khennaoui, X. Wang, G. Grassi, and V. T. Pham, "The fractional form of a new three-dimensional generalized Henon map," *Advances in Difference Equations*, vol. 2019, no. 1, p. 122, 2019.

[10] G. C. Wu and D. Baleanu, "Discrete fractional logistic map and its chaos," *Nonlinear Dynamics*, vol. 75, no. 1-2, pp. 283–287, 2014.

[11] A. A. Khennaoui, A. Ouannas, S. Bendoukha et al., "Chaos, control, and synchronization in some fractional-order difference equations," *Advances in Difference Equations*, vol. 2019, no. 1, pp. 1–23, 2019.

[12] G.-C. Wu and D. Baleanu, "Discrete chaos in fractional delayed logistic maps," *Nonlinear Dynamics*, vol. 80, no. 4, pp. 1697–1703, 2015.

[13] A. Ouannas, A.-A. Khennaoui, G. Grassi, and S. Bendoukha, "On chaos in the fractional-order Grassi-Miller map and its control," *Journal of Computational and Applied Mathematics*, vol. 358, pp. 293–305, 2019.

[14] A. Ouannas, A.-A. Khennaoui, S. Bendoukha, and G. Grassi, "On the dynamics and control of a fractional form of the discrete double scroll," *International Journal of Bifurcation and Chaos*, vol. 29, no. 6, Article ID 1950078, 2019.

[15] A. Ouannas, X. Wang, A.-A. Khennaoui, S. Bendoukha, V.-T. Pham, and F. Alsaadi, "Fractional form of a chaotic map without fixed points: chaos, entropy and control," *Entropy*, vol. 20, no. 10, p. 720, 2018.

[16] A. A. Khennaoui, A. Ouannas, S. Boulaaras, V.-T. Pham, and A. Taher Azar, "A fractional map with hidden attractors: chaos and control," *The European Physical Journal Special Topics*, vol. 229, no. 6-7, pp. 1083–1093, 2020.

[17] A. Ouannas, A. A. Khennaoui, S. Momani, G. Grassi, and V. T. Pham, "Chaos and control of a three-dimensional fractional order discrete-time system with no equilibrium and its synchronization," *AIP Advances*, vol. 10, no. 4, p. 045310, 2020.

[18] A. Ouannas, A.-A. Khennaoui, S. Momani et al., "A quadratic fractional map without equilibria: bifurcation, 0-1 test, complexity, entropy, and control," *Electronics*, vol. 9, no. 5, p. 748, 2020.

[19] A. Ouannas, A. A. Khennaoui, S. Momani, V. T. Pham, and R. El-Khazali, "Hidden attractors in a new fractional-order discrete system: chaos, complexity, entropy, and control," *Chinese Physics B*, vol. 29, no. 5, p. 050504, 2020.

[20] T. Abdeljawad, "On Riemann and Caputo fractional differences," *Computers & Mathematics with Applications*, vol. 62, no. 3, pp. 1602–1611, 2011.

[21] D. Cafagna and G. Grassi, "An effective method for detecting chaos in fractional-order systems," *International Journal of Bifurcation and Chaos*, vol. 20, no. 3, pp. 669–678, 2010.

[22] G. A. Gottwald and I. Melbourne, "A new test for chaos in deterministic systems," *Proceedings of the Royal Society of London. Series A: Mathematical, Physical and Engineering Sciences*, vol. 460, no. 2042, pp. 603–611, 2004.

[23] S. M. Pincus, "Approximate entropy as a measure of system complexity," *Proceedings of the National Academy of Sciences*, vol. 88, no. 6, pp. 2297–2301, 1991.

Hindawi
Mathematical Problems in Engineering
Volume 2020, Article ID 7681479, 16 pages
https://doi.org/10.1155/2020/7681479

Research Article

Mathematical Analysis of Nonlocal Implicit Impulsive Problem under Caputo Fractional Boundary Conditions

Arshad Ali,[1] **Vidushi Gupta**,[2] **Thabet Abdeljawad**,[3,4,5] **Kamal Shah**,[1,3] **and Fahd Jarad**[6]

[1]*Department of Mathematics, University of Malakand, Dir (L), Khyber Pakhtunkhwa, Pakistan*
[2]*Department of Mathematics, Chandigarh University, Chandigarh, Punjab, India*
[3]*Department of Mathematics and General Sciences, Prince Sultan University, Riyadh, Saudi Arabia*
[4]*Department of Medical Research, China Medical University, Taichung, Taiwan*
[5]*Department of Computer Science and Information Engineering, Asia University, Taichung, Taiwan*
[6]*Department of Mathematics, Cankaya University, Ankara, Turkey*

Correspondence should be addressed to Thabet Abdeljawad; tabdeljawad@psu.edu.sa

Received 11 April 2020; Revised 14 August 2020; Accepted 20 August 2020; Published 30 November 2020

Guest Editor: Abdulrahman Al-khedhairi

This paper is related to frame a mathematical analysis of impulsive fractional order differential equations (IFODEs) under nonlocal Caputo fractional boundary conditions (NCFBCs). By using fixed point theorems of Schaefer and Banach, we analyze the existence and uniqueness results for the considered problem. Furthermore, we utilize the theory of stability for presenting Hyers-Ulam, generalized Hyers-Ulam, Hyers-Ulam-Rassias, and generalized Hyers-Ulam-Rassias stability results of the proposed scheme. Finally, some applications are offered to demonstrate the concept and results. The whole analysis is carried out by using Caputo fractional derivatives (CFDs).

1. Introduction

It has been observed that the focus of investigation has shifted from classical integer-order models to fractional-order models. It is because of the fact that many practical systems are excellently described by using fractional-order differential equations (FODEs) instead of classical differential equations. For basic theory and some important applications of fractional-order derivatives, we refer the readers to see [1–4] and the references therein. Many researchers are devoted to work in this area and made significant contribution in this regard; we refer the readers to the recent work in [5–10].

The study of implicit systems of FODEs with impulsive conditions is quite important as such systems appear in a variety of problems of applied nature, especially in biosciences, economics, engineering, etc. Such problems arise due to abrupt changes in the state of systems like earth quack, fluctuation of pendulum, etc. Here, we refer to some recent papers on impulsive problems [11–16]. The important class of FODEs known as IFODEs has been given much devotion by researchers. One of the most important aspects is investigation of problems under boundary conditions. Such problems mostly occur in engineering. Boundary and initial conditions may be local or nonlocal and both are important, and increasingly many problems have been investigated under these conditions. Replacing the local conditions by nonlocal ones produces a significant effect. This is due to the fact that the measurement computed from a nonlocal condition is usually more precise than the only one measurement given by a local condition. Therefore, the area of nonlocal boundary value problems has also attracted enough attention. In the last two decades, the area of IFODEs has been investigated from various directions including qualitative theory of existence of solution/solutions, stability, and numerical analysis. Therefore, IFODEs have also been investigated under nonlocal boundary conditions. For instance, Gupta and Dabas [17] studied the existence and uniqueness results for a class of IFODEs with nonlocal boundary conditions.

$$\begin{cases} {}_0^c\mathscr{D}_t^{\varrho} w(t) + f(t, w(t), w'(t)) = 0, & \varrho \in (1,2],\ t \in [0,1], \\ w(0) = 0,\ {}_0^c\mathscr{D}_t^{\varrho} w(1) = \delta\, {}_0^c\mathscr{D}_t^{\varrho} w(\rho), & 0 < \xi < 1,\ 0 < \rho \le 1. \end{cases} \tag{1}$$

By employing the fixed point technique, the authors obtained the existence and uniqueness results.

This paper can be considered as generalization of the aforesaid work, in which we discuss existence, uniqueness, and various stability results for the following implicit IFODEs with three point NCFBCs of order $\varrho \in (1,2]$:

$$\begin{cases} {}_0^c\mathscr{D}_t^{\varrho} w(t) - f\left(t, w(t), {}_0^c\mathscr{D}_t^{\varrho} w(t)\right) = 0, & t \in [0,T], \\ \Delta w(t_q) = \mathscr{I}_q\left(w(t_q^-)\right), \Delta\left({}_0^c\mathscr{D}_t^{\nu} w(t_q)\right) = \mathscr{J}_q\left(w(t_q^-)\right), & \nu \in (0,1],\ q = 1,2,\dots,\mathbf{r}, \\ w(0) = 0,\ {}_0^c\mathscr{D}_t^{\varrho} w(T) = \delta\, {}_0^c\mathscr{D}_t^{\xi} w(\rho), & 0 < \delta < \xi < 1,\ 0 < \rho < 1. \end{cases} \tag{2}$$

In the proposed problem, the notation ${}_0^c\mathscr{D}_t^{\varrho}$, ${}_0^c\mathscr{D}_t^{\nu}$, and ${}_0^c\mathscr{D}_t^{\xi}$ represent Caputo fractional derivatives of orders ϱ, ν, and ξ, respectively, where the points 0 and t in the subscript of the differential operator $\mathscr{D}$ are actually the limits of the definite integral involved in the definition of CFD. The function $f\colon [0,T] \times \mathscr{R} \times \mathscr{R} \longrightarrow \mathscr{R}$ is continuous, where $\mathscr{R}$ is the set of real numbers. The impulsive functions $\mathscr{I}_q$ and $\mathscr{J}_q$ in C(R, R) are bounded. For the sequence $0 = t^{0<t_1<\cdots<t_{\mathrm{r}}<t_{\mathrm{r}+1}=T}$, we have $\Delta w(t_{\mathrm{q}}) = w(t_{\mathrm{q}}^+) - w(t_{\mathrm{q}}^-)$ and $\Delta\left({}_0^c\mathscr{D}_t^{\nu} w(t_{\mathrm{q}})\right) = \left({}_0^c\mathscr{D}_t^{\nu} w(t_{\mathrm{q}}^+)\right) - \left({}_0^c\mathscr{D}_t^{\nu} w(t_{\mathrm{q}}^-)\right), w(t_{\mathrm{q}}^+) = \lim_{h\longrightarrow 0} w(t_{\mathrm{q}} + h)$, and $w(t_{\mathrm{q}}^-) = \lim_{h\longrightarrow 0} w(t_{\mathrm{q}} - h)$ represents the right-hand and left-hand limits of $w(t)$ at $t = t_{\mathrm{q}}$, respectively, with $w(t_{\mathrm{q}}^-) = w(t_{\mathrm{q}})$. The speciality of this proposed problem is that the nonlinear term depends not only on the unknown function but also on its fractional derivative compared with the available results in the literature. This type of study has rarely been discussed in the literature because of the complexity of fractional impulsive surfaces. The further organization of this manuscript is divided into four parts as follows: The second part of the paper demonstrates the preliminary portion in which we recall to readers the basics of used theory, notations, and definitions. The third part presents an existence result by employing Schaefer's fixed point theorem. The fourth section is introduced to analyze and study several stability results of the considered problem, and the last section is provided to illustrate the applications of the obtained results.

2. Preliminaries

We take $\mathscr{S} = [0,T]$, $\mathscr{S}_0 = [0,t_1]$, and $\mathscr{S}_{\mathrm{q}} = (t_q, t_{q+1}]$. We introduce the following space of piecewise continuous functions by

$$\mathscr{B} = PC(\mathscr{S},\mathscr{R}) = \{w\colon \mathscr{S} \longrightarrow \mathscr{R} \mid w \in C(\mathscr{S}), q = 1,2,\dots,\mathbf{r}, w\left(t_{\mathrm{q}}^+\right), w\left(t_{\mathrm{q}}^-\right) \text{ exist for } q = 1,2,\dots,\mathbf{r}\}, \tag{3}$$

where $\mathscr{B}$ is the Banach space corresponding to the norm $\|w\|_{\mathscr{B}} = \max_{t\in\mathscr{S}} |w(t)|$.

Definition 1 (see [18]). The fractional order integral of function $g \in L^1([a,b],\mathscr{R}^+)$ of order $\varrho \in \mathscr{R}^+$ is defined by

$$I_a^{\varrho} g(t) = \int_a^t \frac{(t-\eta)^{\varrho-1}}{\Gamma(\varrho)} g(\eta)\mathrm{d}\eta, \tag{4}$$

where Γ is the gamma function.

Definition 2 (see [18]). For a function g given on interval $[a,b]$, the CFD of g is defined by

$${}_0^c\mathscr{D}_t^{\varrho} g(t) = \frac{1}{\Gamma(n-\varrho)} \int_a^t (t-\eta)^{n-\varrho-1} g^{(n)}(\eta)\mathrm{d}\eta, \tag{5}$$

where $n = [\varrho] + 1$.

Let there exist constants $\beta > 0$ and $\epsilon > 0$ and a nondecreasing function $\Phi \in C(\mathscr{S},\mathscr{R})$, such that the following inequalities exist for $q = 1,2,\dots,\mathbf{r}$:

$$\begin{cases} \left|{}_0^c\mathscr{D}_t^{\varrho} h(t) - f\left(t, h(t), {}_0^c\mathscr{D}_t^{\varrho} h(t)\right)\right| \le \epsilon, & t \in \mathscr{S}, \\ \left|\Delta h(t_q) - \mathscr{I}_q\left(h(t_q^-)\right)\right| \le \epsilon, \\ \left|\Delta\left({}_0^c\mathscr{D}_t^{\varrho} h(t_q)\right) - \mathscr{J}_q\left(h(t_q^-)\right)\right| \le \epsilon, \end{cases} \tag{6}$$

$$\begin{cases} \left|{}_0^c\mathscr{D}_t^{\varrho} h(t) - f\left(t, h(t), {}_0^c\mathscr{D}_t^{\varrho} h(t)\right)\right| \le \Phi(t), & t \in \mathscr{S}, \\ \left|\Delta h(t_q) - \mathscr{I}_q\left(h(t_q^-)\right)\right| \le \beta, \\ |\Delta\left({}_0^c\mathscr{D}_t^{\varrho}\left(h(t_q)\right) - \mathscr{J}_q\left(h(t_q^-)\right)\right) \le \beta, \end{cases} \tag{7}$$

$$\begin{cases} \left|{}_0^c\mathscr{D}_t^{\varrho} h(t) - f\left(t, h(t), {}_0^c\mathscr{D}_t^{\varrho} h(t)\right)\right| \le \epsilon\Phi(t), & t \in \mathscr{S}, \\ \left|\Delta h(t_q) - \mathscr{I}_q\left(h(t_q^-)\right)\right| \le \epsilon\beta, \\ \left|\Delta\left({}_0^c\mathscr{D}_t^{\nu} h(t_q)\right) - \mathscr{J}_q\left(h(t_q^-)\right)\right| \le \epsilon\beta. \end{cases} \tag{8}$$

Definition 3 (see [19]). If for $\epsilon > 0$ there exists a constant $\mathscr{C} > 0$ such that for any solution $h \in \mathscr{B}$ of inequality (6), there is a unique solution $w \in \mathscr{B}$ of problem (2) which satisfies

$$|h(t) - w(t)| \le \mathscr{C}\epsilon, \quad t \in \mathscr{S}, \tag{9}$$

then problem (2) is called Hyers-Ulam stable.

Definition 4 (see [19]). If for $\epsilon > 0$ and set of positive real numbers $\mathscr{R}^+$ there exists $\psi \in C(\mathscr{R}^+, \mathscr{R}^+)$, such that for any solution $h \in \mathscr{B}$ of inequality (6), there is a unique solution $w \in \mathscr{B}$ of problem (2) which satisfies

$$|h(t) - w(t)| \leq \psi(\varepsilon), \quad t \in \mathscr{S}, \tag{10}$$

then problem (2) is called generalized Hyers-Ulam stable.

Definition 5 (see [19]). If for $\epsilon > 0$ there exists a real number $\mathscr{C} > 0$, such that for any solution $h \in \mathscr{B}$ of inequality (8), there is a unique solution $w \in \mathscr{B}$ of problem (2) which satisfies

$$|h(t) - w(t)| \leq \mathscr{C}\varepsilon(\Phi(t) + \psi), \quad t \in \mathscr{S}, \tag{11}$$

then problem (2) is called Hyers-Ulam-Rassias stable with respect to (Φ, ψ).

Definition 6 (see [19]). If there exists constant $\mathscr{C} > 0$, such that for any solution $h \in \mathscr{B}$ of inequality (7), there is a unique solution $w \in \mathscr{B}$ of problem (2) which satisfies

$$|h(t) - w(t)| \leq \mathscr{C}(\Phi(t) + \psi), \quad t \in \mathscr{S}, \tag{12}$$

then problem (2) is called generalized Hyers-Ulam-Rassias stable with respect to (Φ, ψ).

Here, it is to be noted that Definitions 3–6 have been adopted from the paper [19].

Remark 1. The function $h \in \mathscr{B}$ is called a solution for inequality (6) if there exists a function $\phi \in \mathscr{B}$ together with a sequence ϕ_q, where $q = 1, 2, \ldots, \mathbf{r}$ (which depends on h) such that

(i) $|\phi(t)| \leq \epsilon, |\phi_q| \leq \epsilon$, $t \in \mathscr{S}, q = 1, 2, \ldots, \mathbf{r}$

(ii) ${}_0^c\mathscr{D}_t^\varrho h(t) = f(t, h(t), {}_0^c\mathscr{D}_t^\varrho h(t)) + \phi(t)$, $t \in \mathscr{S}, q = 1, 2, \ldots, \mathbf{r}$

(iii) $\Delta h(t_q) = \mathscr{I}_q(h(t_q^-)) + \phi_q\, t \in \mathscr{S}, q = 1, 2, \ldots, \mathbf{r}$

(iv) $\Delta({}_0^c\mathscr{D}_t^\gamma h(t_q)) = \mathscr{J}_q(h(t_q^-)) + \phi_q$, $t \in \mathscr{S}, q = 1, 2, \ldots, \mathbf{r}$

Remark 2. A function $h \in \mathscr{B}$ is a solution of inequality (8) if there exists a function $\phi \in \mathscr{B}$ and a sequence ϕ_q, where $q = 1, 2, \ldots, \mathbf{r}$ (which depends on h) such that

(i) $|\phi(t)| \leq \epsilon\theta(t), |\phi_q| \leq \epsilon\varphi$, $t \in \mathscr{S}, q = 1, 2, \ldots, \mathbf{r}$

(ii) ${}_0^c\mathscr{D}_t^\varrho h(t) = f(t, h(t), {}_0^c\mathscr{D}_t^\varrho h(t)) + \phi(t)$, $t \in \mathscr{S}, q = 1, 2, \ldots, \mathbf{r}$

(iii) $\Delta h(t_q) = \mathscr{I}_q(h(t_q^-)) + \phi_q$, $t \in \mathscr{S}, q = 1, 2, \ldots, \mathbf{r}$

(iv) $\Delta({}_0^c\mathscr{D}_t^\gamma h(t_q)) = \mathscr{J}_q(h(t_q^-)) + \phi_q$, $t \in \mathscr{S}, q = 1, 2, \ldots, \mathbf{r}$

Lemma 1 (see [20]). *For $\varrho > 0$, the given result holds:*

$${}_0I_t^\varrho({}_0^c\mathscr{D}_t^\varrho g(t)) = g(t) - \sum_{i=0}^{n-1} c_i t^i, \quad \text{where } n = [\varrho] + 1. \tag{13}$$

To investigate the nonlinear IFODE2, we first consider the associated linear problem and obtain its solution.

Lemma 2. *Let $\varrho \in (1,2)$ and σ: $[0,T] \longrightarrow \mathscr{R}$ be continuous. A function $w(t)$ is a solution of the fractional integral equation:*

$$w(t) = \begin{cases} \displaystyle\int_0^t \frac{(t-\eta)^{\varrho-1}}{\Gamma(\varrho)}\sigma(\eta)\mathrm{d}\eta - t\left[\frac{\Gamma(2-\xi)}{\left(\delta\rho^{1-\xi} - T^{1-\xi}\right)}\left(\delta\int_0^\rho \frac{(\rho-\eta)^{\varrho-\xi-1}}{\Gamma(\varrho-\xi)}\sigma(\eta)\mathrm{d}\eta\right.\right. \\ \displaystyle\left.\left. - \int_0^T \frac{(T-\eta)^{\varrho-\xi-1}}{\Gamma(\varrho-\xi)}\sigma(\eta)\mathrm{d}\eta\right) + \sum_{i=1}^{q}\left(\frac{\Gamma(2-\nu)}{t_i^{1-\nu}}\mathscr{J}_i(w(t_i^-))\right)\right], \quad t \in [0, t_1], q = 1, 2, \ldots, \mathbf{r}, \\ \displaystyle\int_0^t \frac{(t-\eta)^{\varrho-1}}{\Gamma(\varrho)}\sigma(\eta)\mathrm{d}\eta + \sum_{i=1}^{q}\mathscr{I}_i(w(t_i^-)) - t\left[\frac{\Gamma(2-\xi)}{\left(\delta\rho^{1-\xi} - T^{1-\xi}\right)}\left(\delta\int_0^\rho \frac{(\rho-\eta)^{\varrho-\xi-1}}{\Gamma(\varrho-\xi)}\sigma(\eta)\mathrm{d}\eta\right.\right. \\ \displaystyle\left.\left. - \int_0^T \frac{(T-\eta)^{\varrho-\xi-1}}{\Gamma(\varrho-\xi)}\sigma(\eta)\mathrm{d}\eta\right) + \sum_{i=1}^{q}\left(\frac{\Gamma(2-\nu)}{t_i^{1-\nu}}\mathscr{J}_i(w(t_i^-))\right)\right] + \sum_{i=1}^{q}(t-t_i) \\ \displaystyle\cdot\left(\frac{\Gamma(2-\nu)}{t_i^{1-\nu}}\mathscr{J}_i(w(t_i^-))\right), \quad t \in \left(t_q, t_{q+1}\right], q = 1, 2, \ldots, \mathbf{r}, \end{cases} \tag{14}$$

if and only if $w(t)$ is a solution of the following BVP:

$$\begin{cases} {}_0^c\mathscr{D}_t^{\varrho} w(t) - \sigma(t) = 0, \quad \varrho \in (1,2], \\ \Delta w\left(t_q\right) = \mathscr{I}_q\left(w\left(t_q^-\right)\right), \quad \Delta\left({}_0^c\mathscr{D}_t^{\nu} w\left(t_q\right)\right) = \mathscr{J}_q\left(w\left(t_q^-\right)\right), \quad \nu \in (0,1],\ q = 1,2,\ldots,\mathbf{r}, \\ w(0) = 0,\ {}_0^c\mathscr{D}_t^{\xi} w(T) = \delta\, {}_0^c\mathscr{D}_t^{\xi} w(\rho), \quad 0 < \delta < \xi < 1. \end{cases} \tag{15}$$

Proof. Let for $t \in [0, t_1)$, $w(t)$ be the solution of (15), then by Lemma 1, we have

$$w(t) = \int_0^t \frac{(t-\eta)^{\varrho-1}}{\Gamma(\varrho)} \sigma(\eta) \mathrm{d}\eta - c_0 - c_1 t. \tag{16}$$

Using the condition $w(0) = 0$, we get

$$c_0 = 0. \tag{17}$$

Substituting c_0 in (16), we get

$$w(t) = \int_0^t \frac{(t-\eta)^{\varrho-1}}{\Gamma(\varrho)} \sigma(\eta) \mathrm{d}\eta - c_1 t. \tag{18}$$

For $t \in (t_1, t_2]$, we get

$$w(t) = \int_0^t \frac{(t-\eta)^{\varrho-1}}{\Gamma(\varrho)} \sigma(\eta) \mathrm{d}\eta - c_2 - c_3 t. \tag{19}$$

Applying the impulsive condition $\Delta w(t_1) = \mathscr{I}_1(w(t_1^-))$, we get

$$\begin{aligned} \mathscr{I}_1\left(w\left(t_1^-\right)\right) &= -c_2 - c_3 t_1 + c_1 t_1, \\ -c_2 &= \mathscr{I}_1\left(w\left(t_1^-\right)\right) + c_3 t_1 - c_1 t_1. \end{aligned} \tag{20}$$

Substituting c_2 in (19), we get

$$w(t) = \int_0^t \frac{(t-\eta)^{\varrho-1}}{\Gamma(\varrho)} \sigma(\eta) \mathrm{d}\eta + \mathscr{I}_1\left(w\left(t_1^-\right)\right) + c_3 t_1 - c_1 t_1 - c_3 t, \tag{21}$$

$$w(t) = \int_0^t \frac{(t-\eta)^{\varrho-1}}{\Gamma(\varrho)} \sigma(\eta) \mathrm{d}\eta + \mathscr{I}_1\left(w\left(t_1^-\right)\right) - c_1 t_1 + c_3 \left(t_1 - t\right). \tag{22}$$

From equations (18) and (22), we get

$$\begin{aligned} {}_0^c\mathscr{D}_t^{\nu} w(t) &= \frac{1}{\Gamma(\varrho-\nu)} \int_0^t (t-\eta)^{\varrho-\nu-1} \sigma(\eta) \mathrm{d}\eta - c_3 \frac{t^{1-\nu}}{\Gamma(2-\nu)}, \\ {}_0^c\mathscr{D}_t^{\nu} w(t) &= \frac{1}{\Gamma(\varrho-\nu)} \int_0^t (t-\eta)^{\varrho-\nu-1} \sigma(\eta) \mathrm{d}\eta - c_1 \frac{t^{1-\nu}}{\Gamma(2-\nu)}. \end{aligned} \tag{23}$$

Now, using the impulsive condition $\Delta({}_0^c\mathscr{D}_t^{\nu} w\ (t_1)) = \mathscr{J}_1(w(t_1^-))$, we get

$$\begin{aligned} \mathscr{J}_1\left(w\left(t_1^-\right)\right) &= -c_3 \frac{t_1^{1-\nu}}{\Gamma(2-\nu)} + c_1 \frac{t_1^{1-\nu}}{\Gamma(2-\nu)}, \\ c_3 &= -\frac{\Gamma(2-\nu)}{t_1^{1-\nu}} \mathscr{J}_1\left(w\left(t_1^-\right)\right) + c_1. \end{aligned} \tag{24}$$

Substituting c_3 in (22), we get

$$\begin{aligned} w(t) = &\int_0^t \frac{(t-\eta)^{\varrho-1}}{\Gamma(\varrho)} \sigma(\eta) \mathrm{d}\eta + \mathscr{I}_1\left(w\left(t_1^-\right)\right) \\ &+ \left(t - t_1\right) \frac{\Gamma(2-\nu)}{t_1^{1-\nu}} \mathscr{J}_1\left(w\left(t_1^-\right)\right) - c_1 t. \end{aligned} \tag{25}$$

For $t \in (t_2, t_3]$, we get

$$w(t) = \int_0^t \frac{(t-\eta)^{\varrho-1}}{\Gamma(\varrho)} \sigma(\eta) \mathrm{d}\eta - c_4 - c_5 t. \tag{26}$$

Applying the impulsive condition $\Delta w(t_2) = \mathscr{I}_2(w(t_2^-))$ in (26) and (25), we get

$$\begin{aligned} \mathscr{I}_2\left(w\left(t_2^-\right)\right) = &-c_4 - c_5 t_2 - \mathscr{I}_1\left(w\left(t_1^-\right)\right) \\ &- \left(t_2 - t_1\right) \frac{\Gamma(2-\nu)}{t_1^{1-\nu}} \mathscr{J}_1\left(w\left(t_1^-\right)\right) + c_1 t_2, \\ -c_4 = &\mathscr{I}_2\left(w\left(t_2^-\right)\right) + c_5 t_2 + \mathscr{I}_1\left(w\left(t_1^-\right)\right) \\ &+ \left(t_2 - t_1\right) \frac{\Gamma(2-\nu)}{t_1^{1-\nu}} \mathscr{J}_1\left(w\left(t_1^-\right)\right) - c_1 t_2. \end{aligned} \tag{27}$$

Substituting c_4 in (26), we get

$$\begin{aligned} w(t) = &\int_0^t \frac{(t-\eta)^{\varrho-1}}{\Gamma(\varrho)} \sigma(\eta) \mathrm{d}\eta + \mathscr{I}_2\left(w\left(t_2^-\right)\right) + c_5 t_2 + \mathscr{I}_1 \\ &\cdot \left(w\left(t_1^-\right)\right) + \left(t_2 - t_1\right) \frac{\Gamma(2-\nu)}{t_1^{1-\nu}} \mathscr{J}_1\left(w\left(t_1^-\right)\right) - c_1 t_2 - c_5 t. \end{aligned} \tag{28}$$

By equations (25) and (28), we get

$$\begin{aligned} {}_0^c\mathscr{D}_t^{\nu} w(t) &= \frac{1}{\Gamma(\varrho-\nu)} \int_0^t (t-\eta)^{\varrho-\nu-1} \sigma(\eta) \mathrm{d}\eta - c_5 \frac{t^{1-\nu}}{\Gamma(2-\nu)}, \\ {}_0^c\mathscr{D}_t^{\nu} w(t) &= \frac{1}{\Gamma(\varrho-\nu)} \int_0^t (t-\eta)^{\varrho-\nu-1} \sigma(\eta) \mathrm{d}\eta \\ &\quad + \left(\frac{\Gamma(2-\nu)}{t_1^{1-\nu}} \mathscr{J}_1\left(w\left(t_1^-\right)\right) - c_1\right) \frac{t^{1-\nu}}{\Gamma(2-\nu)}. \end{aligned} \tag{29}$$

Now, using the impulsive condition $\Delta({}_0^c\mathscr{D}_t^{\nu} w(t_2)) = \mathscr{J}_2(w(t_2^-))$, we get

$$\mathcal{J}_2(w(t_2^-)) = -c_5\frac{t_2^{1-\nu}}{\Gamma(2-\nu)} - \left(\frac{\Gamma(2-\nu)}{t_1^{1-\nu}}\mathcal{J}_1(w(t_1^-)) - c_1\right)\frac{t_2^{1-\nu}}{\Gamma(2-\nu)},$$

$$c_5 = -\frac{\Gamma(2-\nu)}{t_1^{1-\nu}}\mathcal{J}_1(w(t_1^-)) - \frac{\Gamma(2-\nu)}{t_2^{1-\nu}}\mathcal{J}_2(w(t_2^-)) + c_1. \tag{30}$$

Substituting c_5 in (28), we get

$$\begin{aligned} w(t) &= \int_0^t \frac{(t-\eta)^{\varrho-1}}{\Gamma(\varrho)}\sigma(\eta)\mathrm{d}\eta + \mathcal{J}_1(w(t_1^-)) + \mathcal{J}_2(w(t_2^-)) \\ &+ \frac{\Gamma(2-\nu)}{t_1^{1-\nu}}\mathcal{J}_1(w(t_1^-))(t-t_1) \\ &+ \frac{\Gamma(2-\nu)}{t_2^{1-\nu}}\mathcal{J}_2(w(t_2^-))(t-t_2) - c_1 t. \end{aligned} \tag{31}$$

Similarly for $t \in \mathcal{S}_q$, we get

$$\begin{aligned} w(t) &= \int_0^t \frac{(t-\eta)^{\varrho-1}}{\Gamma(\varrho)}\sigma(\eta)\mathrm{d}\eta + \sum_{\imath=1}^{q}\mathcal{J}_\imath(w(t_\imath^-)) - c_1 t \\ &+ \sum_{\imath=1}^{q}(t-t_\imath)\left(\frac{\Gamma(2-\nu)}{t_i^{1-\nu}}\mathcal{J}_\imath(w(t_\imath^-))\right), \\ {}_0^c\mathcal{D}_t^{\nu} w(t) &= \int_0^t \frac{(t-\eta)^{\varrho-\xi-1}}{\Gamma(\varrho-\xi)}\sigma(\eta)\mathrm{d}\eta - c_1\frac{t^{1-\xi}}{\Gamma(2-\xi)} \\ &+ \left(\frac{t^{1-\xi}}{\Gamma(2-\xi)}\right)\sum_{\imath=1}^{q}\left(\frac{\Gamma(2-\nu)}{t_i^{1-\nu}}\mathcal{J}_\imath(w(t_\imath^-))\right). \end{aligned} \tag{32}$$

Using the boundary conditions, ${}_0^c\mathcal{D}_t^{\xi} w(T) = \delta\, {}_0^c\mathcal{D}_t^{\xi} w(\rho)$, we get

$$\begin{aligned} {}_0^c\mathcal{D}_t^{\xi} w(T) &= \int_0^T \frac{(T-\eta)^{\varrho-\xi-1}}{\Gamma(\varrho-\xi)}\sigma(\eta)\mathrm{d}\eta - c_1\frac{T^{1-\xi}}{\Gamma(2-\xi)} + \left(\frac{T^{1-\xi}}{\Gamma(2-\xi)}\right)\sum_{\imath=1}^{q}\left(\frac{\Gamma(2-\nu)}{t_i^{1-\nu}}\mathcal{J}_\imath(w(t_\imath^-))\right), \\ \delta\, {}_0^c\mathcal{D}_t^{\xi} w(\rho) &= \delta\int_0^\rho \frac{(\rho-\eta)^{\varrho-\xi-1}}{\Gamma(\varrho-\xi)}\sigma(\eta)\mathrm{d}\eta - \delta c_1\frac{\rho^{1-\xi}}{\Gamma(2-\xi)} + \delta\left(\frac{\rho^{1-\xi}}{\Gamma(2-\xi)}\right)\sum_{\imath=1}^{q}\left(\frac{\Gamma(2-\nu)}{t_i^{1-\nu}}\mathcal{J}_\imath(w(t_\imath^-))\right), \\ c_1\frac{\left(\delta\rho^{1-\xi} - T^{1-\xi}\right)}{\Gamma(2-\xi)} &= \delta\int_0^\rho \frac{(\rho-\eta)^{\varrho-\xi-1}}{\Gamma(\varrho-\xi)}\sigma(\eta)\mathrm{d}\eta + \delta\left(\frac{\rho^{1-\xi}}{\Gamma(2-\xi)}\right)\sum_{\imath=1}^{q}\left(\frac{\Gamma(2-\nu)}{t_i^{1-\nu}}\mathcal{J}_\imath(w(t_\imath^-))\right) \\ &- \int_0^T \frac{(T-\eta)^{\varrho-\xi-1}}{\Gamma(\varrho-\xi)}\sigma(\eta)\mathrm{d}\eta - \left(\frac{T^{1-\xi}}{\Gamma(2-\xi)}\right)\sum_{\imath=1}^{q}\left(\frac{\Gamma(2-\nu)}{t_i^{1-\nu}}\mathcal{J}_\imath(w(t_\imath^-))\right), \\ c_1 &= \frac{\Gamma(2-\xi)}{\left(\delta\rho^{1-\xi} - T^{1-\xi}\right)}\left[\delta\int_0^\rho \frac{(\rho-\eta)^{\varrho-\xi-1}}{\Gamma(\varrho-\xi)}\sigma(\eta)\mathrm{d}\eta - \int_0^T \frac{(T-\eta)^{\varrho-\xi-1}}{\Gamma(\varrho-\xi)}\sigma(\eta)\mathrm{d}\eta\right] + \sum_{\imath=1}^{q}\left(\frac{\Gamma(2-\nu)}{t_i^{1-\nu}}\mathcal{J}_\imath(w(t_\imath^-))\right). \end{aligned} \tag{33}$$

By substituting the value of c_1 and summarizing, we get the required result.

Conversely, assume that u satisfies the impulsive fractional integral equation (8); then by direct computation, it can be seen that the solution given by (14) satisfies (15).

Corollary 1. *In view of the Lemma 2, problem (2) has the following solution:*

$$w(t) = \begin{cases} \displaystyle\int_0^t \frac{(t-\eta)^{\varrho-1}}{\Gamma(\varrho)} f\left(\eta, w(\eta), {}_0^c\mathcal{D}_t^{\varrho} w(\eta)\right)\mathrm{d}\eta - \mathcal{U}, & t \in [0, t_1], \\ \displaystyle\int_0^t \frac{(t-\eta)^{\varrho-1}}{\Gamma(\varrho)} f\left(\eta, w(\eta), {}_0^c\mathcal{D}_t^{\varrho} w(\eta)\right)\mathrm{d}\eta + \sum_{\imath=1}^{q}\mathcal{J}_\imath(w(t_\imath^-)) - \mathcal{U} & \\ \displaystyle+ \sum_{\imath=1}^{q}(t-t_\imath)\left(\frac{\Gamma(2-\nu)}{t_i^{1-\nu}}\mathcal{J}_\imath(w(t_\imath^-))\right), & t \in \left(t_q, t_{q+1}\right],\ q = 1, 2, \ldots, \mathbf{r}, \end{cases} \tag{34}$$

where

$$\mathcal{U} = \frac{\Gamma(2-\xi)t}{\left(\delta\rho^{1-\xi} - T^{1-\xi}\right)}\delta\int_0^\rho \frac{(\rho-\eta)^{\varrho-\xi-1}}{\Gamma(\varrho-\xi)} f\left(\eta, w(\eta), {}_0^c\mathcal{D}_t^\varrho w(\eta)\right)\mathrm{d}\eta - \frac{\Gamma(2-\xi)t}{\left(\delta\rho^{1-\xi} - T^{1-\xi}\right)}\int_0^T \frac{(T-\eta)^{\varrho-\xi-1}}{\Gamma(\varrho-\xi)} f\left(\eta, w(\eta), {}_0^c\mathcal{D}_t^\varrho w\cdot(\eta)\right)\mathrm{d}\eta + t\sum_{\imath=1}^{q}\left(\frac{\Gamma(2-\nu)}{t_i^{1-\nu}}\mathcal{I}_\imath\left(w\left(t_\imath^-\right)\right)\right), \quad q = 1, 2, \ldots, \mathbf{r}. \tag{35}$$

3. Existence and Uniqueness Results

In this section, we shall prove our main results. For which, we assume the following assumptions:

(H_1) Let there exist positive constants L_1, L_2, L_3, and L_4 such that for $t \in [0, T]$ and all $w_1, w_2, h_1, h_2 \in \mathcal{R}$, the following inequalities hold:

$$\begin{aligned}
\left|f(t, w_1(t), h_1(t)) - f(t, w_2(t), h_2(t))\right| &\leq L_1\left|w_1(t) - w_2(t)\right| + L_2\left|h_1(t) - h_2(t)\right|,\\
\left|\mathcal{I}_\imath(w_1)\left(t_\imath^-\right) - \mathcal{I}_\imath(w_2)\left(t_\imath^-\right)\right| &\leq L_3\left|w_1\left(t_\imath^-\right) - w_2\left(t_\imath^-\right)\right|,\\
\left|\mathcal{J}_\imath(w_1)\left(t_\imath^-\right) - \mathcal{J}_\imath(w_2)\left(t_\imath^-\right)\right| &\leq L_4\left|w_1\left(t_\imath^-\right) - w_2\left(t_\imath^-\right)\right|.
\end{aligned} \tag{36}$$

(H_2) Let the functions $a_1, a_2, a_3 \in C([0, T], \mathcal{R}^+)$, which satisfy

$$\left|f\left(t, w(t), \mathcal{Y}_w(t)\right)\right| \leq a_1(t) + a_2(t)|w| + a_3(t)\left|\mathcal{Y}_w(t)\right|, \quad \text{for } t \in \mathcal{S}, w \in \mathcal{B}. \tag{37}$$

such that $a_3^* = \sup_{t\in[0,T]}|a_3(t)| < 1$.

(H_3) If $f, \mathcal{I}_\imath$, and $\mathrm{J}_\imath$ are continuous functions such that for all $w, h \in \mathcal{R}$, the following inequalities hold:

$$\begin{aligned}
\left|\mathcal{I}_\imath\left(w\left(t_\imath^-\right)\right)\right| &\leq \mathrm{C}_{\mathcal{I}_\imath}|w| + M_{\mathcal{I}}, \mathrm{C}_{\mathcal{I}_\imath}, M_{\mathcal{I}} > 0,\\
\left|\mathrm{J}_\imath\left(w\left(t_\imath^-\right)\right)\right| &\leq \mathrm{C}_{J_\imath}|w| + M_J, \mathrm{C}_{J_\imath}, M_J > 0.
\end{aligned} \tag{38}$$

(H_4) Let there exist constants $\beta > 0$ and $\epsilon > 0$ and a nondecreasing function $\Phi \in C(\mathcal{S}, \mathcal{R})$, such that the following inequalities hold:

$${}_0I_t^\varrho\Phi(t) \leq \beta\Phi(t); \text{ consequently } {}_0I_t^\varrho\Phi(t) \leq \beta\Phi(t). \tag{39}$$

We transform problem (2) into a fixed point problem. Considering an operator $\mathcal{N}: \mathcal{B} \longrightarrow \mathcal{B}$, defined by

$$(\mathcal{N}w)(t) = \begin{cases}
\displaystyle\int_0^t \frac{(t-\eta)^{\varrho-1}}{\Gamma(\varrho)}\mathcal{Y}_w(\eta)\mathrm{d}\eta - \frac{\Gamma(2-\xi)t}{\left(\delta\rho^{1-\xi} - T^{1-\xi}\right)}\delta\int_0^\rho \frac{(\rho-\eta)^{\varrho-\xi-1}}{\Gamma(\varrho-\xi)}\mathcal{Y}_w(\eta)\mathrm{d}\eta + \frac{\Gamma(2-\xi)t}{\left(\delta\rho^{1-\xi} - T^{1-\xi}\right)}\\
\displaystyle\int_0^T \frac{(T-\eta)^{\varrho-\xi-1}}{\Gamma(\varrho-\xi)}\mathcal{Y}_w(\eta)\mathrm{d}\eta - t\sum_{\imath=1}^{\mathrm{q}}\left(\frac{\Gamma(2-\nu)}{t_i^{1-\nu}}\mathcal{I}_\imath\left(w\left(t_\imath^-\right)\right)\right), \quad t \in [0, t_1], q = 1, 2, \ldots, \mathbf{r},\\
\displaystyle\int_0^t \frac{(t-\eta)^{\varrho-1}}{\Gamma(\varrho)}\mathcal{Y}_w(\eta)\mathrm{d}\eta - \frac{\Gamma(2-\xi)t}{\left(\delta\rho^{1-\xi} - T^{1-\xi}\right)}\delta\int_0^\rho \frac{(\rho-\eta)^{\varrho-\xi-1}}{\Gamma(\varrho-\xi)}\mathcal{Y}_w(\eta)\mathrm{d}\eta\\
\displaystyle+\frac{\Gamma(2-\xi)t}{\left(\delta\rho^{1-\xi} - T^{1-\xi}\right)}\int_0^T \frac{(T-\eta)^{\varrho-\xi-1}}{\Gamma(\varrho-\xi)}\mathcal{Y}_w(\eta)\mathrm{d}\eta - t\sum_{\imath=1}^{\mathrm{q}}\left(\frac{\Gamma(2-\nu)}{t_i^{1-\nu}}\mathcal{I}_\imath\left(w\left(t_\imath^-\right)\right)\right)\\
\displaystyle+\sum_{\imath=1}^{\mathrm{q}}\mathcal{I}_\imath\left(w\left(t_\imath^-\right)\right) + \sum_{\imath=1}^{\mathrm{q}}(t-t_\imath)\left(\frac{\Gamma(2-\nu)}{t_i^{1-\nu}}\mathcal{J}_\imath\left(w\left(t_\imath^-\right)\right)\right), \quad t \in \left(t_q, t_{q+1}\right], q = 1, 2, \ldots, \mathbf{r},
\end{cases} \tag{40}$$

where $\mathscr{Y}_w(t) = f(t, w(t), {}_0^c\mathscr{D}_t^{\varrho} w(t)) = f(t, w(t), \mathscr{Y}_w(t))$. In (40), we see that all the terms of solution w in the interval $[0, t_1]$ are contained in the solution w in interval $(t_q, t_{q+1}]$; therefore, for simplicity purpose, we will study the solution in interval $(t_q, t_{q+1}]$ only. Now, we shall prove some theorems. Our first result is based on Schaefer's fixed theorem.

Theorem 1. *If the assumptions $(H_1)-(H_3)$ are satisfied, then problem (2) has at least one solution.*

Proof. We use Schaefer's fixed point theorem. The proof is given in the following four steps.

Step 1: to show that $\mathscr{N}$ is continuous, take a sequence $\{w_n\}$ such that $w_n \longrightarrow w \in \mathscr{B}$. Then, for $t \in \mathscr{S}$, we have

$$\begin{aligned} \left|\mathscr{N}(w_n(t)) - \mathscr{N}(w(t))\right| \leq{}& \int_0^t \frac{(t-\eta)^{\varrho-1}}{\Gamma(\varrho)} \left|\mathscr{Y}_{w_n}(\eta) - \mathscr{Y}_w(\eta)\right| \mathrm{d}\eta \\ &+ \frac{t\Gamma(2-\xi)}{\left|\delta\rho^{1-\xi} - T^{1-\xi}\right|} \delta \int_0^{\rho} \frac{(\rho-\eta)^{\varrho-\xi-1}}{\Gamma(\varrho-\xi)} \left|\mathscr{Y}_{w_n}(\eta) - \mathscr{Y}_w(\eta)\right| \mathrm{d}\eta \\ &+ \frac{t\Gamma(2-\xi)}{\left|\delta\rho^{1-\xi} - T^{1-\xi}\right|} \int_0^{T} \frac{(T-\eta)^{\varrho-\xi-1}}{\Gamma(\varrho-\xi)} \left|\mathscr{Y}_{w_n}(\eta) - \mathscr{Y}_w(\eta)\right| \mathrm{d}\eta \\ &+ t\sum_{\imath=1}^{q} \left(\frac{\Gamma(2-\nu)}{t_i^{1-\nu}}\right) \left|\mathscr{J}_\imath(w_n(t_\imath^-)) - \mathscr{J}_\imath(w(t_\imath^-))\right| + \sum_{\imath=1}^{q} \left|\mathscr{I}_\imath(w_n(t_\imath^-)) - \mathscr{I}_\imath(w(t_\imath^-))\right| \\ &+ \sum_{\imath=1}^{q} \left|t - t_\imath\right| \frac{\Gamma(2-\nu)}{t_i^{1-\nu}} \\ &\times \left|\mathscr{J}_\imath(w_n(t_\imath^-)) - \mathscr{J}_\imath(w(t_\imath^-))\right|, \end{aligned} \tag{41}$$

where $\mathscr{Y}_{w_n}(t) = f(t, w_n(t), \mathscr{Y}_{w_n}(t))$ and $\mathscr{Y}(t) = f(t, w(t), \mathscr{Y}_w(t))$. Using (H_1), we have

$$\begin{aligned} \left|\mathscr{Y}_{w_n}(t) - \mathscr{Y}_w(t)\right| &= \Big|f\big(t, w_n(t), \mathscr{Y}_{w_n}(t)\big) \\ &\quad - f(t, w(t), \mathscr{Y}_w(t))\Big| \\ &\leq L_1\left|w_n(t) - w(t)\right| \\ &\quad + L_2\left|\mathscr{Y}_{w_n}(t) - \mathscr{Y}_w(t)\right|, \end{aligned} \tag{42}$$

which implies

$$\begin{aligned} \left\|\mathscr{Y}_{w_n} - \mathscr{Y}_w\right\|_{\mathscr{B}} &\leq \frac{L_1}{1-L_2}\left\|w_n - w\right\|_{\mathscr{B}}, \\ \left|\mathscr{I}_\imath(w_n)(t_\imath^-) - \mathscr{I}_\imath(w)(t_\imath^-)\right| &\leq L_4\left|w_n(t_\imath^-) - w(t_\imath^-)\right|. \end{aligned} \tag{43}$$

$w_n \longrightarrow w$ implies $\mathscr{Y}_{w_n}(t) \longrightarrow \mathscr{Y}_w(t)$ as $n \longrightarrow \infty$. Now, since every convergent sequence is bounded, there exists a constant $b > 0$ such that $\mathscr{Y}_{w_n}(t) \leq b$ and $\mathscr{Y}_w \leq b$ for $t \in \mathscr{S}$. Thus,

$$\begin{aligned} (t-\eta)^{\varrho-1}\left|\mathscr{Y}_{w_n}(t) - \mathscr{Y}_w(t)\right| &\leq (t-\eta)^{\varrho-1}\Big(\left|\mathscr{Y}_{w_n}(t)\right| + \left|\mathscr{Y}_w(t)\right|\Big) \leq 2b(t-\eta)^{\varrho-1}, \\ (T-\eta)^{\varrho-\xi-1}\left|\mathscr{Y}_{w_n}(t) - \mathscr{Y}_w(t)\right| &\leq (T-\eta)^{\varrho-\xi-1}\Big(\left|\mathscr{Y}_{w_n}(t)\right| + \left|\mathscr{Y}_w(t)\right|\Big) \leq 2b(T-\eta)^{\varrho-\xi-1}, \\ (\rho-\eta)^{\varrho-\xi-1}\left|\mathscr{Y}_{w_n}(t) - \mathscr{Y}_w(t)\right| &\leq (\rho-\eta)^{\varrho-\xi-1}\Big(\left|\mathscr{Y}_{w_n}(t)\right| + \left|\mathscr{Y}_w(t)\right|\Big) \leq 2b(\rho-\eta)^{\varrho-\xi-1}. \end{aligned} \tag{44}$$

The functions $\eta \longrightarrow 2b(t-\eta)^{\varrho-1}$, $\eta \longrightarrow 2b(T-\eta)^{\varrho-\xi-1}$, and $\eta \longrightarrow 2b(\rho-\eta)^{\varrho-\xi-1}$ are integrable for $t \in \mathscr{S}$. Therefore, by the continuity of $f, \mathscr{I}, \text{and} \mathscr{J}$ and the Lebesgue dominated convergent theorem, we conclude from (41) that $|\mathscr{N}(w_n(t)) - \mathscr{N}(w(t))| \longrightarrow 0$ as $n \longrightarrow \infty$ which implies $\|\mathscr{N}(w_n) - \mathscr{N}(w)\|_{\mathscr{B}} \longrightarrow 0 n \longrightarrow \infty$. This proves the continuity of $\mathscr{N}$.

Step 2: in this step, we will show that for each $w \in \mathscr{W}_{\mathbf{b}} = \{w \in \mathscr{B}\colon \|w\| \leq \mathbf{b}\}$, $\|\mathscr{N}w\|_{\mathscr{B}} \leq \mathbb{K}$. For $t \in \mathscr{S}$, consider

$$|\mathcal{N}(w(t))| \leq \int_0^t \frac{(t-\eta)^{\varrho-1}}{\Gamma(\varrho)}|\mathcal{Y}_w(\eta)|\mathrm{d}\eta + \frac{t\Gamma(2-\xi)}{|\delta\rho^{1-\xi}-T^{1-\xi}|}\delta\int_0^\rho \frac{(\rho-\eta)^{\varrho-\xi-1}}{\Gamma(\varrho-\xi)}|\mathcal{Y}_w(\eta)|\mathrm{d}\eta$$
$$+\frac{t\Gamma(2-\xi)}{|\delta\rho^{1-\xi}-T^{1-\xi}|}\int_0^T \frac{(T-\eta)^{\varrho-\xi-1}}{\Gamma(\varrho-\xi)}|\mathcal{Y}_w(\eta)|\mathrm{d}\eta + t\sum_{\imath=1}^{q}\left(\frac{\Gamma(2-\nu)}{t_i^{1-\nu}}\right)|\mathcal{J}_\imath(w(t_\imath^-))| \tag{45}$$
$$+\sum_{\imath=1}^{q}|\mathcal{I}_\imath(w(t_\imath^-))| + \sum_{\imath=1}^{q}|t-t_\imath|\frac{\Gamma(2-\nu)}{t_i^{1-\nu}}|\mathcal{J}_\imath(w(t_\imath^-))|.$$

Using (H_2) and $a_1^* = \sup_{t\in\mathcal{X}} a_1(t)$, $a_2^* = \sup_{t\in\mathcal{X}} a_2(t)$, and $a_3^* = \sup_{t\in\mathcal{X}} a_3(t) < 1$, we have

$$\begin{aligned}|\mathcal{Y}_w(t)| &= |f(t, w(t), \mathcal{Y}_w(t))| \\ &\leq a_1(t) + a_2(t)|w(t)| + a_3(t)|\mathcal{Y}_w(t)|.\end{aligned} \tag{46}$$

Taking the maximum value over the interval $\mathcal{S}$ and simplifying, we get

$$\|\mathcal{Y}_w\|_{\mathcal{B}} \leq \frac{a_1^* + a_2^*\mathbf{b}}{1-a_3^*} =: \mathbb{K}_1. \tag{47}$$

Using this result, (45) implies

$$|\mathcal{N}(w(t))| \leq \mathbb{K}_1\int_0^t \frac{(t-\eta)^{\varrho-1}}{\Gamma(\varrho)}\mathrm{d}\eta + \frac{t\Gamma(2-\xi)\mathbb{K}_1}{|\delta\rho^{1-\xi}-T^{1-\xi}|}\delta\int_0^\rho \frac{(\rho-\eta)^{\varrho-\xi-1}}{\Gamma(\varrho-\xi)}\mathrm{d}\eta$$
$$+\frac{t\Gamma(2-\xi)\mathbb{K}_1}{|\delta\rho^{1-\xi}-T^{1-\xi}|}\int_0^T \frac{(T-\eta)^{\varrho-\xi-1}}{\Gamma(\varrho-\xi)}\mathrm{d}\eta + t\sum_{\imath=1}^{q}\left(\frac{\Gamma(2-\nu)}{t_i^{1-\nu}}\right)\left(C_{J_\imath}|w| + M_J\right) \tag{48}$$
$$+\sum_{\imath=1}^{q}\left(C_{\mathcal{I}_\imath}|w| + M_{\mathcal{I}}\right) + \sum_{\imath=1}^{q}|t-t_\imath|\frac{\Gamma(2-\nu)}{t_i^{1-\nu}}\left(C_{J_\imath}|w| + M_J\right).$$

Further simplification implies

$$\begin{aligned}\|\mathcal{N}w\|_{\mathcal{B}} \leq \mathbb{K}_1&\left(\frac{T^\varrho}{\Gamma(\varrho+1)} + \frac{\delta T\Gamma(2-\xi)\left(\delta\rho^{\varrho-\xi}+T^{\varrho-\xi}\right)}{|\delta\rho^{1-\xi}-T^{1-\xi}|\Gamma(\varrho-\xi+1)}\right)\\ &+2qT\Gamma(2-\nu)\left(C_{J_i}\mathbf{b}+M_J\right) + q\left(C_{\mathcal{I}_i}\mathbf{b}+M_{\mathcal{I}}\right) =: \mathbb{K}.\end{aligned} \tag{49}$$

This shows that the operator $\mathcal{N}$ maps bounded sets into bounded sets.

Step 3: in this step, we will show that $\mathcal{N}$ is equicontinuous. Let $w \in \mathcal{W} \subseteq \mathcal{B}$ and $t_1, t_2 \in \mathcal{S}$ such that $t_1 < t_2$ and consider

$$|\mathcal{N}(w(t_2)) - \mathcal{N}(w(t_1))| \leq \int_{t_1}^{t_2} \frac{(t_2-\eta)^{\varrho-1}}{\Gamma(\varrho)}|\mathcal{Y}_w(\eta)|\mathrm{d}\eta + (t_2-t_1)\frac{\Gamma(2-\xi)}{|\delta\rho^{1-\xi}-T^{1-\xi}|}\delta\int_0^\rho \frac{(\rho-\eta)^{\varrho-\xi-1}}{\Gamma(\varrho-\xi)}|\mathcal{Y}_w(\eta)|\mathrm{d}\eta$$
$$+(t_2-t_1)\frac{\Gamma(2-\xi)}{|\delta\rho^{1-\xi}-T^{1-\xi}|}\int_0^T \frac{(T-\eta)^{\varrho-\xi-1}}{\Gamma(\varrho-\xi)}|\mathcal{Y}_w(\eta)|\mathrm{d}\eta + (t_2-t_1)\sum_{0<t_\imath<t_2-t_1}\left(\frac{\Gamma(2-\nu)}{t_i^{1-\nu}}\right)|\mathcal{J}_\imath(w(t_\imath^-))|$$
$$+\sum_{0<t_\imath<t_2-t_1}|\mathcal{I}_\imath(w(t_\imath^-))| + \sum_{0<t_\imath<t_2-t_1}(t_2-t_1)\frac{\Gamma(2-\nu)}{t_i^{1-\nu}}|\mathcal{J}_\imath(w(t_\imath^-))|. \tag{50}$$

Using assumptions (H_2) and (H_3), we obtain

$$\begin{aligned}\left|\mathcal{N}(w(t_2))-\mathcal{N}(w(t_1))\right| &\leq \mathbb{K}_1\frac{(t_2-t_1)^{\varrho}}{\Gamma(\varrho+1)}+(t_2-t_1)\mathbb{K}_1\frac{\Gamma(2-\xi)}{\left|\delta\rho^{1-\xi}-T^{1-\xi}\right|}\delta\frac{(\rho)^{\varrho-\xi}}{\Gamma(\varrho-\xi+1)}\\ &+(t_2-t_1)\mathbb{K}_1\frac{\Gamma(2-\xi)}{\left|\delta\rho^{1-\xi}-T^{1-\xi}\right|}\frac{(T)^{\varrho-\xi}}{\Gamma(\varrho-\xi+1)}+2(t_2-t_1)q\Gamma(2-\nu)\left(\mathrm{C}_{J_i}\mathbf{b}+M_J\right)\\ &+(t_2-t_1)q\Gamma(2-\nu)\left(\mathrm{C}_{\mathcal{J}_i}\mathbf{b}+M_{\mathcal{J}}\right).\end{aligned} \tag{51}$$

We see that as $t_1 \longrightarrow t_2$, the right-hand side of inequality (51) tends to zero that is $|\mathcal{N}(w(t_2))-\mathcal{N}(w(t_1))| \longrightarrow 0$ as $t_1 \longrightarrow t_2$. Hence, by the Ascoli – Arzela theorem $\mathcal{N}: \mathcal{B} \longrightarrow \mathcal{B}$ is completely continuous.

Step 4: to complete the proof, it remains to show that the set $\mathcal{E}=\{w\in : w=\zeta\mathcal{N}w, \text{ for } 0<\zeta<1\}$ is bounded. Let $w\in\mathcal{E}$, then for any $t\in\mathcal{S}$, we have

$$\begin{aligned}|\mathcal{N}(w(t))| &\leq \zeta\int_0^t\frac{(t-\eta)^{\varrho-1}}{\Gamma(\varrho)}\left|\mathcal{Y}_w(\eta)\right|\mathrm{d}\eta+\frac{\zeta t\Gamma(2-\xi)}{\left|\delta\rho^{1-\xi}-T^{1-\xi}\right|}\delta\int_0^{\rho}\frac{(\rho-\eta)^{\varrho-\xi-1}}{\Gamma(\varrho-\xi)}\left|\mathcal{Y}_w(\eta)\right|\mathrm{d}\eta\\ &+\frac{\zeta t\Gamma(2-\xi)}{\left|\delta\rho^{1-\xi}-T^{1-\xi}\right|}\int_0^T\frac{(T-\eta)^{\varrho-\xi-1}}{\Gamma(\varrho-\xi)}\left|\mathcal{Y}_w(\eta)\right|\mathrm{d}\eta+\zeta t\sum_{\imath=1}^{q}\left(\frac{\Gamma(2-\nu)}{t_i^{1-\nu}}\right)\left|\mathcal{J}_\imath(w(t_\imath^-))\right|\\ &+\zeta\sum_{\imath=1}^{q}\left|\mathcal{J}_\imath(w(t_\imath^-))\right|+\zeta\sum_{\imath=1}^{q}\left|t-t_\imath\right|\frac{\Gamma(2-\nu)}{t_i^{1-\nu}}\left|\mathcal{J}_\imath(w(t_\imath^-))\right|.\end{aligned} \tag{52}$$

Using $0<\zeta<1$ and (47) and (49), from (52), we get the following result:

$$\begin{aligned}\|\mathcal{N}w\|_{\mathcal{B}} &\leq \zeta\left[\mathbb{K}_1\left(\frac{T^{\varrho}}{\Gamma(\varrho+1)}+\frac{\delta T\Gamma(2-\xi)\left(\delta\rho^{\varrho-\xi}+T^{\varrho-\xi}\right)}{\left|\delta\rho^{1-\xi}-T^{1-\xi}\right|\Gamma(\varrho-\xi+1)}\right)\right.\\ &\left.+2qT\Gamma(2-\nu)\left(\mathrm{C}_{J_i}\mathbf{b}+M_J\right)+q\left(\mathrm{C}_{\mathcal{J}_i}\mathbf{b}+M_{\mathcal{J}}\right)\right]=:\zeta\mathbb{K}\leq\mathbb{K}.\end{aligned} \tag{53}$$

This shows that the set $\mathcal{E}$ is bounded. Therefore, by Schaefer's fixed point theorem, problem (2) has at least one solution.

The following and our second result is based on the Banach fixed point theorem.

Theorem 2. *If the assumptions $(H_1)-(H_3)$ and the inequality*

$$\begin{aligned}&\frac{L_1T^{\varrho}}{(1-L_2)\Gamma(\varrho+1)}+\frac{L_1\delta T\Gamma(2-\xi)\left(\delta\rho^{\varrho-\xi}+T^{\varrho-\xi}\right)}{(1-L_2)\left|\delta\rho^{1-\xi}-T^{1-\xi}\right|\Gamma(\varrho-\xi+1)}\\ &+q\left(L_3+2L_4T\Gamma(2-\xi)\right)<1,\end{aligned} \tag{54}$$

are satisfied, then (2) has an unique solution.

Proof. To show that the operator $\mathcal{N}$ as defined above has a unique fixed point, we consider $w_1, w_2\in\mathcal{B}$.

For $t\in t_{\mathrm{q}}, t_{\mathrm{q}+1}]$, we have

$$\left|\mathcal{N}(w_1(t))-\mathcal{N}(w_2(t))\right|\le\int_0^t\frac{(t-\eta)^{\varrho-1}}{\Gamma(\varrho)}\left|\mathcal{Y}_{w_1}(\eta)-\mathcal{Y}_{w_2}(\eta)\right|\mathrm{d}\eta+\frac{t\Gamma(2-\xi)}{\left(\delta\rho^{1-\xi}-T^{1-\xi}\right)}$$
$$\cdot\,\delta\int_0^\rho\frac{(\rho-\eta)^{\varrho-\xi-1}}{\Gamma(\varrho-\xi)}\left|\mathcal{Y}_{w_1}(\eta)-\mathcal{Y}_{w_2}(\eta)\right|\mathrm{d}\eta+\frac{t\Gamma(2-\xi)}{\left(\delta\rho^{1-\xi}-T^{1-\xi}\right)}\int_0^T\frac{(T-\eta)^{\varrho-\xi-1}}{\Gamma(\varrho-\xi)}\left|\mathcal{Y}_{w_1}(\eta)-\mathcal{Y}_{w_2}(\eta)\right|\mathrm{d}\eta$$
$$+t\sum_{\imath=1}^{q}\left(\frac{\Gamma(2-\nu)}{t_\imath^{1-\nu}}\right)\left|\mathcal{J}_\imath(w_1(t_\imath^-))-\mathcal{J}_\imath(w_2(t_\imath^-))\right|+\sum_{\imath=1}^{q}\left|\mathcal{I}_\imath(w_1(t_\imath^-))-\mathcal{I}_\imath(w_2(t_\imath^-))\right|+\sum_{\imath=1}^{q}\left|t-t_\imath\right|\frac{\Gamma(2-\nu)}{t_\imath^{1-\nu}}$$
$$\times\left|\mathcal{J}_\imath(w_1(t_\imath^-))-\mathcal{J}_\imath(w_2(t_\imath^-))\right|, \tag{55}$$

where $\mathcal{Y}_{w_1}(t)=f(t,w_1(t),\mathcal{Y}_{w_1})$ and $\mathcal{Y}_{w_2}(\eta)=f(t,w_2(t),\mathcal{Y}_{w_2})$. Using (H_1), we have

$$\begin{aligned}\left|\mathcal{Y}_{w_1}(t)-\mathcal{Y}_{w_2}(t)\right|&=\left|f\left(t,w_1(t),\mathcal{Y}_{w_1}(t)\right)-f\left(t,w_2(t),\mathcal{Y}_{w_2}(t)\right)\right|\\&\le L_1\left|w_1(t)-w_2(t)\right|+L_2\left|\mathcal{Y}_{w_1}(t)-\mathcal{Y}_{w_2}(t)\right|,\end{aligned} \tag{56}$$

which implies

$$\begin{aligned}\left\|\mathcal{Y}_{w_1}-\mathcal{Y}_{w_2}\right\|_{\mathcal{B}}&\le\frac{L_1}{1-L_2}\left\|w_1-w_2\right\|_{\mathcal{B}},\\\left|\mathcal{J}_\imath(w_1)(t_\imath^-)-\mathcal{J}_\imath(w_2)(t_\imath^-)\right|&\le L_4\left|w_1(t_\imath^-)-w_2(t_\imath^-)\right|.\end{aligned} \tag{57}$$

Thus, from (55), we have

$$\left|\mathcal{N}(w_1)(t)-\mathcal{N}(w_2)(t)\right|\le\frac{L_1T^\varrho}{(1-L_2)\Gamma(\varrho+1)}\max_{t\in\left(t_q,t_{q+1}\right]}\left|w_1(t)-w_2(t)\right|+\frac{\Gamma(2-\xi)\rho^{\varrho-\xi}}{(1-L_2)\left|\delta\rho^{1-\xi}-T^{1-\xi}\right|\Gamma(\varrho-\xi+1)}$$
$$\cdot\max_{t\in\left(t_q,t_{q+1}\right]}(\delta t)\left|w_1(t)-w_2(t)\right|+\frac{L_1\Gamma(2-\xi)T^{\varrho-\xi}}{(1-L_2)\left|\delta\rho^{1-\xi}-T^{1-\xi}\right|\Gamma(\varrho-\xi+1)}\max_{t\in\left(t_q,t_{q+1}\right]}t\left|w_1(t)-w_2(t)\right|$$
$$+\max_{t\in\left(t_q,t_{q+1}\right]}\frac{qt\Gamma(2-\xi)L_4}{t_q^{1-\nu}}\left|w_1(t)-w_2(t)\right|+\max_{t\in\left(t_q,t_{q+1}\right]}qL_3\left|w_1(t_\imath)-w_2(t_\imath)\right|$$
$$+\max_{t\in\left(t_q,t_{q+1}\right]}q\left|t-t_\imath\right|\frac{\Gamma(2-\xi)}{t_\imath^{1-\nu}}L_4\left|w_1(t_\imath)-w_2(t_\imath)\right|,q=1,2,\ldots,\mathbf{r}. \tag{58}$$

By further simplification, we obtain the following inequality:

$$\begin{aligned}\left\|\mathcal{N}(w_1)-\mathcal{N}(w_2)\right\|_{\mathcal{B}}&\le\left[\frac{L_1T^\varrho}{(1-L_2)\Gamma(\varrho+1)}+\frac{L_1\delta T\Gamma(2-\xi)\left(\delta\rho^{\varrho-\xi}+T^{\varrho-\xi}\right)}{(1-L_2)\left|\delta\rho^{1-\xi}-T^{1-\xi}\right|\Gamma(\varrho-\xi+1)}+q\left(L_3+2L_4T\Gamma(2-\xi)\right)\right]\left\|w_1-w_2\right\|_{\mathcal{B}},\\&\frac{L_1T^\varrho}{(1-L_2)\Gamma(\varrho+1)}+\frac{L_1\delta T\Gamma(2-\xi)\left(\delta\rho^{\varrho-\xi}+T^{\varrho-\xi}\right)}{(1-L_2)\left|\delta\rho^{1-\xi}-T^{1-\xi}\right|\Gamma(\varrho-\xi+1)}+q\left(L_3+2L_4T\Gamma(2-\xi)\right)<1.\end{aligned} \tag{59}$$

Therefore, by Banach contraction theorem, problem (2) has a unique fixed point.

4. Stability Analysis

In this section, we study Hyers-Ulam stability of problem (2).

Theorem 3. *If assumptions $(H_1)-(H_3)$ and the inequality*

$$\frac{L_1 T^{\varrho}}{(1-L_2)\Gamma(\varrho+1)}+\frac{L_1\delta T\Gamma(2-\xi)\left(\delta\rho^{\varrho-\xi}+T^{\varrho-\xi}\right)}{(1-L_2)\left|\delta\rho^{1-\xi}-T^{1-\xi}\right|\Gamma(\varrho-\xi+1)} + q\left(L_3+2L_4T\Gamma(2-\xi)\right)<1, \tag{60}$$

are satisfied, then problem (2) is Hyers-Ulam stable.

Proof. Let h be any solution of inequality (6), then by Remark 1, we have

$$\begin{cases} {}_0^c\mathscr{D}_t^{\varrho}h(t)=f\left(t,h(t),{}_0^c\mathscr{D}_t^{\varrho}h(t)\right)+\phi(t), & \varrho\in(1,2], \\ \Delta h\left(t_q\right)=\mathscr{I}_q\left(h\left(t_q^-\right)\right)+\phi_q, \\ \Delta\left({}_0^c\mathscr{D}_t^{\nu}h\left(t_q\right)\right)=\mathscr{J}_q\left(h\left(t_q^-\right)\right)+\phi_q, & \nu\in(0,1],\ q=1,2,\ldots,\mathbf{r}, \\ h(0)=0,\ {}_0^c\mathscr{D}_t^{\xi}h(T)=\delta\,{}_0^c\mathscr{D}_t^{\xi}h(\rho)+\phi_q, & 0<\delta<\xi<1,\ 0<\rho<1, q=1,2,\ldots,\mathbf{r}. \end{cases} \tag{61}$$

In light of Corollary 1, the solution problem (61) is given by

$$h(t)=\begin{cases} \displaystyle\int_0^t\frac{(t-\eta)^{\varrho-1}}{\Gamma(\varrho)}\mathscr{Y}_h(\eta)\mathrm{d}\eta+\int_0^t\frac{(t-\eta)^{\varrho-1}}{\Gamma(\varrho)}\phi(\eta)\mathrm{d}\eta-\frac{\Gamma(2-\xi)t}{\left(\delta\rho^{1-\xi}-T^{1-\xi}\right)}\delta\int_0^{\rho}\frac{(\rho-\eta)^{\varrho-\xi-1}}{\Gamma(\varrho-\xi)}\mathscr{Y}_h(\eta)\mathrm{d}\eta \\ \displaystyle-\frac{\Gamma(2-\xi)t}{\left(\delta\rho^{1-\xi}-T^{1-\xi}\right)}\delta\int_0^{\rho}\frac{(\rho-\eta)^{\varrho-\xi-1}}{\Gamma(\varrho-\xi)}\phi(\eta)\mathrm{d}\eta+\frac{\Gamma(2-\xi)t}{\left(\delta\rho^{1-\xi}-T^{1-\xi}\right)}\int_0^{T}\frac{(T-\eta)^{\varrho-\xi-1}}{\Gamma(\varrho-\xi)}\mathscr{Y}_h(\eta)\mathrm{d}\eta \\ \displaystyle+\frac{\Gamma(2-\xi)t}{\left(\delta\rho^{1-\xi}-T^{1-\xi}\right)}\int_0^{T}\frac{(T-\eta)^{\varrho-\xi-1}}{\Gamma(\varrho-\xi)}\phi(\eta)\mathrm{d}\eta-t\sum_{\imath=1}^{q}\left(\frac{\Gamma(2-\nu)}{t_i^{1-\nu}}\mathscr{J}_\imath\left(h\left(t_\imath^-\right)\right)\right)-t\sum_{\imath=1}^{q}\left(\frac{\Gamma(2-\nu)}{t_i^{1-\nu}}\phi_q\right), \quad t\in\left[0,t_1\right], q=1,2,\ldots,\mathbf{r}, \\ \displaystyle\int_0^t\frac{(t-\eta)^{\varrho-1}}{\Gamma(\varrho)}\mathscr{Y}_h(\eta)\mathrm{d}\eta+\int_0^t\frac{(t-\eta)^{\varrho-1}}{\Gamma(\varrho)}\phi(\eta)\mathrm{d}\eta-\frac{\Gamma(2-\xi)t}{\left(\delta\rho^{1-\xi}-T^{1-\xi}\right)}\delta\int_0^{\rho}\frac{(\rho-\eta)^{\varrho-\xi-1}}{\Gamma(\varrho-\xi)}\mathscr{Y}_h(\eta)\mathrm{d}\eta \\ \displaystyle-\frac{\Gamma(2-\xi)t}{\left(\delta\rho^{1-\xi}-T^{1-\xi}\right)}\delta\int_0^{\rho}\frac{(\rho-\eta)^{\varrho-\xi-1}}{\Gamma(\varrho-\xi)}\phi(\eta)\mathrm{d}\eta+\frac{\Gamma(2-\xi)t}{\left(\delta\rho^{1-\xi}-T^{1-\xi}\right)}\int_0^{T}\frac{(T-\eta)^{\varrho-\xi-1}}{\Gamma(\varrho-\xi)}\mathscr{Y}_h(\eta)\mathrm{d}\eta \\ \displaystyle+\frac{\Gamma(2-\xi)t}{\left(\delta\rho^{1-\xi}-T^{1-\xi}\right)}\int_0^{T}\frac{(T-\eta)^{\varrho-\xi-1}}{\Gamma(\varrho-\xi)}\phi(\eta)\mathrm{d}\eta-t\sum_{\imath=1}^{q}\left(\frac{\Gamma(2-\nu)}{t_i^{1-\nu}}\mathscr{J}_\imath\left(h\left(t_\imath^-\right)\right)\right)-t\sum_{\imath=1}^{q}\left(\frac{\Gamma(2-\nu)}{t_i^{1-\nu}}\phi_q\right) \\ \displaystyle+\sum_{\imath=1}^{q}\mathscr{I}\left(h\left(t_\imath^-\right)\right)_\imath+\sum_{\imath=1}^{q}\phi_q+\sum_{\imath=1}^{q}\left(t-t_\imath\right)\left(\frac{\Gamma(2-\nu)}{t_i^{1-\nu}}\mathscr{J}_\imath\left(h\left(t_\imath^-\right)\right)\right)+\sum_{\imath=1}^{q}\left(t-t_\imath\right)\left(\frac{\Gamma(2-\nu)}{t_i^{1-\nu}}\phi_q\right), \quad t\in\left(t_q,t_{q+1}\right], q=1,2,\ldots,\mathbf{r}, \end{cases} \tag{62}$$

where $\mathscr{Y}_h(t) = f(t, h(t), \mathscr{Y}_h(t))$. Now if w is a unique solution of problem (2), then for $t \in \mathscr{S}$, consider

$$\begin{aligned}
|h(t) - w(t)| \leq{}& \int_0^t \frac{(t-\eta)^{\varrho-1}}{\Gamma(\varrho)} \left|\mathscr{Y}_h(\eta) - \mathscr{Y}_w(\eta)\right| \mathrm{d}\eta + \int_0^t \frac{(t-\eta)^{\varrho-1}}{\Gamma(\varrho)} |\phi(\eta)| \mathrm{d}\eta + \frac{\Gamma(2-\xi)t}{\left|\delta\rho^{1-\xi} - T^{1-\xi}\right|} \\
& \cdot \delta \int_0^\rho \frac{(\rho-\eta)^{\varrho-\xi-1}}{\Gamma(\varrho-\xi)} \left|\mathscr{Y}_h(\eta) - \mathscr{Y}_w(\eta)\right| \mathrm{d}\eta + \frac{\Gamma(2-\xi)t}{\left|\delta\rho^{1-\xi} - T^{1-\xi}\right|} \delta \int_0^\rho \frac{(\rho-\eta)^{\varrho-\xi-1}}{\Gamma(\varrho-\xi)} |\phi(\eta)| \mathrm{d}\eta + \frac{\Gamma(2-\xi)t}{\left|\delta\rho^{1-\xi} - T^{1-\xi}\right|} \\
& \cdot \int_0^T \frac{(T-\eta)^{\varrho-\xi-1}}{\Gamma(\varrho-\xi)} \left|\mathscr{Y}_h(\eta) - \mathscr{Y}_w(\eta)\right| \mathrm{d}\eta \int_0^T \frac{(T-\eta)^{\varrho-\xi-1}}{\Gamma(\varrho-\xi)} |\phi(\eta)| \mathrm{d}\eta \\
& + t \sum_{\imath=1}^{q} \left(\frac{\Gamma(2-\nu)}{t_\imath^{1-\nu}} \left|\mathscr{J}_\imath(h(t_\imath^-)) - \mathscr{J}_\imath(w(t_\imath^-))\right| \right) + t \sum_{\imath=1}^{q} \left(\frac{\Gamma(2-\nu)}{t_\imath^{1-\nu}} \left|\phi_q\right| \right) + \sum_{\imath=1}^{q} \left|\mathscr{I}_\imath(h(t_\imath^-)) - \mathscr{I}_\imath(w(t_\imath^-))\right| + \sum_{\imath=1}^{q} \left|\phi_q\right| \\
& + \sum_{\imath=1}^{q} (t - t_\imath) \left(\frac{\Gamma(2-\nu)}{t_\imath^{1-\nu}} \left|\mathscr{J}_\imath(h(t_\imath^-)) - \mathscr{J}_\imath(w(t_\imath^-))\right| \right) + \sum_{\imath=1}^{q} (t - t_\imath) \left(\frac{\Gamma(2-\nu)}{t_\imath^{1-\nu}} \left|\phi_q\right| \right), \quad t \in \left(t_q, t_{q+1}\right], q = 1, 2, \ldots, \mathbf{r},
\end{aligned} \tag{63}$$

where $\mathscr{Y}_w(t) = f(t, w(t), \mathscr{Y}_w(t))$. By using assumption $(H_1) - (H_3)$, Remark 1, we have from (63)

$$\begin{aligned}
\|h - w\|_{\mathscr{B}} \leq{}& \left[\frac{L_1 T^\varrho}{(1-L_2)\Gamma(\varrho+1)} + \frac{L_1 \delta T \Gamma(2-\xi)\left(\delta\rho^{\varrho-\xi} + T^{\varrho-\xi}\right)}{(1-L_2)\left|\delta\rho^{1-\xi} - T^{1-\xi}\right| \Gamma(\varrho-\xi+1)} + q\left(L_3 + 2L_4 T\Gamma(2-\xi)\right) \right] \|h - w\|_{\mathscr{B}} \\
& + \left[\frac{T^\varrho}{\Gamma(\varrho+1)} + \frac{\delta T \Gamma(2-\xi)\left(\delta\rho^{\varrho-\xi} + T^{\varrho-\xi}\right)}{\left|\delta\rho^{1-\xi} - T^{1-\xi}\right| \Gamma(\varrho-\xi+1)} + q + 2qT\Gamma(2-\xi) \right] \epsilon.
\end{aligned} \tag{64}$$

Let

$$\begin{aligned}
\mathscr{E}_1 &= \frac{L_1 T^\varrho}{(1-L_2)\Gamma(\varrho+1)} + \frac{L_1 \delta T \Gamma(2-\xi)\left(\delta\rho^{\varrho-\xi} + T^{\varrho-\xi}\right)}{(1-L_2)\left|\delta\rho^{1-\xi} - T^{1-\xi}\right| \Gamma(\varrho-\xi+1)} + q\left(L_3 + 2L_4 T\Gamma(2-\xi)\right), \\
\mathscr{E}_2 &= \frac{T^\varrho}{\Gamma(\varrho+1)} + \frac{\delta T \Gamma(2-\xi)\left(\delta\rho^{\varrho-\xi} + T^{\varrho-\xi}\right)}{\left|\delta\rho^{1-\xi} - T^{1-\xi}\right| \Gamma(\varrho-\xi+1)} + q + 2qT\Gamma(2-\xi),
\end{aligned} \tag{65}$$

then

$$\|h - w\|_{\mathscr{B}} \leq \frac{\mathscr{E}_2}{1 - \mathscr{E}_1} \epsilon = \mathscr{C}\epsilon, \tag{66}$$

where $\mathscr{C} = \mathscr{E}_2/1 - \mathscr{E}_1$; $\mathscr{E}_1 < 1$. This shows that problem (2) is Hyers-Ulam stable. Moreover, by setting $\psi(\epsilon) = \mathscr{C}\epsilon$ and $\psi(0) = 0$, then the solution of problem (2) is generalized Hyers-Ulam stable.

Theorem 4. *If assumptions* $(H_1)-(H_4)$ *and the inequality*

$$\mathscr{E}_1=\frac{L_1T^{\varrho}}{(1-L_2)\Gamma(\varrho+1)}+\frac{L_1\delta T\Gamma(2-\xi)\left(\delta\rho^{\varrho-\xi}+T^{\varrho-\xi}\right)}{(1-L_2)\left|\delta\rho^{1-\xi}-T^{1-\xi}\right|\Gamma(\varrho-\xi+1)}+q\left(L_3+2L_4T\Gamma(2-\xi)\right)<1, \tag{67}$$

are satisfied, then problem (2) is Hyers-Ulam-Rassias stable.

Proof. From the proof of Theorem 3, we can write

$$\begin{aligned}|h(t)-w(t)|\le&\int_0^t\frac{(t-\eta)^{\varrho-1}}{\Gamma(\varrho)}\left|\mathscr{Y}_h(\eta)-\mathscr{Y}_w(\eta)\right|\mathrm{d}\eta+\int_0^t\frac{(t-\eta)^{\varrho-1}}{\Gamma(\varrho)}|\phi(\eta)|\mathrm{d}\eta\\&+\frac{\Gamma(2-\xi)t}{\left|\delta\rho^{1-\xi}-T^{1-\xi}\right|}\delta\int_0^{\rho}\frac{(\rho-\eta)^{\varrho-\xi-1}}{\Gamma(\varrho-\xi)}\left|\mathscr{Y}_h(\eta)-\mathscr{Y}_w(\eta)\right|\mathrm{d}\eta+\frac{\Gamma(2-\xi)t}{\left|\delta\rho^{1-\xi}-T^{1-\xi}\right|}\delta\int_0^{\rho}\frac{(\rho-\eta)^{\varrho-\xi-1}}{\Gamma(\varrho-\xi)}|\phi(\eta)|\mathrm{d}\eta\\&+\frac{\Gamma(2-\xi)t}{\left|\delta\rho^{1-\xi}-T^{1-\xi}\right|}\delta\int_0^{T}\frac{(T-\eta)^{\varrho-\xi-1}}{\Gamma(\varrho-\xi)}\left|\mathscr{Y}_h(\eta)-\mathscr{Y}_w(\eta)\right|\mathrm{d}\eta+\frac{\Gamma(2-\xi)t}{\left|\delta\rho^{1-\xi}-T^{1-\xi}\right|}\delta\int_0^{T}\frac{(T-\eta)^{\varrho-\xi-1}}{\Gamma(\varrho-\xi)}|\phi(\eta)|\mathrm{d}\eta\\&+t\sum_{\imath=1}^{q}\left(\frac{\Gamma(2-\nu)}{t_i^{1-\nu}}\left|\mathscr{J}_\imath(h(t_\imath^-))-\mathscr{J}_\imath(w(t_\imath^-))\right|\right)+t\sum_{\imath=1}^{q}\left(\frac{\Gamma(2-\nu)}{t_i^{1-\nu}}\left|\phi_q\right|\right)+\sum_{\imath=1}^{q}\left|\mathscr{I}_\imath(h(t_\imath^-))-\mathscr{I}_\imath(w(t_\imath^-))\right|\\&+\sum_{\imath=1}^{q}\left|\phi_q\right|+\sum_{\imath=1}^{q}(t-t_\imath)\left(\frac{\Gamma(2-\nu)}{t_i^{1-\nu}}\left|\mathscr{J}_\imath(h(t_\imath^-))-\mathscr{J}_\imath(w(t_\imath^-))\right|\right)+\sum_{\imath=1}^{q}(t-t_\imath)\left(\frac{\Gamma(2-\nu)}{t_i^{1-\nu}}\left|\phi_q\right|\right),\\&t\in\left(t_q,t_{q+1}\right],q=1,2,\ldots,\mathbf{r}.\end{aligned} \tag{68}$$

By using assumption $(H_1)-(H_4)$, Remark 2, we have from (68)

$$\begin{aligned}\|h-w\|_{\mathscr{B}}\le\mathscr{E}_1\|h-w\|_{\mathscr{B}}+\epsilon\left(\beta+\frac{\delta T\beta\Gamma(2-\xi)}{\left|\delta\rho^{1-\xi}-T^{1-\xi}\right|}+\frac{T\beta\Gamma(2-\xi)}{\left|\delta\rho^{1-\xi}-T^{1-\xi}\right|}\right)\theta(t)\\+\epsilon(q+2qT\Gamma(2-\nu))\varphi\le\mathscr{E}_1\|h-w\|_{\mathscr{B}}+\mathscr{E}_3(\theta(t)+\varphi)\epsilon,\end{aligned} \tag{69}$$

which implies that

$$\begin{aligned}\|h-w\|_{\mathscr{B}}&\le\frac{\epsilon\mathscr{E}_3(\theta(t)+\varphi)}{1-\mathscr{E}_1},\\\|h-w\|_{\mathscr{B}}&\le\mathscr{C}\epsilon(\theta(t)+\varphi),\end{aligned} \tag{70}$$

where

$$\begin{aligned}\mathscr{E}_1&=\frac{L_1T^{\varrho}}{(1-L_2)\Gamma(\varrho+1)}+\frac{L_1\delta T\Gamma(2-\xi)\left(\delta\rho^{\varrho-\xi}+T^{\varrho-\xi}\right)+q\left(L_3+2L_4T\Gamma(2-\xi)\right)<1}{(1-L_2)\left|\delta\rho^{1-\xi}-T^{1-\xi}\right|\Gamma(\varrho-\xi+1)},\\\mathscr{E}_3&=\frac{\beta\left|\delta\rho^{1-\xi}-T^{1-\xi}\right|+\delta T\beta\Gamma(2-\xi)+T\beta\Gamma(2-\xi)}{\left|\delta\rho^{1-\xi}-T^{1-\xi}\right|}+(q+2qT\Gamma(2-\nu)).\end{aligned} \tag{71}$$

Therefore, problem (2) is Hyers-Ulam-Rassias stable.

5. Example

Consider the following implicit fractional system with given impulsive conditions.

Example 1

$$\begin{cases} {}_0^c\mathscr{D}_t^{3/2} w(t) = \dfrac{|w(t)|}{26(t+1/2)(1+|w(t)|)} + \dfrac{\sin\left|{}_0^c\mathscr{D}_t^{3/2} w(t)\right|}{26+t^3}, \quad t \in \mathscr{S} = [0,1],\ t \neq t_1, q = \mathbf{r} = 1, \\ w(0) = 0, \\ {}_0^c\mathscr{D}_t^{1/2} w(1) = \dfrac{1}{4}\left(\dfrac{12 + |w(\rho)| + \left|{}_0^c\mathscr{D}_t^{1/2} w(\rho)\right|}{72e^{\rho+3}\left(1+|w(\rho)|+\left|{}_0^c\mathscr{D}_t^{1/2} w(\rho)\right|\right)}\right)_{\rho=1/5}, \\ \Delta w(t_1) = \dfrac{|w(t_1^-)|}{40+|w(t_1^-)|}, \\ \Delta {}_0^c\mathscr{D}_t^{1/2} w(t_1) = \dfrac{|w(t_1^-)|}{32+|w(t_1^-)|}. \end{cases} \tag{72}$$

Obviously, the given function f is continuous. We see $\varrho = 5/4$, $\xi = \nu = 1/2$, $T = 1$, $\delta = 1/4$, and $\rho = 1/5$. For $w_1, w_2 \in \mathscr{B}$ and $\mathscr{Y}_{w_1}, \mathscr{Y}_{w_2} \in C(\mathscr{S}, \mathscr{R})$ and $t \in \mathscr{S}$,

$$\begin{aligned} &\left|f\left(t, w_1(t), \mathscr{Y}_{w_1}\right) - f\left(t, w_2(t), \mathscr{Y}_{w_2}\right)\right| \\ &\quad \le \frac{1}{26}\left(\left|w_1(t) - w_2(t)\right| + \left|\mathscr{Y}_{w_1} - \mathscr{Y}_{w_2}\right|\right), \end{aligned} \tag{73}$$

which satisfies (H_1) with $L_1 = L_2 = 1/26$. Further, for $t_1 = 1/5$, let

$$\begin{aligned} \mathscr{I}_1(w(t_1^-)) &= \frac{|w(t_1^-)|}{40+|w(t_1^-)|}, \\ \mathscr{J}_1(w(t_1^-)) &= \frac{|w(t_1^-)|}{32+|w(t_1^-)|}, \quad \text{where } w_1 \in \mathscr{B}. \end{aligned} \tag{74}$$

For any $w_1, w_2 \in \mathscr{B}$, we have

$$\begin{aligned} \left|\mathscr{I}(w_1(t_1^-)) - \mathscr{I}(w_2(t_1^-))\right| &= \left|\frac{|w(t_1^-)|}{40+|w(t_1^-)|} - \frac{|w(t_1^-)|}{40+|w(t_1^-)|}\right| \\ &\le \frac{1}{40}\left|w_1(t_1^-) - w_2(t_1^-)\right|, \\ \left|\mathscr{I}(w_1(t_1^-)) - \mathscr{I}(w_2(t_1^-))\right| &= \left|\frac{|w(t_1^-)|}{32+|w(t_1^-)|} - \frac{|w(t_1^-)|}{32+|w(t_1^-)|}\right| \\ &\le \frac{1}{32}\left|w_1(t_1^-) - w_2(t_1^-)\right|, \end{aligned} \tag{75}$$

which satisfy the 2nd and 3rd inequalities of (H_1) with $L_3 = 1/40$ and $L_4 = 1/32$.

For $\varrho = 1/5$, $\xi = \nu = 1/2$, $T = 1$, $\delta = 1/4, \rho = 1/4, L_1 = L_2 = 1/26, L_3 = 1/40$, and $L_4 = 1/32$, we have

$$\begin{aligned} \mathscr{E}_1 &= \frac{L_1 T^{\varrho}}{(1-L_2)\Gamma(\varrho+1)} + \frac{L_1 \delta T \Gamma(2-\xi)\left(\delta\rho^{\varrho-\xi} + T^{\varrho-\xi}\right)}{(1-L_2)\left|\delta\rho^{1-\xi} - T^{1-\xi}\right|\Gamma(\varrho-\xi+1)} \\ &\quad + q\left(L_3 + 2L_4 T\Gamma(2-\xi)\right) = 0.301 + 0.009 + 0.08 = 0.39 < 1. \end{aligned} \tag{76}$$

Therefore, by Theorem 2, problem (72) has a unique solution. By Theorem 4, problem (52) is Hyers-Ulam stable and consequently generalized Hyers-Ulam stable.

Further, assuming $\Phi(t) = 1$, we have

$${}_0I_1^{3/2}\Phi(t) = \frac{1}{\Gamma(3/2)}\int_0^1 (1-\eta)^{(3/2)-1}\eta \, d\eta \le \frac{1}{3\sqrt{\Pi}}, \tag{77}$$

Consequently,

$${}_0I_1^{(3/2)-1}\Phi(t) = \frac{1}{\Gamma(3/2-1)}\int_0^1 (1-\eta)^{(3/2)-2}\eta d\eta \le \frac{1}{3\sqrt{\Pi}}, \tag{78}$$

which satisfies (H_4) with $\beta = 1/3\sqrt{\Pi}$ and $\Phi(t) = 1$; therefore, by Theorem 4, the solution of (72) is Hyers-Ulam-Rassias stable corresponding to (Φ, ψ). With the help of Matlab, we plot the result by using the RK4 method in Figure 1.

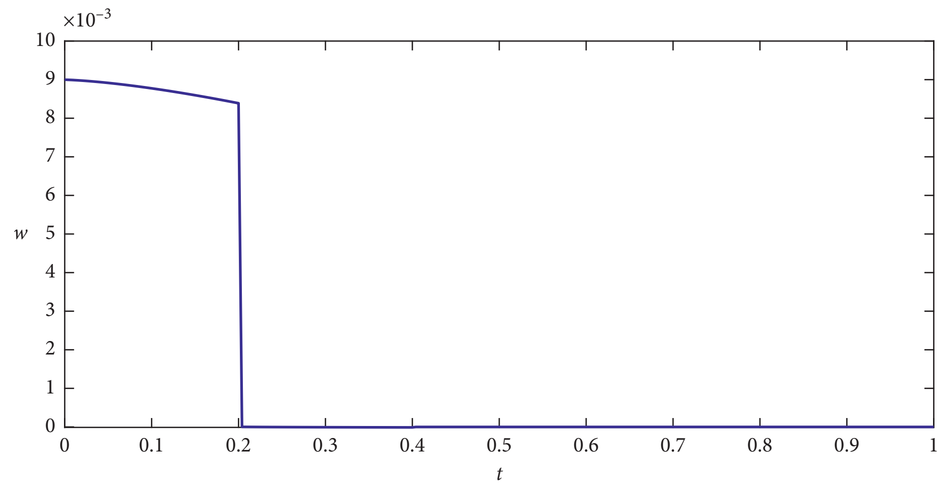

FIGURE 1: Graphical presentation of result of Example 1.

6. Conclusion

In this paper, using Schaefer's fixed point theorem, we have derived sufficient conditions for at least one solution to a class of IFODEs under NCFBC 2. Similarly, using the Banach contraction theorem, we obtained conditions under which problem 2 has unique solution. Moreover, by the application of qualitative theory and nonlinear functional analysis, we established results concerning to various kinds of Hyers-Ulam stability. The concerned results have been verified by a suitable example.

Data Availability

No data were used to support this study.

Conflicts of Interest

The authors declare that they have no conflicts of interest regarding publication of this paper.

Authors' Contributions

All authors have equal contribution in this research paper.

Acknowledgments

The third author T. Abdeljawad would like to thank Prince Sultan University for funding this work through the research group Nonlinear Analysis Methods in Applied Mathematics (NAMAM), group number RG-DES-2017-01-17.

References

[1] A. A. Kilbas, H. M. Srivastava, and J. J. Trujillo, *Theory and Applications of Fractional Diffrential Equations*, Vol. 204, North-Holland Mathematics Studies, Elsevier, Amsterdam, Netherlands, 2006.

[2] A. A. Kilbas, O. I. Marichev, and S. G. Samko, *Fractional Integral and Derivatives (Theory and Applications)*, Gordon & Breach, Basel, Switzerland, 1993.

[3] R. Hilfer, "Fractional time evolution," *Applications of Fractional Calculus in Physics, World Scientific, Singapore*, vol. 35, no. 12, pp. 87–130, 2000.

[4] P. J. Torvik and R. L. Bagley, "On the appearance of the fractional derivative in the behavior of real materials," *Journal of Applied Mechanics*, vol. 51, no. 2, pp. 294–298, 1984.

[5] R. A. Khan and K. Shah, "Existence and uniqueness of solutions to fractional order multi-point boundary value problems," *Communications in Applied Analysis*, vol. 19, pp. 515–526, 2015.

[6] A. Ali and K. Shah, "Existence theory and Ulam-Hyers stability to anti-periodic integral boundary value problem of implicit fractional differential equations," *Applied Mathematics E-Notes*, vol. 19, pp. 228–242, 2019.

[7] J. V. D. C. Sousa and E. C. de Oliveira, "On the ψ-Hilfer fractional derivative," *Communications in Nonlinear Science and Numerical Simulation*, vol. 60, pp. 72–91, 2018.

[8] J. V. D. C. Sousa and E. C. de Oliveira, "Leibniz type rule: ψ-Hilfer fractional operator," *Communications in Nonlinear Science and Numerical Simulation*, vol. 77, pp. 305–311, 2019.

[9] A. Khan, M. I. Syam, A. Zada, and H. Khan, "Stability analysis of nonlinear fractional differential equations with Caputo and Riemann-Liouville derivatives," *The European Physical Journal Plus*, vol. 133, no. 7, pp. 1–9, 2018.

[10] J. V. D. C. Sousa and E. C. de Oliveira, "Ulam-Hyers stability of a nonlinear fractional Volterra integro-differential equation," *Applied Mathematics Letters*, vol. 81, pp. 50–56, 2018.

[11] K. Shah, A. Ali, and S. Bushnaq, "Hyers-Ulam stability analysis to implicit Cauchy problem of fractional differential equations with impulsive conditions," *Mathematical Methods in the Applied Sciences*, vol. 41, no. 17, pp. 1–15, 2018.

[12] N. Ahmad, Z. Ali, K. Shah, A. Zada, and G. ur Rahman, "Analysis of implicit type nonlinear dynamical problem of impulsive fractional differential equations," *Complexity*, vol. 2018, pp. 1–15, 2018.

[13] A. Ali, K. Shah, and D. Baleanu, "Ulam stability results to a class of nonlinear implicit boundary value problems of impulsive fractional differential equations," *Advances in Difference Equations*, vol. 2019, no. 5, pp. 1–21, 2019.

[14] A. Zada and S. Ali, "Stability of integral Caputo-type boundary value problem with noninstantaneous impulses," *International Journal of Applied and Computational Mathematics*, vol. 5, no. 3, pp. 1–55, 2019.

[15] A. Ali, K. Shah, F. Jarad, V. Gupta, and T. Abdeljawad, "Existence and stability analysis to a coupled system of implicit type impulsive boundary value problems of fractional-order differential equations," *Advances in Difference Equations*, vol. 2019, no. 101, pp. 1–21, 2019.

[16] A. Zada and S. Ali, "Stability analysis of multi-point boundary value problem for sequential fractional differential equations with non-instantaneous impulses," *International Journal of Nonlinear Sciences and Numerical Simulation*, vol. 19, no. 7-8, pp. 763–774, 2018.

[17] V. Gupta and J. Dabas, "Existence results for a fractional integro-differential equation with nonlocal boundary conditions and fractional impulsive conditions," *Nonlinear Dynamics and Systems Theory*, vol. 15, no. 4, pp. 370–382, 2015.

[18] R. P. Agarwal, M. Benchohra, and S. Hamani, "A survey on existence results for boundary value problems of nonlinear fractional differential equations and inclusions," *Acta Applicandae Mathematicae*, vol. 109, no. 3, pp. 973–1033, 2010.

[19] I. A. Rus, "Ulam stabilities of ordinary differential equations in a Banach space," *Carpathian Journal of Mathematics*, vol. 26, pp. 103–107, 2010.

[20] A. Cabada and G. Wang, "Positive solutions of nonlinear fractional differential equations with integral boundary value conditions," *Journal of Mathematical Analysis and Applications*, vol. 389, no. 1, pp. 403–411, 2013.

Hindawi
Mathematical Problems in Engineering
Volume 2020, Article ID 1393456, 9 pages
https://doi.org/10.1155/2020/1393456

Research Article

Finite Difference/Fourier Spectral for a Time Fractional Black–Scholes Model with Option Pricing

Juan He[1,2] and Aiqing Zhang [1]

[1]*Business School, Central University of Finance and Economics, Beijing 100081, China*
[2]*Accounting School, Guizhou University of Finance and Economics, Guiyang 550025, Guizhou, China*

Correspondence should be addressed to Aiqing Zhang; zhangaiqing@cufe.edu.cn

Received 4 May 2020; Accepted 27 July 2020; Published 4 September 2020

Academic Editor: Hamdy Nabih Agiza

We study the fractional Black–Scholes model (FBSM) of option pricing in the fractal transmission system. In this work, we develop a full-discrete numerical scheme to investigate the dynamic behavior of FBSM. The proposed scheme implements a known $L1$ formula for the α-order fractional derivative and Fourier-spectral method for the discretization of spatial direction. Energy analysis indicates that the constructed discrete method is unconditionally stable. Error estimate indicates that the $2-\alpha$-order formula in time and the spectral approximation in space is convergent with order $\mathcal{O}(\Delta t^{2-\alpha} + N^{1-m})$, where m is the regularity of $\mathbf{u}$ and Δt and N are step size of time and degree, respectively. Several numerical results are proposed to confirm the accuracy and stability of the numerical scheme. At last, the present method is used to investigate the dynamic behavior of FBSM as well as the impact of different parameters.

1. Introduction

The classical option pricing model is proposed by Black and Scholes [1], which is based on the assumption that stocks and options are in an "ideal state" in the market and Samuelson's model [2]:

$$\mathrm{d}S = \mu S\mathrm{d}t + \sigma S\mathrm{d}B(t), \tag{1}$$

where S be the the stock value, $B(t)$ is the Brownian motion with the unit variance, and μ and σ are two constants. But in many cases, fractional Brownian motion is more accurate than integer order [3]. On the other hand, more and more diffusion processes were found to be non-Fickian [4, 5], and the fractional order stochastic differential equation is considered as an extension of the stochastic differential equation. One view is that fractional order option trading equation is regarded as nonrandom growth process caused by Brownian motion. Therefore, Jumarie [6] and Liang et al. [7] considered fractional Brownian motion in Samuelson's model equation:

$$\begin{aligned} \mathrm{d}S &= \mu S\mathrm{d}t + \sigma S\mathrm{d}B(t,\alpha), \\ \mathrm{d}S &= \mu S\mathrm{d}t + \sigma S w(t)(\mathrm{d}t)^{\alpha}. \end{aligned} \tag{2}$$

Combining Itô lemma and fractional Taylor expansion of the option price V, Jumarie [6] obtained the following FBSM:

$$\begin{aligned} \frac{\partial^{\alpha} V(S,t)}{\partial t^{\alpha}} &= \left(\frac{rV(S,t)}{(1-\alpha)!} - rS^{\alpha}\frac{\partial^{\alpha} V(S,t)}{\partial S^{\alpha}}\right)t^{1-\alpha} \\ &\quad - \frac{(\alpha!)^3[(1-\alpha)!]^2}{(2\alpha)!}\sigma^2 S^2 \frac{\partial^{2\alpha} V(S,t)}{\partial S^{2\alpha}} = 0, \\ \frac{\partial^{\alpha} V(S,t)}{\partial t^{\alpha}} &= \left(rV(S,t) - rS\frac{\partial V}{\partial S}\right)\frac{t^{1-\alpha}}{(1-\alpha)!} \\ &\quad - \frac{\alpha!}{2}\sigma^2 S^2 \frac{\partial^2 V(S,t)}{\partial S^2} = 0. \end{aligned} \tag{3}$$

Jumarie [8] derived new families of the exact solution of the above equations. Moreover, traditional pricing models for double barrier options are often biased when price changes are considered as fractal transmission systems. Chen et al. [9] revealed that it would be better to use fractional order Black–Scholes equation to explain the pricing in fractal transmission systems.

There is a lot of work in the modeling and calculation of fractional equations. Yang et al. [10, 11] developed a new definition of fractional derivative. The advantage of this definition is that it does not contain singular kernel. Inc et al. [12, 13] studied the isolated solutions of a class of fractional equations with Kerr law nonlinearity by Riccati–Bernoulli method. The exact dark optical and periodic singular soliton solution is obtained. Singhet al. [14–16] solved a series of fractional equations by using homotopy analysis technique and Laplace transform algorithm.

As we all know, as an effective method, $L1$ formula [17] has been widely used in the calculation of fractional differential equations. Langlands and Henry [18], Sun and Wu [19], and Lin and Xu [20] discussed the error estimate for $L1$ scheme. De Staelena and Hendybc [21] constructed a numerical method of fourth-order finite difference in space and $2-\alpha$ in time. Stability, uniqueness, and error estimates are analyzed. Zhang et al. [22] presented a discrete implicit finite scheme to solve time fractional Black–Scholes model. They discussed the stability and error estimation of numerical schemes by Fourier analysis. Unfortunately, their analysis methods are local approach. Due to the importance of FBSM, it is necessary to reconstruct an efficient numerical method and analyze global stability and error estimates.

In this work, we will develop an efficient full-discrete scheme to approximate the Black–Scholes model with α-order fractional derivative. We apply $L1$ method to discretize the direction of time and Fourier-spectral method to discretize the direction of space. Using the energy analysis method, we discuss the stability and error estimate of the fully discrete numerical method. The detailed analysis shows that the scheme is unconditionally energy stable, and the error estimates indicate that our full-discrete scheme can achieve $2-\alpha$-order accuracy in time and exponential accuracy in space direction. Finally, some numerical examples are conducted to support the theoretical claims. At the same time, the dynamic behavior of FBSM is studied by the proposed method.

We organize the rest of the paper as follows. Section 2 will briefly introduce the FBSM. In Section 3, we develop a time-discrete method for FBSM and then present its discrete energy law. In Section 4, we will study the error estimate of the full-discrete scheme. In Section 5, we present accuracy/stability tests and numerous numerical examples to demonstrate the validity of the full-discrete method. In addition, we will discuss the properties of the solution of the FBSM. Some concluding remarks are given in Section 6.

2. Black–Scholes Model

In this work, we will consider the following time fractional Black–Scholes model:

$$\frac{\partial^\alpha V(S,t)}{\partial t^\alpha}+\frac{1}{2}\sigma^2 S^2\frac{\partial^2 V(S,t)}{\partial S^2}+rS\frac{\partial V(S,t)}{\partial S}-rV(S,t)=0,\quad (S,t)\in(0,+\infty)\times(0,T), \tag{4}$$

$$\begin{aligned}V(0,t)&=p(t),\\ V(+\infty,t)&=q(t),\end{aligned} \tag{5}$$

$$V(S,T)=w(S), \tag{6}$$

where V is the price of the option, S the price of the underlying asset, r the interest rate, and σ the volatility of the stock price, $0<\alpha\leq 1$; the time fractional derivative $\partial^\alpha V(S,t)/\partial t^\alpha$ is defined by

$$\frac{\partial^\alpha V(\cdot,t)}{\partial t^\alpha}:=\partial_t^\alpha V(\cdot,t)=\frac{1}{\Gamma(1-\alpha)}\int_0^t(t-\mu)^{-\alpha}\frac{\partial V(\cdot,\mu)}{\partial\mu}\mathrm{d}\mu. \tag{7}$$

This is a linear parabolic partial differential equation which has been studied extensively.

We transform the problem to an initial value problem by using the time to mature $t:=T-\tau$, and we then set $x=\ln S, V(S,\tau)=\mathbf{u}(e^x,T-\tau)$; we can rewrite (4) as

$$\begin{aligned}&\partial_t^\alpha\mathbf{u}(x,\tau)-\xi\partial_x^2\mathbf{u}(x,\tau)-\omega\partial_x\mathbf{u}(x,\tau)\\&\quad+r\mathbf{u}(x,\tau)=0,\quad(x,\tau)\in(0,+\infty)\times(0,T),\end{aligned} \tag{8}$$

where $\xi=1/2\sigma^2, \omega=r-\xi$, and with the following boundary (barrier) and initial conditions,

$$\begin{aligned}\mathbf{u}(-\infty,\tau)&=p(\tau),\\ \mathbf{u}(-\infty,\tau)&=q(\tau),\\ \mathbf{u}(x,0)&=\mathbf{u}_0(x),\quad a<x<b.\end{aligned} \tag{9}$$

In order to solve the above model by numerical method, it is necessary to truncate the original unbounded region into a finite interval. Therefore, we will consider problem (8) in bounded interval $(0,2\pi)$. Then, we will study the following problem:

$$\begin{aligned}&\partial_\tau^\alpha\mathbf{u}(x,\tau)-\xi\partial_x^2\mathbf{u}(x,\tau)-\omega\partial_x\mathbf{u}(x,\tau)\\&\quad+r\mathbf{u}(x,\tau)=0,\quad(x,\tau)\in(0,2\pi)\times(0,T),\end{aligned} \tag{10}$$

$$\mathbf{u}(0,\tau)=\mathbf{u}(2\pi,\tau), \tag{11}$$

$$\mathbf{u}(x,0)=\mathbf{u}_0(x). \tag{12}$$

Remark 1. In fact, one can choose homogeneous or inhomogeneous boundary conditions. It all depends on the actual option price. We have tested it, and it does not make any difference in actual numerical examples.

3. $2-\alpha$Order Numerical Method

Here, we will develop the time-discrete method for equation (10). First, given a positive integer K, set $\Delta t = T/K$ be the time step size, and denote $\tau_n = n\Delta t$, $(0 \le n \le K)$ as the mesh point. Then, we introduce an $L1$ method to discrete the Caputo fractional derivative of order α:

$$\partial_t^\alpha \mathbf{u}(x,\tau) = \frac{1}{\Gamma(2-\alpha)} \sum_{j=0}^{n} b_j \frac{\mathbf{u}(\cdot,\tau_{n+1-j}) - \mathbf{u}(\cdot,\tau_{n-j})}{\Delta t^\alpha} + \mathcal{O}\left(\Delta t^{2-\alpha}\right), \tag{13}$$

where $b_j = (j+1)^{1-\alpha} - j^{1-\alpha}$.

Lemma 1 (see [20, 23, 24]). *The coefficients of formula (13) satisfy the following properties:*

$$1 = b_0 > b_1 > b_2 > \cdots b_j \longrightarrow 0, \quad \text{as} j \longrightarrow +\infty. \tag{14}$$

Then, we can obtain the following time-discrete scheme:

$$\begin{aligned} &\frac{1}{a_0}\left(\mathbf{u}^{n+1} - \sum_{j=0}^{n-1}\left(b_j - b_{j+1}\right)\mathbf{u}^{n-j} - b_n\mathbf{u}^0\right) - \xi\partial_x^2\mathbf{u}^{n+1} \\ &\quad - \omega\partial_x\mathbf{u}^{n+1} + r\mathbf{u}^{n+1} = 0, \quad n \ge 0, \end{aligned} \tag{15}$$

where $a_0 = \Delta t^\alpha \Gamma(2-\alpha)$. It should be noted that if $n=0$, we can rewrite the above equation as

$$\frac{1}{a_0}\left(\mathbf{u}^1 - \mathbf{u}^0\right) - \xi\partial_x^2\mathbf{u}^1 - \omega\partial_x\mathbf{u}^1 + r\mathbf{u}^1 = 0. \tag{16}$$

First of all, we have the following energy stability results for time-discrete (15).

Theorem 1. *The time-discrete scheme (15) is unconditionally stable. It satisfies the following energy dissipation law:*

$$\left\|\mathbf{u}^{k+1}\right\| \le \left\|\mathbf{u}^0\right\|, \quad k = 0, 1, \ldots, K. \tag{17}$$

Proof. When $n = 0$, computing the L^2 inner product of (16) with $2\mathbf{u}^1$, we obtain

$$\begin{aligned} &2\left(\mathbf{u}^1 - \mathbf{u}^0, \mathbf{u}^1\right) - 2a_0\xi\left(\partial_x^2\mathbf{u}^1, \mathbf{u}^1\right) \\ &\quad - a_0\omega\left(\partial_x\mathbf{u}^1, \mathbf{u}^1\right) + a_0 r\left(\mathbf{u}^1, \mathbf{u}^1\right) = 0. \end{aligned} \tag{18}$$

It is easy to verify that the following formula is correct:

$$2(A-B, A) = A^2 - B^2 + (A-B)^2. \tag{19}$$

Thus,

$$\left\|\mathbf{u}^1\right\|^2 - \left\|\mathbf{u}^0\right\|^2 + \left\|\mathbf{u}^1 - \mathbf{u}^0\right\|^2 + 2a_0 a\left\|\partial_x\mathbf{u}^1\right\|^2 + 2a_0 r\left\|u^1\right\|^2 = 0. \tag{20}$$

Giving up some positive terms, we have

$$\left\|\mathbf{u}^1\right\|^2 \le \left\|\mathbf{u}^0\right\|^2. \tag{21}$$

Assume the following inequality holds:

$$\left\|\mathbf{u}^j\right\|^2 \le \left\|\mathbf{u}^0\right\|^2, \quad j = 2, 3, \ldots, n. \tag{22}$$

Next, we will show $\|\mathbf{u}^{n+1}\|^2 \le \|\mathbf{u}^0\|^2$ is still valid. If $j = n+1$, taking the L^2 inner product of (15) with $2\mathbf{u}^{n+1}$, we derive

$$\begin{aligned} &2\left\|\mathbf{u}^{n+1}\right\|^2 + 2a_0\xi\left\|\partial_x\mathbf{u}^{n+1}\right\|^2 + 2a_0 r\left\|u^{n+1}\right\|^2 \\ &\quad = 2\left(\sum_{j=0}^{n-1}\left(b_j - b_{j+1}\right)\mathbf{u}^{n-j} + b_n\mathbf{u}^0, \mathbf{u}^{n+1}\right) \\ &\quad \le \sum_{j=0}^{n-1}\left(b_j - b_{j+1}\right)\left(\left\|\mathbf{u}^{n-j}\right\|^2 + \left\|\mathbf{u}^{n+1}\right\|^2\right) \\ &\qquad + b_n\left(\left\|\mathbf{u}^0\right\|^2 + \left\|\mathbf{u}^{n+1}\right\|^2\right). \end{aligned} \tag{23}$$

Note the fact that

$$\sum_{j=0}^{n-1}\left(b_j - b_{j+1}\right) + b_n = 1. \tag{24}$$

Thus, we get

$$\begin{aligned} \left\|\mathbf{u}^{n+1}\right\|^2 &\le \sum_{j=0}^{n-1}\left(b_j - b_{j+1}\right)\left\|\mathbf{u}^{n-j}\right\|^2 + b_n\left\|\mathbf{u}^0\right\|^2 \\ &\le \left(\sum_{j=0}^{n-1}\left(b_j - b_{j+1}\right) + b_n\right)\left\|\mathbf{u}^0\right\|^2 = \left\|\mathbf{u}^0\right\|^2. \end{aligned} \tag{25}$$

This yields (17). □

4. Error Estimate for Full Discretization

In this part, we will study the Fourier-spectral method for the time-discrete method (15). First, we define S_N as the polynomial space. Define $\pi_N\colon L^2(\Omega) \longrightarrow S_N$ be the L^2-projection operator which satisfies

$$\left(\pi_N\phi - \phi, \psi\right) = 0, \quad \forall \psi \in S_N. \tag{26}$$

We have the following estimate [25]:

$$\left\|\phi - \pi_N\phi\right\|_l \le \mathrm{C}N^{l-m}\|\phi\|_m, \quad \forall \phi \in H^m(\Omega), m > l \ge 0. \tag{27}$$

Then, we can develop the following full-discrete scheme:

$$\begin{aligned} &\frac{1}{a_0}\left(\mathbf{u}_N^{n+1} - \sum_{j=0}^{n-1}\left(b_j - b_{j+1}\right)\mathbf{u}_N^{n-j} - b_n\mathbf{u}_N^0, \phi_N\right) \\ &\quad - \xi\left(\partial_x^2\mathbf{u}_N^{n+1}, \phi_N\right) - \omega\left(\partial_x\mathbf{u}^{n+1}, \phi_N\right) + r\left(\mathbf{u}^{n+1}, \phi_N\right) = 0, \quad \phi_N \in S_N. \end{aligned} \tag{28}$$

We now present the stability results of the fully discrete scheme (28).

Theorem 2. *Let $\{\mathbf{u}_N^n\}_{n=1}^{M-1}$ be the solution of (28), then we derive*

$$\left\|\mathbf{u}_N^{n+1}\right\|^2 \le \left\|\mathbf{u}_N^0\right\|^2. \tag{29}$$

Next, we begin to analyze the error estimates of the full-discrete scheme (28). Define the following error function:

$$\begin{aligned} R^{n+1} &= \frac{1}{\Gamma(2-\alpha)}\sum_{j=0}^{n} b_j \frac{\mathbf{u}(\cdot,t_{n+1-j}) - \mathbf{u}(\cdot,t_{n-j})}{\Delta t^{\alpha}} \\ &\quad - \frac{1}{\Gamma(1-\alpha)}\int_0^{t_{n+1}} \frac{\partial \mathrm{u}(\cdot,\mu)}{\partial \mu}\frac{\mathrm{d}\mu}{(t_{n+1}-\mu)^{\alpha}}. \end{aligned} \tag{30}$$

From [20, 19, 24, 23], we know that R^{n+1} satisfies

$$\left\|R^{n+1}\right\| \le C\Delta t^{2-\alpha}. \tag{31}$$

We also define the following error functions:

$$\begin{aligned} \widetilde{e}_u^n &= \pi_N \mathbf{u}(t_n) - \mathbf{u}_N^n, \\ \widehat{e}_u^n &= \mathbf{u}(t_n) - \pi_N \mathbf{u}(t_n), \\ e_u^n &= \widehat{e}_u^n + \widetilde{e}_u^n = \mathbf{u}(t_n) - \mathbf{u}_N^n. \end{aligned} \tag{32}$$

Lemma 2. *For a_0 and b_n, we have the following results:*

$$a_0 \le 2b_n\Gamma(1-\alpha)T^{\alpha}. \tag{33}$$

Proof.

$$\begin{aligned} b_n &= \left((n+1)^{1-\alpha} - (n)^{1-\alpha}\right) \\ &= n^{1-\alpha}\left(\left(1+\frac{1}{n}\right)^{1-\alpha} - 1\right) \\ &= n^{1-\alpha}\left(\frac{(1-\alpha)}{n} + \frac{(1-\alpha)(-\alpha)}{2!}\frac{1}{n^2} + \cdots\right) \\ &\ge n^{1-\alpha}\left(\frac{(1-\alpha)}{n} + \frac{(1-\alpha)(-\alpha)}{2!}\frac{1}{n^2}\right) \\ &= n^{1-\alpha}\left(\frac{(1-\alpha)}{2n} + \frac{(1-\alpha)}{2n} + \frac{(1-\alpha)(-\alpha)}{2!}\frac{1}{n^2}\right). \end{aligned} \tag{34}$$

Note that

$$\frac{(1-\alpha)}{2n} + \frac{(1-\alpha)(-\alpha)}{2!}\frac{1}{n^2} \ge 0. \tag{35}$$

Therefore, we obtain

$$\frac{a_0}{b_n} \le \frac{2n^{\alpha}\Delta t^{\alpha}\Gamma(2-\alpha)}{(1-\alpha)} \le 2\Gamma(1-\alpha)T^{\alpha}. \tag{36}$$

□

Remark 2. In [23, 24], readers will also find similar parameter estimation. This result is very useful for us to analyze error estimate.

Theorem 3. *For the constructed numerical scheme (28), we have the following error estimate:*

$$\left\|\mathbf{u}\left(\tau^k\right) - \mathbf{u}^k\right\| \le C\left(\Delta t^{2-\alpha} + N^{1-m}\right), \quad k = 0,1,\ldots,K = \frac{T}{\Delta t}. \tag{37}$$

Proof. For $n = 0$, we can write equation (28) as

$$\frac{1}{a_0}\left(\mathbf{u}_N^1 - \mathbf{u}_N^0, \phi_N\right) - \xi\left(\partial_x^2\mathbf{u}_N^1, \phi_N\right) - \omega\left(\partial_x\mathbf{u}_N^1, \phi_N\right) + r\left(\mathbf{u}_N^1, \phi_N\right) = 0. \tag{38}$$

Subtracting (38) from (10) at τ_1, we note that

$$\begin{aligned} \partial_\tau^\alpha \mathbf{u}(\cdot,\tau_1) - \frac{\mathbf{u}_N^1 - \mathbf{u}_N^0}{a_0} &= \partial_\tau^\alpha \mathbf{u}(\cdot,\tau_1) - \frac{\mathbf{u}(\cdot,\tau_1) - \mathbf{u}(\cdot,\tau_0)}{a_0} \\ &\quad + \frac{\mathbf{u}(\cdot,\tau_1) - \mathbf{u}(\cdot,\tau_0)}{a_0} - \frac{\pi_N\mathbf{u}(\cdot,\tau_1) - \pi_N\mathbf{u}(\cdot,\tau_0)}{a_0} \\ &\quad + \frac{\pi_N\mathbf{u}(\cdot,\tau_1) - \pi_N\mathbf{u}(\cdot,\tau_0)}{a_0} - \frac{\mathbf{u}_N^1 - \mathbf{u}_N^0}{a_0} \\ &= R^1 + \frac{1}{a_0}(I - \pi_N)(\mathbf{u}(\cdot,\tau_1) - \mathbf{u}(\cdot,\tau_0)) + \frac{1}{a_0}\left(\widetilde{e}_u^1 - \widetilde{e}_u^0\right), \\ \partial_x^2\mathbf{u}(\cdot,\tau_1) - \partial_x^2\mathbf{u}_N^1 &= \partial_x^2\mathbf{u}(\cdot,\tau_1) - \pi_N\partial_x^2\mathbf{u}(\cdot,\tau_1) \\ &\quad + \pi_N\partial_x^2\mathbf{u}(\cdot,\tau_1) - \partial_x^2\mathbf{u}_N^1 \\ &= \partial_x^2\left[(I - \pi_N)\mathbf{u}(\cdot,\tau_1)\right] + \partial_x^2\widetilde{e}_u^1, \\ \partial_x\mathbf{u}(\cdot,\tau_1) - \partial_x\mathbf{u}_N^1 &= \partial_x\mathbf{u}(\cdot,\tau_1) - \pi_N\partial_x\mathbf{u}(\cdot,\tau_1) \\ &\quad + \pi_N\partial_x\mathbf{u}(\cdot,\tau_1) - \partial_x\mathbf{u}_N^1 \\ &= \partial_x\left[(I - \pi_N)\mathbf{u}(\cdot,\tau_1)\right] + \partial_x\widetilde{e}_u^1, \\ \mathbf{u}(\cdot,\tau_1) - \mathbf{u}_N^1 &= \mathbf{u}(\cdot,\tau_1) - \pi_N\mathbf{u}(\cdot,\tau_1) + \pi_N\mathbf{u}(\cdot,\tau_1) - \mathbf{u}_N^1 \\ &= (I - \pi_N)\mathbf{u}(\cdot,\tau_1) + \widetilde{e}_u^1. \end{aligned} \tag{39}$$

Then, we have

$$\begin{aligned} &\left(\widetilde{e}_u^1 - \widetilde{e}_u^0, \phi_N\right) + a_0\xi\left(\partial_x\widetilde{e}_u^1, \partial_x\phi_N\right) - a_0\omega\left(\partial_x\widetilde{e}_u^1, \phi_N\right) + a_0 r\left(\widetilde{e}_u^1, \phi_N\right) \\ &= -a_0\left(R^1, \phi_N\right) + \left(\left(\pi_N - I\right)\left(\mathbf{u}(\cdot,\tau_1) - \mathbf{u}(\cdot,\tau_0)\right), \phi_N\right) \\ &\quad + a_0\xi\left(\left(\pi_N - I\right)\partial_x\mathbf{u}(\cdot,\tau_1), \partial_x\phi_N\right) \\ &\quad - a_0\omega\left(\left(I - \pi_N\right)\mathbf{u}(\cdot,\tau_1), \partial_x\phi_N\right) \\ &\quad + a_0 r\left(\left(\pi_N - I\right)\mathbf{u}(\cdot,\tau_1), \phi_N\right), \quad \phi_N \in S_N. \end{aligned} \tag{40}$$

Set $\phi_N = 2\widetilde{e}_u^1$, we have

$$
\begin{aligned}
&2\|\tilde{e}_u^1\|^2 + 2a_0\xi\|\partial_x\tilde{e}_u^1\|^2 + 2a_0 r\|\tilde{e}_u^1\|^2 \\
&\le a_0\left(\frac{1}{rb_0}\|R^1\|^2 + rb_0\|\tilde{e}_u^1\|^2\right) \\
&\quad + a_0\xi\left(\frac{1}{b_0}\|(\pi_N - I)\partial_x\mathbf{u}(\cdot,\tau_1)\|^2 + b_0\|\partial_x\tilde{e}_u^1\|^2\right) \\
&\quad + a_0\omega\left(\frac{\omega}{\xi b_0}\|(I-\pi_N)\mathbf{u}(\cdot,\tau_1)\|^2 + \frac{\xi b_0}{\omega}\|\partial_x\tilde{e}_u^1\|^2\right).
\end{aligned}
\tag{41}
$$

Dropping some positive terms, we find

$$
\|\tilde{e}_u^1\|^2 \le C_1\frac{a_0}{b_0}\Delta t^{4-2\alpha} + C_2\frac{a_0}{b_0}N^{1-m} + C_3\frac{a_0}{b_0}N^{-m}. \tag{42}
$$

Assume

$$
\|\tilde{e}_u^k\|^2 \le C_1\frac{a_0}{b_{k-1}}\Delta t^4 + C_2\frac{a_0}{b_{k-1}}N^{1-m} + C_3\frac{a_0}{b_{j-1}}N^{-m}, \quad k = 2,3,\ldots,n. \tag{43}
$$

Next, we will prove that it holds also for $k = n+1$. Subtracting (28) from a reformulation of (10) at t_{n+1}, we find

$$
\begin{aligned}
&\left(\tilde{e}_u^{n+1} - \sum_{j=0}^{n-1}(b_j - b_{j+1})\tilde{e}_u^{n-j} - b_n\tilde{e}_u^0, \phi_N\right) + a_0\xi(\partial_x\tilde{e}_u^{n+1}, \partial_x\phi_N) - a_0\omega(\partial_x\tilde{e}_u^{n+1}, \phi_N) + a_0 r(\tilde{e}_u^{n+1}, \phi_N) \\
&= -a_0(R^{n+1}, \phi_N) + \left((\pi_N - I)\left(\mathbf{u}(\cdot,\tau_{n+1}) - \sum_{j=0}^{n-1}(b_j - b_{j+1})\mathbf{u}(\cdot,\tau_{n-j}) - u(\cdot,\tau_0)\right), \phi_N\right) \\
&\quad + a_0\xi((\pi_N - I)\partial_x\mathbf{u}(\cdot,\tau_{n+1}), \partial_x\phi_N) - a_0\omega((I-\pi_N)\mathbf{u}(\cdot,\tau_{n+1}), \partial_x\phi_N) + a_0 r((\pi_N - I)\mathbf{u}(\cdot,\tau_{n+1}), \phi_N).
\end{aligned}
\tag{44}
$$

Let $\phi_N = 2\tilde{e}_u^{n+1}$, we have

$$
\begin{aligned}
&2\|\tilde{e}_u^{n+1}\|^2 + 2a_0\xi\|\partial_x\tilde{e}_u^{n+1}\|^2 + 2a_0 r\|\tilde{e}_u^{n+1}\|^2 \\
&\le 2\left(\sum_{j=0}^{n-1}(b_j - b_{j+1})\tilde{e}_u^{n-j} - b_n\tilde{e}_u^0, \tilde{e}_u^{n+1}\right) - 2a_0(R^{n+1}, \tilde{e}_u^{n+1}) \\
&\quad + 2a_0\xi((\pi_N - I)\partial_x\mathbf{u}(\cdot,\tau_{n+1}), \partial_x\tilde{e}_u^{n+1}) - 2a_0\omega((I-\pi_N)\mathbf{u}(\cdot,\tau_{n+1}), \partial_x\tilde{e}_u^{n+1}) \\
&\le \sum_{j=0}^{n-1}(b_j - b_{j+1})\left(\|\tilde{e}_u^{n-j}\|^2 + \|\tilde{e}_u^{n+1}\|^2\right) + a_0\left(\frac{1}{r}\|R^{n+1}\|^2 + r\|\tilde{e}_u^{n+1}\|^2\right) \\
&\quad + a_0\xi\left(\|(\pi_N - I)\partial_x u(\cdot,\tau_{n+1})\|^2 + \|\partial_x\tilde{e}_u^{n+1}\|^2\right) + a_0\omega\left(\frac{\omega}{\xi}\|(I-\pi_N)\mathbf{u}(\cdot,\tau_{n+1})\|^2 + \frac{\xi}{\omega}\|\partial_x\tilde{e}_u^{n+1}\|^2\right).
\end{aligned}
\tag{45}
$$

Thus, we have

$$
\begin{aligned}
\|\tilde{e}_u^{n+1}\|^2 &\le \sum_{j=0}^{n-1}(b_j - b_{j+1})\|\tilde{e}_u^{n-j}\|^2 + \frac{a_0}{r}\|R^{n+1}\|^2 \\
&\quad + a_0 a\|(\pi_N - I)\partial_x\mathbf{u}(\cdot,\tau_{n+1})\|^2 + \frac{a_0 b^2}{a}\|(I-\pi_N)\mathbf{u}(\cdot,\tau_{n+1})\|^2 \\
&\le \sum_{j=0}^{n-1}(b_j - b_{j+1})\left(C_1\frac{a_0}{b_{j-1}}\Delta t^4 + C_2\frac{a_0}{b_{j-1}}N^{1-m} + C_3\frac{a_0}{b_{j-1}}N^{-m}\right) \\
&\quad + b_n\left(C_1\frac{a_0}{b_n}\Delta t^4 + C_2\frac{a_0}{b_n}N^{1-m} + C_3\frac{a_0}{b_n}N^{-m}\right).
\end{aligned}
\tag{46}
$$

Note that $b_{n-j} \ge b_n$, thus

$$
\begin{aligned}
\|\tilde{e}_u^{n+1}\|^2 &\le \left(C_1\frac{a_0}{b_n}\Delta t^4 + C_2\frac{a_0}{b_n}N^{1-m} + C_3\frac{a_0}{b_n}N^{-m}\right) \\
&\quad \left(\sum_{j=0}^{n-1}(b_j - b_{j+1}) + b_n\right) \\
&= C_1\frac{a_0}{b_n}\Delta t^4 + C_2\frac{a_0}{b_n}N^{1-m} + C_3\frac{a_0}{b_n}N^{-m}.
\end{aligned}
\tag{47}
$$

Note that

$$
\|\mathbf{u}(\tau^k) - \mathbf{u}^k\| \le \|\hat{e}_u^k\| + \|\tilde{e}_u^k\|. \tag{48}
$$

This ends the proof. □

Table 1: Temporal convergence orders of various time steps for Example 1.

$\alpha/\Delta t$	$\Delta t =$ 1/200	$\Delta t =$ 1/400	$\Delta t =$ 1/800	$\Delta t =$ 1/1600	$\Delta t =$ 1/3200
$\alpha = 0.1$	1.8166	1.8263	1.8345	1.8415	1.8475
$\alpha = 0.3$	1.6680	1.6746	1.6797	1.6837	1.6869
$\alpha = 0.5$	1.4892	1.4925	1.4947	1.4963	1.4974
$\alpha = 0.6$	1.3939	1.3960	1.3974	1.3983	1.3989
$\alpha = 0.7$	1.2964	1.2979	1.2987	1.2992	1.2995
$\alpha = 0.9$	1.0980	1.0990	1.0995	1.0997	1.0999

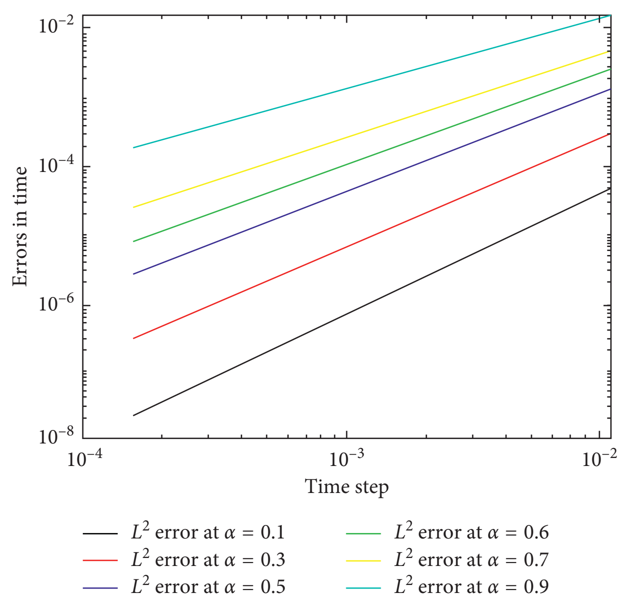

Figure 1: Error in time direction for different α.

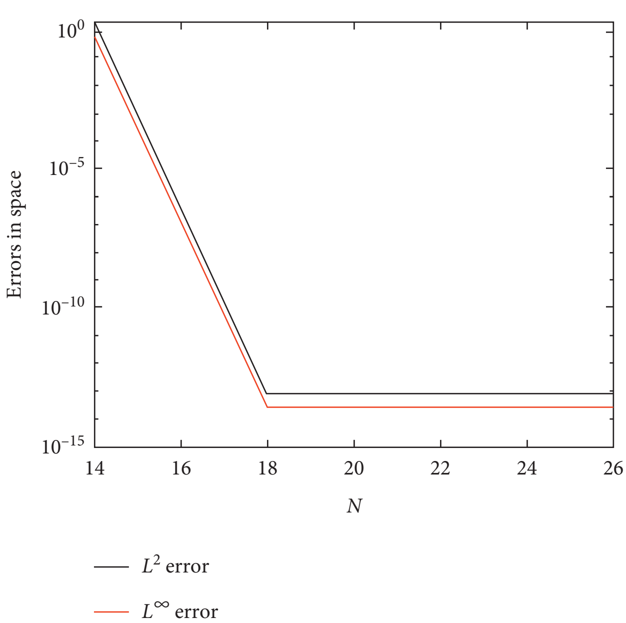

Figure 2: The L^2 and L^∞ errors in space direction with $\alpha = 0.1$.

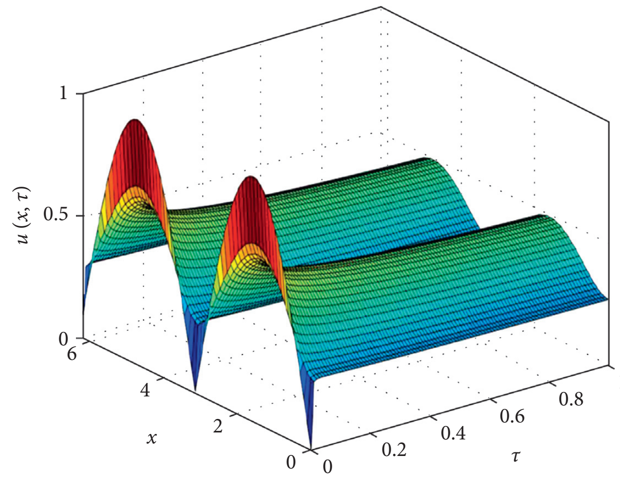

Figure 3: The dynamic behavior of solution to FBSM equation at $\alpha = 0.2$.

5. Numerical Examples

In this section, several numerical examples will be present to confirm the accuracy and applicability of the full-discrete scheme (28). We consider a rectangular computed domain of $[0, 2\pi]$. In order to better simulate the periodic boundary conditions, the Fourier-spectral method will be used to discretize space direction.

5.1. Verification of Convergence of Numerical Method. First, in order to conduct a time accuracy test, an exact solution will be constructed to evaluate the convergence of the full-discrete scheme (28).

Example 1. We consider the following FBSM with α-order Caputo derivative:

$$\partial_\tau^\alpha \mathbf{u}(x,\tau) - \xi\partial_x^2 \mathbf{u}(x,\tau) - \omega\partial_x \mathbf{u}(x,\tau) + r\mathbf{u}(x,\tau) = \mathbf{f}(x,\tau), \tag{49}$$

where

$$\mathbf{f}(x,\tau) = \frac{2T^{2-\alpha}}{\Gamma(3-\alpha)}\sin x + \xi\tau^2 \sin x - \omega\tau^2 \cos x + r\tau^2 \sin x. \tag{50}$$

It is easy to verify that the exact solution will be $\mathbf{u} = \tau^2 \sin x$.

We set $N = 128$. The default values for the parameters are set as $T = 1, \xi = 1, \omega = 0$, and $r = 1$. In Table 1, we show the temporal convergence orders of various time steps. As can be seen from Table 1, our full-discrete scheme is close to $2 - \alpha$-order accuracy in time, which is confirm with the result in Theorem 3.

Fix $N = 128$, in Figure 1, we give L^2 error for different α. It is obvious that our numerical scheme has good convergence in time direction. Let $T = 0.1, \Delta t = 10^{-6}$, $\xi = r = 0.5$, $\omega = 0$, and $u_0 = \cos 8x$. Figure 2 shows that the full-discrete

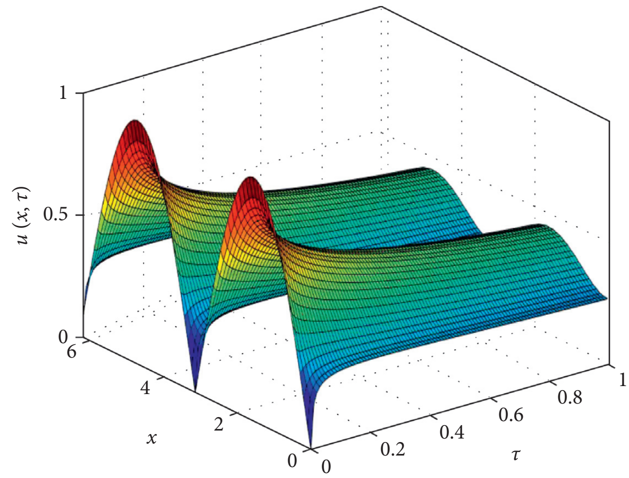

FIGURE 4: The dynamic behavior of solution to FBSM equation at $\alpha = 0.5$.

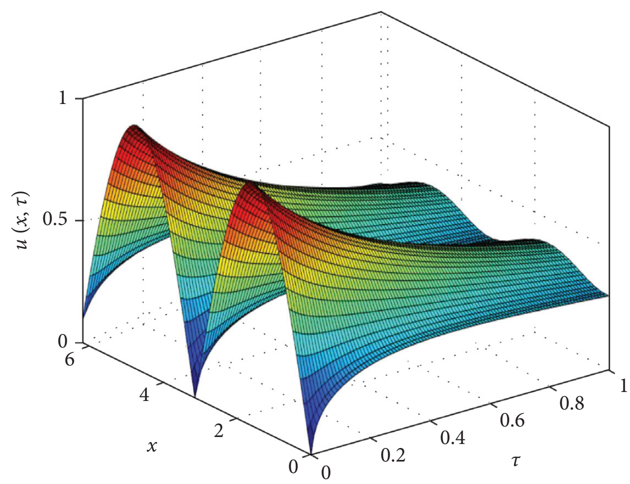

FIGURE 5: The dynamic behavior of solution to FBSM equation at $\alpha = 0.9$.

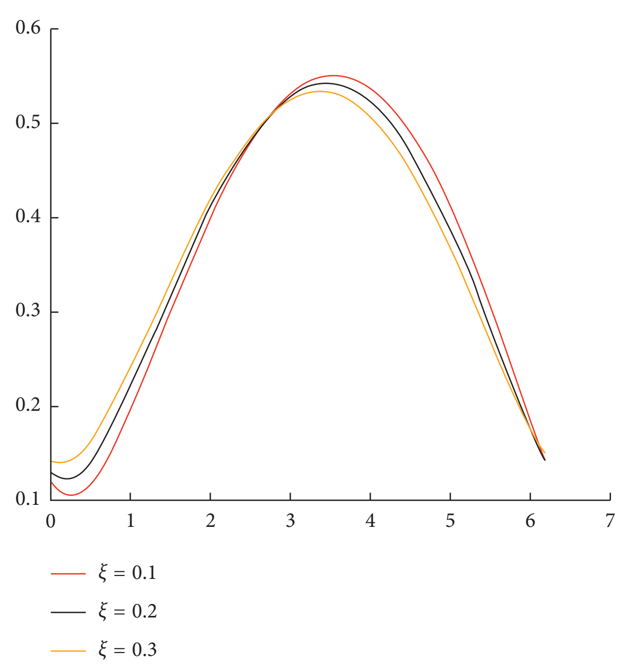

FIGURE 6: The influence of various $\xi (\xi = 0.1, 0.2, 0.3)$ on the option price.

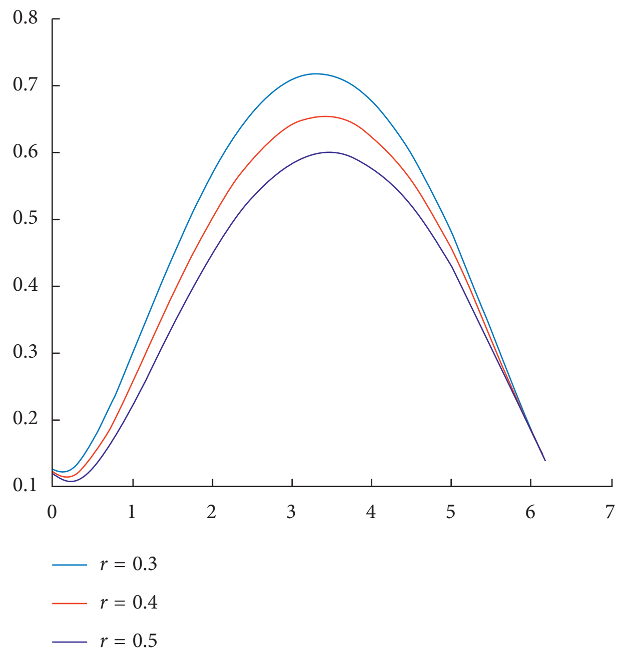

FIGURE 7: The influence of various $r\,(\xi = 0.3, 0.4, 0.5)$ on the option price.

scheme (28) has excellent convergence behavior in space direction.

5.2. Effect of Various Parameters. This section is devoted to investigate the dynamic behavior of FBSM equation with different α. In the following numerical experiments, we fix $\xi = 0.5, w = 0.1, r = 0.6, N = 64, \Delta t = 0.01$, and $u_0 = |\sin x|$. From Figures 3–5, we know that α has certain influence on the solution, as α increases, and the solution becomes smoother. In order to test the influence of ξ on the option price, we set $r = 0.6, u_0 = \sin(x/2)$ and let ξ change at the same time. Figure 6 shows that the parameter ξ has a significant effect on the price of options, and there will be an inflection point around $x = 2.8$. Finally, we investigated the influence of r on the option price, and the results are shown in Figure 7, it can be seen that when r increases, the option price also increases.

6. Conclusion

In this paper, a new full-discrete numerical method is developed to solve the FBSM. An efficient $2-\alpha$-order and unconditionally energy stable method is constructed by combining the $L1$ approach in time and Fourier method in space direction. It is proved that the full-discrete converges to the order $\mathcal{O}(\Delta t^{2-\alpha} + N^{-s} + N^{-m})$ globally. Numerical examples demonstrate the robustness and accuracy of the developed full-discrete method, numerically. Finally, we also study the properties of the solution of the FBSM.

Data Availability

The data used to support the findings of this study are available from the corresponding author upon request.

Conflicts of Interest

The authors declare that they have no conflicts of interest.

Authors' Contributions

Juan He carried out an efficient numerical approach to time fractional Black–Scholes model. Aiqing Zhang helped to draft the manuscript. All authors read and approved the final manuscript.

Acknowledgments

The work of Juan He was supported by the China Scholarship Council (no. 202008520027). The work of Aiqing Zhang was supported by the Cultivation Project of Major Scientic Research Projects of Central University of Finance and Economics (no. 14ZZD007).

References

[1] F. Black and M. Scholes, "The pricing of options and corporate liabilities," *Journal of Political Economy*, vol. 81, no. 3, pp. 637–654, 1973.
[2] R. C. Merton, "Theory of rational option pricing," *The Bell Journal of Economics and Management Science*, vol. 4, no. 1, pp. 141–183, 1973.
[3] R. Cioczek-Georges and B. B. Mandelbrot, "Alternative micropulses and fractional brownian motion," *Stochastic Processes and Their Applications*, vol. 64, no. 2, pp. 143–152, 1996.
[4] W. Min, B. P. English, G. Luo, B. J. Cherayil, S. C. Kou, and X. S. Xie, "Fluctuating enzymes: lessons from single-molecule studies," *Accounts of Chemical Research*, vol. 38, no. 12, pp. 923–931, 2005.
[5] T. A. M. Langlands, B. I. Henry, and S. L. Wearne, "Fractional cable equation models for anomalous electrodiffusion in

nerve cells: infinite domain solutions," *Journal of Mathematical Biology*, vol. 59, no. 6, pp. 761–808, 2009.

[6] G. Jumarie, "Stock exchange fractional dynamics defined as fractional exponential growth driven by (usual) Gaussian white noise. application to fractional black-scholes equations," *Insurance Mathematics and Economics*, vol. 42, no. 1, pp. 271–287, 2007.

[7] J. R. Liang, J. Wang, W. J. Zhang, W. Y. Qiu, and F. Y. Ren, "The solution to a bifractional black-scholes-merton differential equation," *International Journal of Pure and Applied Mathematics*, vol. 58, no. 1, pp. 99–112, 2010.

[8] G. Jumarie, "Derivation and solutions of some fractional Black-Scholes equations in coarse-grained space and time. Application to Merton's optimal portfolio," *Computers & Mathematics with Applications*, vol. 59, no. 3, pp. 1142–1164, 2010.

[9] W. Chen, X. Xu, and S.-P. Zhu, "Analytically pricing double barrier options based on a time-fractional black-scholes equation," *Computers & Mathematics with Applications*, vol. 69, no. 12, pp. 1407–1419, 2015.

[10] X. J. Yang, F. Gao, J. A. Machado, and D. Baleanu, "A new fractional derivative involving the normalized sinc function without singular kernel," *European Physical Journal Special Topics*, vol. 226, no. 16-18, pp. 3567–3575, 2017.

[11] X.-J. Yang, F. Gao, Y. Ju, and H.-W. Zhou, "Fundamental solutions of the general fractional-order diffusion equations," *Mathematical Methods in the Applied Sciences*, vol. 41, no. 18, pp. 9312–9320, 2018.

[12] M. Inc, A. Yusuf, A. I. Aliyu, and D. Baleanu, "Dark and singular optical solitons for the conformable space-time nonlinear Schrödinger equation with Kerr and power law nonlinearity," *Optik*, vol. 162, pp. 65–75, 2018.

[13] M. Inc, A. I. Aliyu, and A. Yusuf, "Dark optical, singular solitons and conservation laws to the nonlinear Schrödinger's equation with spatio-temporal dispersion," *Modern Physics Letters B*, vol. 31, no. 14, p. 1750163, 2017.

[14] J. Singh, D. Kumar, and D. Baleanu, "On the analysis of fractional diabetes model with exponential law," *Advances in Difference Equations*, vol. 231, no. 1, 2018.

[15] J. Singh, D. Kumar, and D. Baleanu, "New aspects of fractional biswas-milovic model with mittag-leffler law," *Mathematical Modelling of Natural Phenomena*, vol. 14, no. 3, p. 303, 2019.

[16] J. Singh, D. Kumar, D. Baleanu, and S. Rathore, "On the local fractional wave equation in fractal strings," *Mathematical Methods in the Applied Sciences*, vol. 42, no. 5, pp. 1588–1595, 2019.

[17] K. B. Oldham and J. Spanier, "The fractional calculus," *Mathematical Gazette*, vol. 56, no. 247, pp. 396–400, 1974.

[18] T. A. M. Langlands and B. I. Henry, "The accuracy and stability of an implicit solution method for the fractional diffusion equation," *Journal of Computational Physics*, vol. 205, no. 2, pp. 719–736, 2005.

[19] Z.-z. Sun and X. Wu, "A fully discrete difference scheme for a diffusion-wave system," *Applied Numerical Mathematics*, vol. 56, no. 2, pp. 193–209, 2006.

[20] Y. Lin and C. Xu, "Finite difference/spectral approximations for the time-fractional diffusion equation," *Journal of Computational Physics*, vol. 225, no. 2, pp. 1533–1552, 2007.

[21] R. H. De Staelena and A. S. Hendybc, "Fractional cable equation models for anomalous electrodiffusion in nerve cells: infinite domain solutions," *Computers and Mathematics with Applications*, vol. 74, no. 6, pp. 1166–1175, 2017.

[22] H. Zhang, F. Liu, I. Turner, and Q. Yang, "Numerical solution of the time fractional black-scholes model governing european options," *Computers & Mathematics with Applications*, vol. 71, no. 9, pp. 1772–1783, 2016.

[23] C. Li, T. Zhao, W. Deng, and Y. Wu, "Orthogonal spline collocation methods for the subdiffusion equation," *Journal of Computational and Applied Mathematics*, vol. 255, pp. 517–528, 2014.

[24] C.-M. Chen, F. Liu, I. Turner, and V. Anh, "A fourier method for the fractional diffusion equation describing sub-diffusion," *Journal of Computational Physics*, vol. 227, no. 2, pp. 886–897, 2007.

[25] A. Quarteroni and A. Valli, *Numerical Approximation of Partial Differential Equations*, Springer, Berlin, Germany, 1994.

Hindawi
Mathematical Problems in Engineering
Volume 2020, Article ID 6529698, 11 pages
https://doi.org/10.1155/2020/6529698

Research Article

n-Dimensional Fractional Frequency Laplace Transform by the Inverse Difference Operator

M. Meganathan,[1] Thabet Abdeljawad ,[2,3,4] G. Britto Antony Xavier,[1] and Fahd Jarad[5]

[1]*Department of Mathematics, Sacred Heart College (Autonomous), Tirupattur District 635601, Vellore, India*
[2]*Department of Mathematics and General Sciences, Prince Sultan University, P.O. Box 66833, Riyadh 11586, Saudi Arabia*
[3]*Department of Medical Research, China Medical University, Taichung 40402, Taiwan*
[4]*Department of Computer Science and Information Engineering, Asia University, Taichung, Taiwan*
[5]*Department of Mathematics, Cankaya University, Etimesgut 06790, Ankara, Turkey*

Correspondence should be addressed to Thabet Abdeljawad; tabdeljawad@psu.edu.sa

Received 11 April 2020; Revised 19 June 2020; Accepted 24 July 2020; Published 24 August 2020

Academic Editor: Abdelalim Elsadany

With the study of extensive literature on the Laplace transform with one and two variables and its properties, applications are available, but there is no work on n-dimensional Laplace transform. In this research article, we define n-dimensional fractional frequency Laplace transform with shift values. Several theorems are derived with properties of the Laplace transform. The results are numerically analyzed and discussed through MATLAB.

1. Introduction

The fractional calculus is a branch of mathematics that focuses on arbitrary order integrals and derivatives. In spite of that, this type of calculus is as older as the conventional calculus, and it has attracted the interest of researchers for the last few decades. This is because of the results reported by these researchers as consequences of their attempts to model real-world phenomena using the fractional operators [1–4]. The discrete version of these operators fetched the attention of research studies as well. Many good results were reported when fractional sums and differences were used in studying related problems (see [5–17] and the references therein).

The integral transforms such as Mellin, Laplace, and Fourier were applied to obtain the solution of differential equations. These transforms made effectively possible changes of a signal in the time domain into a frequency s-domain in the field of digital signal processing (DSP) [18]. The delta Laplace transform was first defined in a very general way by Bohner and Peterson [19]. In 2015, Ivic discussed the discrete Laplace transforms in the view of fast decay factor e^{-sx} and obtained the Laplace transform of $P(x)$ as $\int_0^\infty P(x)e^{-sx}\mathrm{d}x = \pi s^{-2}\sum_{n=1}^{\infty} r(n)e^{-(\pi^2/n)}$. In practice, many applications of Laplace transform (LT), $L[f(x)] = \int_0^\infty f(x)e^{-sx}\mathrm{d}x$, and the forward discrete Laplace transform (DLT), $L[f(n)] = \sum_{n=0}^{\infty} f(n)e^{-sn}$, are discussed and mentioned by several authors in [20–23]. For physical applications of Laplace transform, refer [24–27].

In the existing Laplace transform, the shifting value of time domains is one. In 2016, Britto Antony Xavier et al. [28] defined the Laplace transform with shift value ℓ using the generalized difference operator and obtained the outcomes of polynomial and trigonometric functions. In this fractional frequency Laplace transform, the shift values $\nu_j' s$, $j = 1, 2, \ldots, n$ lie in the interval $[0, 1]$. In [29], the author introduced the double Laplace transform and applied to solve initial and boundary value problems.

In this research work, we extend the work of Laplace transform into an n-dimensional space in discrete case. We present several properties of the fractional transforms for functions such as polynomial factorial, exponential, and trigonometric functions. Also, we derive the relation between Laplace transform and Riemann zeta functions. Furthermore, we present the inverse Laplace transform to compare the results with the existing classical Laplace transform for the particular value of n.

2. Preliminaries

Here, we present some basic definitions and results which will be used further.

Definition 1. Let $u(\overline{t})$ be the function with n-variables and $\overline{h} \in R^n$ be the shift values. Then, the n-dimensional partial difference operator is defined as

$$\underset{h_i}{\Delta} u(\overline{t}) = \frac{u(t_1, t_2, \ldots, t_i + h_i, \ldots, t_n) - u(t_1, t_2, \ldots, t_n)}{h_i}, \tag{1}$$

where $\overline{t} = (t_1, t_2, \ldots, t_n)$ and $\overline{h} = (h_1, h_2, \ldots, h_n)$.

Definition 2 (see [30]). For $h > 0$ and $\mu \in R$, the rising h-polynomial factorial function is defined as

$$t_h^{[\mu]} = h^{\mu} \frac{\Gamma((t/h) + \mu)}{\Gamma(t/h)}, \tag{2}$$

where $t_h^{[0]} = 1$, Γ is the Euler gamma function, and $(t/h) + \mu$, $(t/h) \notin \{0, -1, -2, -3, \ldots\}$ as the division at a pole yields zero.

Lemma 1 (see [31]). *Let $h > 0$ and $u(t)$ and $w(t)$ be real-valued bounded functions. Then,*

$$\Delta_h^{-1}(u(t)w(t)) = u(t)\Delta_h^{-1} w(t) - \Delta_h^{-1}\left(\Delta_h^{-1} w(t+h)\Delta_h u(t)\right). \tag{3}$$

Theorem 1 (see [31]). *Let $t \in (0, \infty)$, $h > 0$, and $s > 0$; then,*

$$L_{h,\nu}\left(t_h^{(\mu)}\right) = \frac{h^{\mu+1}\mu! e^{s^{1/\nu} h}}{\left(e^{s^{1/\nu} h} - 1\right)^{\mu+1}}. \tag{4}$$

2.1. Notations

(i) $\underset{n(h)}{\Delta} u(\overline{t}) = \underset{h_n}{\Delta}\underset{h_{n-1}}{\Delta} \cdots \underset{h_2}{\Delta}\underset{h_1}{\Delta} u(t_1, t_2, \ldots, t_n)$

(ii) $\Delta_{n(h)}^{-1} u(\overline{t}) = \Delta_{h_n}^{-1}\Delta_{h_{n-1}}^{-1} \cdots \Delta_{h_2}^{-1}\Delta_{h_1}^{-1} u(t_1, t_2, \ldots, t_n)$

(iii) $\mathcal{J}(D_n)$ denotes the set of all subsets of $D_n = \{1, 2, \ldots, n\}$

(iv) $n(D_n - \overline{r})$ denotes the number of digits in $D_n - \overline{r}$

Definition 3 (infinite inverse principle law). For the function $u(\overline{t})$, we define the infinite inverse principle law as follows:

$$\Delta_{n(h)}^{-1}\Big|_{\overline{a}}^{\infty} = \left(\prod_{j=1}^{n} h_j\right)\left(\sum_{r_1=0}^{\infty}\sum_{r_2=0}^{\infty} \cdots \sum_{r_n=0}^{\infty} u(a_1 + r_1 h_1, a_2 + r_2 h_2, \ldots, a_n + r_2 h_2)\right), \tag{5}$$

where $\overline{a} = (a_1, a_2, \ldots, a_n)$. In particular, if $\overline{a} = (0, 0, \ldots, 0)$, we obtain

$$\Delta_{n(h)}^{-1}\Big|_{0}^{\infty} = \left(\prod_{j=1}^{n} h_j\right)\left(\sum_{r_1=0}^{\infty}\sum_{r_2=0}^{\infty} \cdots \sum_{r_n=0}^{\infty} u(r_1 h_1, r_2 h_2, \ldots, r_2 h_2)\right). \tag{6}$$

Theorem 2. *Let $\overline{t} \in R^n, h_j > 0, j = 1, 2, \ldots, n$; then,*

$$\Delta_{n(h)}^{-1} a^{-\sum_{j=1}^{n} s_j^{1/\nu_j} t_j} = \frac{\left(\prod_{j=1}^{n} h_j\right) a^{-\sum_{j=1}^{n} s_j^{1/\nu_j} t_j}}{\prod_{j=1}^{n}\left(a^{-s_j^{1/\nu_j} h_j} - 1\right)}. \tag{7}$$

Proof. Taking $u(\overline{t}) = a^{-\sum_{j=1}^{n} s_j^{1/\nu_j} t_j}$ in (1) for the shift value h_1, we obtain

$$\underset{h_1}{\Delta} a^{-\sum_{j=1}^{n} s_j^{1/\nu_j} t_j} = \frac{a^{-\left(s_1^{1/\nu_1}(t_1+h_1) - \sum_{j=1}^{n} s_j^{1/\nu_j} t_j\right)} - a^{-\sum_{j=1}^{n} s_j^{1/\nu_j} t_j}}{h_1} = \frac{h_1 a^{-\sum_{j=1}^{n} s_j^{1/\nu_j} t_j}}{\left(a^{-s_1^{1/\nu_1} h_1} - 1\right)}. \tag{8}$$

In (8), applying $\Delta_{h_2}^{-1}$ on both sides, we get

$$\Delta_{h_2}^{-1}\Delta_{h_1}^{-1}a^{-\sum_{j=1}^{n}s_j^{1/\nu_j}t_j} = \frac{h_1}{\left(a^{-s_1^{1/\nu_1}h_1}-1\right)}\Delta_{h_2}^{-1}a^{-\sum_{j=1}^{n}s_j^{1/\nu_j}t_j}$$
$$= \frac{h_1}{\left(a^{-s_1^{1/\nu_1}h_1}-1\right)}\frac{h_2}{\left(a^{-s_2^{1/\nu_2}h_2}-1\right)}a^{-\sum_{j=1}^{n}s_j^{1/\nu_j}t_j},$$
$$\Delta_{h_2}^{-1}\Delta_{h_1}^{-1}a^{-\sum_{j=1}^{n}s_j^{1/\nu_j}t_j} = \frac{\left(\prod_{j=1}^{2}h_j\right)a^{-\sum_{j=1}^{n}s_j^{1/\nu_j}t_j}}{\prod_{j=1}^{2}\left(a^{-s_j^{1/\nu_j}h_j}-1\right)}. \tag{9}$$

Proceeding like this for the induction on n, we get the proof of (7).

Corollary 1. *Let $\bar{t}\in R^n, h_j>0$ and $j=1,2,\ldots,n$. Then, we have*

$$\Delta_{\overline{n(h)}}^{-1}e^{-\sum_{j=1}^{n}s_j^{1/\nu_j}t_j} = \frac{\left(\prod_{j=1}^{n}h_j\right)e^{-\sum_{j=1}^{n}s_j^{1/\nu_j}t_j}}{\prod_{j=1}^{n}\left(e^{-s_j^{1/\nu_j}h_j}-1\right)}. \tag{10}$$

Proof. In the proof of Theorem 2, replacing a by e, we get (10).

Corollary 2. *In Theorem 2, applying $a=3$, we get*

$$\Delta_{\overline{n(h)}}^{-1}3^{-\sum_{j=1}^{n}s_j^{1/\nu_j}t_j} = \frac{\left(\prod_{j=1}^{n}h_j\right)3^{-\sum_{j=1}^{n}s_j^{1/\nu_j}t_j}}{\prod_{j=1}^{n}\left(3^{-s_j^{1/\nu_j}h_j}-1\right)}. \tag{11}$$

Example 1. Let $n=2$ in (11); we get the result for the shift values h_1 and h_2 as

$$\Delta_{h_2}^{-1}\Delta_{h_1}^{-1}3^{-\left(s_1^{1/\nu_1}t_1+s_2^{1/\nu_2}t_2\right)} = \frac{h_1h_2 3^{-\left(s_1^{1/\nu_1}t_1+s_2^{1/\nu_2}t_2\right)}}{\left(3^{-s_1^{1/\nu_1}h_1}-1\right)\left(3^{-s_2^{1/\nu_2}h_2}-1\right)}. \tag{12}$$

Summing from 0 to ∞ for t_1 and t_2 on both sides yields

$$\Delta_{h_2}^{-1}\Delta_{h_1}^{-1}3^{-\left(s_1^{1/\nu_1}t_1+s_2^{1/\nu_2}t_2\right)}\Big|_0^\infty\Big|_0^\infty = \frac{h_1h_2}{\left(3^{-s_1^{1/\nu_1}h_1}-1\right)\left(3^{-s_2^{1/\nu_2}h_2}-1\right)}. \tag{13}$$

For $n=2$, the infinite principle law reads

$$\Delta_{h_2}^{-1}\Delta_{h_1}^{-1}u(t_1,t_2)\Big|_0^\infty\Big|_0^\infty = h_1h_2\sum_{r_1=0}^{\infty}\sum_{r_2=0}^{\infty}u(r_1h_1,r_2h_2). \tag{14}$$

Equating (13) and (14) for the function $u(t_1,t_2)=3^{-\left(s_1^{1/\nu_1}t_1+s_2^{1/\nu_2}t_2\right)}$, we obtain

$$h_1h_2\sum_{r_1=0}^{\infty}\sum_{r_2=0}^{\infty}3^{-\left(s_1^{1/\nu_1}r_1h_1+s_2^{1/\nu_2}r_2h_2\right)} = \frac{h_1h_2}{\left(3^{-s_1^{1/\nu_1}h_1}-1\right)\left(3^{-s_2^{1/\nu_2}h_2}-1\right)}, \tag{15}$$

which is verified for the particular values $s_1=2, s_2=3, \nu_1=0.3, \nu_2=0.5, h_1=0.4,$ and $h_2=0.7$ by MATLAB coding as follows: ((0.4). ∗ (0.7)). ∗ symsum (symsum (3.∧(− (2.∧(1./0.3). ∗ 0.4. ∗ $r1$ + 3.∧(1./0.5). ∗ 0.7. ∗ $r2$)), $r1$, 0, ∞), $r2$, 0, ∞)= (0.4. ∗ 0.7)/ ((3.∧(− (2.∧(1./ 0.3). ∗ 0.4)) − 1). ∗ (3.∧(−(3.∧(1./0.5). ∗ 0.7))− 1)) = 0.2837.

3. n-Dimensional Fractional Frequency Laplace Transform

Definition 4. For the function $u(\bar{t})$ with n-variables $t_1,t_2,\ldots,t_n$, the n-dimensional fractional frequency Laplace transform is defined as

$$\mathscr{L}_{n(h)}[u(\bar{t})] = U_n(\bar{s}) = \Delta_{\overline{n(h)}}^{-1}u(\bar{t})e^{-\sum_{j=1}^{n}s_j^{1/\nu_j}t_j}\Big|_{t_j=0,j=1,2,\ldots,n}^{\infty}$$
$$= \left(\prod_{j=1}^{n}h_j\right)\sum_{r_1=0}^{\infty}\sum_{r_2=0}^{\infty}\cdots\sum_{r_n=0}^{\infty}u(r_1h_1,r_2h_2,\ldots,r_nh_n)e^{-\sum_{j=1}^{n}s_j^{1/\nu_j}r_jh_j}. \tag{16}$$

Remark 1

(i) The n-dimensional fractional frequency Laplace transform satisfies the linear property.

(ii) In the aforesaid equation (16), we represent the Laplace transform of the functions in two ways: one in the closed-form solution and another one in the summation form solution. In this paper, we numerically verified and analyzed with MATLAB that both solutions are equal.

Theorem 3. *Let $\bar{t}\in R^n, \bar{h}>0$, ν_j be a fraction, and $s_j>0, j=1,2,\ldots,n$. Then, we have*

$$\mathscr{L}_{n(h)}[1] = \frac{\prod_{j=1}^{n}h_j}{\prod_{j=1}^{n}\left(e^{-s_j^{1/\nu_j}h_j}-1\right)}. \tag{17}$$

Proof. Taking $u(\bar{t})=1$ in (16) yields

$$\mathscr{L}_{n(h)}[1] = \Delta_{n(h)}^{-1} e^{-\sum\sum_{j=1}^{n} s_j^{1/\nu_j} t_j} \Big|_{t_j=0,j=1,2,\dots,n}^{\infty}$$
$$= \Delta_{h_n}^{-1} e^{-s_n^{1/\nu_n} t_n} \Big|_0^{\infty} \cdots \Delta_{h_2}^{-1} e^{-s_2^{1/\nu_2} t_2} \Big|_0^{\infty} \Delta_{h_1}^{-1} e^{-s_1^{1/\nu_1} t_1} \Big|_0^{\infty}$$
$$= \frac{h_n}{\left(e^{-s_n^{1/\nu_n} h_n} - 1\right)} \cdots \frac{h_2}{\left(e^{-s_2^{1/\nu_2} h_2} - 1\right)} \frac{h_1}{\left(e^{-s_1^{1/\nu_1} h_1} - 1\right)}, \tag{18}$$

(using Corollary 1), which completes the proof.

Theorem 4. *Let $\bar{t} \in R^n, \bar{h} > 0$, ν_j be a fraction, and $s_j > 0$, $j = 1, 2, \dots, n$; then,*

$$\mathscr{L}_{n(h)}\left[e^{\sum_{j=1}^{n} a_j t_j}\right] = \frac{\prod_{j=1}^{n} h_j}{\prod_{j=1}^{n}\left(e^{-\left(s_j^{1/\nu_j} - a_j\right)h_j} - 1\right)}. \tag{19}$$

Proof. Taking $u(\bar{t}) = e^{\sum_{j=1}^{n} a_j t_j}$ in (16), we have

$$\mathscr{L}_{n(h)}\left[e^{\sum_{j=1}^{n} a_j t_j}\right] = \Delta_{n(h)}^{-1} e^{\sum_{j=1}^{n} a_j t_j} e^{-\sum_{j=1}^{n} s_j^{1/\nu_j} t_j} \Big|_{t_j=0,j=1,2,\dots,n}^{\infty}$$
$$= \Delta_{h_n}^{-1} e^{-\left(s_n^{1/\nu_n} - a_n\right)t_n} \Big|_0^{\infty} \cdots \Delta_{h_2}^{-1} e^{-\left(s_2^{1/\nu_2} - a_2\right)t_2} \Big|_0^{\infty} \Delta_{h_1}^{-1} e^{-\left(s_1^{1/\nu_1} - a_1\right)t_1} \Big|_0^{\infty} \tag{20}$$
$$= \frac{h_n}{\left(e^{-\left(s_n^{1/\nu_n} - a_n\right)h_n} - 1\right)} \cdots \frac{h_2}{\left(e^{-\left(s_2^{1/\nu_2} - a_2\right)h_2} - 1\right)} \frac{h_1}{\left(e^{-\left(s_1^{1/\nu_1} - a_1\right)h_1} - 1\right)},$$

which gives (19).

Example 2. For $n = 2$, the summation solution of the exponential function given by the infinite inverse principle law and the closed form of the solution given as

$$\mathscr{L}_{n(h)}\left[e^{a_1 t_1 + a_2 t_2}\right] = h_1 h_2 \sum_{r_2=0}^{\infty}\sum_{r_1=0}^{\infty} e^{-\left[\left(s_1^{1/\nu_1} - a_1\right) r_1 h_1 + \left(s_2^{1/\nu_2} - a_2\right) r_2 h_2\right]}$$
$$= \frac{h_2}{\left(e^{-\left(s_2^{1/\nu_2} - a_2\right)h_2} - 1\right)} \frac{h_1}{\left(e^{-\left(s_1^{1/\nu_1} - a_1\right)h_1} - 1\right)}, \tag{21}$$

is numerically verified for the particular values $h_1 = 7, h_2 = 3, a_1 = 5, a_2 = 9, \nu_1 = 0.1, \nu_2 = 0.3, s_1 = 11$, and $s_2 = 13$ by MATLAB coding as follows: 21. ∗ (symsum (symsum (exp (− (11.∧ (1./1.0) − 5). ∗ 7. ∗ r1 + (13.∧ (1./0.3) − 9. ∗ 3. ∗ r2)), r1, 0, 10), r2, 0, 10))= 21./ ((exp (− (11.∧(1./0.1) −5). ∗ 7) − 1). ∗ (exp (− (13.∧ (1./0.3) −9). ∗ 3) − 1)).

The following are the graphical representations of the exponential function in time and frequency domains. Figure 1 is the graphical representation of the input function $e^{5t_1+9t_2}$ in the time domain, and Figure 2 is the graphical representation of the output in the frequency domain for the particular values of $\nu_1 = 0.0001, \nu_2 = 0.0003$. One can easily choose the values of fraction $\nu_i' s$ to get the output in the frequency domain.

Theorem 5. *Let $\bar{t} \in R^n, \bar{h} > 0$, ν_j be a fraction, and $s_j > 0$, $j = 1, 2, \dots, n$; then,*

$$\mathscr{L}_{n(h)}\left[e^{i\sum_{j=1}^{n} a_j t_j}\right] = \frac{\prod_{j=1}^{n} h_j \sum_{\bar{r}\in\mathcal{J}(D_n)} (-1)^{n(D_n - \bar{r})} e_{-i(a_{\bar{r}} h_{\bar{r}})} e_{s_{D_n-\bar{r}} h_{D_n-\bar{r}}}}{2^n\left[\prod_{j=1}^{n}\left(\cosh s_j^{1/\nu_j} h_j - \cos a_j h_j\right)\right]}, \tag{22}$$

where $e_{-i(a_{\bar{r}} h_{\bar{r}})} = e^{-i(a_1 h_1 + a_2 h_2 + \cdots + a_n h_n)}$ *for* $\bar{r} = \{1, 2, \dots, n\}$, $e_{s_{D_n-\bar{r}} h_{D_n-\bar{r}}} = e^{s_1^{1/\nu_1} h_1 + s_2^{1/\nu_2} h_2 + \cdots + s_n^{1/\nu_n} h_n}$ *for* $D_n - \bar{r} = \{1, 2, \dots, n\}$, *and* $e_{-i(a_0 h_0)} = e_{s_0 h_0} = 1$.

Proof. From the previous theorem, we obtain the Laplace transform for the trigonometric function $e^{i\sum_{j=1}^{n} a_j t_j}$ as

$$\mathscr{L}_{n(h)}\left[e^{i\sum_{j=1}^{n} a_j t_j}\right] = \frac{\prod_{j=1}^{n} h_j}{\prod_{j=1}^{n}\left(e^{-\left(s_j^{1/\nu_j} - i a_j\right)h_j} - 1\right)}. \tag{23}$$

The proof then can be continued by making use of the conjugate and the product of each term in n-variables.

Theorem 6. *Let $\bar{t} \in R^n, \bar{h} > 0$, ν_j be a fraction, and $s_j > 0$, $j = 1, 2, \dots, n$; then,*

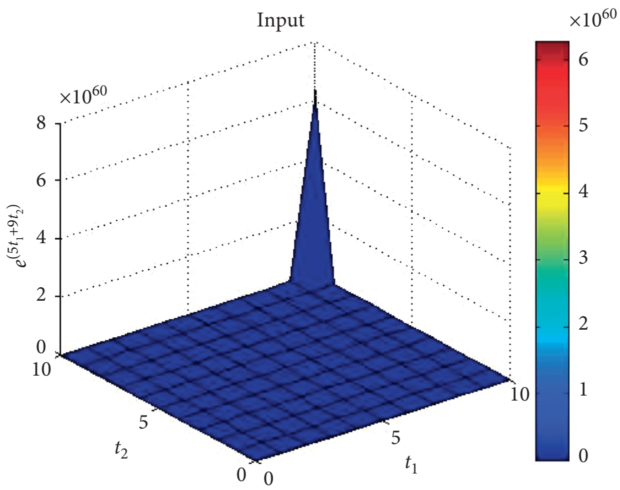

Figure 1: Time signal (function) $e^{5t_1+9t_2}$.

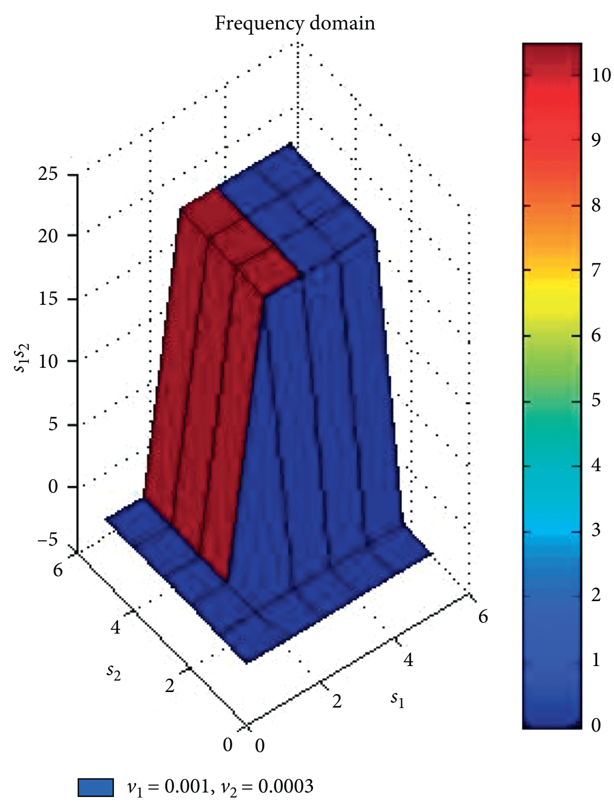

Figure 2: Frequency signal for $\nu_1 = 0.0001$ and $\nu_2 = 0.0003$.

$$\mathscr{L}_{2(h)}\left[\sin\left(\sum_{j=1}^{2}a_jt_j\right)\right]=\frac{h_1h_2\left(e^{s_2^{1/\nu_2}h_2}\sin a_1h_1+e^{s_1^{1/\nu_1}h_1}\sin a_2h_2-\sin\left(a_1h_1+a_2h_2\right)\right)}{4\left(\prod_{j=1}^{2}\left(\cosh s_j^{1/\nu_j}h_j-\cos a_jh_j\right)\right)}, \tag{24}$$

$$\mathscr{L}_{2(h)}\left[\cos\left(\sum_{j=1}^{2}a_jt_j\right)\right]=\frac{h_1h_2\left(\cos\left(\sum_{j=1}^{2}a_jt_j\right)-e^{s_2^{1/\nu_2}h_2}\cos a_1h_1-e^{s_1^{1/\nu_1}h_1}\cos a_2h_2+e^{\sum_{j=1}^{2}s_j^{1/\nu_j}h_j}\right)}{4\left(\prod_{j=1}^{2}\left(\cosh s_j^{1/\nu_j}h_j-\cos a_jh_j\right)\right)}. \tag{25}$$

Proof. The proof follows by taking $n=2$ in Theorem 5, making the product by its conjugate terms and separating the real and imaginary parts to get the double Laplace transform for the sine and cosine terms.

Example 3. Equation (24) is the closed-form solution of the sine function. Now, for $n=2$, the summation solution of the sine function given by the infinite inverse principle law is

$$\mathscr{L}_{2(h)}\left[\sin\left(\sum_{j=1}^{2}a_jt_j\right)\right]=h_1h_2\sum_{r_2=0}^{\infty}\sum_{r_1=0}^{\infty}\sin\left(a_1r_1h_1+a_2r_2h_2\right)e^{-\left(s_1^{1/\nu_1}r_1h_1+s_2^{1/\nu_2}r_2h_2\right)}. \tag{26}$$

Now, (24) and (26) are numerically verified for the particular values $h_1=2, h_2=3, a_1=1, a_2=4, \nu_1=0.4, \nu_2=0.6, s_1=5$, and $s_2=6$ by MATLAB coding as follows: 6. ∗ symsum (symsum (sin (2. ∗ r1 + 12. ∗ r2). ∗ exp (− (5.∧ (1./0.4). ∗ 2. ∗ r1 + 6.∧ (1./0.6). ∗ 3. ∗ r2)), r1, 0, 10), r2, 0, ∞) = (6. ∗ (exp (6.∧ (1./0.6). ∗ 3). ∗ sin (2) − exp ((5.∧ (1./ 0.4). ∗ 2). ∗ sin (12) − sin (14)))/ (4. ∗ (cosh (6.∧ (1./ 0.6). ∗ 3) − cos (12)). ∗ ((cosh (5.∧ (1./0.4)). ∗ 2) − cos (2)))).

The following are the graphical representations of the sine function in time and frequency domains. Figure 3 represents the input time-domain signal (function) for the sine function. Figure 4 represents the output in the frequency domain for the particular values of $\nu_1=0.4$ and $\nu_2=0.6$. Figure 5 represents the output in the frequency domain for the particular values of $\nu_1=0.3$ and $\nu_2=0.5$. Figure 6 represents the output in the frequency domain for the particular values of $\nu_1=0.1$ and $\nu_2=0.7$. Similarly, one can analyze the solution in the frequency domain by choosing diverse values of fraction $\nu_i's$.

Theorem 7. *Let $\bar{t}\in R^n, \bar{h}>0$, ν_j be a fraction, and $s_j, \mu_j>0$, $j=1,2,\ldots,n$; then,*

$$\mathscr{L}_{n(h)}\left[\prod_{j=1}^{n}\left(t_j\right)_{h_j}^{(\mu_j)}\right]=\prod_{j=1}^{n}\frac{h_j^{\mu_j+1}\mu_j!e^{s_j^{1/\nu_j}h_j}}{\left(e^{-s_j^{1/\nu_j}}-1\right)}. \tag{27}$$

Proof. Taking $u(\bar{t})=\prod_{j=1}^{n}(t_j)_{h_j}^{(\mu_j)}$ in (16), we have

$$\begin{aligned}\mathscr{L}_{n(h)}\left[\prod_{j=1}^{n}\left(t_j\right)_{h_j}^{(\mu_j)}\right]&=\Delta_{n(h)}^{-1}\prod_{j=1}^{n}\left(t_j\right)_{h_j}^{(\mu_j)}e^{-\sum_{j=1}^{n}s_j^{1/\nu_j}t_j}\Big|_{t_j=0,j=1,2,\ldots,n}^{\infty}\\&=\Delta_{h_n}^{-1}\left(t_n\right)_{h_n}^{(\mu_n)}e^{-s_n^{1/\nu_n}t_n}\Big|_0^{\infty}\cdots\Delta_{h_2}^{-1}\left(t_2\right)_{h_2}^{(\mu_2)}e^{-s_2^{1/\nu_2}t_2}\Big|_0^{\infty}\Delta_{h_1}^{-1}\left(t_1\right)_{h_1}^{(\mu_1)}e^{-s_1^{1/\nu_1}t_1}\Big|_0^{\infty}\\&=\frac{h_n^{\mu_n+1}\mu_n!e^{s_n^{1/\nu_n}h_n}}{\left(e^{-\left(s_n^{1/\nu_n}\right.}-1\right)}\cdots\frac{h_2^{\mu_2+1}\mu_2!e^{s_2^{1/\nu_2}h_2}}{\left(e^{-\left(s_2^{1/\nu_2}\right.}-1\right)}\frac{h_1^{\mu_1+1}\mu_1!e^{s_1^{1/\nu_1}h_1}}{\left(e^{-\left(s_1^{1/\nu_1}\right.}-1\right)},\end{aligned} \tag{28}$$

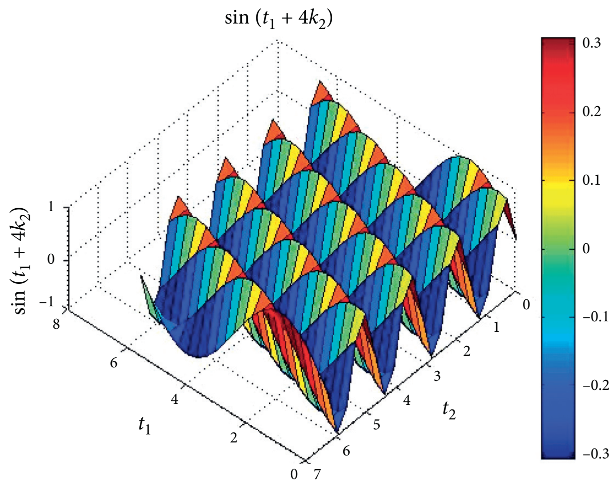

Figure 3: Time signal for $\sin(t_1 + 4t_2)$.

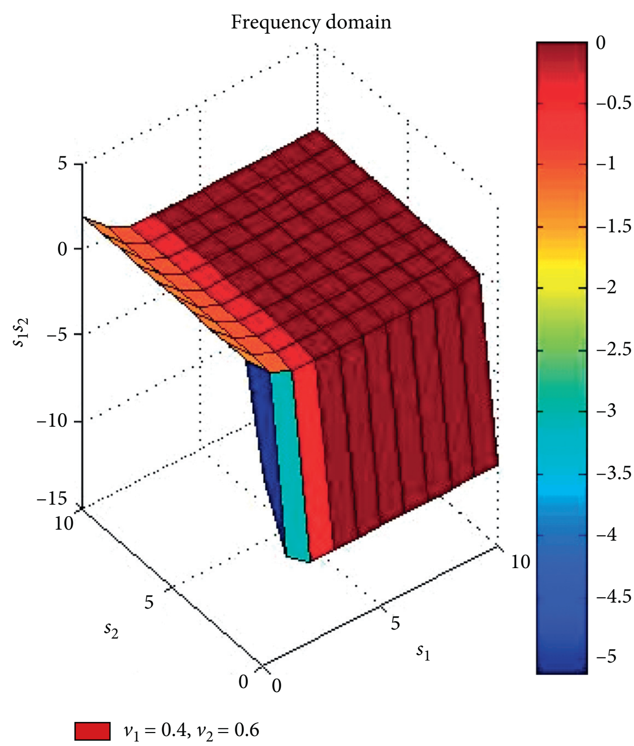

Figure 4: Frequency signal for $\nu_1 = 0.4$ and $\nu_2 = 0.6$.

by Lemma 1, which gives (4).

3.1. n-Kind Riemann Zeta Function in the Discrete Case. In Theorem 7, when $\nu_j = 1$ and $h_j \longrightarrow 0$ for $j = 1, 2, \ldots, n.$, we get

$$\mathscr{L}_{n(h)}\left[t_1^{\mu_1-1} t_2^{\mu_2-1} \ldots t_n^{\mu_n-1}\right] = \frac{\Gamma(\mu_n) \ldots \Gamma(\mu_2)\Gamma(\mu_1)}{s_n^{\mu_n} \ldots s_2^{\mu_2} s_1^{\mu_1}}. \tag{29}$$

We know that the Riemann zeta function is defined as

$$\zeta(\mu) = \sum_{s=1}^{\infty} \frac{1}{s^{\mu}}. \tag{30}$$

Equation (29) can be written as

$$\frac{\Gamma(\mu_n) \ldots \Gamma(\mu_2)\Gamma(\mu_1)}{s_n^{\mu_n} \ldots s_2^{\mu_2} s_1^{\mu_1}} = \Delta_{h_n}^{-1} t_n^{\mu_n-1} e^{-s_n t_n}\Big|_0^{\infty} \cdots \Delta_{h_2}^{-1} t_2^{\mu_2-1} e^{-s_2 t_2}\Big|_0^{\infty} \cdot \Delta_{h_1}^{-1} t_1^{\mu_1-1} e^{-s_1 t_1}\Big|_0^{\infty}. \tag{31}$$

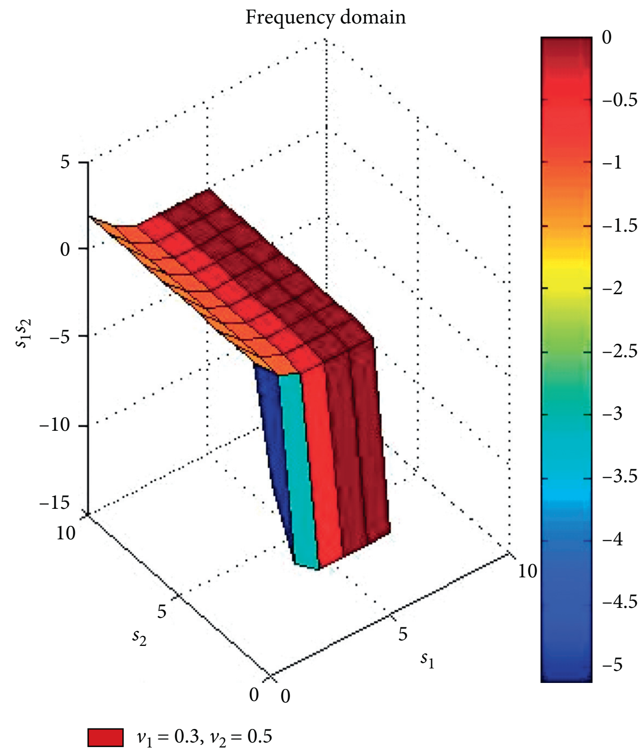

FIGURE 5: Frequency signal for $\nu_1 = 0.3$ and $\nu_2 = 0.5$.

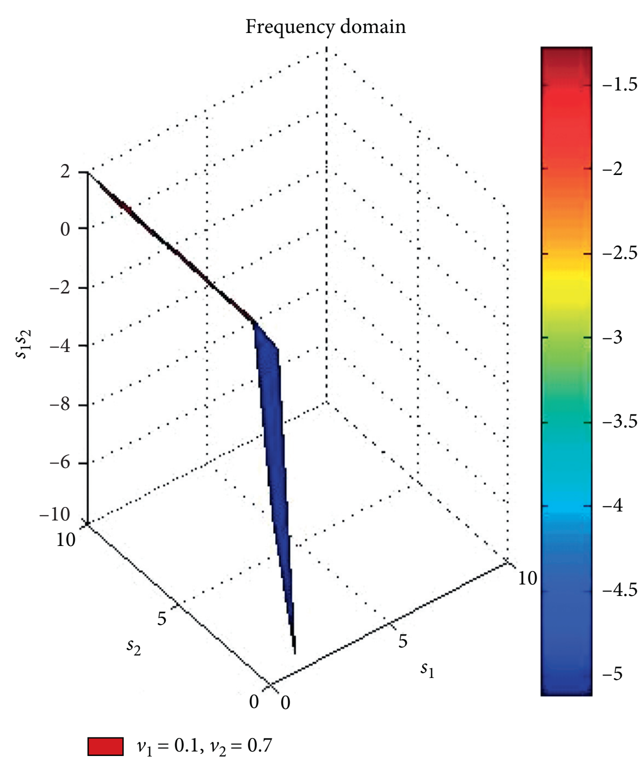

FIGURE 6: Frequency signal for $\nu_1 = 0.1$ and $\nu_2 = 0.7$.

Taking summation on s_j, $j = 1, 2, \ldots, \infty$, on both sides, we get

$$\prod_{j=1}^{n}\Gamma(\mu_j)\sum_{s_n=1}^{\infty}\frac{1}{s_n^{\mu_n}}\cdots\sum_{s_2=1}^{\infty}\frac{1}{s_2^{\mu_2}}\sum_{s_1=1}^{\infty}\frac{1}{s_1^{\mu_1}} = \Delta_{h_n}^{-1}t_n^{\mu_n-1}\sum_{s_n=1}^{\infty}e^{-s_n t_n}\Big|_0^{\infty}\cdots\Delta_{h_2}^{-1}t_2^{\mu_2-1}\sum_{s_2=1}^{\infty}e^{-s_2 t_2}\Big|_0^{\infty}\Delta_{h_1}^{-1}t_1^{\mu_1-1}\sum_{s_1=1}^{\infty}e^{-s_1 t_1}\Big|_0^{\infty},$$

$$\prod_{j=1}^{n}\Gamma(\mu_j)\zeta(\mu_n)\cdots\zeta(\mu_2)\zeta(\mu_1) = \Delta_{h_n}^{-1}t_n^{\mu_n-1}\frac{1}{(e^{t_n}-1)}\Bigg|_0^{\infty}\cdots\Delta_{h_2}^{-1}t_2^{\mu_2-1}\frac{1}{(e^{t_2}-1)}\Bigg|_0^{\infty}\Delta_{h_1}^{-1}t_1^{\mu_1-1}\frac{1}{(e^{t_1}-1)}\Bigg|_0^{\infty}, \tag{32}$$

$$\zeta(\mu_n)\cdots\zeta(\mu_2)\zeta(\mu_1) = \frac{1}{\Gamma(\mu_n)}\Delta_{h_n}^{-1}\frac{t_n^{\mu_n-1}}{(e^{t_n}-1)}\Bigg|_0^{\infty}\cdots\frac{1}{\Gamma(\mu_2)}\Delta_{h_2}^{-1}\frac{t_2^{\mu_2-1}}{(e^{t_2}-1)}\Bigg|_0^{\infty}\frac{1}{\Gamma(\mu_1)}\Delta_{h_1}^{-1}\frac{t_1^{\mu_1-1}}{(e^{t_1}-1)}\Bigg|_0^{\infty},$$

which is the product of n^{th}-kind Riemann zeta function in the discrete case.

3.2. One-Dimensional Laplace Transform on the Fractional Difference Equation. Let $u(t)$ and $v(t)$ be the two functions. The Leibniz rule of noninteger order is $\overset{\nu}{\Delta}[u(t)v(t)] = \sum_{r=0}^{\infty}\binom{\nu}{r}\overset{\nu-r}{\Delta}u(t)\overset{r}{\Delta}v(t+\nu-r)$. Here, we present the product formula on the fractional difference operator as $\Delta_h^{\nu}[u(t)v(t)] = \sum_{r=0}^{\infty}\binom{\nu}{r}\Delta_h^{\nu-r}u(t)\Delta_h^{r}v(t+(\nu-r)h)$.

The following theorem plays an important role in solving the fractional difference equation by one-dimensional Laplace transform.

Theorem 8. *Let $u(t_1)$ be a real-valued function and $s_1, h_1, \nu_1 > 0$. Then, we have*

$$L_{h_1}\left[\Delta_{h_1}^{\nu}u(t)\right] = \frac{\left(1-e^{-s_1^{1/\nu_1}h_1}\right)^{\nu_1}}{h_1^{\nu_1}}L_{h_1}\left[u(t_1+\nu_1 h_1)\right] - \sum_{r_1=1}^{\infty}\frac{\left(1-e^{-s_1^{1/\nu_1}h_1}\right)^{\nu_1-r_1}}{h_1^{\nu_1-r_1}}\Delta_{h_1}^{r_1-1}u((\nu_1-r_1)h_1). \tag{33}$$

Proof. Taking $u(t_1) = \underset{h_1}{\Delta}u(t_1)$ in (16), we get $L_{h_1}[\underset{h_1}{\Delta}u(t_1)] = \Delta_{h_1}^{-1}[\underset{h_1}{\Delta}u(t_1)e^{-s_1^{h_1/\nu_1}t_1}]|_0^{\infty}$. Now, applying (3) and solving, we get

$$L_{h_1}\left[\underset{h_1}{\Delta}u(t_1)\right] = \frac{\left(1-e^{-s_1^{1/\nu_1}h_1}\right)}{h_1}L_{h_1}\left[u(t_1+h_1)\right] - u(0). \tag{34}$$

Again taking $u(t_1) = \Delta_{h_1}^2 u(t_1)$, using (3) and (16), and applying (34) give

$$L_{h_1}\left[\Delta_{h_1}^{2}u(t_1)\right] = \frac{\left(1-e^{-s_1^{1/\nu_1}h_1}\right)^{2}}{h_1^{2}}L_{h_1}\left[u(t_1+2h_1)\right] - \frac{\left(1-e^{-s_1^{1/\nu_1}h_1}\right)}{h_1}u(h_1) - \underset{h_1}{\Delta}u(0). \tag{35}$$

Continuing this process for integer n, we arrive at

$$L_{h_1}\left[\Delta_{h_1}^{n}u(t_1)\right] = \frac{\left(1-e^{-s_1^{1/\nu_1}h_1}\right)^{n}}{h_1^{n}}L_{h_1}\left[u(t_1+nh_1)\right] - \sum_{r_1=1}^{n}\frac{\left(1-e^{-s_1^{1/\nu_1}h_1}\right)^{n-r_1}}{h_1^{n-r_1}}\Delta_{h_1}^{r_1-1}u((n-r_1)h_1). \tag{36}$$

Since the order is a fraction, we consider (36) for fraction ν as mentioned in (33).

4. n-Dimensional Inverse Laplace Transform

The n-dimensional inverse Laplace transform is defined by

$$\mathscr{L}_{n(h)}^{-1}\left[U_n(\bar{s})\right] = u(\bar{t}) = \Delta_{\overline{n(h)}}^{-1} U_n(\bar{s}) e^{\sum_{j=1}^{n} s_j^{1/\nu_j} t_j}\Big|_{c_j-i\infty}^{c_j+i\infty}, \quad j = 1, 2, \ldots, n. \tag{37}$$

Since we can easily represent the n-dimensional Laplace transform of the functions mentioned, we can present some results listed as follows:

$$\begin{aligned}
&\mathscr{L}_{n(h)}^{-1}\left[\frac{\prod_{j=1}^{n} h_j}{\prod_{j=1}^{n}\left(e^{-s_j^{1/\nu_j} h_j} - 1\right)}\right] = 1,\\
&\mathscr{L}_{n(h)}^{-1}\left[\frac{\prod_{j=1}^{n} h_j}{\prod_{j=1}^{n}\left(e^{-\left(s_j^{1/\nu_j} - a_j\right) h_j} - 1\right)}\right] = e^{\sum_{j=1}^{n} a_j t_j},\\
&\mathscr{L}_{n(h)}^{-1}\left[\frac{\prod_{j=1}^{n} h_j \sum_{\bar{r}\in\mathscr{J}(D_n)} (-1)^{n(D_n-\bar{r})} e_{-i(a_{\bar{r}} h_{\bar{r}})} e_{s_{D_n-\bar{r}} h_{D_n-\bar{r}}}}{2^n\left[\prod_{j=1}^{n}\left(\cosh s_j^{1/\nu_j} h_j - \cos a_j h_j\right)\right]}\right] = e^{i\sum_{j=1}^{n} a_j t_j},\\
&\mathscr{L}_{n(h)}^{-1}\left[\prod_{j=1}^{n} \frac{h_j^{\mu_j+1} \mu_j! e^{s_j^{1/\nu_j} h_j}}{\left(e^{-\left(s_j^{1/\nu_j}\right.} - 1\right)}\right] = \prod_{j=1}^{n} \left(t_j\right)_{h_j}^{(\mu_j)},\\
&\mathscr{L}_{n(h)}^{-1}\left[\frac{\Gamma(\mu_n)\ldots\Gamma(\mu_2)\Gamma(\mu_1)}{s_n^{\mu_n}\ldots s_2^{\mu_2} s_1^{\mu_1}}\right] = t_1^{\mu_1-1} t_2^{\mu_2-1} \ldots t_n^{\mu_n-1}.
\end{aligned} \tag{38}$$

5. Results and Discussion

When $n = 2$, $\nu_1 = \nu_2 = 1$, and $h_1, h_2 \longrightarrow 0$, in all the above results, we have

(i) $\mathscr{L}_2[1] = 1/s_1 s_2$.

(ii) $\mathscr{L}_2[e^{a_1 t_1 + a_2 t_2}] = 1/(s_1 - a_1)(s_2 - a_2)$.

(iii) $\mathscr{L}_2[\sin(a_1 t_1 + a_2 t_2)] = a_1 a_2/(s_1^2 + a_1^2)(s_2^2 + a_2^2)$.

(iv) $\mathscr{L}_2[\cos(a_1 t_1 + a_2 t_2)] = s_1 s_2/(s_1^2 + a_1^2)(s_2^2 + a_2^2)$.

Similarly, the following result for the hyperbolic functions can be obtained:

(i) $\mathscr{L}_2[t_1^{\mu_1} t_2^{\mu_2}] = \mu_1! \mu_2! / s_1^{\mu_1+1} s_2^{\mu_2+1}$.

These results match the formulas of the double Laplace transform of functions available in the literature.

6. Conclusion

The fractional frequency is used to derive the n-dimensional Laplace transform with shift values h_j, $j = 1, 2, \ldots, n$, that presents more accuracy outputs of the input functions such as exponential, polynomial factorial, polynomial, and trigonometric functions. Also, the numerical results and the solutions are analyzed graphically by MATLAB. The major application of this research work is also provided by considering the classical Laplace transform according to particular values of n which are $\nu_j = 1$ and $h_j \longrightarrow 0$, $j = 1, 2, \ldots, n$.

Data Availability

The data used to support the findings of this study are available from the corresponding author upon request.

Conflicts of Interest

The authors declare that they have no conflicts of interest.

Acknowledgments

This research was catalyzed and financially supported by the Tamil Nadu State Council for Science and Technology, Department of Higher Education, Government of Tamil Nadu.

References

[1] I. Podlubny, *Fractional Differential Equations*, Academic Press, San Diego, CA, USA, 1999.

[2] G. Samko, A. A. Kilbas, and S. Marichev, *Fractional Integrals and Derivatives: Theory and Applications*, Gordon & Breach, Yverdon, Switzerland, 1993.

[3] A. A. Kilbas, M. H. Srivastava, and J. J. Trujillo, "Theory and application of fractional differential equations," *North-Holland Mathematics Studies*, Vol. 204, Elsevier, Amsterdam, Netherland, 2006.

[4] R. L. Magin, *Fractional Calculus in Bioengineering*, Begell House Publishers, Danbury, CT, USA, 2006.

[5] T. Abdeljawad, "On Riemann and Caputo fractional differences," *Computers & Mathematics with Applications*, vol. 62, no. 3, pp. 1602–1611, 2011.

[6] F. M. Atıcı and P. W. Eloe, "A transform method in discrete fractional calculus," *International Journal Difference Equations*, vol. 2, no. 2, pp. 165–176, 2007.

[7] F. M. Atıcı and P. W. Eloe, "Initial value problems in discrete fractional calculus," *Proceedings of the American Mathematical Society*, vol. 137, no. 3, pp. 981–989, 2009.

[8] F. M. Atıcı and P. W. Eloe, "Discrete fractional calculus with the nabla operator," *Electronic Journal of Qualitative Theory of Differential Equations*, vol. 3, 2009.

[9] F. M. Atıcı and S. Şengül, "Modelling with fractional difference equations," *Journal of Mathematical Analysis and Applications*, vol. 369, no. 1, pp. 1–9, 2010.

[10] K. S. Miller and B. Ross, "Fractional difference calculus," in *Proceedings of the International Symposium on Univalent Functions, Fractional Calculus and Their Applications*, pp. 139–152, Nihon, Japan, 1989.

[11] T. Abdeljawad and D. Baleanu, "Fractional differences and integration by parts," *Journal of Computational Analysis and Applications*, vol. 13, no. 3, pp. 574–582, 2011.

[12] N. R. O. Bastos, R. A. C. Ferreira, and D. F. M. Torres, "Discrete-time fractional variational problems," *Signal Processing*, vol. 91, no. 3, pp. 513–524, 2011.

[13] H. L. Gray and N. F. Zhang, "On a new definition of the fractional difference," *Mathematics of Computation*, vol. 50, no. 182, p. 513, 1988.

[14] T. Abdeljawad and F. M. Atici, "On the definitions of nabla fractional operators," *Abstract and Applied Analysis*, vol. 2012, pp. 1–13, Article ID 406757, 2012.

[15] T. Abdeljawad, F. Jarad, and D. Baleanu, "A semigroup-like property for discrete Mittag-Leffler functions," *Advances in Difference Equations*, vol. 2012, no. 1, p. 72, 2012.

[16] G.-C. Wu, D. Baleanu, S.-D. Zeng, and Z.-G. Deng, "Discrete fractional diffusion equation," *Nonlinear Dynamics*, vol. 80, no. 1-2, pp. 281–286, 2015.

[17] G.-C. Wu, D. Baleanu, and S.-D. Zeng, "Several fractional differences and their applications to discrete maps," *Journal of Applied Nonlinear Dynamics*, vol. 4, no. 4, pp. 339–348, 2015.

[18] S. W. Smith, *The Scientist and Engineer's Guide to Digital Signal Processing*, California Technical Publishing, San Diego, CA, USA, 2nd edition, 1999.

[19] M. Bohner and A. Peterson, *Dynamic Equation on Time Scales: An Introduction with Applications*, Birkhuser, Boston, MA, USA, 2001.

[20] A. Ivic, "Some applications of Laplace transforms in analytic number theory," *Novi Sad Journal of Mathematics*, vol. 45, no. 1, pp. 31–44, 2015.

[21] A. Ivic, "The Laplace transform of the fourth moment of of the zeta-function," *Univ. Beograd. Publ. Elektrotehn. Fak. Ser. Mat.*vol. 11, pp. 41–48, 2000.

[22] A. M. Sedletskii, *Fourier Transforms and Approximations*, Gordon and Breach Science Publishers, Amsterdam, Netherland, 2000.

[23] M. Jutila, "The Mellin transform of the square of Riemann's zeta-function," *Periodica Mathematica Hungarica*, vol. 42, pp. 179–190, 2001.

[24] I. A. Abbas and M. Marin, "Analytical solution of thermoelastic interaction in a half-space by pulsed laser heating," *Physica E: Low-Dimensional Systems and Nanostructures*, vol. 87, pp. 254–260, 2017.

[25] M. Marin, M. A. Othman, and I. Abbas, "An extension of the domain of influence theorem for generalized thermoelasticity of anisotropic material with voids," *Journal of Computational and Theoretical Nanoscience*, vol. 12, no. 8, pp. 1594–1598, 2015.

[26] M. Marin, I. Abbas, and R. Kumar, "Relaxed Saint-Venant principle for thermoelastic micropolar diffusion," *Structural Engineering and Mechanics*, vol. 51, no. 4, pp. 651–662, 2014.

[27] M. I. A. Othman and I. A. Abbas, "Effect of rotation on plane waves at the free surface of a fibre-reinforced thermoelastic half-space using the finite element method," *Meccanica*, vol. 46, no. 2, pp. 413–421, 2011.

[28] G. Britto Antony Xavier, B. Govindan, S. John Borg, and M. Meganathan, "Generalized Laplace transform arrived from an inverse difference operator," *Global Journal of Pure and Applied Mathematics*, vol. 12, no. 3, pp. 661–666, 2016.

[29] L. Debnath, "The double Laplace transforms and their properties with applications to functional, integral and partial differential equations," *International Journal of Applied and Computational Mathematics*, vol. 2, no. 2, pp. 223–241, 2016.

[30] M. Meganathan, G. Britto Antony Xavier, and T. Abdeljawad, "Modeling with fractional Laplace transform by h-difference operator," *Progress in Fractional Differentiation and Applications*, In press.

[31] S. Pinelas, M. Meganathan, M. Murugesan, and B. A. X. G. Gnanaprakasam, "Fractional frequency Laplace transform by inverse difference operator with shift value," *Open Journal of Mathematical Sciences*, vol. 3(2019), no. 1, pp. 121–128, 2019.

Hindawi
Mathematical Problems in Engineering
Volume 2020, Article ID 4308589, 12 pages
https://doi.org/10.1155/2020/4308589

Research Article

A Discrete Fractional-Order Prion Model Motivated by Parkinson's Disease

M. F. Elettreby,[1,2] **E. Ahmed**,[2] **and A. S. Alqahtani**[1]

[1]*Mathematics Department, Faculty of Science, King Khalid University, Abha 9004, Saudi Arabia*
[2]*Mathematics Department, Faculty of Science, Mansoura University, Mansoura 35516, Egypt*

Correspondence should be addressed to M. F. Elettreby; mohfathy@yahoo.com

Received 2 June 2020; Accepted 14 July 2020; Published 17 August 2020

Academic Editor: Carlo Cosentino

A prion differential equation model motivated by Parkinson's disease (PD) is studied. A fractional-order form of this model is proposed. After that, we discretized fractional-order Parkinson's disease model. A sufficient condition for the existence and the uniqueness of a solution to the system is obtained. The stability of the fixed points of the system is achieved by using the Jury test. The impacts of varying the parameters of the system are examined. Under certain conditions, the system undergoes some kinds of bifurcations. We observe that the model loses its stability through double-period bifurcation to chaotic behavior as the growth rate increases. Also, the system stabilizes by increasing the memory parameter, and the contact rate between the two types of prions increases. The system shows rich dynamical behavior for a wide range of the values of the parameters.

1. Introduction

Parkinson's disease (PD) is a long-term neurodegenerative disorder of the central nervous system that gradually develops and affects how sufferers move [1, 2]. Typically, this disease affects elderly persons. Also, it can occur in adults as well. Striking approximately one percent of the individuals (1%), the condition is slightly less common in women and usually begins to manifest between the ages of 50 to 65. The cause of Parkinson's disease is generally unknown.

The symptoms are caused by the gradual degeneration of nerve cells located in the region of the brain responsible for controlling movement. It can slow and stiffen a person's movement, and tremors are the most recognized symptom of the disease. Although there is no surgery, cure and medications can reduce symptoms and improve patient outlook. Medicines can reduce the disabling effects of the disease. Hence, trying different approaches to early diagnosis may be helpful [3, 4].

Recently, mathematics, graph theory, and computer science have been used to study early diagnoses of PD [5–9]. Also, prions are related to PD [10]. Prions are misfolded proteins that replicate by converting their properly folded counterparts. Prion models have been used to study some brain diseases [11–13]. In most cases, diffusion models have been used. While in [13], a difference equation model has been used. Since 1695, many different applications appeared in different fields which can be described by using fractional calculus [14–24]. Fractional models and systems allow more authentic interpretation for a lot of real phenomena. Hence, fractional-order equations are more natural and more appropriate than integer-order ones to model systems with memory which exist in most biological phenomena [25]. Recently, a large number of authors are interested in studying qualitative behavior and the properties of fractional-order models [26–30].

Actually, discrete mathematics is appropriate and realistic to represent the complex dynamics of a population especially if the populations have nonoverlapping generations such as Parkinson's disease. Since the examinations of the patient, laboratory blood tests performed, and the doses of drugs that are prescribed to be taken are a discrete process, we need to discretize the fractional-order models arising from nature [31, 32].

In Section 2, we started with a simple model as a system of two ordinary differential equations. The stability conditions of its fixed points are obtained. In Section 3, we proposed and studied the corresponding fractional-ordered form of Parkinson's disease. In Section 4, we discretized the fractional-order model and investigated the stability of its fixed points. The dynamical behavior of the model is rich and complex. In Section 5, some numerical simulations were carried out to support our analytical results. Finally, we summarized and concluded our results in Section 6.

2. Model of Parkinson's Disease

Let $x(t)$ be the properly folded (healthy) prions and $y(t)$ be the wrongly folded (infected) ones in the brain. Then, their interaction can be modeled by the following simple mathematical differential equation model:

$$\begin{aligned} \frac{\mathrm{d}x}{\mathrm{d}t} &= ax(1-x) - \frac{bxy}{x+y}, \\ \frac{\mathrm{d}y}{\mathrm{d}t} &= \frac{bxy}{x+y} - y, \end{aligned} \tag{1}$$

which models the change rates of both the healthy and the infected prions. The constants a and b are positive constants that represent the growth rate of healthy prions and the contact rate between the healthy and the infected prions, respectively. We rescaled the other parameters.

Model (1) is a nonlinear system, and it is difficult to obtain a time-dependent explicit solution. Hence, we will study the qualitative behavior of the model. Equating the equations in (1) by zero and solving the resulting system with respect to the equilibrium state variables $\overline{x}$ and $\overline{y}$, we get the following fixed points: the healthy state $e_1 = (1, 0)$ and the infected one $e_2 = (((1+a-b)/a), (((1+a-b)(b-1))/a))$. The necessary condition of the existence of the disease state e_2 is $1 < b < 1 + a$. We will study the case where the value of b is outside this interval later.

The local stability analysis of these equilibria is established by studying the following Jacobian matrix of system (1) at these equilibria:

$$J = \begin{pmatrix} a(1-2\overline{x}) - \dfrac{b\overline{y}^2}{(\overline{x}+\overline{y})^2} & \dfrac{-b\overline{x}^2}{(\overline{x}+\overline{y})^2} \\ \\ \dfrac{b\overline{y}^2}{(\overline{x}+\overline{y})^2} & \dfrac{b\overline{x}^2}{(\overline{x}+\overline{y})^2} - 1 \end{pmatrix}. \tag{2}$$

Proposition 1. *System (1) has a stable healthy state e_1 if the contact rate is less than one $(b < 1)$.*

Proof. The Jacobian matrix computed at the healthy state $e_1 = (1, 0)$ is

$$J_{e_1} = \begin{pmatrix} -a & -b \\ 0 & b-1 \end{pmatrix}. \tag{3}$$

It has the eigenvalues $\lambda_1 = -a < 0$ and $\lambda_2 = b - 1$. Then, the healthy fixed state e_1 is stable if $b < 1$.

In Figure 1, we plot the time t versus the two classes of prions $x(t)$ and $y(t)$ to check their qualitative behavior. We start with the initial point $(x_0, y_0) = (0.1, 0.7)$, fixing the growth rate parameter at $a = 1.1$ and four different values of the contact rate $b = 0.3, 0.5, 0.7,$ and 0.9. In the figures, all curves of the healthy prions tend to one and all curves of the infected prions tend to zero as t increases. This shows the extinction of the infection when the contact rate is less than one $(b < 1)$. Also, from Figure 1, note that increasing the value of the contact parameter b increases the time to reach the stability state. ☐

Proposition 2. *The infected state e_2 is stable whenever it exists.*

Proof. The local stability analysis of the infected state can be established by studying the following Jacobian matrix of system (1) at e_2:

$$J_{e_2} = \begin{pmatrix} b - a - \dfrac{1}{b} & \dfrac{-1}{b} \\ \\ b - 2 + \dfrac{1}{b} & \dfrac{1}{b} - 1 \end{pmatrix}, \tag{4}$$

which has the characteristic equation $m^2 - \beta m + \gamma = 0$, where m is the eigenvalue of the Jacobian matrix J_{e_2}, $\beta = b - a - 1 < 0$ (from the existence condition of e_2), and $\gamma = ((b-1)(1+a-b)/b) > 0$. So, both eigenvalues are negative. Then, the infected fixed state e_2 is stable whenever it exists.

In Figure 2, we plot the time t versus the two classes of prions $x(t)$ and $y(t)$ to check their qualitative behavior. We start with the initial point $(x_0, y_0) = (0.1, 0.7)$ and four different pairs of the parameter's values $(a, b) = (2.2, 1.1), (2.8, 1.5), (3.8, 2.7),$ and $(5.1, 3.9)$ which satisfy the existence and stability conditions. In the figures, all curves of the healthy prions and the infected prions tend to infected states $(0.9545, 0.0954)$, $(0.8241, 0.4107)$, $(0.5526, 0.9395)$, and $(0.4314, 1.251)$ as t increases. This shows the existence of the healthy and the infected prions when the growth rate and the contact rate satisfy the condition $1 < b < a + 1$. Also, note that increasing the value of the contact parameter b increases the infected prions and, consequently, decreases healthy prions. We find that the stability of this fixed point does not depend on the initial point. ☐

3. Fractional-Order Form of the Parkinson's Disease Model

Let us start by stating the definitions of fractional-order integral and derivative [33]. Let $f(x)\colon \mathbb{R}^+ \longrightarrow \mathbb{R}$ be a piecewise continuous function which is integrable on any finite subinterval of $\mathbb{R}^+$. Then, for $x > 0$, the Riemann–Liouville fractional integral of order α of the function $f(x)$ is defined by

$$I^{\alpha} f(x) = \frac{1}{\Gamma(\alpha)} \int_0^x (x-t)^{\alpha-1} f(t)\mathrm{d}t, \tag{5}$$

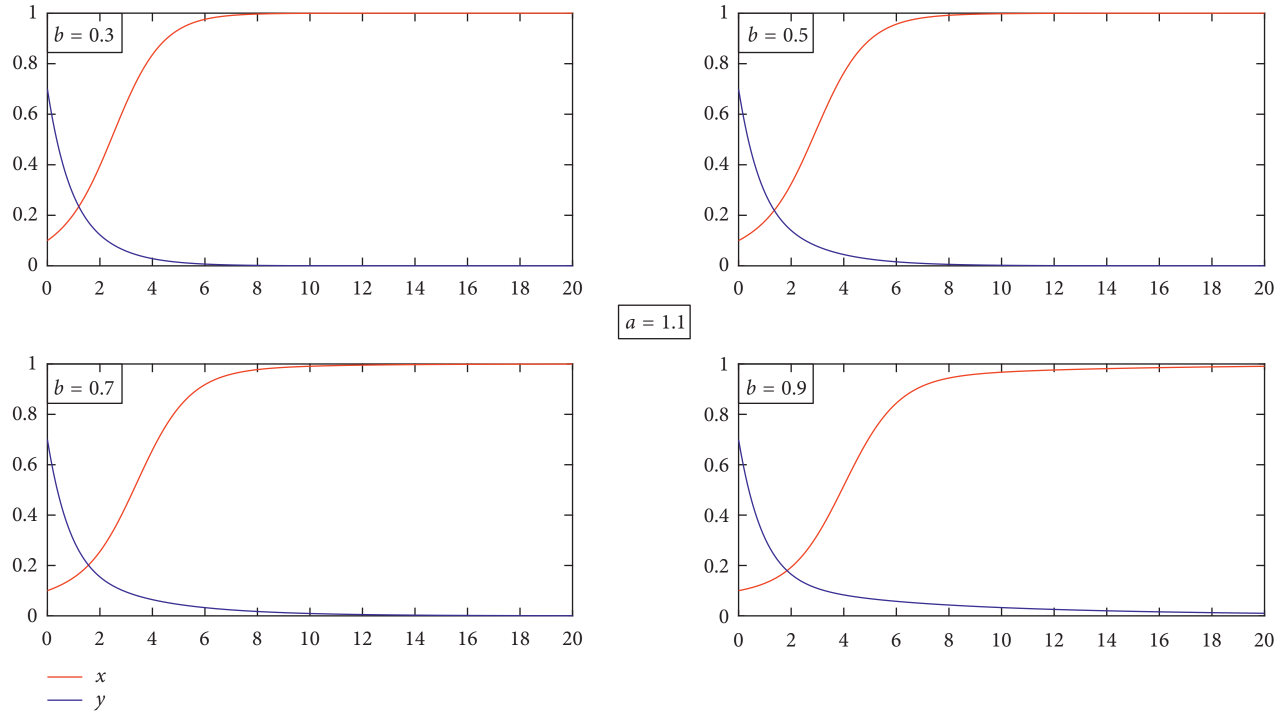

FIGURE 1: Four figures showing the two classes of the prion curves $x(t)$ and $y(t)$ at a constant growth rate $a = 1.1$ and the contact rates $b = 0.3$, $b = 0.5$, $b = 0.7$, and $b = 0.9$, at the initial values of $(x(0), y(0)) = (0.1, 0.7)$.

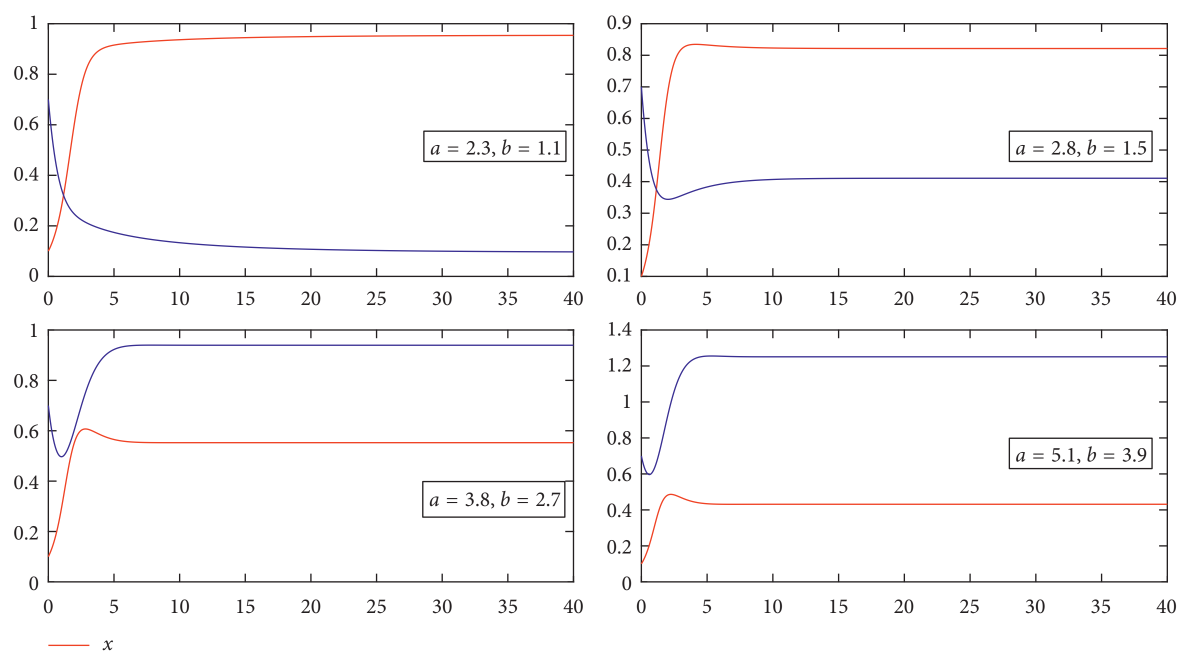

FIGURE 2: The two classes of the prion curves $x(t)$ and $y(t)$ exist at different values of a and b. (a) $a = 2.3$, $b = 1.1$. (b) $a = 2.8$, $b = 1.5$. (c) $a = 3.8$, $b = 2.7$. (d) $a = 5.1$, $b = 3.9$.

where $\Gamma(\cdot)$ is the Euler–Gamma function [34]. Let $m \in \mathbb{N}$ and $\alpha > 0$ such that $m - 1 \leq \alpha < m$; then, the Riemann–Liouville fractional derivative of the function $f(x)$ of order α is given as

$$D^{\alpha} f(x) = D^{m} [I^{m-\alpha} f(x)], \quad x > 0, \tag{6}$$

which exists for $m - \alpha > 0$ [35]. Consider the following system:

$$D^{\alpha}X(t)=f(X(t)),\quad X(0)=X_0, \tag{7}$$

where $X(t)=(x_1,x_2,\ldots,x_n)^T\in\mathbb{R}^n$, $f:\mathbb{R}^n\longrightarrow\mathbb{R}^n$, and $\alpha\in(0,1]$ be a nonlinear autonomous fractional-order system. Matignon's results [36] determine the local stability conditions of the fixed points of the linearized fractional-order form of system (7):

$$\left|\arg(\lambda_i)\right|>\frac{\alpha\pi}{2},\quad i=1,2,\ldots,n, \tag{8}$$

where λ_i are eigenvalues of the Jacobian matrix J of system (7) evaluated at the fixed points of the system.

Now, the fractional-order form of system (1) is given by

$$\begin{aligned} D_t^{\alpha}x(t)&=ax(1-x)-\frac{bxy}{x+y},\\ D_t^{\alpha}y(t)&=\frac{bxy}{x+y}-y, \end{aligned} \tag{9}$$

where $\alpha\in(0,1]$ is the fractional order and $D=(\mathrm{d}^{\alpha}/\mathrm{d}t^{\alpha})$ is the Caputo derivative [35]. The conditions $x(0)=x_0$ and $y(0)=y_0$ are the initial conditions of system (9).

3.1. Discretization of the Fractional-Order PD Model. In the following steps, we will generalize the forward Euler discretization method in integer-order to fractional-order one. The process of discretization of fractional-order system (9) with piecewise constant argument is given as follows [32, 37, 38]:

$$\begin{aligned} D_t^{\alpha}(x)&=ax\left(\left[\frac{t}{h}\right]h\right)\left(1-x\left(\left[\frac{t}{h}\right]h\right)\right)-\frac{bx([t/h]h)y([t/h]h)}{x([t/h]h)+y([t/h]h)},\\ D_t^{\alpha}(y)&=\frac{bx([t/h]h)y([t/h]h)}{x([t/h]h)+y([t/h]h)}-y\left(\left[\frac{t}{h}\right]h\right). \end{aligned} \tag{10}$$

Now, let $0\le t<h$, which is equivalent to $0\le(t/h)<1$. Then,

$$\begin{aligned} D_t^{\alpha}x_1&=ax_0(1-x_0)-\frac{bx_0y_0}{x_0+y_0},\\ D_t^{\alpha}y_1&=\frac{bx_0y_0}{x_0+y_0}-y_0, \end{aligned} \tag{11}$$

which has the following solution:

$$\begin{aligned} x_1&=x_0+\frac{h^{\alpha}}{\Gamma(1+\alpha)}\left[ax_0(1-x_0)-\frac{bx_0y_0}{x_0+y_0}\right],\\ y_1&=y_0+\frac{h^{\alpha}}{\Gamma(1+\alpha)}\left[\frac{bx_0y_0}{x_0+y_0}-y_0\right]. \end{aligned} \tag{12}$$

Continuing the process of discretization n times, we obtain the following:

$$\begin{aligned} x_{n+1}&=x_n+L^{\alpha}\left[ax_n(1-x_n)-\frac{bx_ny_n}{x_n+y_n}\right],\\ y_{n+1}&=y_n+L^{\alpha}\left[\frac{bx_ny_n}{x_n+y_n}-y_n\right], \end{aligned} \tag{13}$$

where $L^{\alpha}=h^{\alpha}/(\Gamma(1+\alpha))$. Note that if α tends to 1 in system (13), we will obtain the forward Euler discretization of dynamical system (9).

3.2. The Existence and the Uniqueness of the Solution. System (9) can be rewritten in the matrix form as [33, 39]

$$D^{\alpha}X(t)=F(X(t)),\quad t\in(0,T],\ \alpha\in(0,1],\ X(0)=X_0, \tag{14}$$

where $X=\begin{pmatrix}x\\ y\end{pmatrix}$, $X_0=\begin{pmatrix}x_0\\ y_0\end{pmatrix}$, and $F(X)=\begin{pmatrix}ax(1-x)(bxy/(x+y))\\ (bxy/(x+y))-y\end{pmatrix}$. Let $\|\phi\|=\sup_{t\in(0,T]}|\phi(t)|$ denote the supremum norm of the function $\phi(t)$ and $\|M\|=\sum_{I,J}\sup_{t\in(0,T]}|M_{i,j}(t)|$ denote the norm of the matrix M, and the region of existence and uniqueness is given by $\Omega\times(0,T]$, where $\Omega=\{(x,y,z):\ \max(|x|,|y|,|z|)\le\eta\}$.

Now, the solution of system (9) is obtained as follows:

$$\begin{aligned} X(t)&=X_0+I^{\alpha}(F(X(t)))=X_0+\frac{1}{\Gamma(\alpha)}\int_0^t(t-s)^{\alpha-1}\\ &\quad F(X(s))\mathrm{d}s=H(X). \end{aligned} \tag{15}$$

Then,

$$\begin{aligned} H(X_1)-H(X_2)&=\frac{1}{\Gamma(\alpha)}\int_0^t(t-s)^{\alpha-1}(F(X_1(s))-F(X_2(s)))\mathrm{d}s,\\ \left|H(X_1)-H(X_2)\right|&\le\frac{1}{\Gamma(\alpha)}\int_0^t\left|(t-s)^{\alpha-1}(F(X_1(s))-F(X_2(s)))\right|\mathrm{d}s,\\ \left|H(X_1)-H(X_2)\right|&\le\frac{1}{\Gamma(\alpha)}F\int_0^t(t-s)^{\alpha-1}\left|F(X_1(s))-F(X_2(s))\right|\mathrm{d}s,\\ \left\|H(X_1)-H(X_2)\right\|&\le\frac{T^{\alpha}}{\Gamma(\alpha+1)}\max\{a(1-2\eta,\mu)\}\left\|X_1-X_2\right\|,\\ \left\|H(X_1)-H(X_2)\right\|&\le K\left\|X_1-X_2\right\|, \end{aligned} \tag{16}$$

where

$$K=\frac{T^{\alpha}}{\Gamma(\alpha+1)}\max\{a(1-2\eta),\eta\}, \tag{17}$$

where the map $X=H(X)$ contracts if $K<1$.

Theorem 1. *The sufficient condition for the existence and the uniqueness of the solution of system (9) in the indicated region $\Omega\times(0,T]$ with initial conditions $X(0)=X_0$ and $t(0,T]$ is*

$$K = \frac{T^{\alpha}}{\Gamma(\alpha+1)} \max\{a(1-2\eta), \eta\} < 1. \tag{18}$$

3.3. Stability Analysis of the Fractional-Order System. System (13) is a nonlinear system, and it is difficult to obtain a time-dependent explicit solution. Hence, we will study the qualitative behavior of the model. Equating the equations in (1) by zero and solving the resulting system with respect to the equilibrium state variables $\overline{x}$ and $\overline{y}$, we obtain the following fixed points: the healthy one $E_1 = (1,0)$ and the diseased one $E_2 = (((1+1-b)/a), ((1+a=b)(b-1)/a))$. The necessary condition of the existence of the disease state E_2 is $1 < b < a+1$.

The local stability analysis of these equilibria is established by studying the Jacobian matrix of system (13) at these equilibria.

4. Dynamical Behavior of the Discretized Fractional-Order Model

Here, we investigate the dynamics of discretized fractional-order model (13). The Jacobian matrix J of system (13) at any fixed point $(\overline{x}, \overline{y})$ is given by

$$J = \begin{pmatrix} 1 + \frac{h^{\alpha}}{\Gamma(1+\alpha)}\left(a(1-2\overline{x}) - \frac{b\overline{y}^2}{(\overline{x}+\overline{y})^2}\right) & \frac{-h^{\alpha}}{\Gamma(1+\alpha)} \frac{b\overline{x}^2}{(\overline{x}+\overline{y})^2} \\ \frac{h^{\alpha}}{\Gamma(1+\alpha)} \frac{b\overline{y}^2}{(\overline{x}+\overline{y})^2} & 1 + \frac{h^{\alpha}}{\Gamma(1+\alpha)}\left(\frac{b\overline{x}^2}{(\overline{x}+\overline{y})^2} - 1\right) \end{pmatrix}. \tag{19}$$

Theorem 2. *The fixed point $E_1 = (1,0)$, where $b < 1$, is*

(a) *a sink point if $h < \min\{\sqrt[\alpha]{(2\Gamma(1+\alpha))/a}, \sqrt[\alpha]{(2\Gamma(1+\alpha))/1-b}\}$*

(b) *a source point if $h > \max\{\{\sqrt[\alpha]{(2\Gamma(1+\alpha))/a}, \sqrt[\alpha]{(2\Gamma(1+\alpha))/1-b}\}\}$*

(c) *a saddle point if $\sqrt[\alpha]{(2\Gamma(1+\alpha))/a} < h < \sqrt[\alpha]{(2\Gamma(1+\alpha))/1-b}$ (or $\sqrt[\alpha]{(2\Gamma(1+\alpha))/1-b} < h < \sqrt[\alpha]{(2\Gamma(1+\alpha))/a}$)*

(d) *a nonhyperbolic point if $h = \sqrt[\alpha]{(2\Gamma(1+\alpha))/a}$ (or $h = \sqrt[\alpha]{(2\Gamma(1+\alpha))/1-b}$)*

Proof (a) At E_1, the Jacobian matrix is written as

$$J_1 = J(1,0) = \begin{pmatrix} 1 - \frac{ah^{\alpha}}{\Gamma(1+\alpha)} & -\frac{bh^{\alpha}}{\Gamma(1+\alpha)} \\ 0 & 1 + \frac{(b-1)h^{\alpha}}{\Gamma(1+\alpha)} \end{pmatrix}, \tag{20}$$

whose eigenvalues are $\lambda_1 = 1 - (ah^{\alpha}/(\Gamma(1+\alpha)))$ and $\lambda_2 = 1 - (((1-b)h^{\alpha})/\Gamma(1+\alpha))$. Since $(h^{\alpha}/(\Gamma(1+\alpha))) > 0$ for $0 < \alpha \le 1$ and $b < 1$, it is obvious that $|\lambda_i| < 1$, $i = 1, 2$, if $0 < h < (\sqrt[\alpha]{(2\Gamma(1+\alpha))/a})$ and $0 < h < (\sqrt[\alpha]{(2\Gamma(1+\alpha))/1-b})$. Then, E_1 is a sink point if

$$h < \min\left\{\left(\sqrt[\alpha]{\frac{2\Gamma(1+\alpha)}{a}}\right), \sqrt[\alpha]{\frac{2\Gamma(1+\alpha)}{1-b}}\right\}. \tag{21}$$

(b) E_1 is a source point if $|\lambda_i| > 1$, $i = 1, 2$, $|1 - (ah^{\alpha}/(\Gamma(1+\alpha)))| > 1$ which violates condition (21), i.e., $h > \max\{\sqrt[\alpha]{(2\Gamma(1+\alpha))/a}, \sqrt[\alpha]{(2\Gamma(1+\alpha))/1-b}\}$.

(c) E_1 is a saddle point if $|\lambda_1| > 1, |\lambda_2| < 1$ (or $|\lambda_1| < 1$, $|\lambda_2| > 1$).

(d) E_1 is a nonhyperbolic point if $|\lambda_1| = 1$, $|\lambda_2| \ne 1$ (or $|\lambda_1| \ne 1, |\lambda_2| = 1$). □

Theorem 3. *The fixed point $E_2 = (\overline{x}, t(b-1)n\overline{x})$, where $1 < b < a+1$, of system (13) is locally asymptotically stable, if and only if*

(i) $0 < ((h^{\alpha}/(b\Gamma(1+\alpha)))(b-1)) < 1$

(ii) $0 < ((h^{\alpha}/(\Gamma(1+\alpha)))(1+a-b)) < 4$

Proof. The Jacobian matrix at the fixed point E_2 is

$$J_2 = \begin{pmatrix} 1 + \frac{h^{\alpha}(b^2 - ab - 1)}{b\Gamma(1+\alpha)} & \frac{-h^{\alpha}}{b\Gamma(1+\alpha)} \\ \frac{h^{\alpha}(b^2 - 2b + 1)}{b\Gamma(1+\alpha)} & 1 - \frac{h^{\alpha}(b-1)}{b\Gamma(1+\alpha)} \end{pmatrix}. \tag{22}$$

The characteristic equation of Jacobian matrix (22) is $\lambda^2 - \beta\lambda + \gamma = 0$, where

$$\begin{aligned} \beta &= 2 - \frac{h^{\alpha}(1+a-b)}{\Gamma(1+\alpha)}, \\ \gamma &= 1 - \frac{h^{\alpha}(1+a-b)}{\Gamma(1+\alpha)} + \frac{h^{2\alpha}(1+a-b)(b-1)}{b\Gamma^2(1+\alpha)}. \end{aligned} \tag{23}$$

Using Jury's stability condition, $|\beta| < 1 + \gamma < 2$ [40–42], we obtain the following stability conditions:

$$\left|2 - \frac{h^{\alpha}(1+a-b)}{\Gamma(1+\alpha)}\right| < 2 - \frac{h^{\alpha}(1+a-b)}{\Gamma(1+\alpha)} + \frac{h^{2\alpha}(1+a-b)(b-1)}{b\Gamma^2(1+\alpha)} < 2. \tag{24}$$

The left inequality of (24), $-1-\gamma < \beta < 1+\gamma$, gives

$$0 < \frac{2h^{\alpha}(1+a-b)}{\Gamma(1+\alpha)} < 4 + \frac{h^{2\alpha}(1+a-b)(b-1)}{b\Gamma^2(1+\alpha)}, \tag{25}$$

$$0 < \frac{h^{2\alpha}(1+a-b)(b-1)}{b\Gamma^2(1+\alpha)}. \tag{26}$$

The right inequality of (24), $1+\gamma < 2$, gives

$$0 < \frac{h^{\alpha}}{b\Gamma(1+\alpha)}(b-1) < 1. \tag{27}$$

From the conditions of the existence of E_2, we find that inequality (26) is satisfied. Also, using inequality (27) in inequality (25), we obtain

$$0 < \frac{h^{\alpha}}{\Gamma(1+\alpha)}(1+a-b) < 4. \tag{28}$$

□

4.1. Bifurcation. We will discuss the bifurcation dynamics of discretized system (13). Three kinds of bifurcations show the changes in the dynamical behavior of the system due to the changes in its parameters. This behavior depends on four parameters a, b, h,and α. The first kind is the Neimark–Sacker (NS) bifurcation which is analogous to the Hopf bifurcation. NS bifurcation is a good tool to prove the existence of quasiperiodic orbits for the map [43]. The second kind is the flip (period-doubling) bifurcation which occurs when a new limit cycle born from an existing limit cycle with period equal twice of the old one. Finally, the third one is the fold (saddle-node) bifurcation which is a collision or disappearance of two equilibria in the system.

Lemma 1. *The interior fixed point E_2 loses its stability*

(1) via NS bifurcation when $(h^{\alpha}/(\Gamma(1+\alpha))) = (b/(b-1))$

(2) via flip bifurcation when $(2h^{\alpha}(1+a-b)/(\Gamma(1+\alpha))) = 4 + (h^{2\alpha}(1+a-b)(b-1)/(b\Gamma^2(1+\alpha)))$

Proof. (1) NS bifurcation occurs when the Jacobian matrix J_2 has two complex conjugate eigenvalues of modulus 1 [42]. Then, NS bifurcation occurs when $\gamma = 1$ and $-2 < \beta < 2$. Substituting by the form of the values of β and γ above, we obtain

$$\frac{h^{\alpha}}{\Gamma(1+\varepsilon)} = \frac{b}{b-1}. \tag{29}$$

Condition (29) contradicts with condition (27), which is one of the stability conditions of the fixed point E_2. The other condition is the same as condition (25).

(2) Flip bifurcation occurs when one of the two eigenvalues equal -1. It requires the condition $1+\beta+\gamma = 0$:

$$\frac{2h^{\alpha}(1+a-b)}{\Gamma(1+\alpha)} = 4 + \frac{h^{2\alpha}(1+a-b)(b-1)}{b\Gamma^2(1+\alpha)}. \tag{30}$$

Note that the fold bifurcation requires the condition $1-\beta+\gamma = 0$:

$$(1+a-b)(b-1) = 0, \tag{31}$$

but from the existence conditions of the fixed point E_2, $1 < b < 1+a$, we find that this condition is not satisfied. Then, there is no fold bifurcation. □

5. Numerical Simulations

Tremendous numerical simulations have been carried out to study the dynamical behavior of system (13), which prove our analytical findings for different sets of parameters. These simulations show that the behavior does not depend on the initial conditions. So, we fixed the initial point to be $(x_0, y_0) = (0.3, 0.5)$ for all following figures. In all figures, we plot the healthy prions $x(t)$ (blue curves) and the infected ones $y(t)$ (red curves) in the brain versus the steps n. Also, we choose the values of the parameters that satisfy the necessary stability conditions of the fixed points E_1 (21) and E_2 (27) and (28).

In Figure 3, we vary the value of the step size h to check its effect on the behavior of the prions. This figure shows that all curves of the infected prions tend to zero as n increases while the healthy prions approach the value one, whenever the fixed point E_1 is stable. Note that the steps needed to reach the fixed point increases as the step size h decreases. Also in Figure 4, we vary the value of the fractional-order α to check its impact on the behavior of the system. We found that the steps needed to reach the fixed point decreases as the parameter α decreases.

Figure 5 shows the stable dynamics of system (13) at fixed point E_2. For the parameter values at $a = 1.1$, $\alpha = 0.5$, and $h = 0.05$ and four different values of b, system (13) admits a stable focus $E_2 = (0.9091, 0.0909)$, $(0.5455, 0.2727)$, $(0.3636, 0.2545)$, and $(0.0909, 0909)$. Note that reaching the stability point E_2 is delayed by increasing the value of b. Also, Figure 6 shows four different stable fixed points E_2 for $b = 1.1$, $\alpha = 0.5$, and $h = 0.05$ and four different values of the parameter a. Note that reaching the stability point E_2 is delayed by decreasing the value of a. At these values, system (13) admits a stable focus $E_2 = (0.5, 0.05)$, $(0.8889, 0.0889)$, $(0.9286, 0.0929)$, and $(0.9524, 0952)$.

Bifurcation diagram for the healthy prions of system (13) is plotted with respect to a for parameter values $b = 1.1$, $\alpha = 0.3$, and $h = 0.05$ in Figure 7. The system exhibits

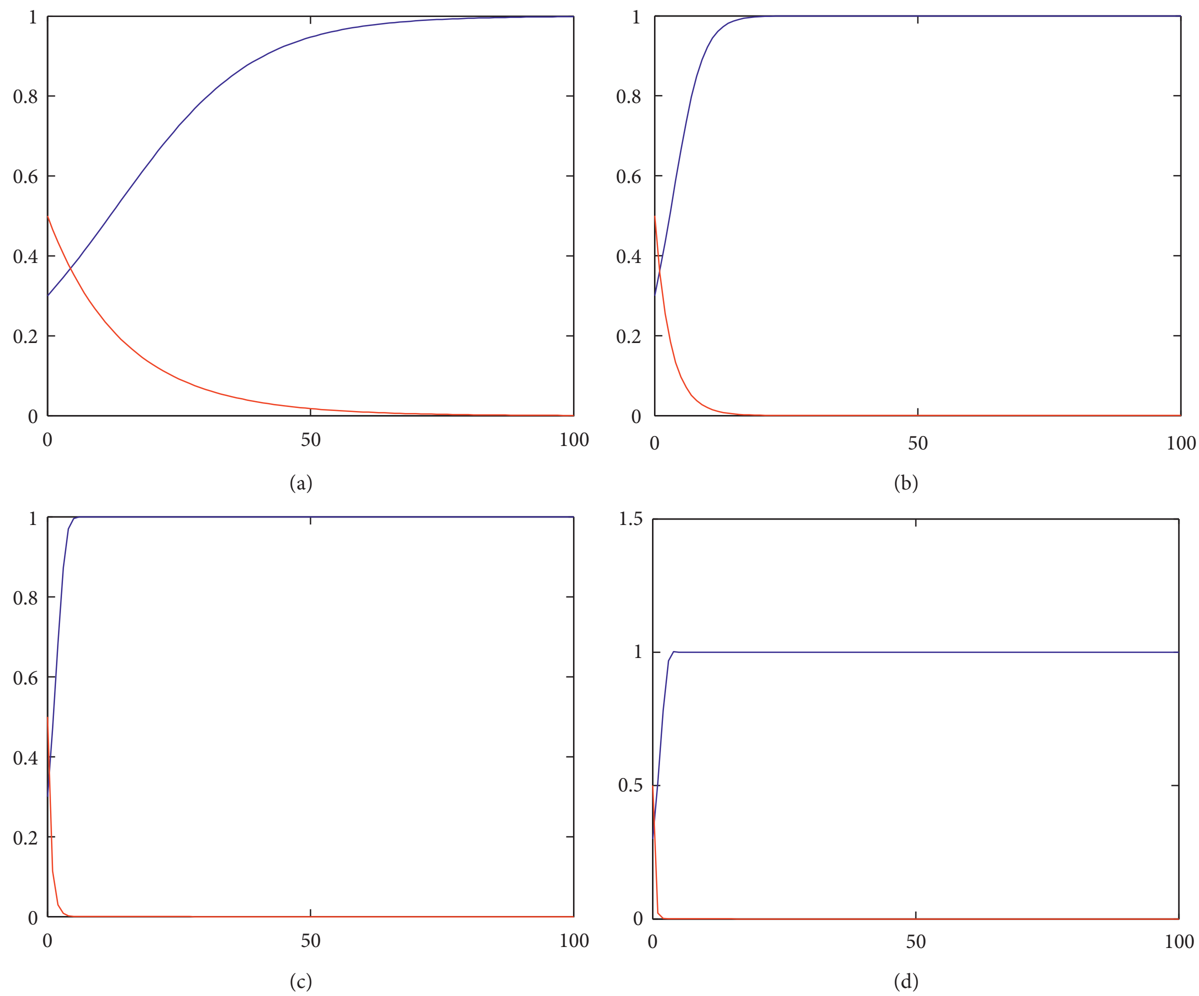

Figure 3: Four figures showing the two classes of the prion curves $x(t)$ and $y(t)$ at $a = 1.1$, $b = 0.1$, and $\alpha = 0.9$ and four different values of h. (a) $h = 0.05$. (b) $h = 0.25$. (c) $h = 0.75$. (d) $h = 0.95$.

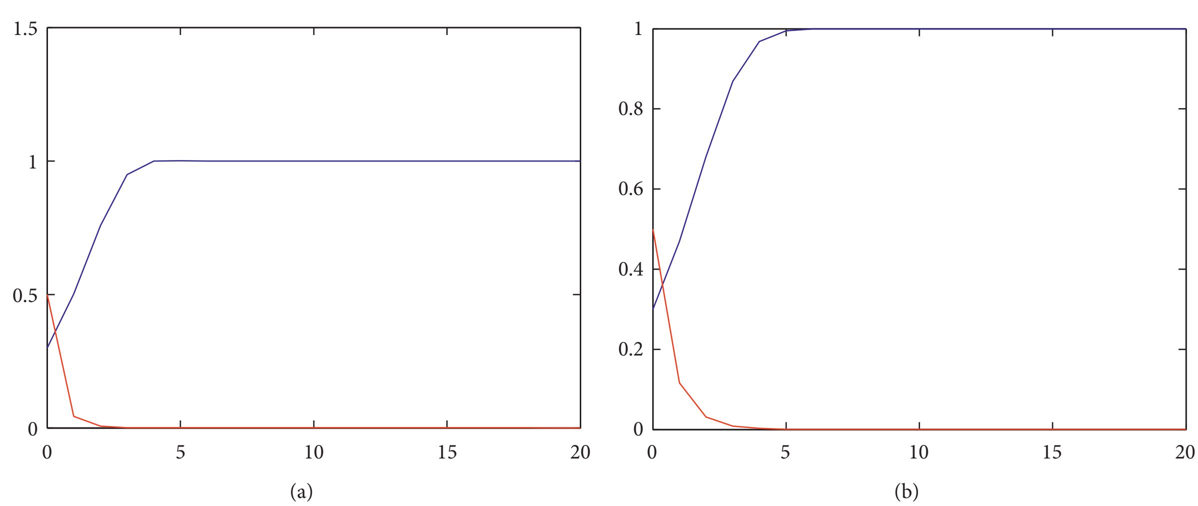

Figure 4: Continued.

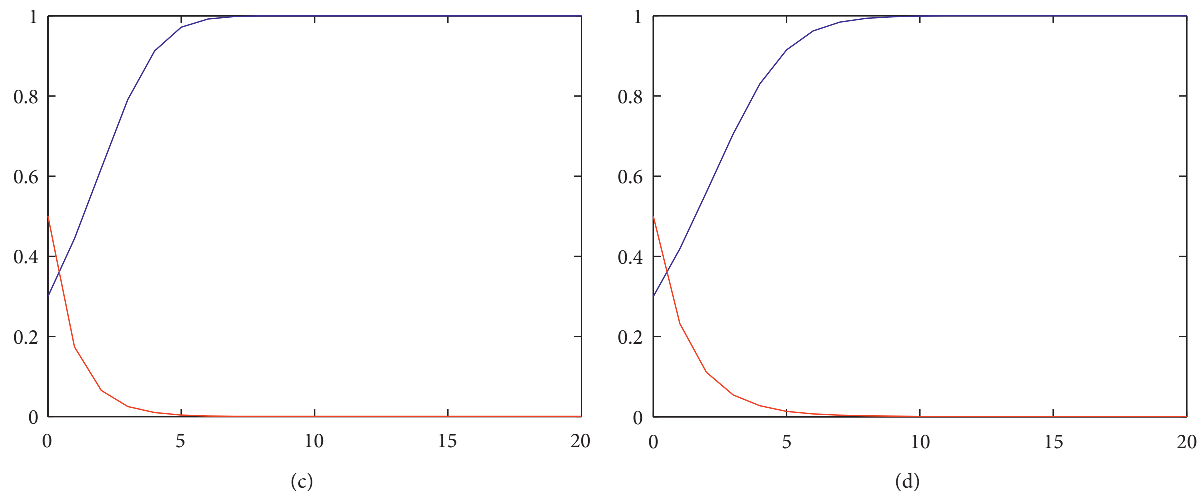

FIGURE 4: Four figures showing the two classes of the prion curves $x(t)$ and $y(t)$ at $a = 1.1$, $b = 0.1$, and $h = 0.5$ and four different values of α. (a) $\alpha = 0.2$. (b) $\alpha = 0.5$. (c) $\alpha = 0.7$. (d) $\alpha = 0.9$.

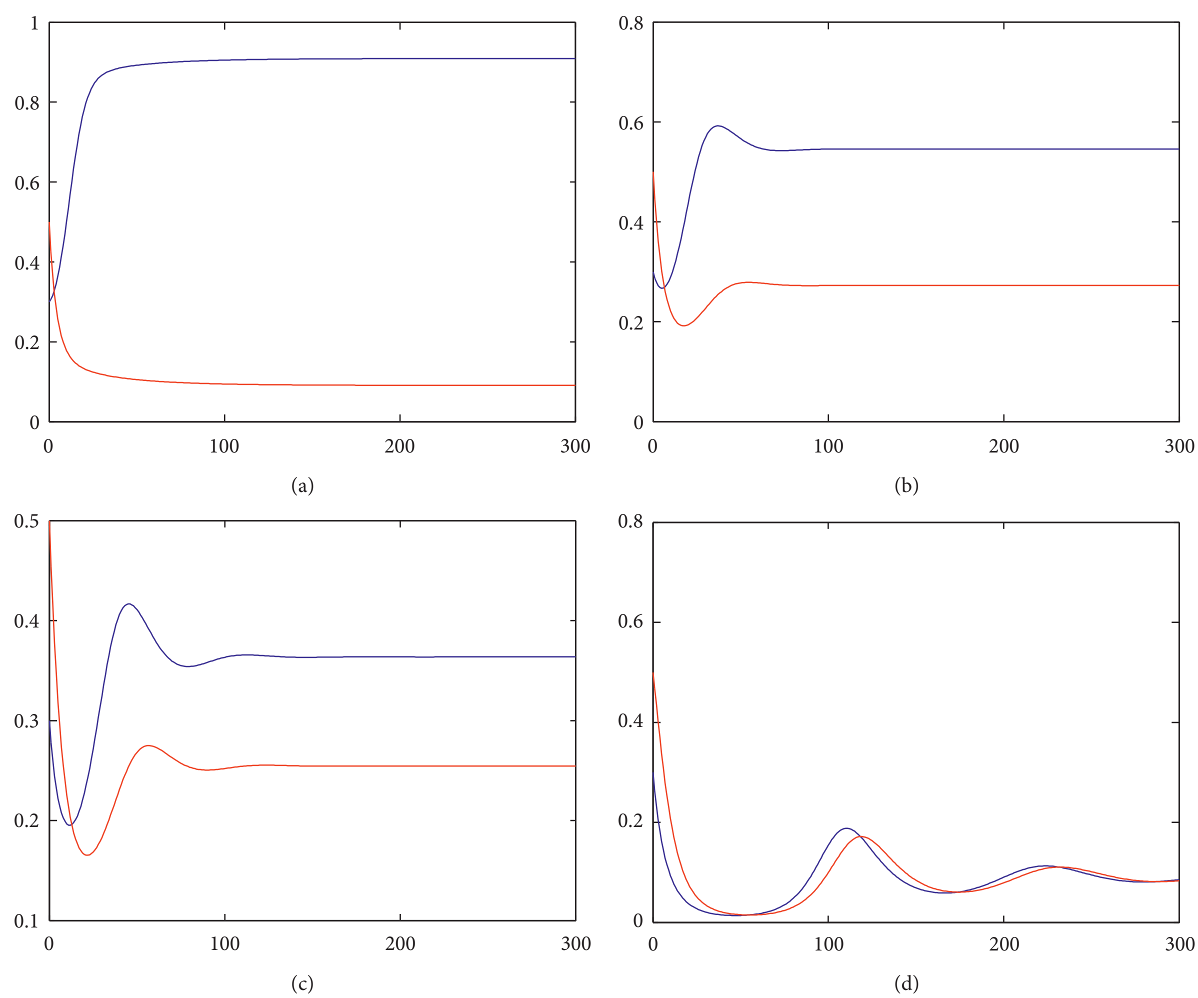

FIGURE 5: Stable fixed point E_2 at $a = 1.1$, $\alpha = 0.5$, and $h = 0.5$ and four different values of b. (a) $b = 1.1$. (b) $b = 1.5$. (c) $b = 1.7$. (d) $b = 2.0$.

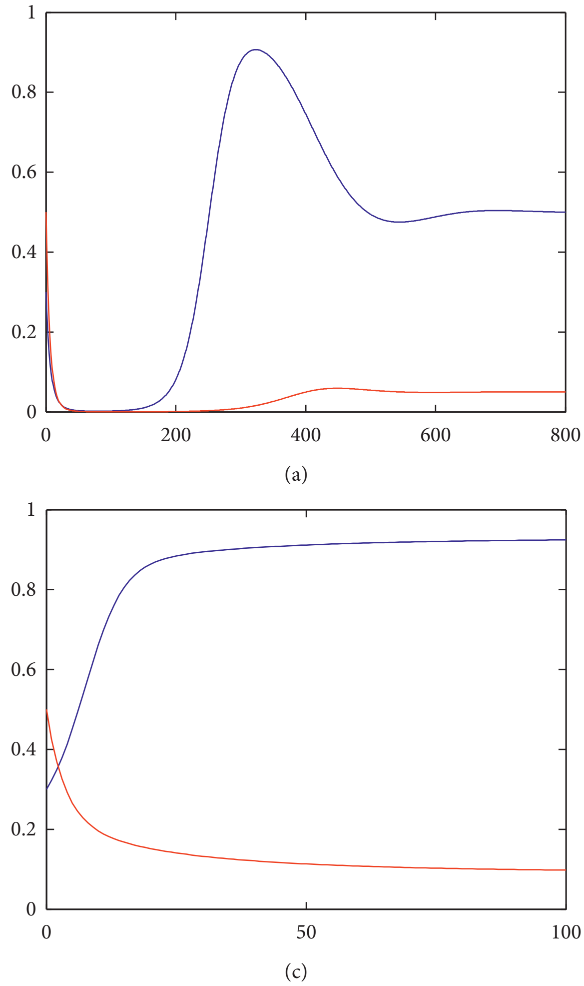

Figure 6: Stable fixed point E_2 at $b = 1.1$, $\alpha = 0.5$, and $h = 0.5$ and four different values of a. (a) $a = 0.2$. (b) $a = 0.9$. (c) $a = 1.4$. (d) $a = 2.1$.

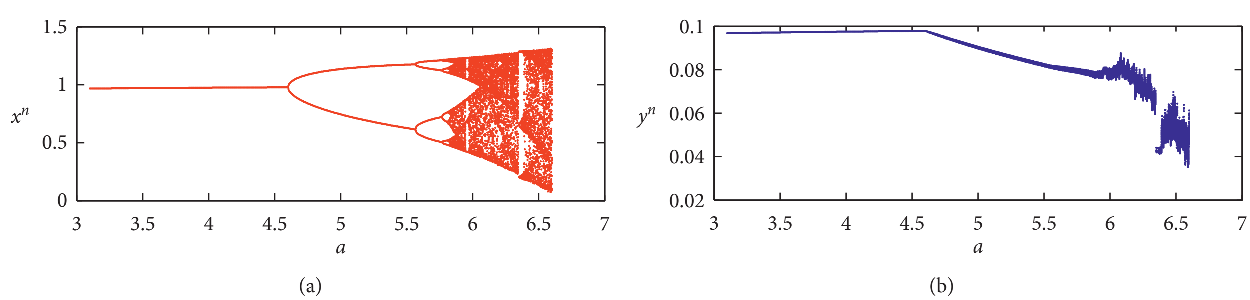

Figure 7: Bifurcation diagram with respect to a at $b = 1.1$, $\alpha = 0.3$, and $h = 0.05$.

stability up to $a = 4.3$. The system shows chaotic behavior for higher values of a started by intermittent multiperiodic windows to chaos. Figure 8 depicts the associated largest Lyapunov exponent (LLE) plot corresponding to the case presented in Figure 7. The positive Largest Lyapunov exponent confirms the existence of chaos in the system.

In Figure 9, bifurcation diagram is drawn with respect to the parameter values α using parameters $a = 3.1$, $b = 1.3$, and $h = 0.5$. A chaos to period-doubling route (flip bifurcation) along with intermittent periodic windows is clearly visible (up to $\alpha = 0.54$). For higher values beyond $\alpha = 0.54$, the solution goes to be stable. Also, the LLE corresponding with Figure 9 is plotted in Figure 10.

In another bifurcation diagram with respect to b for $a = 3.1$, $\alpha = 0.03$, and $h = 0, 5$, the system exhibits a wide range of dynamics from chaotic (up to $b = 1.3$) to

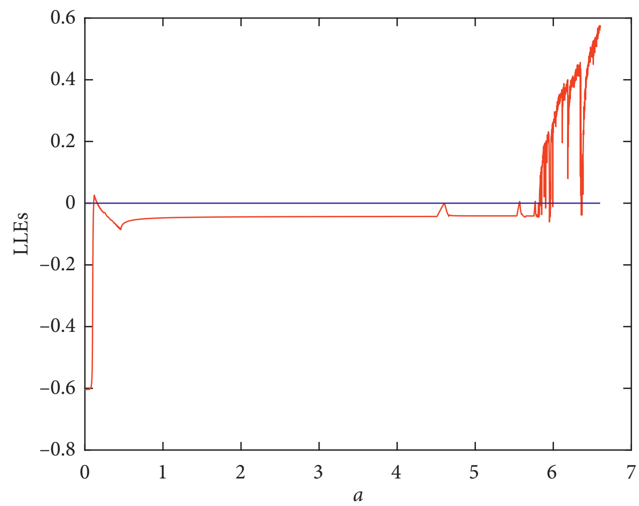

Figure 8: Largest Lyapunov exponent at $b = 1.1$, $\alpha = 0.3$, and $h = 0.05$.

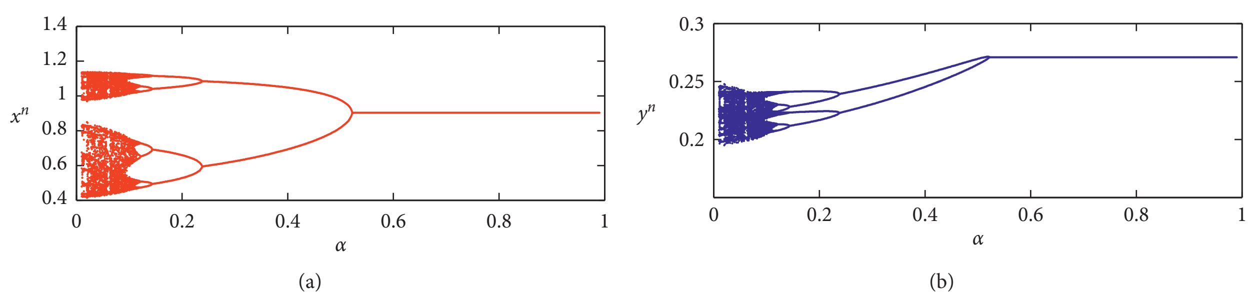

Figure 9: Bifurcation diagram with respect to α at $a = 3.1$, $b = 1.3$, and $h = 0.5$.

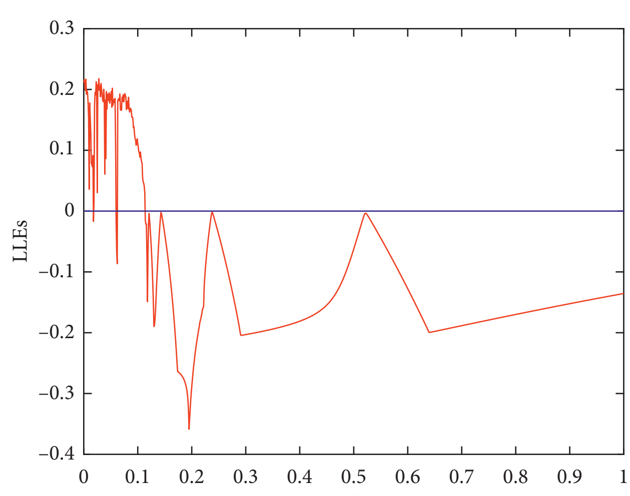

Figure 10: Largest Lyapunov exponent at $a = 3.1$, $b = 1.3$, and $h = 0.05$.

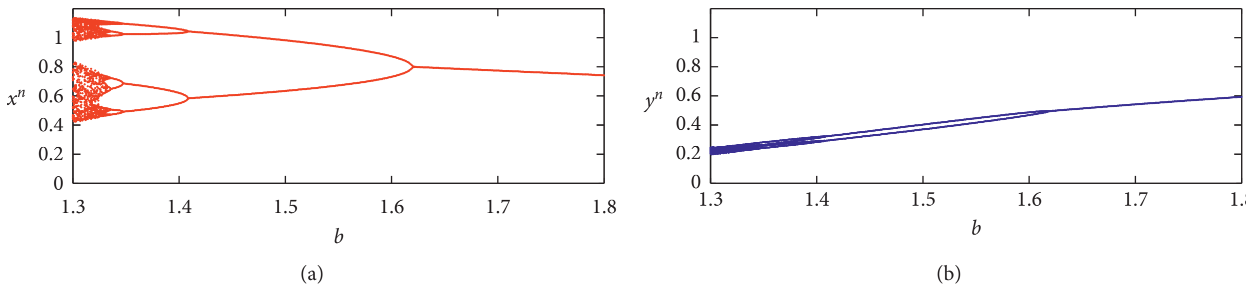

FIGURE 11: Bifurcation diagram with respect to b at $a = 3.1$, $\alpha = 0.03$, and $h = 0.5$.

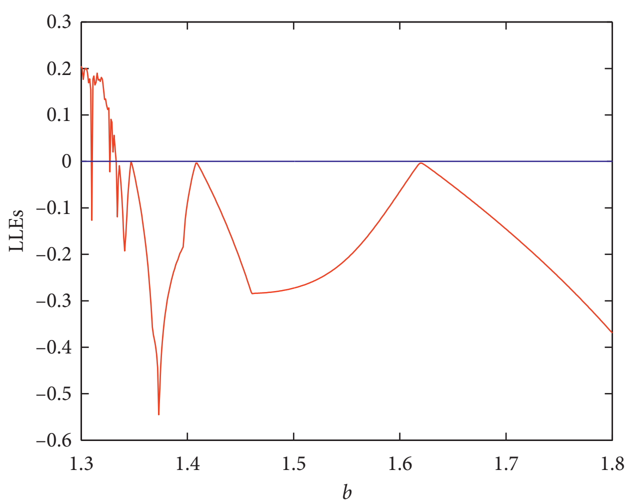

FIGURE 12: Largest Lyapunov exponent at $a = 3.1$, $\alpha = 0.03$, and $h = 0.5$.

period-doubling route with multiperiodic windows until (up to $b = 1.42$) stable state. Also, the LLE corresponding with Figure 11 is plotted in Figure 12.

6. Summary and Conclusion

Initially, a simple mathematical model was proposed to describe Parkinson's disease which consists of two ordinary differential equations. Since memory plays an essential role in PD, we proposed a fractional-order form to study this disease. The existence and the uniqueness of a solution of this model were proved. The stability conditions of its fixed points were achieved. The examinations of the patient, laboratory blood tests performed, and the doses of drugs that are prescribed to be taken are a discrete process. So, a discretized form of the fractional-order model is presented. The fixed points existence and stability conditions are obtained. Also, bifurcation studies to the model are achieved.

Our discretized model depends on the intrinsic growth rate a, the contact rate b, the order α, and the size step h. We find that decreasing the size step h delays the time needed to reach the stable the healthy state E_1 (see Figure 3). Decreasing the order α accelerates the time needed to reach the stable the healthy state E_1 (see Figure 4). With the increase in the contact parameter b, the time required to reach the fixed point E_2 increases. Also, the value of healthy prions decreases and the value of infected prions increases until they become equal (see Figure 5). While increasing the growth parameter a, the time required to reach the fixed point E_2 decreases. Also, the value of healthy prions increases and the value of infected prions decreases (see Figure 6).

The Neimark–Sacker (NS) bifurcation appears as the value of the parameter a increases. The fixed point E_2 is stable up to $a = 4.7$. After that value, the route to chaos starts (see Figure 7). Also, the flip bifurcation occurs as the values of the two parameters b and α decrease (see Figures 9 and 11). All these complex behaviors are consistent with the above theoretical results.

Data Availability

No data were used to support this study.

Conflicts of Interest

The authors declare that they have no conflicts of interest.

Acknowledgments

The authors extend their appreciation to the Deanship of Scientific Research at King Khalid University for funding this work through Big Group Research Project under grant number R.G.P.1/198/41.

References

[1] D. J. Gelb, E. Oliver, and S. Gilman, "Diagnostic criteria for Parkinson disease," *Archives of Neurology*, vol. 56, no. 1, pp. 33–39, 1999.

[2] G. E. Nam, N. H. Kim, K. Han et al., "Reply to: kidney dysfunction and risk of Parkinson's disease: the issue of equations and large number," *Movement Disorders*, vol. 35, p. 519, 2020.

[3] G. Wu, Z.-H. Lu, J. H. Seo, S. K. Alselehdar, S. DeFrees, and R. W. Ledeen, "Mice deficient in GM1 manifest both motor and non-motor symptoms of Parkinson's disease; successful treatment with synthetic GM1 ganglioside," *Experimental Neurology*, vol. 329, Article ID 113284, 2020.

[4] D. N. van Deursen, O. A. van den Heuvel, J. Booij, H. W. Berendse, and C. Vriend, "Autonomic failure in Parkinson's disease is associated with striatal dopamine deficiencies," *Journal of Neurology*, vol. 267, no. 7, pp. 1922–1930, 2020.

[5] J. M. Hausdorff, "Gait dynamics in Parkinson's disease: common and distinct behavior among stride length, gait variability, and fractal-like scaling," *Chaos: An Interdisciplinary Journal of Nonlinear Science*, vol. 19, Article ID 26113, 2009.

[6] C. Lainscsek, L. Schettino, P. Rowat et al., *Applications of Nonlinear Dynamics, Understanding Complex Systems*, Springer, Berlin, Germany, 2009.

[7] J. H. Ko, P. G. Spetsieris, and D. Eidelberg1, "Network structure and function in Parkinsons disease," *Cerebral Cortex*, vol. 28, pp. 4121–4135, 2018.

[8] Y. Sarbaz, M. Banaie, M. Pooyan, S. Gharibzadeh, F. Towhidkhah, and A. Jafari, "Modeling the gait of normal and Parkinsonian persons for improving the diagnosis," *Neuroscience Letters*, vol. 509, no. 2, pp. 72–75, 2012.

[9] Y. Sarbaz and H. Pourakbari, "A review of presented mathematical models in Parkinson's disease: black- and gray-box models," *Medical & Biological Engineering & Computing*, vol. 54, no. 6, pp. 855–868, 2016.

[10] S. Pandya, Y. Zeighami, B. Freeze et al., "Predictive model of spread of Parkinson's pathology using network diffusion," *Neuroimage*, vol. 192, pp. 178–194, 2019.

[11] M. Al-Zoughool and S. El Saadany, "Mathematical models for estimating the risk of vCJD transmission," in *Proceedings of the OCCAM Fields MITACS Biomedical Problem Solving Workshop*, pp. 81–98, Toronto, Canada, June 2009.

[12] S. S. Sindi, *Mathematical Modeling of Prion Disease, Prion-An Overview*, Intech, London, UK, 2017.

[13] S. M. Salman and E. Ahmed, "A mathematical model for Creutzfeldt Jacob disease (CJD)," *Chaos, Solitons & Fractals*, vol. 116, pp. 249–260, 2018.

[14] A. M. A. El-Sayed, "Fractional-order diffusion-wave equation," *International Journal of Theoretical Physics*, vol. 35, no. 2, pp. 311–322, 1996.

[15] C. Li and G. Peng, "Chaos in Chen's system with a fractional order," *Chaos, Solitons & Fractals*, vol. 22, no. 2, pp. 443–450, 2004.

[16] A. E. M. El-Misiery and E. Ahmed, "On a fractional model for earthquakes," *Applied Mathematics and Computation*, vol. 178, no. 2, pp. 207–211, 2006.

[17] F. C. Meral, T. J. Royston, and R. Magin, "Fractional calculus in viscoelasticity: an experimental study," *Communications in Nonlinear Science and Numerical Simulation*, vol. 15, no. 4, pp. 939–945, 2010.

[18] J. T. Machado, V. Kiryakova, and F. Mainardi, "Recent history of fractional calculus," *Communications in Nonlinear Science and Numerical Simulation*, vol. 16, no. 3, pp. 1140–1153, 2011.

[19] D. A. Benson, M. M. Meerschaert, and J. Revielle, "Fractional calculus in hydrologic modeling: a numerical perspective," *Advances in Water Resources*, vol. 51, pp. 479–497, 2013.

[20] A. Sapora, P. Cornetti, and A. Carpinteri, "Wave propagation in nonlocal elastic continua modelled by a fractional calculus approach," *Communications in Nonlinear Science and Numerical Simulation*, vol. 18, no. 1, pp. 63–74, 2013.

[21] M. P. Aghababa and M. Borjkhani, "Chaotic fractional-order model for muscular blood vessel and its control via fractional control scheme," *Complexity*, vol. 20, no. 2, pp. 37–46, 2014.

[22] J. A. Tenreiro Machado and M. E. Mata, "Pseudo phase plane and fractional calculus modeling of western global economic downturn," *Communications in Nonlinear Science and Numerical Simulation*, vol. 22, no. 1-3, pp. 396–406, 2015.

[23] M. F. Elettreby, T. Nabil, and A. A. Al-Raezah, "Dynamical analysis of a prey-predator fractional model," *Journal of Fractional Calculus and Applications*, vol. 8, pp. 237–245, 2017.

[24] M. F. Elettreby, A. A. Al-Raezah, and T. Nabil, "Fractional-order model of two-prey one-predator system," *Mathematical Problems in Engineering*, vol. 2017, Article ID 6714538, 12 pages, 2017.

[25] M. F. Elettreby, A. S. Alqahtani, and E. Ahmed, "Fractional-order model for multi-drug antimicrobial resistance," *Computer Modeling in Engineering & Sciences*, vol. 124, no. 2, pp. 665–682, 2020.

[26] E. Ahmed, A. M. A. El-Sayed, and H. A. A. El-Saka, "Equilibrium points, stability and numerical solutions of fractional-order predator-prey and rabies models," *Journal of Mathematical Analysis and Applications*, vol. 325, no. 1, pp. 542–553, 2007.

[27] S. Das, P. K. Gupta, and Rajeev, "A fractional predator prey model and its solution," *International Journal of Nonlinear Sciences and Numerical Simulation*, vol. 10, no. 7, pp. 873–876, 2009.

[28] M. Rivero, J. J. Trujillo, L. Pilar Velasco, and M. P. Velasco, "Fractional dynamics of populations," *Applied Mathematics and Computation*, vol. 218, no. 3, pp. 1089–1095, 2011.

[29] M. Javidi and N. Nyamoradi, "Dynamic analysis of a fractional order prey-predator interaction with harvesting," *Applied Mathematical Modelling*, vol. 37, no. 20-21, pp. 8946–8956, 2013.

[30] M. Javidi and B. Ahmad, "A study of a fractional-order cholera model," *Applied Mathematics & Information Sciences*, vol. 8, no. 5, pp. 2195–2206, 2014.

[31] A. E. Matouk, A. A. Elsadany, E. Ahmed, and H. N. Agiza, "Dynamical behavior of fractional-order Hastings-Powell food chain model and its discretization," *Communications in Nonlinear Science and Numerical Simulation*, vol. 27, no. 1-3, pp. 153–167, 2015.

[32] A. Singh, A. A. Elsadany, and A. Elsonbaty, "Complex dynamics of a discrete fractional-order Leslie-Gower predator-prey model," *Math. Meth. Appl. Sci.* vol. 42, pp. 1–16, 2019.

[33] I. Podlubny, *Fractional Differential Equations*, Academic Press, New York, NY, USA, 1999.

[34] E. D. Rainville, *Special Functions*, Macmillan Company, New York, NY, USA, 1960.

[35] M. Caputo, "Linear models of dissipation whose Q is almost frequency independent--II," *Geophysical Journal International*, vol. 13, no. 5, pp. 529–539, 1967.

[36] D. Matignon, "Stability results for fractional differential equations with applications to control processing," *Computational Engineering in Systems Applications*, vol. 2, pp. 963–968, 1996.

[37] R. P. Agarwal, A. M. El-Sayed, and S. M. Salman, "Fractional-order Chua's system: discretization, bifurcation and chaos," *Advances in Differential Equations*, vol. 320, 2013.

[38] A. M. El-Sayed, Z. F. El-Raheem, and S. M. Salman, "Discretization of forced Duffing system with fractional-orderd amping," *Advances in Differential Equations*, vol. 66, 2014.

[39] J. Shen and J. Lam, "Non-existence of finite-time stable equilibria in fractional-order nonlinear systems," *Automatica*, vol. 50, no. 2, pp. 547–551, 2014.

[40] M. Kot, *Elements of Mathematical Ecology*, Cambridge University Press, 2001.

[41] L. Edelstein-Keshet, *Mathematical Models in Biology*, McGraw-Hill, New York, NY, USA, 2005.

[42] S. Elaydi, *Discrete Chaos with Applications in Science and Engineering*, Chapman and Hall/CRC, Boca Raton, FL, USA, 2nd edition, 2008.

[43] R. Asheghi, "Bifurcations and dynamics of a discrete predator-prey system," *Journal of Biological Dynamics*, vol. 8, pp. 161–186, 2018.

Hindawi
Mathematical Problems in Engineering
Volume 2020, Article ID 1405764, 4 pages
https://doi.org/10.1155/2020/1405764

Research Article

Forecasting Confirmed Cases, Deaths, and Recoveries from COVID-19 in China during the Early Stage

Lianyi Liu, Yan Chen, and Lifeng Wu

College of Management Engineering and Business, Hebei University of Engineering, Handan 056038, China

Correspondence should be addressed to Lifeng Wu; wlf6666@126.com

Received 23 May 2020; Accepted 7 July 2020; Published 29 July 2020

Academic Editor: Abdelalim A. Elsadany

To provide a theoretical basis for the prevention and control of COVID-19 in China, confirmed cases, deaths, and recoveries from COVID-19 in China were predicted using a fractional grey model. The results indicated that the grey model has high forecasting accuracy in the prediction of disease spread.

1. Introduction

The outbreak of the novel coronavirus disease-2019 (COVID-19) caused by SARS-CoV-2 took place in December 2019 in Wuhan, China. This disease can cause severe fever and, in the worst cases, acute respiratory failure syndrome [1]. There were 1016 recorded deaths from this outbreak as of February 10, 2020, in China. It has also spread across other countries, starting with Japan and then Australia, France, and the United States. The SARS-CoV-2 virus continues to evolve in alarming ways, with the spread of COVID-19, putting enormous strain on health systems around the world. There is no indication that China will succeed in beating COVID-19 in the short term. Accurately forecasting the epidemic tendency can provide a theoretical basis for the prevention and control of COVID-19.

Statistical methods are widely used for forecasting of epidemic diseases [2]. Traditional prediction methods often require a large number of data samples, which follow a certain typical distribution. However, because of the limited information available during the early stages of disease transmission, the spreading mechanism of COVID-19 is yet to be fully understood [3]. The grey prediction theory provides a new way to solve the systemic problems that occur in cases of limited information. Thus, the grey prediction theory is more suitable for the prediction of the incidence of COVID-19 in China than other theories.

The rest of the paper is arranged as follows. Section 2 introduces the forecasting model. Section 3 shows in detail the prediction results. Conclusions are drawn in Section 4.

2. Fractional Grey Model

Grey system theory mainly focuses on systems with incomplete or uncertain information [4]. In recent years, grey system theory has been successfully applied to the prediction of infectious diseases [5–8].

Despite the widespread outbreak of COVID-19, data on this disease in China are limited. Many methods cannot make accurate predictions if the data samples are small. For this reason, the fractional grey model (FGM(1,1)) is used to deal with the forecasting problem with limited samples [9]. The FGM(1,1) model is an optimized form of the grey prediction model. Its detailed modeling process has been described previously [9, 10].

3. Results

In this section, the data are from the National Health Commission of the People's Republic of China (http://www.nhc.gov.cn/). The Chinese government has made every effort

Table 1: Prediction of confirmed cases of COVID-19 in China.

Data	Actual values	FGM(1,1)	MAPE
21-Jan	291		
22-Jan	440		
23-Jan	571		
24-Jan	1287		
25-Jan	1975		
26-Jan	2744	3207	16.89
27-Jan	4515	3961	12.27
28-Jan	5974	6462	8.17
29-Jan	7711	8362	8.44
30-Jan	9692	9881	1.95
31-Jan	11,791	12,037	2.08
1-Feb	14,380	14,103	1.92
2-Feb	17,205	17,271	0.38
3-Feb	20,438	20,418	0.10
4-Feb	24,324	23,973	1.44
5-Feb	28,018	28,593	2.05
6-Feb	28,985	31,792	9.68
7-Feb	31,774	30,893	2.77
8-Feb	33,738	33,145	1.76
9-Feb	35,982	35,965	0.05
Mean			4.66

Table 2: Prediction of the death toll due to COVID-19.

Data	Actual values	FGM(1,1)	MAPE
22-Jan	9		
23-Jan	17		
24-Jan	41		
25-Jan	56		
26-Jan	80		
27-Jan	106	109	2.79
28-Jan	132	143	8.63
29-Jan	170	164	3.26
30-Jan	213	212	0.33
31-Jan	259	267	3.22
1-Feb	304	311	2.22
2-Feb	361	351	2.87
3-Feb	425	422	0.78
4-Feb	490	500	2.02
5-Feb	563	559	0.69
6-Feb	636	643	1.16
7-Feb	722	714	1.13
8-Feb	811	813	0.28
9-Feb	908	908	0.05
Mean			2.10

to fight the epidemic and has continued to release relevant data since January 21, 2020. Data released after January 21 were used to test the performance of the forecasts.

A rolling forecast approach was taken in the experiment. Here, the data of every five consecutive days were used as observations to predict the data for the next day. The mean absolute percentage error (MAPE) was used to test the performance of the model. The prediction results of the confirmed cases are presented in Table 1.

As shown in Table 1, the mean MAPE is 4.66%, which meets our expectations for accurate forecasting. The FGM(1,1) model only needs five consecutive days of data to predict the next day's data. It needs very little data and follows the principle of new information priority. Even for the most uncontrollable first days of the epidemic, FGM(1,1) showed accurate prediction. Since February 28, the predicted MAPE has been less than 10%, which demonstrates the adaptability of the model.

The number of deaths due to COVID-19 and the number of people who have recovered are shown in Tables 2 and 3, respectively.

As shown in Tables 2 and 3, the MAPE of the number of deaths and recoveries from COVID-19 was 2.10% and 3.61%, respectively. All the MAPE values of the prediction results were less than 10%, which means that the prediction results met the requirement of highly accurate prediction.

Table 3: Prediction of the number of people recovered from COVID-19.

Data	Actual values	FGM(1,1)	MAPE (%)
24-Jan	38		
25-Jan	49		
26-Jan	51		
27-Jan	60		
28-Jan	103		
29-Jan	124	129	3.84
30-Jan	171	169	1.00
31-Jan	243	225	7.38
1-Feb	328	318	3.01
2-Feb	475	441	7.09
3-Feb	632	646	2.28
4-Feb	892	843	5.51
5-Feb	1153	1217	5.54
6-Feb	1540	1536	0.25
7-Feb	2050	1975	3.64
8-Feb	2649	2669	0.75
9-Feb	3281	3381	3.05
Mean			3.61

Table 4: The forecasting results of FGM(1,1).

Data	Number of confirmed cases	Growth rate of confirmed cases (%)	Number of deaths	Number of recoveries
10-Feb	37,857	5.21	1011	4160
11-Feb	39,742	4.98	1123	5240
12-Feb	41,585	4.64	1244	6582
13-Feb	43,397	4.36	1373	8253
14-Feb	45,186	4.12	1513	10,333

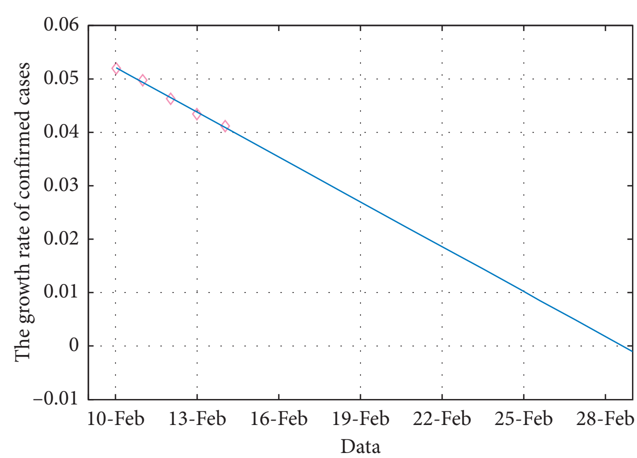

Figure 1: Prediction of the growth rate of the number of confirmed cases.

Therefore, we took the next step to predict the future number of confirmed, dead, and recovered cases, as shown in Table 4.

The predictions show that the growth rate of the number of confirmed cases was on the decline, and the number of recoveries was on the rise. Based on the above results, we further predicted the growth rate of confirmed cases. From the existing data, the growth rate showed a straight-line downward trend, so linear regression was used for prediction. The predictive effect is shown in Figure 1. We could draw the conclusion that the inflection point would be reached around February 29, the spread of COVID-19 would be effectively controlled, and the number of people infected would not increase much.

4. Conclusions

The spread of COVID-19 has caused great damage to the world's health care systems, so it is very necessary to predict the spread of disease in the future. In the early stages of the outbreak, data are limited and not absolutely accurate. The FGM(1,1) model is a good choice at the early stage of disease transmission for the prediction of trends of this new disease. FGM(1,1) is suitable for short-term prediction of time series. Using the characteristics of fractional-order accumulation, the grey model can analyze the rules in short-term data well based on the principle of new information first. Hence, FGM(1,1) could accurately predict the number of confirmed cases, the number of deaths, and the number of recoveries. The predicted results indicate that the spread of COVID-19 will be further suppressed in China, more people will be cured, and infection rates will fall further.

Data Availability

The data used to support the findings of this study are available from the corresponding author upon request.

Conflicts of Interest

The authors declare that there are no conflicts of interest regarding the publication of this paper.

Acknowledgments

This research was supported by the National Natural Science Foundation of China (71871084), the Scientist Foundation of Hebei Education Department (SQ201027 and ZD202007), and the Excellent Young Scientist Foundation of Hebei Education Department (SLRC2019001).

References

[1] WHO, *WHO to Accelerate Research and Innovation for New Coronavirus*, WHO, Geneva, Switzerland, 2020, https://www.who.int/news-room/detail/06-02-2020-who-to-accelerate-research-and-innovation-for-new-coronavirus.

[2] R. Xu, "Global dynamics of an SEIS epidemic model with saturation incidence and latent period," *Applied Mathematics and Computation*, vol. 218, no. 15, pp. 7927–7938, 2012.

[3] J. T. Wu, K. Leung, and G. M. Leung, "Nowcasting and forecasting the potential domestic and international spread of the 2019-nCoV outbreak originating in Wuhan, China: a modelling study," *The Lancet*, vol. 395, no. 10225, https://www.sciencedirect.com/science/article/pii/S0140673620302609, 2020.

[4] K. K. Emmanuel, "Forecasting the total energy consumption in Ghana using grey models," *Grey Systems: Theory and Application*, vol. 9, no. 4, pp. 488–501, 2019.

[5] X. Guo, S. Liu, and Y. Yang, "A prediction method for plasma concentration by using a nonlinear grey Bernoulli combined model based on a self-memory algorithm," *Computers in Biology and Medicine*, vol. 105, pp. 81–91, 2019.

[6] X. J. Shen, L. M. Ou, X. J. Chen et al., "The application of the grey disaster model to forecast epidemic peaks of typhoid and paratyphoid fever in China," *PLoS One*, vol. 8, Article ID e60601, 2013.

[7] L. Zhang, Y. Zheng, K. Wang et al., "An optimized Nash nonlinear grey Bernoulli model based on particle swarm optimization and its application in prediction for the incidence of Hepatitis B in Xinjiang, China," *Computers in Biology and Medicine*, vol. 33, no. 4, pp. 1073–1078, 2014.

[8] Y. Wang, Q. Du, F. Ren et al., "Spatio-temporal variation and prediction of Ischemic heart disease hospitalizations in Shenzhen, China," *International Journal of Environmental Research and Public Health*, vol. 11, no. 5, pp. 4799–4824, 2014.

[9] L. Liang, S. Liu, L. Yao, and D. Liu, "Grey system model with the fractional order accumulation," *Communications in Nonlinear Science and Numerical Simulation*, vol. 18, no. 7, pp. 1775–1785, 2013.

[10] Y. Yan, W. Lifeng, L. Lianyi, and Z. Kai, "Fractional Hausdorff grey model and its properties," *Chaos, Solitons & Fractals*, vol. 138, p. 109915, 2020.

Hindawi
Mathematical Problems in Engineering
Volume 2020, Article ID 3902931, 14 pages
https://doi.org/10.1155/2020/3902931

Research Article

A Transformation Method for Delta Partial Difference Equations on Discrete Time Scale

Syed Sabyel Haider,[1] **Mujeeb Ur Rehman**,[1] **and Thabet Abdeljawad**[2,3,4]

[1]*School of Natural Sciences, National University of Sciences and Technology, H-12, Islamabad, Pakistan*
[2]*Department of Mathematics and General Sciences, Prince Sultan University, P.O. Box 66833, Riyadh 11586, Saudi Arabia*
[3]*Department of Medical Research, China Medical University, Taichung 40402, Taiwan*
[4]*Department of Computer Science and Information Engineering, Asia University, Taichung, Taiwan*

Correspondence should be addressed to Thabet Abdeljawad; tabdeljawad@psu.edu.sa

Received 3 May 2020; Revised 28 May 2020; Accepted 18 June 2020; Published 10 July 2020

Guest Editor: Baogui Xin

The aim of this study is to develop a transform method for discrete calculus. We define the double Laplace transforms in a discrete setting and discuss its existence and uniqueness with some of its important properties. The delta double Laplace transforms have been presented for integer and noninteger order partial differences. For illustration, the delta double Laplace transforms are applied to solve partial difference equation.

1. Introduction

The origin of calculus of finite differences is found from Brook Taylor (1717), rather it was Jacob Stirling, who found the theory (1730) and introduce the delta Δ symbol for the difference, which is in common use nowadays. The development on calculus of finite differences in the beginning of the nineteenth century by Lacroix and remarkable work of George Boole, Narlund, and Steffensen appeared later in the nineteenth century. Jordan discussed calculus of finite differences with the classical approach in [1]. In modern era, the focus of mathematician is to correlate the continuous and the discrete, to shape in comprehensive unified mathematics, and to eliminate ambiguity. The calculus of finite differences is applicable to both continuous and discrete functions. For difference equations, Bohner and Peterson treat the dynamic equations on time scales in [2] and get surprisingly different results from continuous counterpart. Some results can be found in [3–19] which has helped to construct the theory of discrete fractional calculus.

Coon and Bernstein [20–22] defined the double Laplace transforms (continuous) and investigated many properties. Debnath [23] modified the properties and use the double Laplace transforms (continuous) to solve functional, integral, and partial differential equations. Dhunde and Waghmare [24] discussed convergence and absolute convergence of the double Laplace transforms (continuous) and, by application of double Laplace transforms, presented the solution of Volterra Integropartial differential equation. For applications of triple, quadruple, and n-dimensional Laplace transforms (continuous), we refer the readers to [25–27]. Goodrich and Peterson [10] developed discrete delta Laplace transforms analogous to Laplace transforms discussed by Bohner and Peterson [2] in the continuous case, to solve difference and summation equations with initial data by applying the delta Laplace transforms. The delta Laplace transforms is given for newly defined Hilfer difference operator [28] and substantial difference operator in [29]. Bohner et al. [30] generalized properties of the Laplace transforms to the delta Laplace transforms on arbitrary time scales and discussed translation theorems and transforms of periodic functions. Compatible discrete time Laplace transforms with Laplace transforms was introduced in [31]. Savoye [32] highlighted the importance of discrete time problems and relationship of Z transforms to Laplace transforms on time scale. Fractional double Laplace transform was introduced in [33]; during derivation of Corollary 1, authors neglected the violation of semigroup property of Mittage-Leffler functions, and a counter example for semigroup property of Mittage-Leffler functions is given in [34]. The qualitative analysis of delay partial difference equations is considered as discrete analog of delay partial differential equations by Zhang and Zhou [35]. For solving partial difference equations Ozpinar and Belgacem introduced discrete homotopy perturbation Sumudu transform method in [36]. For solving partial differential equations, double Laplace transform was applied in [37, 38].

Here, we introduce the delta double Laplace transforms similar to the one presented by Bernstein [20] in such a way that properties and expressions bear a resemblance to that appearing in Debnath [23] for the continuous calculus. The double convolution product, we consider in this article, resemble with the convolution product defined for delta calculus in [2, 10], but it differs from the one defined by Atici in [8]. We consider the problem with constant coefficients in two independent variables and solve by applying the delta double Laplace transforms to partial difference equations with initial data.

This paper is divided into five sections. In Section 2, we shall present basic definitions and results from discrete calculus. Definition, existence, uniqueness, and series representation of the delta double Laplace transforms are given in Section 3. Some properties of the delta double Laplace transforms are proved in Section 4. In Section 5, we present the delta double Laplace transforms of partial differences.

2. Preliminaries

For convenience, this section comprises of some basic definitions and results from discrete calculus for later use in the following sections. The functions we consider usually are defined on the set $\mathbb{N}_a := \{a, a+1, a+2, \ldots\}$ and $\mathbb{N}_a^b := \{a, a+1, a+2, \ldots, b\}$, for fixed $a, b \in \mathbb{R}$.

The following concepts are discussed in [10, 16].

Falling function is defined for positive integer n by

$$x^{\underline{n}} = x(x-1)(x-2)\cdots(x-n+1). \tag{1}$$

The forward jump operator is defined for $x \in \mathbb{N}_a$ by $\sigma(x) = x + 1$.

The set of regressive functions is defined for $x \in \mathbb{N}_a$ by $\mathscr{R} = \{p_i\colon 1 + p_i(x) \neq 0\}$.

The circle plus sum of $p_1, p_2 \in \mathscr{R}$ is given by $p_1 \oplus p_2 = p_1 + p_2 + p_1 p_2$.

The additive inverse of $p_1 \in \mathscr{R}$ is given by $\ominus p_1(x) = -p_1(x)/(1 + p_1(x))$ for $x \in \mathbb{N}_a$.

Definition 1 (see [10]). Assume $p_1 \in \mathscr{R}$ and $s \in \mathbb{N}_a$. Then, the delta exponential function is given by

$$e_{p_1}(x,s) = \begin{cases} \prod_{t=s}^{x-1} [1 + p_1(t)], & \text{if } x \in \mathbb{N}_s, \\ \prod_{t=x}^{s-1} [1 + p_1(t)]^{-1}, & \text{if } x \in \mathbb{N}_a^{s-1}. \end{cases} \tag{2}$$

By the empty product convention, $\prod_{t=s}^{s-1}[h(t)] := 1$ for any function h.

Example 1. If $p_1(x) = c$ is a constant such that $c \in \mathscr{R}$ (that is $c \neq -1$), then the delta exponential function for a constant is given by

$$e_{p_1}(x,s) = e_c(x,s) = [1 + c]^{x-s}, \quad \text{for } x \in \mathbb{N}_a. \tag{3}$$

For a particular choice of $s = a$, that is, the initial point of the domain of definition,

$$e_c(x,a) = [1 + c]^{x-a}, \quad \text{for } x \in \mathbb{N}_a. \tag{4}$$

Definition 2 (see [10]). Assume $f\colon \mathbb{N}_a \longrightarrow \mathbb{R}$ and $b \le c$ are in $\mathbb{N}_a$; then, the delta definite integral is defined by

$$\int_b^c f(x)\Delta x = \sum_{x=b}^{c-1} f(x). \tag{5}$$

Note that the value of integral $\int_b^c f(x)\Delta x$, depending on the set $\{b, b+1, \ldots, c-1\}$. Also, by the empty sum convention,

$$\sum_{x=b}^{b-k} f(x) = 0, \quad \text{whenever } k \in \mathbb{N}_1. \tag{6}$$

The delta indefinite integral is defined by

$$\int_b^\infty f(x)\Delta x = \sum_{x=b}^{\infty} f(x). \tag{7}$$

Definition 3 (see [10]). Assume $f\colon \mathbb{N}_a \longrightarrow \mathbb{R}$. Then, the delta Laplace transform of f based at a is defined by

$$\mathscr{L}_x\{f\}(p) = \int_a^\infty e_{\ominus p}(\sigma(x), a) f(x)\Delta x, \tag{8}$$

for all complex numbers $p \neq -1$ such that this improper integral converges.

Note that throughout this article, we take the delta Laplace transform at the initial point a of the set $\mathbb{N}_a$, unless stated otherwise.

The following concepts are also discussed in [10, 16].

Definition 4 (see [10]). A function f is of exponential order $r_1 > 0$ if there exist a constant $A_1 > 0$ and the following inequality:

$$|f(x)| \le A_1 r_1^x, \quad \text{holds for sufficiently large } x \in \mathbb{N}_a. \tag{9}$$

If f is of exponential order, then $\mathscr{L}_x\{f\}(p)$ converges absolutely for $|p+1| > r_1$, which ensures the existence of the Laplace transform. Even though the converse in not true, we restrict ourselves to only exponential order functions. For $f\colon \mathbb{N}_a \longrightarrow \mathbb{R}$, the following are useful expressions for the delta Laplace transform of f based at a:

$$\begin{aligned} \mathscr{L}_x\{f\}(p) = \widetilde{F}(p) &= \int_0^\infty \frac{f(a+j)}{(p+1)^{j+1}}\Delta j \\ &= \sum_{j=0}^{\infty} \frac{f(a+j)}{(p+1)^{j+1}}, \end{aligned} \tag{10}$$

for all complex numbers $p \neq -1$ such that this infinite series converges.

Example 2. If $c \neq -1$, then for $|p+1| > |c+1|$, we have

$$\mathscr{L}_x\{e_c(x,a)\}(p) = \frac{1}{p-c}. \tag{11}$$

Definition 5 (see [10]). Assume $f, g\colon \mathbb{N}_a \longrightarrow \mathbb{R}$. The convolution product is defined by

$$(f * g)(x) = \sum_{r=a}^{x-1} f(r) g(x - \sigma(r) + a), \quad \text{for } x \in \mathbb{N}_a. \tag{12}$$

Note that by the empty sum convention $(f * g)(a) = 0$.

Lemma 1 (convolution theorem, see [10]). *Assume $f, g\colon \mathbb{N}_a \longrightarrow \mathbb{R}$. If both $\mathscr{L}_x f(x)$ and $\mathscr{L}_x g(x)$ exist, then the delta Laplace transform of the convolution product is given by*

$$\mathscr{L}_x\{(f * g)(x)\} = \mathscr{L}_x\{f(x)\}\mathscr{L}_x\{g(x)\} = \mathscr{L}_x\{(g * f)(x)\}. \tag{13}$$

Lemma 2 (see [10]). *Assume two functions $v, w\colon \mathbb{N}_a \longrightarrow \mathbb{R}$. Let $b_1, b_2 \in \mathbb{N}_a$ such that $b_1 < b_2$, and we have the summation by parts formula:*

$$\int_{b_1}^{b_2} v(\sigma(t))\Delta w(t)\Delta t = v(t)w(t)\Big|_{b_1}^{b_2} - \int_{b_1}^{b_2} w(t)\Delta v(t)\Delta t. \tag{14}$$

Definition 6. The generalized falling function is defined in term of gamma function by

$$t^{\underline{\mu}} = \frac{\Gamma(\sigma(t))}{\Gamma(\sigma(t) - \mu)}, \quad \text{for } t \in \mathbb{N}_a, \mu \in \mathbb{R}, \tag{15}$$

given that the expression in the above equation is justifiable. It is convenient to take $t^{\underline{\mu}} = 0$, whenever $t + 1$ is natural number and $t - \mu + 1$ is a zero or negative integer.

Definition 7. The discrete Taylor monomial based at $s = a$ is defined by

$$h_n(x,a) = \frac{(x-a)^{\underline{n}}}{n!}, \quad \text{for } x \in \mathbb{N}_a, \tag{16}$$

and the μ^{th} order Taylor monomial is defined by

$$h_\mu(x,a) = \frac{(x-a)^{\underline{\mu}}}{\Gamma(\mu+1)}, \quad \text{for } x \in \mathbb{N}_a. \tag{17}$$

Lemma 3 (see [10]). *ie following hold for delta Laplace of Taylor monomial:*

(i) $\mathscr{L}_x\{h_n(x,a)\}(p) = 1/p^{n+1}$, *for* $|p+1| > 1$, $n \in \mathbb{N}_0$
(ii) $\mathscr{L}_x\{(x-a)^{\underline{n}}\}(p) = n!/p^{n+1}$, *for* $|p+1| > 1$, $n \in \mathbb{N}_0$
(iii) $\mathscr{L}_x\left\{(x-a)^{\underline{\mu}}\right\}(p) = (\Gamma(\mu+1)(p+1)^{\mu})/p^{\mu+1}$, *for* $|p+1| > 1$, $\mu \geq 0$.

In the next definition, we consider only delta difference with increment 1, and do not bother the different operators that we will not be using here. One can find the details of Definition 8 in [1, 39].

Definition 8. Assume $u\colon \mathbb{N}_a \times \mathbb{N}_a \longrightarrow \mathbb{R}$, a function of two independent variables. Then, the partial difference of $u(x,y)$ with respect to x, regarding y as a constant is given by

$$\Delta_x[u(x,y)] = u(x+1,y) - u(x,y). \tag{18}$$

The partial difference of $u(x,y)$ with respect to y, regarding x as a constant, is given by

$$\Delta_y[u(x,y)] = u(x,y+1) - u(x,y). \tag{19}$$

Partial difference equation is an equation containing partial differences.

Note that $\Delta_{xy} = \Delta_y\Delta_x = \Delta_x\Delta_y = \Delta_{yx}$. Followed by the rule for integer order difference operator $\Delta^n = \Delta\Delta^{n-1}$, we adopt the symbol for partial differences as follows: $\Delta_x^n = \Delta_x\Delta_x^{n-1}$ and $\Delta_y^m = \Delta_y\Delta_y^{m-1}$.

3. The Delta Double Laplace Transforms

In this section, we give abstract definition of the delta double Laplace transform. For convenience, we simplify definition to series representation followed by Goodrich and Peterson [10] simplification of the delta Laplace transform. Also, condition for existence, uniqueness, and linearity of the delta double Laplace transform has been revealed.

Definition 9. Assume $f\colon \mathbb{N}_a \times \mathbb{N}_a \longrightarrow \mathbb{R}$. Then, the delta double Laplace transform of f based at (a,a) is the successive application of the delta Laplace transform on x and y in any order

$$\begin{aligned}
\mathscr{L}_2[f(x,y)](p,q) &= \mathscr{L}_x\left[\mathscr{L}_y\{f(x,y); y \longrightarrow q\}; x \longrightarrow p\right] \\
&= \mathscr{L}_y\left[\mathscr{L}_x\{f(x,y); x \longrightarrow p\}; y \longrightarrow q\right] \\
&= \mathscr{L}_y[\widetilde{F}(p,y); y \longrightarrow q] \\
&= \widetilde{\widetilde{F}}(p,q),
\end{aligned} \tag{20}$$

where $\mathscr{L}_x$ and $\mathscr{L}_y$ are the delta Laplace transforms (single) based at a with respect to x and y, respectively, and $\mathscr{L}_2$ is the delta double Laplace transform based at (a,a). The delta double Laplace transform of a function $f(x,y)$ of two variables x and y is defined in p-q plane provided the following double sum converges:

$$\mathscr{L}_2\{f\}(p,q) = \int_a^\infty \int_a^\infty e_{\ominus p}(\sigma(x),a) e_{\ominus q}(\sigma(y),a) f(x,y)\Delta x \Delta y, \tag{21}$$

for all complex numbers $p \neq -1$ and $q \neq -1$.

One can easily verify by using Lemma 4 that $\mathscr{L}_x\mathscr{L}_y = \mathscr{L}_y\mathscr{L}_x$. Later, in Theorem 2, we will prove that the double infinite series is absolutely convergent. It is well known that absolutely convergent series behave nicely and change in the order of summation $\sum_{k=0}^\infty \sum_{j=0}^\infty$ allowed. Therefore, we can operate in either way $\mathscr{L}_x\mathscr{L}_y = \mathscr{L}_y\mathscr{L}_x$.

Lemma 4. *Assume $f: \mathbb{N}_a \times \mathbb{N}_a \longrightarrow \mathbb{R}$. Then,*

$$\mathscr{L}_2[f(x,y)] = \sum_{k=0}^{\infty}\sum_{j=0}^{\infty}\frac{f(a+j,a+k)}{(p+1)^{j+1}(q+1)^{k+1}}, \tag{22}$$

for all complex numbers $p \neq -1$ and $q \neq -1$ such that the infinite series converges.

Proof. By using the definition of the delta double Laplace transform, consider the following:

$$\mathscr{L}_2\{f\}(p,q) = \int_a^{\infty}\int_a^{\infty} e_{\ominus p}(\sigma(x),a)e_{\ominus q}(\sigma(y),a)f(x,y)\Delta x\Delta y. \tag{23}$$

Now, by the definition of delta integral from discrete calculus, we obtain

$$\begin{aligned}
&= \sum_{y=a}^{\infty}\sum_{x=a}^{\infty} e_{\ominus p}(\sigma(x),a)e_{\ominus q}(\sigma(y),a)f(x,y)\\
&= \sum_{y=a}^{\infty}\sum_{x=a}^{\infty}(1\ominus p)^{\sigma(x)-a}(1\ominus q)^{\sigma(y)-a}f(x,y)\\
&= \sum_{y=a}^{\infty}\sum_{x=a}^{\infty}\frac{f(x,y)}{(p+1)^{x+1-a}(q+1)^{y+1-a}}.
\end{aligned} \tag{24}$$

In preceding steps, we use the definition of delta exponential function and the fact that $1\ominus p = 1/(1+p)$ and $1\ominus q = 1/(1+q)$, since p and q are regressive functions. In the following step, we use $x-a=j$ and $y-a=k$ to reindex the sums as follows:

$$\mathscr{L}_2[f(x,y)] = \sum_{k=0}^{\infty}\sum_{j=0}^{\infty}\frac{f(a+j,a+k)}{(p+1)^{j+1}(q+1)^{k+1}}. \tag{25}$$

□

Theorem 1. *Assume functions $f(x,y): \mathbb{N}_a \times \mathbb{N}_a \longrightarrow \mathbb{R}$, $g(x): \mathbb{N}_a \longrightarrow \mathbb{R}$, and $h(y): \mathbb{N}_a \longrightarrow \mathbb{R}$ such that the delta double Laplace transforms exist, then the following holds:*

(i) $\mathscr{L}_2\{g(x)\}(p,q) = (1/q)\mathscr{L}_x\{g(x)\}(p)$

(ii) $\mathscr{L}_2\{h(y)\}(p,q) = (1/p)\mathscr{L}_y\{h(y)\}(q)$

(iii) For $f(x,y) = g(x)h(y)$, $\mathscr{L}_2\{f(x,y)\}(p,q) = \mathscr{L}_x\{g(x)\}(p)\mathscr{L}_y\{h(y)\}(q)$

Proof. Under the assumption stated above and by Lemma 4,

(i) For $p \neq -1$ and $q \neq 0,-1$, we have

$$\begin{aligned}
\mathscr{L}_2\{g(x)\}(p,q) &= \sum_{k=0}^{\infty}\sum_{j=0}^{\infty}\frac{g(a+j)}{(p+1)^{j+1}(q+1)^{k+1}}\\
&= \sum_{k=0}^{\infty}\frac{1}{(q+1)^{k+1}}\sum_{j=0}^{\infty}\frac{g(a+j)}{(p+1)^{j+1}}\\
&= \frac{1}{q}\mathscr{L}_x\{g(x)\}(p).
\end{aligned} \tag{26}$$

(ii) The proof is similar to part (i).

(iii) For $p \neq -1$ and $q \neq -1$, we have

$$\begin{aligned}
\mathscr{L}_2\{f(x,y)\}(p,q) &= \sum_{k=0}^{\infty}\sum_{j=0}^{\infty}\frac{g(a+j)h(a+k)}{(p+1)^{j+1}(q+1)^{k+1}}\\
&= \sum_{j=0}^{\infty}\frac{g(a+j)}{(p+1)^{j+1}}\sum_{k=0}^{\infty}\frac{h(a+k)}{(q+1)^{k+1}}\\
&= \mathscr{L}_x\{g(x)\}(p)\mathscr{L}_y\{h(y)\}(q).
\end{aligned} \tag{27}$$

□

Example 3

(i) If $f(x,y)=1$ for $x,y\in\mathbb{N}_a$, then $\mathscr{L}_2\{1\} = 1/pq$,

(ii) If $f(x,y) = (x-a)^{\underline{m}}(y-a)^{\underline{n}}$ for $x,y\in\mathbb{N}_a$, then $\mathscr{L}_2\{(x-a)^{\underline{m}}(y-a)^{\underline{n}}\} = (m!n!)/(p^{m+1}q^{n+1})$.

(iii) By Lemma 4

$$\begin{aligned}
\mathscr{L}_2\{1\} &= \sum_{k=0}^{\infty}\sum_{j=0}^{\infty}\frac{1}{(p+1)^{j+1}(q+1)^{k+1}}\\
&= \sum_{k=0}^{\infty}\frac{1}{(q+1)^{k+1}}\sum_{j=0}^{\infty}\frac{1}{(p+1)^{j+1}}\\
&= \frac{1}{pq}, \quad \text{for } p,q\neq 0,-1.
\end{aligned} \tag{28}$$

(iv) By using Theorem 1 part (iii), we obtain

$$\mathscr{L}_2\left\{(x-a)^{\underline{m}}(y-a)^{\underline{n}}\right\} = \mathscr{L}_x\left\{(x-a)^{\underline{m}}\right\}\mathscr{L}_y\left\{(y-a)^{\underline{n}}\right\}. \tag{29}$$

By using Lemma 3,

$$\begin{aligned}
&= \frac{m!}{p^{m+1}}\mathscr{L}_y\left\{(y-a)^{\underline{n}}\right\}\\
&= \frac{m!}{p^{m+1}}\frac{n!}{q^{n+1}}.
\end{aligned} \tag{30}$$

If we choose either $m=0$ or $n=0$, then as a special case of the above

$$\begin{aligned}
\mathscr{L}_2\{(y-a)^{\underline{n}}\} &= \frac{n!}{pq^{n+1}}, \quad \text{for } p,q\neq 0,-1,\\
\mathscr{L}_2\{(x-a)^{\underline{m}}\} &= \frac{m!}{p^{m+1}q}, \quad \text{for } p,q\neq 0,-1.
\end{aligned} \tag{31}$$

Coon and Bernstein [20, 21] defined the double Laplace transforms and discussed convergence and existence for the continuous case. We discuss discrete analogue of the double Laplace transforms.

Definition 10. A function $f(x,y)\colon \mathbb{N}_a \times \mathbb{N}_a \longrightarrow \mathbb{R}$ is of exponential order $r_1, r_2 > 0$ with respect to x and y, respectively, if there exist a constant $A > 0$ and $m, n \in \mathbb{N}_0$ such that, for each $x \in \mathbb{N}_{a+m}$ and $y \in \mathbb{N}_{a+n}$, the inequality $|f(x,y)| \le A r_1^x r_2^y$ holds, where $A = \max\{A_1, A_2\}$ for $|f(x,a)| \le A_1 r_1^x$ and $|f(a,y)| \le A_2 r_2^y$.

Theorem 2. *If a function $f(x,y)\colon \mathbb{N}_a \times \mathbb{N}_a \longrightarrow \mathbb{R}$ is of exponential order $r_1, r_2 > 0$, then the delta double Laplace transform $\mathscr{L}_2\{f\}(p,q)$ converges absolutely for p and q provided $|p+1| > r_1$, $|q+1| > r_2$.*

Proof. Assume $f(x,y)\colon \mathbb{N}_a \times \mathbb{N}_a \longrightarrow \mathbb{R}$ is of exponential order $r_1, r_2 > 0$. Then, there exists a constant $A > 0$ and $m, n \in \mathbb{N}_0$ such that, for each $x \in \mathbb{N}_{a+m}$ and $y \in \mathbb{N}_{a+n}$, $|f(x,y)| \le A r_1^x r_2^y$. Thus, for $|p+1| > r_1$ and $|q+1| > r_2$, we consider the following:

$$\begin{aligned}
&\sum_{k=n}^{\infty}\sum_{j=m}^{\infty}\left|\frac{f(a+j,a+k)}{(p+1)^{j+1}(q+1)^{k+1}}\right| \\
&\quad\le \sum_{k=n}^{\infty}\sum_{j=m}^{\infty}\frac{A r_1^{j+a} r_2^{k+a}}{|p+1|^{j+1}|q+1|^{k+1}} \\
&\quad= \frac{A r_1^a r_2^a}{|p+1||q+1|}\sum_{k=n}^{\infty}\sum_{j=m}^{\infty}\left(\frac{r_1}{|p+1|}\right)^j\left(\frac{r_2}{|q+1|}\right)^k \\
&\quad= \frac{A r_1^a r_2^a}{|p+1||q+1|}\,\frac{(r_1/|p+1|)^m}{(1-(r_1/|p+1|))}\,\frac{(r_2/|q+1|)^n}{(1-(r_2/|q+1|))} \\
&\quad= \frac{A r_1^{a+m} r_2^{a+n}}{|p+1|^m|q+1|^n\left[(|p+1|-r_1)(|q+1|-r_2)\right]} \\
&\quad< \infty.
\end{aligned} \tag{32}$$

Since $|p+1| > r_1$ and $|q+1| > r_2$, therefore $|p+1| - r_1 > 0$ and $|q+1| - r_2 > 0$. Hence, the delta double Laplace transform of f converges absolutely.

Theorem 2 ensures the existence of the delta double Laplace transform. In general, the converse does not hold. We should consider functions f of some exponential order $r > 0$, to ensure the delta double Laplace transform of f which does converge somewhere in the complex plane outside the both closed balls of radius r_1, r_2, centered at -1, that is, we can choose $r = max\{r_1, r_2\}$ for $|p+1| > r_1$ and $|q+1| > r_2$. □

Theorem 3. *Suppose $f, g\colon \mathbb{N}_a \times \mathbb{N}_a \longrightarrow \mathbb{R}$. If the delta double Laplace transform of f, g converges for $|p+1| > r_1$ and $|q+1| > r_2$, where $r_1, r_2 > 0$, and let c_1, $c_2 \in \mathbb{C}$, then the delta double Laplace transform of $c_1 f + c_2 g$ converges for $|p+1| > r_1$, $|q+1| > r_2$, and $\mathscr{L}_2\{c_1 f + c_2 g\}(p,q) = c_1\mathscr{L}_2\{f\}(p,q) + c_2\mathscr{L}_2\{g\}(p,q)$, converges for $|p+1| > r_1$ and $|q+1| > r_2$.*

Proof. Since $f, g\colon \mathbb{N}_a \times \mathbb{N}_a \longrightarrow \mathbb{R}$ and the delta double Laplace transform of f, g converges for $|p+1| > r_1$ and $|q+1| > r_2$, where $r_1, r_2 > 0$. We have that, for $|p+1| > r_1$ and $|q+1| > r_2$,

$$\begin{aligned}
&c_1\mathscr{L}_2\{f\}(p,q) + c_2\mathscr{L}_2\{g\}(p,q) \\
&\quad= c_1\sum_{k=0}^{\infty}\sum_{j=0}^{\infty}\frac{f(a+j,a+k)}{(p+1)^{j+1}(q+1)^{k+1}} \\
&\qquad+ c_2\sum_{k=0}^{\infty}\sum_{j=0}^{\infty}\frac{g(a+j,a+k)}{(p+1)^{j+1}(q+1)^{k+1}} \\
&\quad= \sum_{k=0}^{\infty}\sum_{j=0}^{\infty}\frac{(c_1 f + c_2 g)(a+j,a+k)}{(p+1)^{j+1}(q+1)^{k+1}} \\
&\quad= \mathscr{L}_2\{c_1 f + c_2 g\}(p,q).
\end{aligned} \tag{33}$$

Theorem 3 exposed the linearity property of the delta double Laplace transform, and Theorem 4 revealed the uniqueness.

Theorem 4. *Suppose $f, g\colon \mathbb{N}_a \times \mathbb{N}_a \longrightarrow \mathbb{R}$ and $r_1 > 0$, $r_2 > 0$. If $\mathscr{L}_2\{f\}(p,q) = \mathscr{L}_2\{g\}(p,q)$, provided $|p+1| > r_1$, $|q+1| > r_2$, and $p, q \ne 0, -1$, then $f(x,y) = g(x,y)$ for all $x, y \in \mathbb{N}_a$.*

Proof. By hypothesis, we have

$$\mathscr{L}_2\{f\}(p,q) = \mathscr{L}_2\{g\}(p,q), \tag{34}$$

for $|p+1| > r_1$ and $|q+1| > r_2$. This implies that

$$\sum_{k=0}^{\infty}\sum_{j=0}^{\infty}\frac{f(a+j,a+k)}{(p+1)^{j+1}(q+1)^{k+1}} = \sum_{k=0}^{\infty}\sum_{j=0}^{\infty}\frac{g(a+j,a+k)}{(p+1)^{j+1}(q+1)^{k+1}}, \tag{35}$$

for $|p+1| > r_1$ and $|q+1| > r_2$. Since, by Theorem 2, the double infinite series is absolute convergent, therefore comparison of both sides implies that

$$f(a+j,a+k) = g(a+j,a+k), \quad \text{for all } j,k \in \mathbb{N}_0. \tag{36}$$

For each fix j and for all $y \in \mathbb{N}_a$, this implies that

$$f(a+j,y) = g(a+j,y). \tag{37}$$

For each fix k, we obtain

$$f(x,y) = g(x,y), \quad \text{for all } x, y \in \mathbb{N}_a. \tag{38}$$

□

4. Basic Properties of the Delta Double Laplace Transform

In this section, following Bohner et al. [30], we prove some properties of the delta double Laplace transform. We also define double convolution product of discrete functions followed by Goodrich and Peterson [10] convolution product (single) of discrete functions. We present, the delta double Laplace transform of double convolution product for later use to solve difference equations.

Theorem 5. *Assume* $f: \mathbb{N}_a \times \mathbb{N}_a \longrightarrow \mathbb{R}$ *and* $\mathscr{L}_2[f(x,y)]$ *exists. If* $\mathscr{L}_2[f(x,y)] = \tilde{\tilde{F}}(p,q)$, *then*

$$\mathscr{L}_2[f(x-\alpha, y-\beta)H(x-\alpha, y-\beta)] = e_{\ominus p}(\alpha,0)e_{\ominus q}(\beta,0)\left[\tilde{\tilde{F}}(p,q) - \sum_{s=0}^{c-a-1}\sum_{\tau=0}^{c-a-1}\frac{f(a+\tau,a+s)}{(p+1)^{\tau+1}(q+1)^{s+1}}\right], \tag{39}$$

where $H(x,y)$ *is the Heaviside unit step function defined by*

$$H(x-\alpha, y-\beta) = \begin{cases} 0, & \text{if } x-\alpha, y-\beta \in \mathbb{N}_a^{c-1}, \\ 1, & \text{if } x-\alpha, y-\beta \in \mathbb{N}_c. \end{cases} \tag{40}$$

Proof. We have, by Lemma 4,

$$\mathscr{L}_2[f(x-\alpha, y-\beta)H(x-\alpha, y-\beta)] = \sum_{k=0}^{\infty}\sum_{j=0}^{\infty}\frac{f(a-\alpha+j, a-\beta+k)H(a-\alpha+j, a-\beta+k)}{(p+1)^{j+1}(q+1)^{k+1}} = \sum_{k=\beta+c-a}^{\infty}\sum_{j=\alpha+c-a}^{\infty}\frac{f(a-\alpha+j, a-\beta+k)}{(p+1)^{j+1}(q+1)^{k+1}}. \tag{41}$$

Reindex by $j-\alpha = \tau$ and $k-\beta = s$,

$$= \sum_{s=c-a}^{\infty}\sum_{\tau=c-a}^{\infty}\frac{f(a+\tau,a+s)}{(p+1)^{\alpha+\tau+1}(q+1)^{\beta+s+1}} = \frac{1}{(p+1)^{\alpha}(q+1)^{\beta}}\left[\sum_{s=0}^{\infty}\sum_{\tau=0}^{\infty}\frac{f(a+\tau,a+s)}{(p+1)^{\tau+1}(q+1)^{s+1}} - \sum_{s=0}^{c-a-1}\sum_{\tau=0}^{c-a-1}\frac{f(a+\tau,a+s)}{(p+1)^{\tau+1}(q+1)^{s+1}}\right], \tag{42}$$

$$\mathscr{L}_2[f(x-\alpha, y-\beta)H(x-\alpha, y-\beta)] = e_{\ominus p}(\alpha,0)e_{\ominus q}(\beta,0)\left[\tilde{\tilde{F}}(p,q) - \sum_{s=0}^{c-a-1}\sum_{\tau=0}^{c-a-1}\frac{f(a+\tau,a+s)}{(p+1)^{\tau+1}(q+1)^{s+1}}\right].$$

In the last step, we use Lemma 4 with the fact $e_{\ominus p}(\alpha,0) = 1/(p+1)^{\alpha}$ and $e_{\ominus q}(\beta,0) = 1/(q+1)^{\beta}$.

Theorem 5 gives different results from its continuous counterpart stated in [23]. We state the useful shifting Theorem 6 for discrete setting. □

Theorem 6. *Assume* $f: \mathbb{N}_a \times \mathbb{N}_a \longrightarrow \mathbb{R}$ *and* $\mathscr{L}_2[f(x,y)]$ *exist. If* $\mathscr{L}_2[f(x,y)] = \tilde{\tilde{F}}(p,q)$, *then*

(i) $\mathscr{L}_2[f(x-(c-a), y-(c-a))H(x,y)] = 1/[(p+1)(q+1)]^{c-a}\tilde{\tilde{F}}(p,q)$.

(ii) $\mathscr{L}_2[f(x+(c-a), y+(c-a))] = [(p+1)(q+1)]^{c-a}[\tilde{\tilde{F}}(p,q) - \sum_{s=0}^{c-a-1}\sum_{\tau=0}^{c-a-1} f(a+\tau,a+s)/((p+1)^{\tau+1}(q+1)^{s+1})]$,

where $H(x,y)$ *is the Heaviside unit step function defined by*

$$H(x,y) = \begin{cases} 0, & \text{if } x,y \in \mathbb{N}_a^{c-1}, \\ 1, & \text{if } x,y \in \mathbb{N}_c. \end{cases} \tag{43}$$

Proof

(i) We have by Lemma 4, $\mathscr{L}_2[f(x-(c-a), y-(c-a))H(x,y)]$

$$= \sum_{k=0}^{\infty}\sum_{j=0}^{\infty}\frac{f(j+2a-c, k+2a-c)H(a+j,a+k)}{(p+1)^{j+1}(q+1)^{k+1}} = \sum_{k=c-a}^{\infty}\sum_{j=c-a}^{\infty}\frac{f(j+2a-c, k+2a-c)}{(p+1)^{j+1}(q+1)^{k+1}}. \tag{44}$$

Reindex by $\tau = j+a-c$ and $s = k+a-c$,

$$= \sum_{s=0}^{\infty}\sum_{\tau=0}^{\infty}\frac{f(a+\tau,a+s)}{(p+1)^{\tau+c-a+1}(q+1)^{s+c-a+1}} = \frac{1}{[(p+1)(q+1)]^{c-a}}\sum_{s=0}^{\infty}\sum_{\tau=0}^{\infty}\frac{f(a+\tau,a+s)}{(p+1)^{\tau+1}(q+1)^{s+1}} = \frac{1}{[(p+1)(q+1)]^{c-a}}\tilde{\tilde{F}}(p,q). \tag{45}$$

(ii) By use of Lemma 4 and reindex by $\tau = j+c-a$ and $s = k+c-a$,

$$\mathscr{L}_2[f(x+(c-a), y+(c-a))] = \sum_{k=0}^{\infty}\sum_{j=0}^{\infty}\frac{f(j+c,k+c)}{(p+1)^{j+1}(q+1)^{k+1}} = \sum_{s=c-a}^{\infty}\sum_{\tau=c-a}^{\infty}\frac{f(a+\tau,a+s)}{(p+1)^{\tau+a-c+1}(q+1)^{s+a-c+1}} = [(p+1)(q+1)]^{c-a}\sum_{s=c-a}^{\infty}\sum_{\tau=c-a}^{\infty}\frac{f(a+\tau,a+s)}{(p+1)^{\tau+1}(q+1)^{s+1}} = [(p+1)(q+1)]^{c-a}\left[\tilde{\tilde{F}}(p,q) - \sum_{s=0}^{c-a-1}\sum_{\tau=0}^{c-a-1}\frac{f(a+\tau,a+s)}{(p+1)^{\tau+1}(q+1)^{s+1}}\right]. \tag{46}$$

□

Theorem 7. *Assume $f(x,y)$ is periodic with $T_1, T_2 \in \mathbb{N}_1$ and $\mathscr{L}_2[f(x,y)]$ exist; then,*

$$\mathscr{L}_2[f(x,y)] = \frac{1}{\left[1 - e_{\ominus p}(T_1,0)e_{\ominus q}(T_2,0)\right]} \sum_{j=0}^{T_1-1}\sum_{k=0}^{T_2-1} \frac{f(a+j,a+k)}{(p+1)^{j+1}(q+1)^{k+1}}. \tag{47}$$

Proof. Under the assumption, we have, by Lemma 4,

$$\begin{aligned}\mathscr{L}_2[f(x,y)] &= \sum_{k=0}^{\infty}\sum_{j=0}^{\infty} \frac{f(a+j,a+k)}{(p+1)^{j+1}(q+1)^{k+1}} \\ &= \sum_{k=0}^{T_2-1}\sum_{j=0}^{T_1-1} \frac{f(a+j,a+k)}{(p+1)^{j+1}(q+1)^{k+1}} + \sum_{k=T_2}^{\infty}\sum_{j=T_1}^{\infty} \frac{f(a+j,a+k)}{(p+1)^{j+1}(q+1)^{k+1}} \\ &= \sum_{k=0}^{T_2-1}\sum_{j=0}^{T_1-1} \frac{f(a+j,a+k)}{(p+1)^{j+1}(q+1)^{k+1}} + \sum_{v=0}^{\infty}\sum_{u=0}^{\infty} \frac{f(a+u+T_1,a+v+T_2)}{(p+1)^{T_1+u+1}(q+1)^{T_2+v+1}}.\end{aligned} \tag{48}$$

In the last step, we used $j = T_1 + u$ and $k = T_2 + v$ to reindex second double summation. In second double summation, periodicity of f implies that

$$\begin{aligned}\mathscr{L}_2[f(x,y)] &= \sum_{k=0}^{T_2-1}\sum_{j=0}^{T_1-1} \frac{f(a+j,a+k)}{(p+1)^{j+1}(q+1)^{k+1}} + \sum_{v=0}^{\infty}\sum_{u=0}^{\infty} \frac{f(a+u,a+v)}{(p+1)^{T_1+u+1}(q+1)^{T_2+v+1}} \\ &= \sum_{k=0}^{T_2-1}\sum_{j=0}^{T_1-1} \frac{f(a+j,a+k)}{(p+1)^{j+1}(q+1)^{k+1}} + \left[\frac{1}{(p+1)}\right]^{T_1}\left[\frac{1}{(q+1)}\right]^{T_2} \sum_{v=0}^{\infty}\sum_{u=0}^{\infty} \frac{f(a+u,a+v)}{(p+1)^{u+1}(q+1)^{v+1}} \\ &= \sum_{k=0}^{T_2-1}\sum_{j=0}^{T_1-1} \frac{f(a+j,a+k)}{(p+1)^{j+1}(q+1)^{k+1}} + e_{\ominus p}(T_1,0)e_{\ominus q}(T_2,0) \sum_{v=0}^{\infty}\sum_{u=0}^{\infty} \frac{f(a+u,a+v)}{(p+1)^{u+1}(q+1)^{v+1}} \\ &= \sum_{k=0}^{T_2-1}\sum_{j=0}^{T_1-1} \frac{f(a+j,a+k)}{(p+1)^{j+1}(q+1)^{k+1}} + e_{\ominus p}(T_1,0)e_{\ominus q}(T_2,0)\mathscr{L}_2[f(x,y)] \\ &= \frac{1}{\left[1 - e_{\ominus p}(T_1,0)e_{\ominus q}(T_2,0)\right]} \sum_{k=0}^{T_2-1}\sum_{j=0}^{T_1-1} \frac{f(a+j,a+k)}{(p+1)^{j+1}(q+1)^{k+1}}.\end{aligned} \tag{49}$$

□

Definition 11. Assume $f, g \colon \mathbb{N}_a \times \mathbb{N}_a \longrightarrow \mathbb{R}$. The double convolution product is defined by

$$\begin{aligned}(f ** g)(x,y) = \sum_{r=a}^{x-1}\sum_{s=a}^{y-1} f(r,s) g(x - \sigma(r) + a, \\ y - \sigma(s) + a) \quad \text{for } x, y \in \mathbb{N}_a.\end{aligned} \tag{50}$$

Note, by empty sum convention, $(f ** g)(a,a) = 0$.

Lemma 5. *Assume $f, g \colon \mathbb{N}_a \times \mathbb{N}_a \longrightarrow \mathbb{R}$. The double convolution product is commutative:*

$$(f ** g)(x,y) = (g ** f)(x,y) \quad \text{for } x, y \in \mathbb{N}_a. \tag{51}$$

Proof. By Definition 11 and the change of variables $x - r - 1 + a = u$ and $y - s - 1 + a = v$, we have

$$(g ** f)(x,y) = \sum_{r=a}^{x-1}\sum_{s=a}^{y-1} g(r,s) f(x-\sigma(r)+a, y-\sigma(s)+a) \quad \text{for } x,y \in \mathbb{N}_a,$$
$$= \sum_{u=a}^{x-1}\sum_{v=a}^{y-1} g(x-\sigma(u)+a, y-\sigma(v)+a) f(u,v),$$
$$= (f ** g)(x,y), \quad \text{for } x,y \in \mathbb{N}_a. \tag{52}$$

□

Theorem 8 (convolution theorem). *Assume f, g: $\mathbb{N}_a \times \mathbb{N}_a \longrightarrow \mathbb{R}$. If both $\mathscr{L}_2[f(x,y)]$ and $\mathscr{L}_2[g(x,y)]$ exist, then the delta double Laplace transform of double convolution product is*

$$\mathscr{L}_2\{(f ** g)(x,y)\} = \mathscr{L}_2\{f(x,y)\}\mathscr{L}_2\{g(x,y)\}. \tag{53}$$

Proof. Under given assumption, we have, by Lemma 4 and the fact $(f ** g)(a,a) = 0$,

$$\mathscr{L}_2\{(f ** g)(x,y)\} = \sum_{k=0}^{\infty}\sum_{j=0}^{\infty} \frac{(f ** g)(a+j, a+k)}{(p+1)^{j+1}(q+1)^{k+1}}$$
$$= \sum_{k=1}^{\infty}\sum_{j=1}^{\infty} \frac{(f ** g)(a+j, a+k)}{(p+1)^{j+1}(q+1)^{k+1}}$$
$$= \sum_{k=1}^{\infty}\sum_{j=1}^{\infty} \frac{1}{(p+1)^{j+1}(q+1)^{k+1}}$$
$$\sum_{r=a}^{a+k-1}\sum_{s=a}^{a+j-1} f(r,s) g(a+j-\sigma(r)+a, a+k-\sigma(s)+a). \tag{54}$$

In the last step, we used Definition 11; next, making the change of variables $r \longrightarrow a+r$ and $s \longrightarrow a+s$ gives us that

$$= \sum_{k=1}^{\infty}\sum_{j=1}^{\infty}\sum_{r=0}^{k-1}\sum_{s=0}^{j-1} \frac{f(a+r,a+s) g(a+j-\sigma(r), a+k-\sigma(s))}{(p+1)^{j+1}(q+1)^{k+1}}$$
$$= \sum_{k=1}^{\infty}\sum_{r=0}^{k-1}\sum_{j=1}^{\infty}\sum_{s=0}^{j-1} \frac{f(a+r,a+s) g(a+j-\sigma(r), a+k-\sigma(s))}{(p+1)^{j+1}(q+1)^{k+1}}$$
$$= \sum_{r=0}^{\infty}\sum_{k=1}^{\infty}\sum_{s=0}^{\infty}\sum_{j=1}^{\infty} \frac{f(a+r,a+s) g(a+j-\sigma(r), a+k-\sigma(s))}{(p+1)^{j+1}(q+1)^{k+1}}$$
$$= \sum_{r=0}^{\infty}\sum_{\tau_2=0}^{\infty}\sum_{s=0}^{\infty}\sum_{\tau_1=0}^{\infty} \frac{f(a+r,a+s) g(a+\tau_1, a+\tau_2)}{(p+1)^{\tau_1+r+2}(q+1)^{\tau_2+s+2}}$$
$$= \sum_{s=0}^{\infty}\sum_{r=0}^{\infty} \frac{f(a+r,a+s)}{(p+1)^{r+1}(q+1)^{s+1}} \sum_{\tau_2=0}^{\infty}\sum_{\tau_1=0}^{\infty} \frac{g(a+\tau_1, a+\tau_2)}{(p+1)^{\tau_1+1}(q+1)^{\tau_2+1}}$$
$$= \mathscr{L}_2\{f(x,y)\}\mathscr{L}_2\{g(x,y)\}. \tag{55}$$

In the previous steps, we interchanged the order of first pairs and second pairs of summation and change variables $j-r-1 = \tau_1$ and $k-s-1 = \tau_2$. □

Corollary 1. *Assume f, g: $\mathbb{N}_a \times \mathbb{N}_a \longrightarrow \mathbb{R}$. If $f(x,y) = u_1(x)v_1(y)$ and $g(x,y) = u_2(x)v_2(y)$ and the delta Laplace transform exists, then*

$$\mathscr{L}_2\{(f ** g)(x,y)\} = \mathscr{L}_x\{(u_1 * u_2)(x)\}\mathscr{L}_y\{(v_1 * v_2)(y)\}, \tag{56}$$

where the product on right- and left-hand sides is given by Definitions 5 and 11, respectively.

Proof. By double convolution theorem, we have

$$\mathscr{L}_2\{(f ** g)(x,y)\} = \mathscr{L}_2\{f(x,y)\}\mathscr{L}_2\{g(x,y)\}. \tag{57}$$

Since $\mathscr{L}_2[f(x,y)] = \mathscr{L}_2[u_1(x)v_1(y)] = \mathscr{L}_x[u_1(x)]\mathscr{L}_y[v_1(y)]$ and $\mathscr{L}_2[g(x,y)] = \mathscr{L}_2[u_2(x)v_2(y)] = \mathscr{L}_x[u_2(x)]\mathscr{L}_y[v_2(y)]$,

$$\begin{aligned} &\text{consider } \mathscr{L}_2\{(f ** g)(x,y)\} \\ &= \mathscr{L}_x[u_1(x)]\mathscr{L}_y[v_1(y)]\mathscr{L}_x[u_2(x)]\mathscr{L}_y[v_2(y)] \\ &= \mathscr{L}_x[u_1(x)]\mathscr{L}_x[u_2(x)]\mathscr{L}_y[v_1(y)]\mathscr{L}_y[v_2(y)] \\ &= \mathscr{L}_x\{(u_1 * u_2)(x)\}\mathscr{L}_y\{(v_1 * v_2)(y)\}. \end{aligned} \tag{58}$$

The last step is followed from single convolution Lemma 1. □

5. The Delta Double Laplace Transforms of Partial Differences

In this section, we examine the action of the delta double Laplace transforms on first order partial differences. The results developed for first order partial differences are further used to establish properties of the delta double Laplace transforms of generalized order partial difference, similar to that appeared in [40] for fractional order partial derivatives. We usually consider functions $u(x,y)$: $\mathbb{N}_a \times \mathbb{N}_a \longrightarrow \mathbb{R}$, of exponential order $r_1, r_2 > 0$ with respect to x and y, respectively, ensuring that delta Laplace and the delta double Laplace transforms of $u(x,y)$ and its partial differences does exist.

Lemma 6. *Assume $u(x,y)$: $\mathbb{N}_a \times \mathbb{N}_a \longrightarrow \mathbb{R}$, such that the delta Laplace transforms exist for constants $p \neq -1$ and $q \neq -1$. Then,*

$$\mathscr{L}_x\Delta_x[u(x,y)] = p\mathscr{L}_x\{u(x,y)\} - u(a,y), \tag{59}$$

$$\mathscr{L}_y\Delta_y[u(x,y)] = q\mathscr{L}_y\{u(x,y)\} - u(x,a), \tag{60}$$

$$\mathscr{L}_x\Delta_y[u(x,y)] = \Delta_y\mathscr{L}_x u(x,y), \tag{61}$$

$$\mathscr{L}_y\Delta_x[u(x,y)] = \Delta_x\mathscr{L}_y u(x,y). \tag{62}$$

Proof. By definition of the delta Laplace transforms on x,

$$\mathscr{L}_x\Delta_x[u(x,y)] = \int_a^{\infty} e_{\ominus p}(\sigma(x),a)\Delta_x u(x,y)\Delta x. \quad (63)$$

Apply summation by parts (Lemma 2) on x, and using the fact $\Delta_x[e_{\ominus p}(\sigma(x),a)] = \ominus p e_{\ominus p}(x,a)$, we have that

$$= e_{\ominus p}(x,a)u(x,y)|_{x=a}^{\infty} - \int_a^{\infty} u(x,y)\left[\ominus p e_{\ominus p}(x,a)\right]\Delta x. \quad (64)$$

Use the fact $e_{\ominus p}(x,a) = 1/(p+1)^{x-a}$ and $\ominus p = -p/(p+1)$,

$$= \frac{1}{(p+1)^{x-a}}u(x,y)|_{x=a}^{\infty} - \int_a^{\infty} u(x,y)\left(\frac{-p}{(p+1)}\right)e_{\ominus p}(x,a)\Delta x. \quad (65)$$

Since $(p+1)e_{\ominus p}(\sigma(x),a) = e_{\ominus p}(x,a)$,

$$\begin{aligned} &= [0 - u(a,y)] + p\int_a^{\infty} u(x,y)e_{\ominus p}(\sigma(x),a)\Delta x \\ &= -u(a,y) + p\mathscr{L}_x\{u(x,y)\}, \\ \mathscr{L}_x\Delta_x[u(x,y)] &= p\mathscr{L}_x\{u(x,y)\} - u(a,y). \end{aligned} \quad (66)$$

Let $\mathscr{L}_x u(x,y) = \tilde{u}(p,y)$. Consider the left-hand side of equation (61) and use the definition of delta difference:

$$\mathscr{L}_x\Delta_y[u(x,y)] = \mathscr{L}_x[u(x,y+1) - u(x,y)]. \quad (67)$$

By using linearity property of the delta Laplace transforms, we obtain

$$\begin{aligned} &= \mathscr{L}_x u(x,y+1) - \mathscr{L}_x u(x,y) \\ &= \tilde{u}(p,y+1) - \tilde{u}(p,y). \end{aligned} \quad (68)$$

Now, consider the right-hand side of equation (61) and use $\mathscr{L}_x u(x,y) = \tilde{u}(p,y)$:

$$\Delta_y\mathscr{L}_x[u(x,y)] = \Delta_y\tilde{u}(p,y). \quad (69)$$

By using the definition of delta difference, we obtain

$$= \tilde{u}(p,y+1) - \tilde{u}(p,y). \quad (70)$$

Equality holds in equation (61) from equations (68) and (70). Proof of equations (60) and (62) is similar to proof of equations (59) and (61), respectively. □

Theorem 9. *Assume* $u(x,y)\colon \mathbb{N}_a \times \mathbb{N}_a \longrightarrow \mathbb{R}$, *such that the delta double Laplace transforms exist for constants* $p \neq -1$ *and* $q \neq -1$. *Then,*

(i) $\mathscr{L}_2\Delta_x[u(x,y)] = p\mathscr{L}_2\{u(x,y)\} - \mathscr{L}_y\{u(a,y)\}$

(ii) $\mathscr{L}_2\Delta_y[u(x,y)] = q\mathscr{L}_2\{u(x,y)\} - \mathscr{L}_x\{u(x,a)\}$

Proof. Since, by definition, the delta double Laplace transforms is the successive application of the delta Laplace transforms on x and y in any order, therefore $\mathscr{L}_2 = \mathscr{L}_x\mathscr{L}_y = \mathscr{L}_y\mathscr{L}_x$.

(i) Consider

$$\mathscr{L}_2\Delta_x[u(x,y)] = \mathscr{L}_y[\mathscr{L}_x\Delta_x u(x,y)]. \quad (71)$$

By using equation (59) of Lemma 6, we obtain

$$= \mathscr{L}_y[p\mathscr{L}_x\{u(x,y)\} - u(a,y)]. \quad (72)$$

Use linearity property of the delta Laplace transforms for $\mathscr{L}_y$,

$$= p\mathscr{L}_2\{u(x,y)\} - \mathscr{L}_y[u(a,y)]. \quad (73)$$

(ii) The proof is similar to part (i).

Note that, for constant a, $\Delta_x\{u(a,y)\} = u(a,y) - u(a,y) = 0$. We adopt the following symbols in our result which are nonzero, in general, $\Delta_x\{u(a,y)\} = \Delta_x\{u(x,y)\}|_{x=a}$ and $\Delta_y\{u(x,a)\} = \Delta_y\{u(x,y)\}|_{y=a}$, that is, first we take difference and then evaluate at a. □

Lemma 7. *Assume* $u(x,y)\colon \mathbb{N}_a \times \mathbb{N}_a \longrightarrow \mathbb{R}$, *such that the delta Laplace transforms exist for constants* $p \neq -1$ *and* $q \neq -1$. *Then,*

(i) $\mathscr{L}_x\Delta_x^n[u(x,y)] = p^n\mathscr{L}_x\{u(x,y)\} - \sum_{k=0}^{n-1} p^{n-1-k}\Delta_x^k u(a,y)$

(ii) $\mathscr{L}_y\Delta_y^m[u(x,y)] = q^m\mathscr{L}_y\{u(x,y)\} - \sum_{j=0}^{m-1} q^{m-1-j}\Delta_y^j u(x,a)$

(iii) $\mathscr{L}_x\Delta_{xy}^{nm}[u(x,y)] = p^n\mathscr{L}_x\Delta_y^m\{u(x,y)\} - \sum_{k=0}^{n-1} p^{n-1-k}\Delta_x^k\Delta_y^m u(a,y)$

(iv) $\mathscr{L}_y\Delta_{xy}^{nm}[u(x,y)] = q^m\mathscr{L}_y\Delta_x^n\{u(x,y)\} - \sum_{j=0}^{m-1} q^{m-1-j}\Delta_x^n\Delta_y^j u(x,a)$

Proof

(i) We prove this part by induction on n, and result for $n=1$ has been proved in Lemma 6. Assume the result is true for $n \geq 1$:

$$\mathscr{L}_x\Delta_x^n[u(x,y)] = p^n\mathscr{L}_x\{u(x,y)\} - \sum_{k=0}^{n-1} p^{n-1-k}\Delta_x^k u(a,y). \quad (74)$$

We will try to establish result for $n+1$, beginning with the following:

$$\mathscr{L}_x\Delta_x^{n+1}[u(x,y)] = \mathscr{L}_x[\Delta_x\Delta_x^n u(x,y)]. \quad (75)$$

Let $w(x,y) = \Delta_x^n[u(x,y)]$, and we have that

$$= \mathscr{L}_x[\Delta_x w(x,y)]. \quad (76)$$

Again using equation (59) of Lemma 6,

$$\begin{aligned} &= p\mathscr{L}_x\{w(x,y)\} - w(a,y)] \\ &= p\mathscr{L}_x\{\Delta_x^n[u(x,y)]\} - \Delta_x^n[u(a,y)]. \end{aligned} \quad (77)$$

By using assumption for n,

$$\begin{aligned} &= p\left[p^n\mathscr{L}_x\{u(x,y)\} - \sum_{k=0}^{n-1} p^{n-1-k}\Delta_x^k u(a,y)\right] - \Delta_x^n[u(a,y)] \\ &= p^{n+1}\mathscr{L}_x\{u(x,y)\} - \sum_{k=0}^{n-1} p^{n-k}\Delta_x^k u(a,y) - p^{n-n}\Delta_x^n[u(a,y)] \\ \mathscr{L}_x\Delta_x^{n+1}[u(x,y)] &= p^{n+1}\mathscr{L}_x\{u(x,y)\} - \sum_{k=0}^{n} p^{n-k}\Delta_x^k u(a,y). \end{aligned} \quad (78)$$

The result holds for $n+1$, whenever it holds for n. Hence, by induction, result in part (i) holds.

(ii)

$$\mathscr{L}_x\Delta_{xy}^{nm}[u(x,y)] = \mathscr{L}_x\Delta_x^n\left[\Delta_y^m u(x,y)\right]. \tag{79}$$

Let $v(x,y) = \Delta_y^m u(x,y)$, and use part (i) of the same Lemma:

$$\begin{aligned}
&= \mathscr{L}_x\Delta_x^n[v(x,y)] \\
&= p^n\mathscr{L}_x\{v(x,y)\} - \sum_{k=0}^{n-1} p^{n-1-k}\Delta_x^k v(a,y) \\
&= p^n\mathscr{L}_x\Delta_y^m\{u(x,y)\} - \sum_{k=0}^{n-1} p^{n-1-k}\Delta_x^k\Delta_y^m u(a,y).
\end{aligned} \tag{80}$$

Proof of (ii) and (iv) is similar as proof of part (i) and (iii), respectively. □

Theorem 10. *Assume $u(x,y)\colon \mathbb{N}_a\times\mathbb{N}_a \longrightarrow \mathbb{R}$, such that the delta double Laplace transforms exist for constants $p \neq -1$ and $q \neq -1$. Then,*

(i) $\mathscr{L}_2\Delta_x^n[u(x,y)] = p^n\mathscr{L}_2\{u(x,y)\} - \sum_{k=0}^{n-1}p^{n-1-k}\mathscr{L}_y\times\left\{\Delta_x^k u(a,y)\right\}$

(ii) $\mathscr{L}_2\Delta_y^m[u(x,y)] = q^m\mathscr{L}_2\{u(x,y)\} - \sum_{j=0}^{m-1}q^{m-1-j}\mathscr{L}_x\times\left\{\Delta_y^j u(x,a)\right\}$

(iii) $\mathscr{L}_2\Delta_{xy}^{nm}[u(x,y)] = p^nq^m[\mathscr{L}_2\{u(x,y)\} - \sum_{k=0}^{n-1}p^{-1-k}\mathscr{L}_y\left\{\Delta_x^k u(a,y)\right\} - \sum_{j=0}^{m-1}q^{-1-j}\mathscr{L}_x\left\{\Delta_y^j u(x,a)\right\} + \sum_{j=0}^{m-1}\sum_{k=0}^{n-1}p^{-1-k}q^{-1-j}\left\{\Delta_{xy}^{kj}u(a,a)\right\}]$

Proof. Since by definition, the delta double Laplace transforms is the successive application of the delta Laplace transforms on x and y in any order; therefore, $\mathscr{L}_2 = \mathscr{L}_x\mathscr{L}_y = \mathscr{L}_y\mathscr{L}_x$.

(i) Using Lemma 7 part (i) and linearity of Laplace, we consider the following:

$$\begin{aligned}
\mathscr{L}_2\Delta_x^n[u(x,y)] &= \mathscr{L}_y\left[\mathscr{L}_x\Delta_x^n u(x,y)\right] \\
&= \mathscr{L}_y\left[p^n\mathscr{L}_x\{u(x,y)\} - \sum_{k=0}^{n-1}p^{n-1-k}\Delta_x^k u(a,y)\right] \\
&= p^n\mathscr{L}_y\mathscr{L}_x\{u(x,y)\} - \mathscr{L}_y\sum_{k=0}^{n-1}p^{n-1-k}\Delta_x^k u(a,y) \\
&= p^n\mathscr{L}_2\{u(x,y)\} - \sum_{k=0}^{n-1}p^{n-1-k}\mathscr{L}_y\left\{\Delta_x^k u(a,y)\right\}.
\end{aligned} \tag{81}$$

(ii) Proof is similar as in part (i).

(iii) Using Lemma 7 part (iii) and linearity of Laplace, we consider the following:

$$\begin{aligned}
\mathscr{L}_2\Delta_{xy}^{nm}[u(x,y)] &= \mathscr{L}_y\left[\mathscr{L}_x\Delta_{xy}^{nm}u(x,y)\right] \\
&= \mathscr{L}_y\left[p^n\mathscr{L}_x\Delta_y^m\{u(x,y)\} - \sum_{k=0}^{n-1}p^{n-1-k}\Delta_x^k\Delta_y^m u(a,y)\right] \\
&= p^n\left[\mathscr{L}_y\mathscr{L}_x\Delta_y^m\{u(x,y)\}\right] - p^n\sum_{k=0}^{n-1}p^{-1-k}\left[\mathscr{L}_y\Delta_x^k\Delta_y^m u(a,y)\right] \\
&= p^n\left[\mathscr{L}_2\Delta_y^m\{u(x,y)\}\right] - p^n\sum_{k=0}^{n-1}p^{-1-k}\left[q^m\mathscr{L}_y\Delta_x^k\{u(a,y)\} - \sum_{j=0}^{m-1}q^{m-1-j}\Delta_x^k\Delta_y^j u(a,a)\right].
\end{aligned} \tag{82}$$

In the previous step, we used Lemma 7 part (iv). In the following step, using Theorem 10 part (ii),

$$\begin{aligned}
&= p^n\left[q^m \mathscr{L}_2\{u(x,y)\} - \sum_{j=0}^{m-1} q^{m-1-j}\mathscr{L}_y\left\{\Delta_y^j u(x,a)\right\}\right] \\
&\quad - p^n \sum_{k=0}^{n-1} p^{-1-k}\left[q^m \mathscr{L}_y \Delta_x^k\{u(a,y)\} - \sum_{j=0}^{m-1} q^{m-1-j}\Delta_x^k\Delta_y^j u(a,a)\right] \\
&= p^n q^m\left[\mathscr{L}_2\{u(x,y)\} - \sum_{k=0}^{n-1} p^{-1-k}\mathscr{L}_y\left\{\Delta_x^k u(a,y)\right\} - \sum_{j=0}^{m-1} q^{-1-j}\mathscr{L}_x\left\{\Delta_y^j u(x,a)\right\} + \sum_{j=0}^{m-1}\sum_{k=0}^{n-1} p^{-1-k}q^{-1-j}\left\{\Delta_{xy}^{kj}u(a,a)\right\}\right].
\end{aligned} \tag{83}$$

□

Theorem 11. *Assume $f(x,y)$: $\mathbb{N}_a \times \mathbb{N}_a \longrightarrow \mathbb{R}$. If $\mathscr{L}_2[f(x,y)] = \tilde{\tilde{F}}(p,q)$, then for constants $p \neq 0,-1$ and $q \neq 0,-1$, and we have*

$$\mathscr{L}_2\left[\int_a^x\int_a^y f(t,\tau)\Delta\tau\Delta t\right] = \frac{\tilde{\tilde{F}}(p,q)}{pq}. \tag{84}$$

Proof. For $x, y \in \mathbb{N}_a$, let

$$u(x,y) = \int_a^x\int_a^y f(t,\tau)\Delta\tau\Delta t. \tag{85}$$

Then, the difference Δ_{xy} is

$$\begin{aligned}
\Delta_{xy}u(x,y) &= \Delta_y\left[\Delta_x u(x,y)\right] \\
&= \Delta_y\left[\int_a^{x+1}\int_a^y f(t,\tau)\Delta\tau\Delta t - \int_a^x\int_a^y f(t,\tau)\Delta\tau\Delta t\right] \\
&= \Delta_y\left[\sum_{t=a}^{x}\sum_{\tau=a}^{y-1} f(t,\tau) - \sum_{t=a}^{x-1}\sum_{\tau=a}^{y-1} f(t,\tau)\right].
\end{aligned} \tag{86}$$

By separating last term for $t = x$, from the first double sum, we obtain

$$\begin{aligned}
&= \Delta_y\left[\sum_{\tau=a}^{y-1} f(x,\tau) + \sum_{t=a}^{x-1}\sum_{\tau=a}^{y-1} f(t,\tau) - \sum_{t=a}^{x-1}\sum_{\tau=a}^{y-1} f(t,\tau)\right] \\
&= \Delta_y\left[\sum_{\tau=a}^{y-1} f(x,\tau)\right] \\
&= \sum_{\tau=a}^{y} f(x,\tau) - \sum_{\tau=a}^{y-1} f(x,\tau).
\end{aligned} \tag{87}$$

By separating last term for $\tau = y$, from the first sum, we obtain

$$\begin{aligned}
&= f(x,y) + \sum_{\tau=a}^{y-1} f(x,\tau) - \sum_{\tau=a}^{y-1} f(x,\tau) \\
f(x,y) &= \Delta_{xy}u(x,y).
\end{aligned} \tag{88}$$

Now, for constants $p \neq 0,-1$ and $q \neq 0,-1$, taking the delta double Laplace transforms on both sides,

$$\mathscr{L}_2 f(x,y) = \mathscr{L}_2\Delta_{xy}u(x,y). \tag{89}$$

By application of Theorem 10 (iii) for $m = 1 = n$, $\mathscr{L}_2\Delta_{xy}[u(x,y)] = pq\mathscr{L}_2\ [u(x,y)] - q\mathscr{L}_y\{u(a,y)\} - p\mathscr{L}_x\{u(x,a)\} + u(a,a)$. On right-hand side, we obtain

$$\begin{aligned}
&= pq\mathscr{L}_2[u(x,y)] - q\mathscr{L}_y\{u(a,y)\} \\
&\quad - p\mathscr{L}_x\{u(x,a)\} + u(a,a)
\end{aligned} \tag{90}$$

$$\mathscr{L}_2 f(x,y) = pq\mathscr{L}_2[u(x,y)].$$

In the last step, $u(x,a), u(a,y), u(a,a)$ are zero by empty sum convention, and on further simplification, we obtain

$$\mathscr{L}_2\left[\int_a^x\int_a^y f(t,\tau)\Delta\tau\Delta t\right] = \frac{\tilde{\tilde{F}}(p,q)}{pq}. \tag{91}$$

□

Example 4

(a) Solve the partial difference equation:

$$\begin{aligned}
&\Delta_x u(x,y) - \Delta_y u(x,y) = 0 \\
&\text{with } u(x,a) = (x-a)^{\underline{1}}, u(a,y) = (y-a)^{\underline{1}}.
\end{aligned} \tag{92}$$

Application of the delta Laplace transforms to initial conditions by Lemma 3,

$$\begin{aligned}
\mathscr{L}_x u(x,a) &= \mathscr{L}_x (x-a)^{\underline{1}} = \frac{1}{p^2}, \\
\mathscr{L}_y u(a,y) &= \mathscr{L}_y (y-a)^{\underline{1}} = \frac{1}{q^2}.
\end{aligned} \tag{93}$$

Apply the delta double Laplace transforms to difference equation and then use linearity property:

$$\begin{aligned}
&\mathscr{L}_2\left[\Delta_x u(x,y) - \Delta_y u(x,y)\right] = 0, \\
&\mathscr{L}_2\Delta_x u(x,y) - \mathscr{L}_2\Delta_y u(x,y) = 0.
\end{aligned} \tag{94}$$

Using Theorem 9,

$$\begin{aligned}
&\left[p\mathscr{L}_2\{u(x,y)\} - \mathscr{L}_y\{u(a,y)\}\right] \\
&\quad - \left[q\mathscr{L}_2\{u(x,y)\} - \mathscr{L}_x\{u(x,a)\}\right] = 0, \\
&(p-q)\mathscr{L}_2\{u(x,y)\} = \frac{1}{q^2} - \frac{1}{p^2}, \\
&\mathscr{L}_2\{u(x,y)\} = \frac{1}{pq^2} + \frac{1}{p^2 q}.
\end{aligned} \tag{95}$$

Inverting the delta Laplace transforms pairs

$$u(x,y) = (x-a)^{\underline{1}} + (y-a)^{\underline{1}}. \tag{96}$$

(b) Solve the same partial difference equation with slightly different initial conditions:

$$u(x,a) = (x-a)^{\underline{2}},\quad u(a,y) = (y-a)^{\underline{2}}. \tag{97}$$

Application of the delta Laplace transforms to initial conditions by Lemma 3:

$$\mathscr{L}_x u(x,a) = \mathscr{L}_x (x-a)^{\underline{2}} = \frac{2}{p^3},$$

$$\mathscr{L}_y u(a,y) = \mathscr{L}_y (y-a)^{\underline{2}} = \frac{2}{q^3}.$$

$$\text{From equation (7)}\,(p-q)\mathscr{L}_2\{u(x,y)\} = \frac{2}{q^3} - \frac{2}{p^3},$$

$$\mathscr{L}_2\{u(x,y)\} = \frac{2}{pq^3} + \frac{2}{p^2q^2} + \frac{2}{p^3q}. \tag{98}$$

Inverting delta Laplace transforms pairs,

$$u(x,y) = (x-a)^{\underline{2}} + 2(x-a)^{\underline{1}}(y-a)^{\underline{1}} + (y-a)^{\underline{2}}. \tag{99}$$

Assume $f\colon \mathbb{N}_a \longrightarrow \mathbb{R}$, then the Riemann–Liouville fractional difference of order $N-1<\alpha\le N$, for $N\in\mathbb{N}_1$ is given by $\Delta_a^\alpha f(x) = \Delta^N \Delta_a^{-(N-\alpha)} f(x)$, for $x\in\mathbb{N}_{a+N-\alpha}$. By using the discussion and results, from Theorem 2.65 to Theorem 2.70, in [10], we take the starting point of the double Laplace $a+\alpha-N$ and $a+N-\alpha$, respectively, for sum and difference operator.

Corollary 2. *Assume $u(x,y)\colon \mathbb{N}_a\times\mathbb{N}_a \longrightarrow \mathbb{R}$, such that the delta double Laplace transforms exists for constants $p\neq -1$ and $q\neq -1$ and denote $\mathscr{L}_2 u(x,y) = \tilde{\tilde{u}}(p,q)$. Then, for $\lceil N-\alpha\rceil = M$ and $\lceil k+\alpha-N\rceil = L$, the delta double Laplace transforms of fractional order operators is given by*

$$\text{(i)}\mathscr{L}_2\left[\Delta_a^{-\alpha} u(x,y)\right](p,q) = \frac{(p+1)^{\alpha-N}(q+1)^{\alpha-N}}{p^\alpha q^\alpha}\tilde{\tilde{u}}(p,q),\quad \text{where } N-1<\alpha<N, \tag{100}$$

$$\begin{aligned}\text{(ii)}\mathscr{L}_2\left[\Delta_x^\alpha u(x,y)\right](p,q) = {} & p^\alpha q^{\alpha-N}(p+1)^{N-\alpha-M}(q+1)^{N-\alpha-M}\tilde{\tilde{u}}(p,q)\\ & -\sum_{k=0}^{N-1} p^{N-1-k}\left[q^{k+\alpha-N}(q+1)^{L-(k+\alpha-N)}\tilde{u}(a,q) - \sum_{j=0}^{L-1} q^j \Delta_x^{k+\alpha-N-1} u(a,a+L-(k+\alpha-N))\right],\end{aligned} \tag{101}$$

$$\begin{aligned}\text{(iii)}\mathscr{L}_2\left[\Delta_y^\alpha u(x,y)\right](p,q) = {} & p^{\alpha-N} q^{\alpha}(p+1)^{N-\alpha-M}(q+1)^{N-\alpha-M}\tilde{\tilde{u}}(p,q)\\ & -\sum_{k=0}^{N-1} q^{N-1-k}\left[p^{k+\alpha-N}(p+1)^{L-(k+\alpha-N)}\tilde{u}(p,a) - \sum_{j=0}^{L-1} p^j \Delta_y^{k+\alpha-N-1} u(a+L-(k+\alpha-N),a)\right].\end{aligned} \tag{102}$$

Proof

(i) Proof is an implication of Definition 3.1 and Theorem 2.67 of [10]

(ii) Result is obtained by application of Theorem 5.4 part (i) and Theorem 2.70 of [10]

(iii) Result is obtained by application of Theorem 5.4 part (ii) and Theorem 2.70 of [10] □

Example 5. Solve the fractional difference equation for $0<\alpha<1$:

$$\Delta_x^\alpha u(x,y) = (y-a)^{\underline{1}},\quad \text{with } u(a,y)=0. \tag{103}$$

Apply the delta Laplace transforms to initial condition $\mathscr{L}_y u(a,y) = \mathscr{L}_y 0 = 0$. For $0<\alpha<1$, we have $N=1$ which implies $k=0$ and therefore $\lceil k+\alpha-1\rceil = L = 0$, also $\lceil 1-\alpha\rceil = M = 1$. Application of the delta double Laplace transforms on both sides of fractional difference equation (103) and making use of equation (101) on left-hand side, and on the right-hand side we used Example 3 to obtain

$$\frac{p^\alpha q^{\alpha-1}}{(p+1)^\alpha (q+1)^\alpha}\tilde{\tilde{u}}(p,q) - p^0 q^{\alpha-1}(q+1)^{1-\alpha}\tilde{u}(a,q) = \frac{1}{pq^2}. \tag{104}$$

Using $\tilde{u}(a,q)=0$ and simplifying the above,

$$\tilde{\tilde{u}}(p,q) = \frac{(p+1)^\alpha (q+1)^\alpha}{p^{\alpha+1}q^{\alpha+1}}. \tag{105}$$

Inverting the delta Laplace transforms pairs by making use of Theorem 1 (iii), together with Lemma 3 (iii),

$$u(x,y) = \frac{(x-a)^{\underline{\alpha}}}{\Gamma(\alpha+1)}\frac{(y-a)^{\underline{\alpha}}}{\Gamma(\alpha+1)}. \tag{106}$$

Data Availability

The data used to support the findings of this study are available from the corresponding author upon request.

Conflicts of Interest

The authors declare no conflicts of interest.

Authors' Contributions

All authors contributed in writing review and editing the article and have read and agreed to the published version of the manuscript.

Acknowledgments

The authors would like to thank Prince Sultan University for funding this work through research group Nonlinear Analysis Methods in Applied Mathematics (NAMAM), Group no. RG-DES-2017-01-17.

References

[1] C. Jordan, *Calculus of Finite Differences*, AMS Chelsea Publishing, Chelsea, NY, USA, 1979.

[2] M. Bohner and A. C. Peterson, *Dynamic Equations on Time Scales an Introduction with Applications*, Birkhauser Boston, Cambridge, MA, USA, 2001.

[3] T. Abdeljawad and D. Baleanu, "On fractional derivatives with exponential kernel and their discrete versions," *Reports on Mathematical Physics*, vol. 80, no. 1, pp. 11–27, 2017.

[4] T. Abdeljawad, "On Riemann and Caputo fractional differences," *Computers & Mathematics with Applications*, vol. 62, no. 3, pp. 1602–1611, 2011.

[5] T. Abdeljawad, D. Baleanu, F. Jarad, and R. P. Agarwal, "Fractional sums and differences with binomial coefficients," *Discrete Dynamics in Nature and Society*, vol. 2013, Article ID 104173, 6 pages, 2013.

[6] T. Abdeljawad, S. Banerjee, and G. C. Wu, "Discrete tempered fractional calculus for new chaotic systems with short memory and image encryption," *Optik*, Article ID 163698, 2019.

[7] T. Abdeljawad, "On delta and nabla Caputo fractional differences and dual identities," *Discrete Dynamics in Nature and Society*, vol. 2013, Article ID 406910, 12 pages, 2013.

[8] F. M. Atici and P. W. Eloe, "A transform method in discrete fractional calculus," *International Journal of Differential Equations*, vol. 2, no. 2, 2007.

[9] A. Ivan, J. Losada, and J. J. Nieto, "On quasi-periodic properties of fractional sums and fractional differences of periodic functions," *Applied Mathematics and Computation*, vol. 273, pp. 190–200, 2016.

[10] C. S. Goodrich and A. C. Peterson, *Discrete Fractional Calculus*, Springer, New York, NY, USA, 2015.

[11] C. S. Goodrich, "Existence and uniqueness of solutions to a fractional difference equation with nonlocal conditions," *Computers & Mathematics with Applications*, vol. 61, no. 2, pp. 191–202, 2011.

[12] L.-L. Huang, J. H. Park, G.-C. Wu, and Z.-W. Mo, "Variable-order fractional discrete-time recurrent neural networks," *Journal of Computational and Applied Mathematics*, vol. 370, p. 112633, 2020.

[13] G.-C. Wu, D. Baleanu, and W.-H. Luo, "Lyapunov functions for Riemann-Liouville-like fractional difference equations," *Applied Mathematics and Computation*, vol. 314, pp. 228–236, 2017.

[14] G. C. Wu, Z. G. Deng, D. Baleanu, and D. Q. Zeng, "New variable-order fractional chaotic systems for fast image encryption," *Chaos*, vol. 29, Article ID 083103, 2019.

[15] M. T. Holm, "The Laplace transform in discrete fractional calculus," *Computers & Mathematics with Applications*, vol. 62, no. 3, pp. 1591–1601, 2011.

[16] M. T. Holm, *The Theory of Discrete Fractional Calculus: Development and Application*, University of Nebraska-Lincoln, Lincoln, NE, USA, 2011.

[17] S. S. Haider and M. U. Rehman, "Ulam-Hyers-Rassias stability and existence of solutions to nonlinear fractional difference equations with multipoint summation boundary condition," *Acta Mathematica Scientia*, vol. 40, no. 2, pp. 589–602, 2020.

[18] S. S. Haider and M. U. Rehman, "Construction of fixed point operators for nonlinear difference equations of non integer order with impulses," *Fractional Calculus and Applied Analysis*, vol. 23, no. 3, 2020.

[19] F. Jarad, K. Taş, and K. Ta, "A new transform method in nabla discrete fractional calculus," *Advances in Difference Equations*, vol. 2012, no. 1, 190 pages, 2012.

[20] D. L. Bernstein, "The double Laplace integral," *Duke Mathematical Journal*, vol. 8, no. 3, pp. 460–496, 1941.

[21] G. A. Coon and D. L. Bernstein, *Some Properties of the Double Laplace Transformation*, Taylor Instrument Companies, University of Rochester Press, Rochester, NY, USA, 1953.

[22] G. A. Coon and D. L. Bernstein, "Some general formulas for double Laplace transformations," *Proceedings of the American Mathematical Society*, vol. 14, no. 1, p. 52, 1963.

[23] L. Debnath, "The double Laplace transforms and their properties with applications to functional, integral and partial differential equations," *International Journal of Applied and Computational Mathematics*, vol. 2, no. 2, pp. 223–241, 2016.

[24] R. R. Dhunde and G. L. Waghmare, "On some convergence theorems of double Laplace transform," *Journal of Informatics and Mathematical Sciences*, vol. 6, pp. 45–54, 2014.

[25] A. Atangana, "A note on the triple Laplace transform and its applications to some kind of third-order differential equation," *Abstract and Applied Analysis*, vol. 2013, Article ID 769102, 10 pages, 2013.

[26] R. S. Dahiya and M. Vinayagamoorthy, "Laplace transform pairs of n-dimensions and heat conduction problem," *Mathematical and Computer Modelling*, vol. 13, no. 10, pp. 35–50, 1990.

[27] H. U. Rehman, M. Iftikhar, S. Saleem, M. Younis, and A. Mueed, "A computational quadruple Laplace transform for the solution of partial differential equations," *Applied Mathematics*, vol. 5, no. 21, pp. 3372–3382, 2014.

[28] S. S. Haider, M. U. Rehman, and T. Abdeljawad, "On Hilfer fractional difference operator," *Advances in Difference Equations*, vol. 122, pp. 1–20, 2020.

[29] S. S. Haider and M. U. Rehman, "On substantial fractional difference operator," *Advances in Difference Equations*, no. 1, , 2020.

[30] M. Bohner, G. S. Guseinov, and B. Karpuz, "Further properties of the Laplace transform on time scales with arbitrary graininess," *Integral Transforms and Special Functions*, vol. 24, no. 4, pp. 289–301, 2013.

[31] M. D. Ortigueira, F. J. V. Coito, and J. J. Trujillo, "Discrete-time differential systems," *Signal Processing*, vol. 107, pp. 198–217, 2015.

[32] P. Savoye, "On the inclusion of difference equation problems and Z Transform methods in sophomore differential equation classes," *Primus*, vol. 19, no. 6, pp. 491–499, 2009.

[33] M. Omran and A. Kiliman, "Fractional double Laplace transform and its properties," in *Proceedings of the AIP Conference*, vol. 1795, no. 1, January 2017.

[34] J. Peng and K. Li, "A note on property of the Mittag-Leffler function," *Journal of Mathematical Analysis and Applications*, vol. 370, no. 2, pp. 635–638, 2010.

[35] B. Zhang and Y. Zhou, *Qualitative Analysis of Delay Partial Difference Equations, Contemporary Mathematics and its Applications*, Hindawi, New York, NY, USA, 2007.

[36] F. Ozpinar and F. M. Belgacem, "The discrete homotopy perturbation Sumudu transform method for solving partial difference equations," *Discrete & Continuous Dynamical Systems*, vol. 12, no. 3, pp. 615–624, 2019.

[37] A. Aghili and M. R. Masomi, "Solving systems of fractional partial differential equations via two dimensional Laplace transforms," *International Journal of Research–Granthaalayah*, vol. 5, no. 12, pp. 406–420, 2017.

[38] S. K. Elagan, M. Sayed, and M. Higazy, "An analytical study on fractional partial differential equations by Laplace transform operator method," *International Journal of Applied Engineering Research*, vol. 13, no. 1, pp. 545–549, 2018.

[39] A. M. Haghighi and D. P. Mishev, *Difference and Differential Equations with Applications in Queueing Theory*, John Wiley and Sons, Hoboken, NJ, USA, 2013.

[40] A. M. O. Anwar, F. Jarad, D. Baleaun, and F. Ayaz, "Fractional Caputo heat equation within the double Laplace transform," *Romanian Journal of Physics*, vol. 58, pp. 15–18, 2013.

Hindawi
Mathematical Problems in Engineering
Volume 2020, Article ID 7898109, 9 pages
https://doi.org/10.1155/2020/7898109

Research Article

Design of Static Output Feedback Controller for Fractional-Order T-S Fuzzy System

Zhile Xia

Department of Mathematics, TaiZhou University, ZheJiang, TaiZhou 318000, China

Correspondence should be addressed to Zhile Xia; zhilexia@163.com

Received 12 April 2020; Revised 18 May 2020; Accepted 20 May 2020; Published 15 June 2020

Guest Editor: Amr Elsonbaty

This paper studies the design of fuzzy static output feedback controllers for two kinds of fractional-order T-S fuzzy systems. The fractional order α satisfies $0 < \alpha < 1$ and $1 \leq \alpha < 2$. Based on the fractional order theory, matrix decomposition technique, and projection theorem, four new sufficient conditions for the asymptotic stability of the system and the corresponding controller design methods are given. All the results can be expressed by linear matrix inequalities, and the relationship between fuzzy subsystems is also considered. These have great advantages in solving the results and reducing the conservatism. Finally, a simulation example is given to show the effectiveness of the proposed method.

1. Introduction

Compared with the integer-order system, the fractional-order system has many advantages, for example, the integer order is a special case of the fractional-order system; the fractional-order system has global properties, and the system state depends not only on the current time but also on the past time; it can accurately describe the memory and genetic properties in physics and engineering. Therefore, in recent decades, fractional-order control systems have also been widely concerned, and important results have been obtained. For example, Chen et al. [1–3] made a comprehensive introduction and in-depth study of fractional-order systems. Specifically, the paper [1] considered the robust stability and stabilization of fractional-order linear systems with polyhedral uncertainties. The results obtained are not only applicable to the fractional order α satisfying $0 < \alpha < 1$ but also to the fractional order α satisfying $1 \leq \alpha < 2$. For the fractional-order neural network system with time-varying delay, the literature [2] solved a challenging problem: the delay-dependent stability and stabilization of the fractional-order delay system. The literature [3] studied the stability and synchronization of the delayed neural network, and a series of very important results were given, including delay-independent stability criterion, measurable algebra criterion, and synchronization criterion. Gallegos and Duarte-Mermoud [4] investigated the stability of fractional-order and integral-order coupled systems, in which the concepts of dissipativity and passivity were extended, and the theorems of small gain and passivity for correlated systems were obtained. Liu et al. [5] used the fractional filtering method to study the backstepping controller design of the actuator fault fuzzy neural network system with completely unknown parameters and modes. Combined with the fractional adaptive law, the tracking error and compensation tracking error converged to a small enough area. Based on Lyapunov functions and the comparison principle, Jia et al. [6] designed delayed state feedback control and coupling state feedback control for fractional-order memristor-based neural networks with time delay. To sum up, the control problem of the fractional-order system is a hot issue at present, attracting a large number of researchers to participate in it.

In addition, the fuzzy theory opens up a new way to deal with the fuzzy uncertainty in nature with strict mathematical methods and proposes the method of the membership function to describe the degree of the element set [7]. When the membership degree is 1, it means that the element belongs to the set completely, when the membership degree is 0, it means that the element does not belong to the set at all, and when the membership degree belongs to the interval $(0, 1)$, it means that the element belongs to the set but does not completely belong to the set. Obviously, this is a generalization of the classical set theory. Fuzzy control is based on the fuzzy theory. By using expert language, fuzzy control can achieve good and effective control for some complex nonlinear control objects which are difficult to establish the mathematical model accurately [8, 9]. So far, two main fuzzy models have been proposed. The first model is based on the input-output model proposed in document [9]. The disadvantage is that there is a lot of useful information which is not used. The second model is the T-S fuzzy model proposed by Japanese scholars Takagi and Sugeno in 1985 [10, 11]. In [12–14], it is proved that this kind of fuzzy system has the ability of universal approximation. Some recent literature studies are listed to show that the T-S fuzzy system has been widely studied. For example, based on the T-S fuzzy model, in [15], the design of the fuzzy filter for the discrete-time nonlinear networked system is studied, and a new method is proposed to ensure that the filtering error system is dissipative by using the method of event triggering and quantization. For continuous-time nonlinear time-delay systems, by using repetitive control, Rathinasamy et al. [16] proposed an improved output feedback controller design method. This method ensures that the system can track the given reference signal within the allowable error range. Li et al. [17] studied the finite-time H_∞ control problem, and the sufficient conditions based on LMI were given. The research results of the output feedback can be found in the literature studies [18–28]. There are also a large number of references related to the T-S fuzzy model, which we cannot be enumerated here.

Compared with many research results of the integer-order T-S fuzzy system, the research results of the fractional-order T-S fuzzy system are less. For the fractional-order T-S fuzzy system, Zheng et al. [29] studied the stabilization of the chaotic system by using the adaptive method. When the order of the fractional order considered satisfies $1 \le \alpha < 2$ and $0 < \alpha < 1$, respectively, the stability conditions based on LMI were proposed in [30, 31]. Huang et al. [32] studied the stabilization of the state feedback that can be applied to both the following situations: $1 \le \alpha < 2$ and $0 < \alpha < 1$. However, in the practical engineering field, the state of the system is often difficult to obtain directly. At this time, the state observer or output feedback control methods need to be considered. Based on the T-S fuzzy model, Duan et al. [33] studied the design problem of the nonfragile observer by using singular value decomposition of the matrix and put forward sufficient conditions of linear matrix inequalities, which guarantee that the corresponding closed-loop system is stochastic asymptotically stable; when the fuzzy antecedent variables are unmeasurable, Duan and Li [34] considered the design problem of dynamic output feedback controllers and proposed sufficient conditions for the system to be asymptotically stable; Karthick et al. [35] designed a dynamic output feedback controller by means of interference suppression and quantization; and Lin et al. and Ji et al. [36, 37] studied the design of the fuzzy static output feedback controller. The design of the static fuzzy output feedback controller will increase the fuzzy relation in the stabilization condition by a certain multiple because the product term of coefficient matrices $B_iF_jC_k$ appears, while the design state feedback only contains the product term of coefficient matrices B_iF_j $(i, j, k = 1, 2, \ldots, r)$, where r is an integer, indicating the number of fuzzy rules. For the traditional T-S fuzzy system, Chaibi et al. [38] used the matrix decomposition technique to effectively separate the coefficient term $B_iF_jC_k$ and effectively reduced the fuzzy relation of one layer and proposed the design method based on the linear matrix inequality. In this paper, we try to extend the research results of Chaibi et al. [38] to the fractional-order T-S fuzzy system.

In conclusion, this paper studies the fuzzy static output feedback control of the fractional-order T-S fuzzy system. The order includes two cases: $0 < \alpha < 1$ and $1 \le \alpha < 2$. According to the theory of fractional differential correlation and the projection theorem, several new stabilization design methods are given. All the results are expressed by the linear matrix inequality. The main contributions of this paper are as follows: (1) the control method of the fuzzy static output feedback is extended from the integer-order fuzzy system to the fractional-order fuzzy system, so it is more practical; (2) the condition of system stabilization and controller design methods are all expressed by LMIs. Therefore, LMI toolbox of Matlab can be used to program and calculate; (3) output matrix $C_1, C_2, \ldots, C_r$ of the system can still be completely different; (4) for some similar Lyapunov matrices, only symmetry or antisymmetry is required, no further diagonal is required, and stability conditions are relaxed; and (5) the stabilization conditions are also considered. Finally, a numerical simulation example is given to show the effectiveness of the proposed method.

Notations. Throughout this paper, $\mathbb{R}^n$ denotes the n–dimensional Euclidean space; $\mathbb{R}^{n\times m}$ is the set of all $n \times m$ real matrices; I and O represent the identity matrix and the zero matrix with appropriate dimensions; $P > 0\,(P < 0)$ represents the positive definite (negative definite) matrix; the right superscript T denotes the transposition of the matrix; the symbol $\mathrm{sym}\{S\}$ means $S + S^T$; the diagonal block matrix is denoted by $\mathrm{diag}\{A_1, A_2, \ldots, A_n\}$; and the symbol $*$ shows the symmetric part of the block matrix.

2. Basic Definition and Lemmas

Several definitions of fractional-order differential are given in monograph [39], among which Caputo and Riemann–Liouville fractional-order differential are widely used. In this paper, we adopt the definition of Caputo fractional-order differential.

Definition 1 (see Podlubny [39]). The Caputo-type fractional derivative of order $\alpha > 0$ for a function $f(t)$ is defined as follows:

$$D^\alpha f(t) = \frac{1}{\Gamma(m-\alpha)} \int_0^t \frac{f^{(m)}(\tau)}{(t-\tau)^{\alpha+1-m}} \mathrm{d}\tau, \quad (1)$$

where $\Gamma(\cdot)$ is the gamma function defined as $\Gamma(q) = \int_0^\infty t^{q-1} e^{-t} \mathrm{d}t$ and the integer m satisfies the condition $m - 1 < \alpha \le m$.

Next, we give the following lemmas that will be used in this paper.

Lemma 1 (see Zhang et al. [40, 41]). *Let $A \in \mathbb{R}^{n\times n}$ be a real matrix. The fractional-order system $D^{\alpha}x(t) = Ax(t)$ with $0<\alpha<1$ is asymptotically stable if and only if there exist real symmetric positive definite matrices P_{11} and P_{21} and skew-symmetric matrices P_{12} and P_{22} such that*

$$\begin{bmatrix} P_{11} & P_{12} \\ -P_{12} & P_{11} \end{bmatrix} > 0,$$
$$\begin{bmatrix} P_{21} & P_{22} \\ -P_{22} & P_{21} \end{bmatrix} > 0, \tag{2}$$
$$\sum_{i=1}^{2}\sum_{j=1}^{2} \mathrm{sym}\left(\theta_{ij} \otimes \left(AP_{ij}\right)\right) < 0,$$

where $\theta_{11} = \begin{bmatrix} a & b \\ b & a \end{bmatrix}$, $\theta_{12} = \begin{bmatrix} b & a \\ -a & b \end{bmatrix}$, $\theta_{21} = \begin{bmatrix} a & b \\ -b & a \end{bmatrix}$, *and* $\theta_{22} = \begin{bmatrix} -b & a \\ -a & -b \end{bmatrix}$, $a = \sin\theta_1, b = \cos\theta_1,\ \theta_1 = \pi\alpha/2$.

Lemma 2 (see Chilali et al. [42]). *Let $A \in \mathbb{R}^{n\times n}$ be a real matrix. The fractional-order system $D^{\alpha}x(t) = Ax(t)$ with $1\le\alpha<2$ is asymptotically stable if and only if there exists a symmetric positive definite matrix $P \in \mathbb{R}^{n\times n}$ such that*

$$\begin{bmatrix} c\left(AP+PA^T\right) & d\left(AP-PA^T\right) \\ * & c\left(AP+PA^T\right) \end{bmatrix} < 0, \tag{3}$$

where $c = \sin\theta_2$ and $d = \cos\theta_2$, $\theta_2 = \pi - \pi\alpha/2$.

Lemma 3 (see Chaibi et al. [38]). *For matrices T, Q, U, and W with proper dimensions, scalar ξ, if inequality*

$$\begin{bmatrix} T & \xi Q + W^T U \\ * & -\mathrm{sym}(\xi U) \end{bmatrix} < 0 \tag{4}$$

holds, then

$$T + \mathrm{sym}(QW) < 0. \tag{5}$$

Lemma 4 (see Gahinet and Apkarian [43]). *Given a symmetric matrix $Z_0 \in R^{m\times m}$ and two matrices X, Y of column m, there exists a matrix Z such that the LMI*

$$Z_0 + \mathrm{sym}\left(X^T Z Y\right) < 0 \tag{6}$$

holds if and only if the following two projection inequalities are satisfied:

$$\begin{aligned} X_{\perp}^T Z_0 X_{\perp} &< 0, \\ Y_{\perp}^T Z_0 Y_{\perp} &< 0, \end{aligned} \tag{7}$$

where $X_{\perp}$ and $Y_{\perp}$ are arbitrary matrices whose columns form bases of the null bases of X and Y, respectively.

3. Problem Description and Formation

Consider the following fractional-order T-S fuzzy systems.

Plant rule i: if $\theta_1(t)$ is $\mu_{i1}(t)$, and ..., and $\theta_p(t)$ is $\mu_{ip}(t)$, then

$$\begin{cases} D^{\alpha}x(t) = A_i x(t) + B_i u(t), \\ y(t) = C_i x(t), \quad i = 1, 2, \ldots, r, \end{cases} \tag{8}$$

where the order α satisfies $0<\alpha<1$ or $1\le\alpha<2$; r is the number of if-then rules; $\theta_j(t)$ and $\mu_{ij}(t)\,(j = 1, 2, \ldots, p)$ are the premise variables and the fuzzy sets, respectively; $x(t) \in \mathbb{R}^n, u(t) \in \mathbb{R}^l$, and $y(t) \in \mathbb{R}^m$ are the state, the measurable output, and the controller, respectively; and A_i, B_i, and C_i are matrices with appropriate dimensions.

Using fuzzy reasoning technology, the final output of fuzzy system (8) is

$$\begin{cases} D^{\alpha}x(t) = \sum_{i=1}^{r} h_i(\theta(t))\left(A_i x(t) + B_i u(t)\right), \\ y(t) = \sum_{i=1}^{r} h_i(\theta(t)) C_i x(t), \end{cases} \tag{9}$$

where $\theta(t) = [\theta_1(t), \theta_2(t), \ldots, \theta_p(t)]$ and $h_i(\theta(t)) = \omega_i(\theta(t))/\sum_{i=1}^{r}\omega_i(\theta(t))$, $\omega_i(\theta(t)) = \Pi_{j=1}^{p}\mu_{ij}(\theta_j(t))$; $\mu_{ij}(\theta_j(t))$ is the membership degree of $\theta_j(t)$ in fuzzy set $\mu_{ij}(t)$.

According to the definition of the membership function, we can easily get the following properties:

$$\omega_i(\theta(t)) \ge 0,$$
$$0 \le h_i(\theta(t)) \le 1, \quad i = 1, 2, \ldots, r; \ \sum_{i=1}^{r} h_i(\theta(t)) = 1. \tag{10}$$

For system (8), we will design the following fuzzy static output feedback controller:

$$u(t) = \sum_{i=1}^{r} h_i(\theta(t)) F_i y(t), \tag{11}$$

where $F_i\,(i = 1, 2, \ldots, r)$ are the matrices with proper dimensions to be designed.

By bringing controller (11) into system (8), we can get the closed-loop system:

$$D^{\alpha}x(t) = \sum_{i=1}^{r}\sum_{j=1}^{r}\sum_{k=1}^{r} h_i(\theta(t)) h_j(\theta(t)) h_k(\theta(t))\left(A_i + B_i F_j C_k\right)x(t). \tag{12}$$

The main purpose of this paper is to design static fuzzy controller (11) for system (8) so that the corresponding closed-loop system (12) is asymptotically stable.

4. Design of the Fuzzy Static Output Feedback Controller

In this section, the design methods of the fuzzy static output feedback controller for fractional-order fuzzy system (8) are given, and the corresponding closed-loop system is guaranteed to be asymptotically stable. Now, we can prove the following results.

Theorem 1. *Fractional-order closed-loop system (12) with $0<\alpha<1$ is asymptotically stable if there is scalar $\xi>0$, proper dimensional matrices $U, G_{1i}, G_{2i}, G_{3i}, G_{4i}, K_i\,(i = 1, 2, \ldots, r)$,* *symmetric matrices P_{11}, P_{21}, and skew-symmetric matrices P_{21}, P_{22} such that the following LMIs are satisfied:*

$$\begin{bmatrix} P_{11} & P_{12} \\ -P_{12} & P_{11} \end{bmatrix} > 0, \quad \begin{bmatrix} P_{21} & P_{22} \\ -P_{22} & P_{21} \end{bmatrix} > 0, \tag{13}$$

$$\Omega_{ii} < 0, \quad i = 1, 2, \ldots, r, \tag{14}$$

$$\Omega_{ij} + \Omega_{ji} < 0, \quad i = 1, 2, \ldots, r-1, \; j = i+1, \ldots, r. \tag{15}$$

In addition, the controller gain matrices can be designed as

$$F_i = K_i U^{-1}, \quad i = 1, 2, \ldots, r, \tag{16}$$

where

$$\Omega_{ij} = \begin{bmatrix} -\mathrm{sym}(G_{1i}) & \Gamma_1 + G_{1i}A_j^T - G_{2i}^T & 0 & \Gamma_2 & \\ * & \mathrm{sym}\left(G_{2i}A_j^T\right) & -\Gamma_2^T & 0 & \xi Q_{ij} + W_{ij}^T \\ * & * & -\mathrm{sym}(G_{3i}) & \Gamma_1 + G_{3i}A_j^T - G_{4i}^T & \\ * & * & * & \mathrm{sym}\left(G_{4i}A_j^T\right) & \\ * & * & * & * & -\mathrm{sym}(\xi \mathbb{U}) \end{bmatrix},$$
$$\Gamma_1 = aP_{11} + bP_{12} + aP_{21} - bP_{22},$$
$$\Gamma_2 = -bP_{11} + aP_{12} + bP_{21} + aP_{22},$$
$$a = \sin\left(\frac{\pi\alpha}{2}\right),$$
$$b = \cos\left(\frac{\pi\alpha}{2}\right),$$
$$Q_{ij} = \mathrm{diag}\left\{G_{1i}C_j^T, G_{2i}C_j^T, G_{3i}C_j^T, G_{4i}C_j^T\right\},$$
$$\mathbb{U} = \mathrm{diag}\{U, U, U, U\},$$
$$W_{ij} = \mathrm{diag}\left\{\left[0, K_j^T B_i^T; 0, K_j^T B_i^T\right], \left[0, K_j^T B_i^T; 0, K_j^T B_i^T\right]\right\}. \tag{17}$$

Proof. Let

$$\Omega = \begin{bmatrix} -\mathrm{sym}(\overline{G}_{1i}) & \Gamma_1 + \overline{G}_{1i}\overline{A}_i^T - \overline{G}_{2i}^T & 0 & \Gamma_2 & \\ * & \mathrm{sym}\left(\overline{G}_{2i}\overline{A}_i^T\right) & -\Gamma_2^T & 0 & \xi \overline{Q}_i + \overline{W}_{iu}^T \mathbb{U} \\ * & * & -\mathrm{sym}(\overline{G}_{3i}) & \Gamma_1 + \overline{G}_{3i}\overline{A}_i^T - \overline{G}_{4i}^T & \\ * & * & * & \mathrm{sym}\left(\overline{G}_{4i}\overline{A}_i^T\right) & \\ * & * & * & * & -\mathrm{sym}(\xi \mathbb{U}) \end{bmatrix}, \tag{18}$$

where $\overline{Q}_i = \mathrm{diag}\left\{\overline{G}_{1i}\overline{C}_i^T, \overline{G}_{2i}\overline{C}_i^T, \overline{G}_{3i}\overline{C}_i^T, \overline{G}_{4i}\overline{C}_i^T\right\}$, $\overline{W}_{iu} = \mathrm{diag}\{[0, U^{-T} \; \overline{K}_i^T \overline{B}_i^T; 0, U^{-T}\overline{K}_i^T \overline{B}_i^T], [0, U^{-T}\overline{K}_i^T \overline{B}_i^T; 0, \; U^{-T}\overline{K}_i^T \overline{B}_i^T]\}$, and $[\overline{A}_i, \overline{B}_i, \overline{C}_i, \overline{K}_i, \overline{G}_{1i}, \overline{G}_{2i}, \overline{G}_{3i}, \overline{G}_{4i}] = \sum_{i=1}^r h_i(\theta(t))[A_i, B_i, C_i, K_i, G_{1i}, G_{2i}, G_{3i}, G_{4i}]$.

According to inequalities (14) and (15) and the properties of the membership function, we can get

$$\Omega = \sum_{i=1}^{r}\sum_{i=1}^{r} h_i(\theta(t))h_j(\theta(t))\Omega_{ij} = \sum_{i=1}^{r} h_i^2(\theta(t))\Omega_{ii} + \sum_{i=1}^{r-1}\sum_{j=i+1}^{r} h_i(\theta(t))h_j(\theta(t))\left(\Omega_{ij}+\Omega_{ji}\right) < 0. \tag{19}$$

Replacing $\overline{K}_i U^{-1}$ with $\overline{F}_i$ in Ω, we obtain

$$\begin{bmatrix} -\mathrm{sym}(\overline{G}_{1i}) & \Gamma_1 + \overline{G}_{1i}\overline{A}_i^T - \overline{G}_{2i}^T & 0 & \Gamma_2 & \\ * & \mathrm{sym}\left(\overline{G}_{2i}\overline{A}_i^T\right) & -\Gamma_2^T & 0 & \xi\overline{Q}_i + \overline{W}_{if}^T\mathbb{U} \\ * & * & -\mathrm{sym}(\overline{G}_{3i}) & \Gamma_1 + \overline{G}_{3i}\overline{A}_i^T - \overline{G}_{4i}^T & \\ * & * & * & \mathrm{sym}\left(\overline{G}_{4i}\overline{A}_i^T\right) & \\ * & * & * & * & -\mathrm{sym}(\xi\mathbb{U}) \end{bmatrix} < 0, \tag{20}$$

where $\overline{W}_{if} = \mathrm{diag}\left\{[0,\overline{F}_i^T\overline{B}_i^T;0,\overline{F}_i^T\overline{B}_i^T],[0,\overline{F}_i^T\overline{B}_i^T;0,\overline{F}_i^T\overline{B}_i^T]\right\}$.

According to Lemma 3, if inequality (20) holds, then

$$\begin{bmatrix} -\mathrm{sym}(\overline{G}_{1i}) & \Gamma_1 + \overline{G}_{1i}\overline{A}_i^T - \overline{G}_{2i}^T & 0 & \Gamma_2 \\ * & \mathrm{sym}\left(\overline{G}_{2i}\overline{A}_i^T\right) & -\Gamma_2^T & 0 \\ * & * & -\mathrm{sym}(\overline{G}_{3i}) & \Gamma_1 + \overline{G}_{3i}\overline{A}_i^T - \overline{G}_{4i}^T \\ * & * & * & \mathrm{sym}\left(\overline{G}_{4i}\overline{A}_i^T\right) \end{bmatrix} + \mathrm{sym}\left(\overline{Q}_i\overline{W}_{if}\right) < 0. \tag{21}$$

Let

$$\widetilde{A} = \sum_{i=1}^{r}\sum_{j=1}^{r}\sum_{k=1}^{r} h_i(\theta(t))h_j(\theta(t))h_k(\theta(t))\left(A_i + B_iF_jC_k\right). \tag{22}$$

Then, $\widetilde{A} = \overline{A}_i + \overline{B}_i\overline{F}_i\overline{C}_i$.

Therefore, inequality (21) can be rewritten as

$$\begin{bmatrix} 0 & \Gamma_1 & 0 & \Gamma_2 \\ * & 0 & -\Gamma_2^T & 0 \\ * & * & 0 & \Gamma_1 \\ * & * & * & 0 \end{bmatrix} + \mathrm{sym}\left(\begin{bmatrix} \overline{G}_{1i} & 0 \\ \overline{G}_{2i} & 0 \\ 0 & \overline{G}_{3i} \\ 0 & \overline{G}_{4i} \end{bmatrix}\begin{bmatrix} -I & \widetilde{A}^T & 0 & 0 \\ 0 & 0 & -I & \widetilde{A}^T \end{bmatrix}\right) < 0. \tag{23}$$

Taking $\Psi = \begin{bmatrix} \widetilde{A} & I & 0 & 0 \\ 0 & 0 & \widetilde{A} & I \end{bmatrix}$ and using Lemma 4, we have

$$\Psi\begin{bmatrix} 0 & \Gamma_1 & 0 & \Gamma_2 \\ * & 0 & -\Gamma_2^T & 0 \\ * & * & 0 & \Gamma_1 \\ * & * & * & 0 \end{bmatrix}\Psi^T + \mathrm{sym}\left(\Psi\begin{bmatrix} \overline{G}_{1i} & 0 \\ \overline{G}_{2i} & 0 \\ 0 & \overline{G}_{3i} \\ 0 & \overline{G}_{4i} \end{bmatrix}\begin{bmatrix} -I & \widetilde{A}^T & 0 & 0 \\ 0 & 0 & -I & \widetilde{A}^T \end{bmatrix}\Psi^T\right) < 0,$$

which is equivalent to

$$\begin{bmatrix} \widetilde{A}\Gamma_1 + \Gamma_1^T\widetilde{A}^T & \widetilde{A}\Gamma_2 - \Gamma_2^T\widetilde{A}^T \\ * & \widetilde{A}\Gamma_1 + \Gamma_1^T\widetilde{A}^T \end{bmatrix} < 0. \tag{24}$$

The above inequality can be rewritten as

$$\mathrm{sym}\left\{\begin{bmatrix} \widetilde{A}\Gamma_1 & \widetilde{A}\Gamma_2 \\ -\widetilde{A}\Gamma_2 & \widetilde{A}\Gamma_1 \end{bmatrix}\right\} < 0. \tag{25}$$

According to the definition of the Kronecker product, one has from (25)

$$\mathrm{sym}\left\{\begin{bmatrix} a & -b \\ b & a \end{bmatrix}\otimes\left(\widetilde{A}P_{11}\right) + \begin{bmatrix} b & a \\ -a & b \end{bmatrix}\otimes\left(\widetilde{A}P_{12}\right) + \begin{bmatrix} a & b \\ -b & a \end{bmatrix}\otimes\left(\widetilde{A}P_{21}\right) + \begin{bmatrix} -b & a \\ -a & -b \end{bmatrix}\otimes\left(\widetilde{A}P_{22}\right)\right\} < 0. \tag{26}$$

According to Lemma 1, if inequalities (13) and (26) hold, closed-loop system (12) with $0 < \alpha < 1$ is asymptotically stable. This completes the proof. □

Remark 1. Compared with [19–26], this paper studies the design of the fuzzy static output feedback controller for fractional-order fuzzy systems. In general, the fuzzy static output feedback controller will generate the term $B_iF_jC_k$ $(i,j,k = 1,2,\ldots,r)$, which increases the fuzzy r-times relationship. At the same time, the controller gain matrix is located between the two matrices, which makes the design of the control more difficult. In this paper, Lemma 3 is used to ingeniously separate this item and eliminate the above-mentioned difficulties. Furthermore, the relationship between fuzzy systems is considered.

Considering the relationship between fuzzy subsystems, we can prove the following conclusions.

Theorem 2. *Fractional-order closed-loop system (12) with $0<\alpha<1$ is asymptotically stable if there is scalar $\xi>0$, proper dimensional matrices $U, G_{1i}, G_{2i}, G_{3i}, G_{4i}, K_i, Z_{ij}\,(i=1,2,\ldots,r)$, symmetric matrices P_{11}, P_{21}, Z_{ii}, and skew-symmetric matrices P_{21}, P_{22} such that (13) and the following LMIs hold:*

$$\Omega_{ii}<Z_{ii},\quad i=1,2,\ldots,r, \tag{27}$$

$$\Omega_{ij}+\Omega_{ji}<Z_{ij}+Z_{ij}^T,\quad i=1,2,\ldots,r-1,\ j=i+1,\ldots,r,$$
$$Z=\begin{bmatrix} Z_{11} & Z_{12} & \cdots & Z_{1r} \\ Z_{12}^T & Z_{22} & \cdots & Z_{2r} \\ \vdots & \vdots & \ddots & \vdots \\ Z_{1r}^T & Z_{2r}^T & \cdots & Z_{rr} \end{bmatrix}<0. \tag{28}$$

If the above matrix inequalities hold, the controller gain matrices can be designed as

$$F_i=K_iU^{-1},\quad i=1,2,\ldots,r. \tag{29}$$

Proof. According to inequalities (27) and (28), we can easily get

$$\begin{aligned}&\sum_{i=1}^{r}\sum_{j=1}^{r}h_i(\theta(t))h_j(\theta(t))\Omega_{ij}\\ &\quad=\sum_{i=1}^{r}h_i^2(\theta(t))\Omega_{ii}+\sum_{i=1}^{r-1}\sum_{j=i+1}^{r}h_i(\theta(t))h_j(\theta(t))\left(\Omega_{ij}+\Omega_{ji}\right)\\ &\quad<\sum_{i=1}^{r}h_i^2(\theta(t))Z_{ii}+\sum_{i=1}^{r-1}\sum_{j=i+1}^{r}h_i(\theta(t))h_j(\theta(t))\left(Z_{ij}+Z_{ij}^T\right)\\ &\quad=\left[h_1(\theta(t)),h_2(\theta(t)),\ldots,h_r(\theta(t))\right]\\ &\qquad\cdot Z\left[h_1(\theta(t)),h_2(\theta(t)),\ldots,h_r(\theta(t))\right]^T.\end{aligned} \tag{30}$$

If $Z<0$ holds, there is $\sum_{i=1}^{r}\sum_{j=1}^{r}h_i(\theta(t))h_j(\theta(t))\Omega_{ij}<0$, i.e., inequality (19) holds. According to the proof process of Theorem 1, closed-loop system (12) with 0 asymptotically stable. This completes the proof. □

For fractional-order system (12) with order greater than zero and less than one, two new controller design methods are proposed. Using the similar method, when the order is greater than or equal to 1 but less than 2, we can prove the following results. □

Theorem 3. *Fractional-order closed-loop system (12) with $1\le\alpha<2$ is asymptotically stable if there is scalar $\xi>0$, proper dimensional matrices $U, G_{1i}, G_{2i}, G_{3i}, G_{4i}, K_i\,(i=1,2,\ldots,r)$, symmetric positive definite matrices $P_i\,(i=1,2,\ldots,r)$, and the following LMIs are satisfied:*

$$\Xi_{ii}<0,\quad i=1,2,\ldots,r, \tag{31}$$

$$\begin{aligned}&\Xi_{ij}+\Xi_{ji}<0,\quad i=1,2,\ldots,r-1, j=i+1,\ldots,r,\\ &F_i=K_iU^{-1},\quad i=1,2,\ldots,r,\end{aligned} \tag{32}$$

where

$$\Omega_{ij}=\begin{bmatrix} -\mathrm{sym}(G_{1i}) & cP_i+G_{1i}A_j^T-G_{2i}^T & 0 & dP_i & \\ * & \mathrm{sym}\left(G_{2i}A_j^T\right) & -dP_i & 0 & \xi Q_{ij}+W_{ij}^T \\ * & * & -\mathrm{sym}(G_{3i}) & cP_i+G_{3i}A_j^T-G_{4i}^T & \\ * & * & * & \mathrm{sym}\left(G_{4i}A_j^T\right) & \\ * & * & * & * & -\mathrm{sym}(\xi\mathbb{U}) \end{bmatrix}, \tag{33}$$

$c=\sin(\pi-\pi\alpha/2), d=\cos(\pi-\pi\alpha/2)$, and the definitions of other symbols are the same as those in Theorem 1.

Proof. Let $\overline{P}_i=\sum_{i=1}^{r}h_i(\theta(t))P_i$. Because every P_i is a symmetric positive definite matrix and the membership function is greater than 0, $\overline{P}_i$ is also a symmetric positive definite matrix.

In the process of proving Theorem 2, let $\Gamma_1=c\overline{P}_i$ and $\Gamma_2=d\overline{P}_i$; starting from inequalities (31) and (32), we can get the following results from (24):

$$\begin{bmatrix} c\left(\widetilde{A}_{ijk}\overline{P}_i+\overline{P}_i\widetilde{A}_{ijk}^T\right) & d\left(\widetilde{A}_{ijk}\overline{P}_i-\overline{P}_i\widetilde{A}_{ijk}^T\right) \\ * & c\left(\widetilde{A}_{ijk}\overline{P}_i+\overline{P}_i\widetilde{A}_{ijk}^T\right) \end{bmatrix}<0. \tag{34}$$

According to Lemma 2, Theorem 3 ensures that closed-loop system (12) with $1\le\alpha<2$ is asymptotically stable. This completes the proof. □

Similar to Theorem 1, we can prove the following result. □

Theorem 4. *Fractional-order closed-loop system (12) is asymptotically stable if there is scalar $\xi > 0$, proper dimensional matrices $U, G_{1i}, G_{2i}, G_{3i}, G_{4i}, K_i, \ Z_{ij}\,(i = 1, 2, \ldots, r)$, and symmetric positive definite matrices $P_i\,(i = 1, 2, \ldots, r)$ such that the following linear matrix inequalities hold:*

$$\Xi_{ii} < Z_{ii}, \quad i = 1, 2, \ldots, r, \tag{35}$$

$$\Xi_{ij} + \Omega_{ji} < Z_{ij} + Z_{ij}^T, \quad i = 1, 2, \ldots, r-1, \ j = i+1, \ldots, r. \tag{36}$$

$$Z = \begin{bmatrix} Z_{11} & Z_{12} & \cdots & Z_{1r} \\ Z_{12}^T & Z_{22} & \cdots & Z_{2r} \\ \vdots & \vdots & \ddots & \vdots \\ Z_{1r}^T & Z_{2r}^T & \cdots & Z_{rr} \end{bmatrix} < 0. \tag{37}$$

The corresponding controller can be selected as

$$F_i = K_i U^{-1}, \quad i = 1, 2, \ldots, r. \tag{38}$$

Proof. The proof process of Theorem 4 is exactly the same as that of Theorem 2, so it is omitted here. □

5. Numerical Example

In order to illustrate the effectiveness of the proposed methods, a numerical simulation example is given in this part. Since the simulation methods are similar, we only verify Theorem 1.

Example 1. For system (9), the corresponding simulation parameters are selected as follows:

$$\begin{gathered} A_1 = \begin{bmatrix} -1 & 1 & 2 \\ 1 & 0 & 1 \\ -2 & -1 & 2 \end{bmatrix}, \\ A_2 = \begin{bmatrix} -6 & -3 & 4 \\ 1 & 0 & 0 \\ -2 & -2 & 2 \end{bmatrix}, \\ B_1 = \begin{bmatrix} 0.8 \\ -3 \\ 3.8 \end{bmatrix}, \\ B_2 = \begin{bmatrix} 2 \\ -1 \\ 2 \end{bmatrix}, \\ C_1 = \begin{bmatrix} -2 & 1 & 0 \end{bmatrix}, \\ C_2 = \begin{bmatrix} 4 & -3 & 2 \end{bmatrix}. \end{gathered} \tag{39}$$

Membership functions are taken as $h_1(\theta(t)) = 0.5(1 - \sin(x_1(t)))$, $h_2(\theta(t)) = 1 - h_1(\theta(t))$.

Take fractional order $\alpha = 0.75$ and initial condition of the system $x_0 = [1, -3, 1.8]^T$. When the controller $u(t) = 0$, the state trajectory of the system is shown in Figure 1. Obviously, the system is unstable.

According to Theorem 1, the following feasible solutions can be obtained by using the linear matrix inequality toolbox and making $\xi = 1$:

$$\begin{gathered} P_{11} = P_{21} = \begin{bmatrix} 47.9949 & -4.9576 & 10.1684 \\ -4.9576 & 9.6889 & 7.9151 \\ 10.1684 & 7.9151 & 25.3468 \end{bmatrix}, \\ P_{12} = P_{22} = \begin{bmatrix} 0 & -1.0326 & 5.4116 \\ 1.0326 & 0 & -2.1499 \\ -5.4116 & 2.1499 & 0 \end{bmatrix}, \\ G_{11} = \begin{bmatrix} 17.3758 & -2.2678 & -11.9404 \\ -0.8326 & 27.6204 & -8.6416 \\ 15.0427 & 23.0184 & 17.4726 \end{bmatrix}, \\ G_{12} = \begin{bmatrix} 6.3362 & -3.5964 & -15.0566 \\ 0.6207 & 32.8234 & 14.5413 \\ 9.2638 & 33.9112 & 34.1965 \end{bmatrix}, \\ G_{21} = \begin{bmatrix} 9.6221 & -16.8697 & -25.2363 \\ -20.4052 & 4.4510 & -25.1853 \\ 21.6206 & 42.4479 & 27.6159 \end{bmatrix}, \\ G_{22} = \begin{bmatrix} 11.1564 & -5.6354 & -5.2083 \\ -8.3296 & 7.0806 & -4.8982 \\ 10.2057 & 25.5957 & 24.3865 \end{bmatrix}, \\ G_{31} = \begin{bmatrix} 25.1420 & 8.5343 & -88.6732 \\ 13.2014 & 34.9178 & -175.9623 \\ 79.6915 & 184.1028 & 38.7372 \end{bmatrix}, \\ G_{32} = \begin{bmatrix} 23.7128 & 192.8158 & 254.9889 \\ -163.7837 & 31.1085 & 364.0394 \\ -275.7049 & -347.9581 & 36.6636 \end{bmatrix}, \\ G_{41} = \begin{bmatrix} -19.3450 & -67.0576 & -2.1058 \\ -32.3201 & -11.7544 & -7.8586 \\ 1.8301 & -29.0457 & -38.1671 \end{bmatrix}, \\ G_{42} = \begin{bmatrix} -14.0099 & -123.5301 & -127.9458 \\ -13.0018 & -23.2141 & -30.4210 \\ 6.7847 & 9.8925 & -0.7920 \end{bmatrix}, \\ K_1 = 6.1395, \\ K_2 = -21.5572, \\ U = 101.1738. \end{gathered} \tag{40}$$

Gain matrices of the controller can be obtained by calculation:

$$\begin{gathered} F_1 = K_1^{-1} U^{-1} = 0.0607, \\ F_2 = K_2^{-1} U^{-1} = -0.2131. \end{gathered} \tag{41}$$

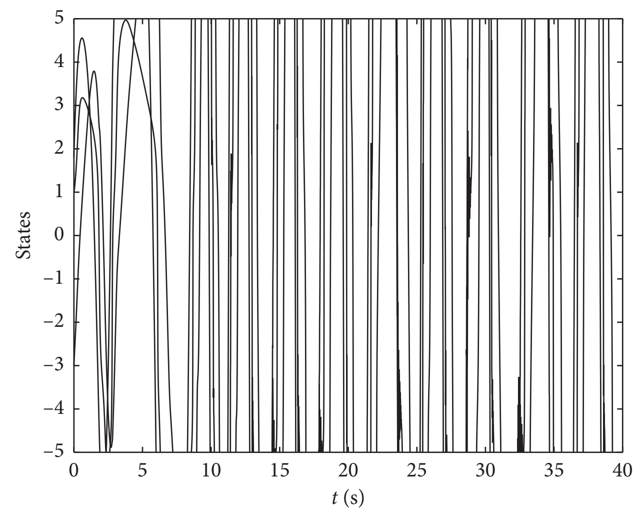

Figure 1: The state trajectories of the system when the controller $u(t) = 0$.

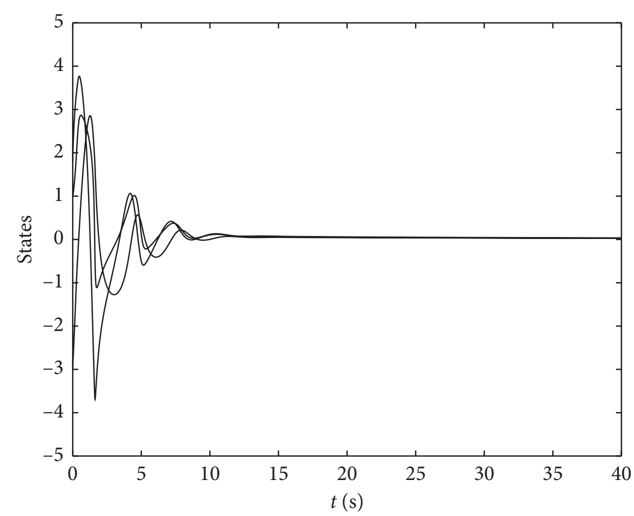

Figure 2: State trajectories of the system after adding the controller.

Using fuzzy controller (11), the state trajectories of closed-loop system (12) can be obtained as shown in Figure 2. As can be seen from Figure 2, the controller designed is effective.

6. Conclusion

For the fractional-order T-S fuzzy system, the controller design methods with order in two different intervals are studied. Four theorems are given to ensure that the closed-loop system is asymptotically stable. The result is expressed by the linear matrix inequality, which fully considers the feasibility and conservatism. In order to consider the feasibility, the condition of each theorem is the strict linear matrix inequality. This can be solved directly by the linear matrix inequality toolbox of Matlab. In order to reduce the conservatism, we try to make the matrix correspond to the fuzzy rule. Theorems 2 and 4 further consider the relationship between fuzzy subsystems.

Data Availability

The simulation results of this paper can be obtained by MATLAB software.

Conflicts of Interest

The author declares that there are no conflicts of interest.

References

[1] L. Chen, R. Wu, Y. He, and L. Yin, "Robust stability and stabilization of fractional-order linear systems with polytopic uncertainties," *Applied Mathematics and Computation*, vol. 257, pp. 274–284, 2015.

[2] L. Chen, T. Huang, J. A. Tenreiro Machado, A. M. Lopes, Y. Chai, and R. Wu, "Delay-dependent criterion for asymptotic stability of a class of fractional-order memristive neural networks with time-varying delays," *Neural Networks*, vol. 118, pp. 289–299, 2019.

[3] L. Chen, J. Cao, R. Wu, J. A. Tenreiro Machado, A. M. Lopes, and H. Yang, "Stability and synchronization of fractional-order memristive neural networks with multiple delays," *Neural Networks*, vol. 94, pp. 76–85, 2017.

[4] J. A. Gallegos and M. A. Duarte-Mermoud, "A dissipative approach to the stability of multi-order fractional systems," *IMA Journal of Mathematical Control and Information*, vol. 37, no. 1, pp. 143–158, 2018.

[5] H. Liu, Y. P. Pan, J. D. Cao, H. X. Wang, and Y. Zhou, "Adaptive neural network backstepping control of fractional-order nonlinear systems with actuator faults," *IEEE Transactions on Neural Networks and Learning Systems*, pp. 1–12. In press, 2020.

[6] J. Jia, X. Huang, Y. Li, J. Cao, and A. Alsaedi, "Global stabilization of fractional-order memristor-based neural networks with time delay," *IEEE Transactions on Neural Networks and Learning Systems*, vol. 31, no. 3, pp. 997–1009, 2020.

[7] L. A. Zadeh, "Fuzzy sets," *Information and Control*, vol. 8, no. 3, pp. 338–353, 1965.

[8] X. J. Zeng and M. G. Singh, "Approximation theory of fuzzy systems: SISO case," *IEEE Transactions on Systems, Man, and cybernetics*, vol. 24, no. 2, pp. 332–342, 1994.

[9] L. X. Wang, "Fuzzy systems are universal approximations," in *Proceedings of the IEEE International Conference on Fuzzy Systems*, pp. 1163–1170, San Diego, CA, USA, March 1992.

[10] T. Takagi and M. Sugeno, "Fuzzy identification of systems and its applications to modeling and control," *IEEE Transactions on Systems, Man, and Cybernetics*, vol. SMC-15, no. 1, pp. 116–132, 1985.

[11] M. Sugeno and T. Yasukawa, "A fuzzy-logic-based approach to qualitative modeling," *IEEE Transactions on Fuzzy Systems*, vol. 1, no. 1, pp. 7–25, 1993.

[12] L.-X. Wang and J. M. Mendel, "Fuzzy basis functions, universal approximation, and orthogonal least-squares learning," *IEEE Transactions on Neural Networks*, vol. 3, no. 5, pp. 807–814, 1992.

[13] L. Wang, *Adaptive Fuzzy System and Control Design and Stability Analysis*, National Defense Industry Press, Beijing, China, 1995.

[14] S. G. Cao, N. W. Rees, and G. Feng, "Analysis and design of fuzzy control systems using dynamic fuzzy global models," *Fuzzy Sets and Systems*, vol. 75, no. 1, pp. 47–62, 1995.

[15] Z. Chen, B. Zhang, Y. Zhang, and Z. Zhang, "Dissipative fuzzy filtering for nonlinear networked systems with limited communication links," *IEEE Transactions on Systems, Man, and Cybernetics: Systems*, vol. 50, no. 3, pp. 962–971, 2020.

[16] S. Rathinasamy, S. Palanisamy, and K. Boomipalagan, "Modified repetitive control design for nonlinear systems with time delay based on T-S fuzzy model," *IEEE Transactions on Systems, Man, and Cybernetics: Systems*, vol. 50, no. 2, pp. 646–655, 2020.

[17] Y. Li, L. Liu, and G. Feng, "Finite-time H_∞ controller synthesis of T-S fuzzy systems," *IEEE Transactions on Systems, Man, and Cybernetics: Systems*, vol. 50, no. 5, pp. 1956–1963, 2020.

[18] Y.-C. Chang, S.-S. Chen, S.-F. Su, and T.-T. Lee, "Static output feedback stabilization for nonlinear interval time-delay systems via fuzzy control approach," *Fuzzy Sets and Systems*, vol. 148, no. 3, pp. 395–410, 2004.

[19] D. Huang and S. K. Nguang, "Static output feedback controller design for fuzzy systems: an ILMI approach," *Information Sciences*, vol. 177, no. 14, pp. 3005–3015, 2007.

[20] H. N. Wu, "An ILMI approach to robust static output feedback fuzzy control for uncertain discrete-time nonlinear systems," *Automatica*, vol. 44, no. 9, pp. 2333–2339, 2008.

[21] S.-W. Kau, H.-J. Lee, C.-M. Yang, C.-H. Lee, L. Hong, and C.-H. Fang, "Robust fuzzy static output feedback control of T-S fuzzy systems with parametric uncertainties," *Fuzzy Sets and Systems*, vol. 158, no. 2, pp. 135–146, 2007.

[22] J. Dong and G.-H. Yang, "Static output feedback control of a class of nonlinear discrete-time systems," *Fuzzy Sets and Systems*, vol. 160, no. 19, pp. 2844–2859, 2009.

[23] H.-Y. Chung and S.-M. Wu, "Hybrid approaches for regional Takagi-Sugeno static output feedback fuzzy controller design," *Expert Systems with Applications*, vol. 36, no. 2, pp. 1720–1730, 2009.

[24] J. C. Lo and M. L. Lin, "Robust H_∞ nonlinear control via fuzzy static output feedback," *IEEE Transactions on Circuits and Systems I: Fundamental Theory and Applications*, vol. 50, no. 11, pp. 1494–1502, 2003.

[25] D. Huang and S. K. Sing Kiong Nguang, "Robust H_∞ static output feedback control of fuzzy systems: an ILMI approach," *IEEE Transactions on Systems, Man and Cybernetics, Part B (Cybernetics)*, vol. 36, no. 1, pp. 216–222, 2006.

[26] H. N. Wu and H. Y. Zhang, "Reliable mixed L_2/H_∞ fuzzy static output feedback control for nonlinear systems with sensor faults," *Automatica*, vol. 41, no. 11, pp. 1925–1932, 2005.

[27] H. J. Lee and D. W. Kim, "Fuzzy static output feedback may be possible in LMI framework," *IEEE Transactions on Fuzzy Systems*, vol. 17, no. 5, pp. 1229-1230, 2009.

[28] C. H. Fang, Y. S. Liu, S. W. Kau et al., "A new LMI-based approach to relaxed quadratic stabilization of T-S fuzzy control systems," *IEEE Transactions on Fuzzy Systems*, vol. 14, no. 3, pp. 386–397, 2006.

[29] Y. Zheng, Y. Nian, and D. Wang, "Controlling fractional order chaotic systems based on Takagi-Sugeno fuzzy model and adaptive adjustment mechanism," *Physics Letters A*, vol. 375, no. 2, pp. 125–129, 2010.

[30] J. Li and Y. Li, "Robust stability and stabilization of fractional order systems based on uncertain Takagi-Sugeno fuzzy model with the fractional order $1 \leq \alpha < 2$." *Journal of Computing and Nonlinear Dynamics*, vol. 8, no. 4, pp. 1–7, 2013.

[31] Y. Li and J. Li, "Stability analysis of fractional order systems based on T-S fuzzy model with the fractional order α:$0 < \alpha < 1$," *Nonlinear Dynamics*, vol. 78, no. 4, pp. 2909–2919, 2014.

[32] X. Huang, Z. Wang, Y. Li, and J. Lu, "Design of fuzzy state feedback controller for robust stabilization of uncertain fractional-order chaotic systems," *Journal of the Franklin Institute*, vol. 351, no. 12, pp. 5480–5493, 2014.

[33] R. Duan, J. Li, and J. Chen, "Mode-dependent non-fragile observer-based controller design for fractional-order T-S fuzzy systems with Markovian jump via non-PDC scheme," *Nonlinear Analysis: Hybrid Systems*, vol. 34, pp. 74–91, 2019.

[34] R. Duan and J. Li, "Observer-based non-PDC controller design for T-S fuzzy systems with the fractional-order $0 < \alpha < 0$," *IET Control Theory & Applications*, vol. 12, no. 5, pp. 661–668, 2018.

[35] S. A. Karthick, R. Sakthivel, Y. K. Ma, S. Mohanapriya, and A. Leelamani, "Disturbance rejection of fractional-order T-S fuzzy neural networks based on quantized dynamic output feedback controller," *Applied Mathematics and Computation*, vol. 361, pp. 846–857, 2019.

[36] C. Lin, B. Chen, and Q.-G. Wang, "Static output feedback stabilization for fractional-order systems in T-S fuzzy models," *Neurocomputing*, vol. 218, pp. 354–358, 2016.

[37] Y. Ji, L. Su, and J. Qiu, "Design of fuzzy output feedback stabilization for uncertain fractional-order systems," *Neurocomputing*, vol. 173, pp. 1683–1693, 2016.

[38] R. Chaibi, E. Tissir, A. Hmamed et al., "Static output feedback controller for continuous-time fuzzy systems," *International Journal of Innovative Computing, Information and Control*, vol. 15, no. 4, pp. 1469–1484, 2019.

[39] L. Podlubny, *Fractional Differential Equations*, Academie Press, New York, NY, USA, 1999.

[40] X. F. Zhang and Y. Q. Chen, "D-stability based LMI criteria of stability and stabilization for fractional order systems," in *Proceedings of the ASME 2015 ASME/IEEE International Conference on Mechatronic and Embedded Systems and Applications*, Boston, MA, USA, August 2015.

[41] B. Li and X. Zhang, "Observer-based robust control of ($0 < \alpha$ <1) fractional-order linear uncertain control systems," *IET Control Theory & Applications*, vol. 10, no. 14, pp. 1724–1731, 2016.

[42] M. Chilali, P. Gahinet, and P. Apkarian, "Robust pole placement in LMI regions," *IEEE Transactions on Automatic Control*, vol. 44, no. 12, pp. 2257–2270, 1999.

[43] P. Gahinet and P. Apkarian, "A linear matrix inequality approach to H_∞ control," *International Journal of Robust and Nonlinear Control*, vol. 4, no. 4, pp. 421–448, 1994.